594
29/10/92

Indian J Chem
NOVEMBER 1992
CODEN : IJOCAP 31A(11) 811-902 (1992)
ISSN : 0376-4710

INDIAN JOURNAL OF CHEMISTRY

SECTION A

(Inorganic, Bio-inorganic, Physical, Theoretical & Analytical Chemistry)

Published by
PUBLICATIONS & INFORMATION DIRECTORATE, CSIR, NEW DELHI
in association with
THE INDIAN NATIONAL SCIENCE ACADEMY, NEW DELHI

The Treatise on Indian Medicinal Plants

Editors: Asima Chatterjee and Satyesh Chandra Pakrashi

Pages: 172
Price: Rs. 250/-

Ayurveda, the indigenous system of medicine, advocates the application of various Indian herbs in curing many maladies. Several drugs of plant origin are used in Ayurveda.

The Treatise on Indian Medicinal Plants, Vol. I, the first in a series of six volumes, covers 111 plants. The write-up on each plant includes its vernacular name,occurrence and distribution, botanical description, and therapeutic uses along with important chemical constituents of the plant extract. A distinctive feature of the book is inclusion of authentic Sanskrit *slokas*, both in Devnagri and Roman scripts. The *slokas* explain the therapeutic uses of individual plants. A glossary gives the meanings of Sanskrit/Ayurvedic and medical terms. Also, a list of books referred to has been given for ready reference.

The book is profusely illustrated with both coloured and black and white pictures to enable proper identification of plant species.

The editors of the book are eminent scientists in the field. Professor Chatterjee, a Padma Bhushan and a winner of the S.S. Bhatnagar Award, is a chemist of world repute. She is currently the coordinator of the Centre of Advanced Studies on Natural Products, Department of Pure Chemistry, Calcutta University. Dr Pakrashi, the former Director of Indian Institute of Chemical Biology, Calcutta and a Fellow of the Indian National Science Academy is at present a Distinguished CSIR Fellow.

This volume would prove immensely useful to teachers, researchers and specialists in the field of Ayurveda and medicinal plants.

Insight into Scientific Research in Indian Universities & the Institutes of Technology

Rais Ahmed and Madhulika Rakesh

Pages : v + 155
Price : Rs 140/-

The role of scientific research in industry, trade, defence and in the day-to-day life of an individual cannot be over-emphasized. It, therefore, becomes pertinent to take a holistic view not only of the various parameters of research but also to assess its organizational patterns, and human relations, values and attitudes associated with it, which are the main factors responsible for the germination and growth of research *per se*.

Insight into Scientific Research encompasses an exhaustive yet interesting study of the quality, character and efficiency of scientific research in Indian universities and other research institutions.

Several recommendations ranging from adequate financial support, reform of education leading to research, and utilization of research results would enlighten the reader. The book also throws light on what should be the research policy for Indian universities and research institutions.

One of the authors, Professor Ahmed, a Padma Bhushan is a renouned physicist. At present he is Executive Director of the Tertiary Education Commission in Mauritius. The coauthor Ms. Rakesh is an experienced researcher in the field of investigating conditions, process and value systems of scientific research.

Well illustrated with graphs and tables, which aid the text, the book should be a valuable possession for all involved in the scientific and technological development of the country.

Order for the books should be accompanied by M.O./D.D. made payable to **"Publications & Information Directorate"** and sent to:
Sales and Distribution Officer.
PUBLICATIONS & INFORMATION DIRECTORATE
Dr. K.S. Krishnan Marg,
New Delhi-110012.

RENEWAL NOTICE

Your subscription which expires with the despatch of December 1992 issue of the journal, stands for renewal. We request you to be so good as to return the enclosed order form duly filled, early, so as to ensure continuity in despatch.

Sales & Distribution Officer

Order No.....

DATED :

The Sales & Distribution Officer
Publications & Information Directorate, C.S.I.R.
Dr. K.S. Krishnan Marg, New Delhi-110012 (INDIA)

Dear Sir,

Please renew my subscription/enrol me as a subscriber to :

			Rs	$	£
1.	Journal of Scientific & Industrial Research	(Monthly)	250.00	100.00	80.00
2.	Indian Journal of Chemistry, Section A	(Monthly)	400.00	150.00	100.00
3.	Indian Journal of Chemistry, Section B	(Monthly)	400.00	150.00	100.00
4.	Indian Journal of Experimental Biology	(Monthly)	350.00	150.00	80.00
5.	Indian Journal of Technology	(Monthly)	300.00	150.00	80.00
6.	Indian Journal of Pure & Applied Physics	(Monthly)	300.00	150.00	80.00
7.	Indian Journal of Biochemistry & Biophysics	(Bimonthly)	150.00	75.00	40.00
8.	Indian Journal of Marine Sciences	(Quarterly)	160.00	65.00	40.00
9.	Indian Journal of Radio & Space Physics	(Bimonthly)	150.00	75.00	40.00
10.	Indian Journal of Fibre & Textile Research	(Quarterly)	160.00	65.00	40.00
11.	Research & Industry	(Quarterly)	160.00	65.00	40.00
12.	Medicinal & Aromatic Plants Abstracts	(Bimonthly)	300.00	125.00	75.00
13.	Current Literature on Science of Science	(Monthly)	150.00	90.00	48.00
14.	C.S.I.R. News	(Semi-Monthly)	50.00	20.00	12.00

(Please tick the periodicals you would like to subscribe).

for one year from January 1993 for which I am/we are enclosing a cheque/Demand Draft No .....dated ..... for a sum of Rs .....
£ .....$ ..... in favour of

PUBLICATIONS & INFORMATION DIRECTORATE, NEW DELHI

COMPLETE MAILING ADDRESS

Name .....

Address .....

Country/State .....

(Signature)

Notes :

1. Subscription at annual rates for all the periodicals are enlisted for the full volumes, i.e. for the period from January to December only.
2. The Cheque/Demand Draft may please be drawn in favour of "PUBLICATIONS & INFORMATION DIRECTORATE, NEW DELHI". Banking charges shall be borne by the subscriber. For inland/outstation cheques please add Rs.10.00 for Foreign Cheques please add $ 2.00 or £ 1.00.
3. The supply will commence on receipt of subscription in advance.
4. Foreign subscription rates are for delivery by surface mail. Air mail rates will be supplied on request.

INDIAN JOURNAL OF CHEMISTRY

Section A: Inorganic, Bio-inorganic, Physical, Theoretical & Analytical Chemistry

Editorial Board

Prof. R C Mehrotra
Vice-Chancellor
Allahabad University
Allahabad 211 002

Prof. D V S Jain
Chemistry Department
Panjab University
Chandigarh 160 014

Prof. A Chakravorty
Department of Inorganic Chemistry
Indian Association for the
Cultivation of Science
Calcutta 700 032

Prof. V Krishnan
Department of Inorganic
& Physical Chemistry
Indian Institute of Science
Bangalore 560 012

Prof. K K Rohatgi Mukherjee
Department of Chemistry
Jadavpur University
Calcutta 700 032

Dr J P Mittal
Chemistry Division
Bhabha Atomic Research Centre
Bombay 400 085

Prof. S K Rangarajan
Director
Central Electrochemical Research Institute
Karaikudi 623 006

Prof. R C Srivastava
Department of Chemistry
Banaras Hindu University
Varanasi 221 005

Prof. E D Jemmis
Department of Chemistry
University of Hyderabad
Hyderabad 500 134

Dr S K Date
Physical Chemistry Division
National Chemical Laboratory
Pune 411 008

Prof. I Gutman
Faculty of Science
Yu. 34000, Kragujevac
Radoja Domanovica
Yugoslavia

Prof. A B Sannigrahi
Department of Chemistry
IIT, Kharagpur 721 302

Dr D Papousek
Institute of Atomic and
Molecular Sciences
Academia Sinica
P.O. Box 23-166
Taipei, TAIWAN 10764

Prof. P P Singh
Department of Chemistry
M.D. University
Rohtak 124 001

Dr Pradip K Mascharak
Department of Chemistry
University of California
Santa Cruz
California 65064
USA

Dr G P Phondke Director, PID

Editors : Dr B.C. Sharma, Dr S. Sivakamasundari and Dr S.K. Bhasin
Sr. Scientific Assistant : Geeta Mahadevan

Published by the Publications & Information Directorate, CSIR, Dr K.S. Krishnan Marg, New Delhi 110012

Director: Dr G P Phondke

Copyright, 1992, by the Council of Scientific & Industrial Research, New Delhi 110 012

The Indian Journal of Chemistry is issued monthly in two sections: A and B. Communications regarding contributions for publication in the journal should be addressed to the Editor, Indian Journal of Chemistry, Publications & Information Directorate, Hillside Road, New Delhi 110 012.

Correspondence regarding subscriptions and advertisements should be addressed to the Sales & Distribution Officer, Publications & Information Directorate, Dr K.S. Krishnan Marg, New Delhi 110 012.
Phone 586301 Gram: PUBLIFORM Telex: 031-77271

The Publications & Information Directorate (CSIR) assumes no responsibility for the statements and opinions advanced by contributors. The Editorial Board in its work of examining papers received for publication is assisted, in an honorary capacity by a large number of distinguished scientists, working in various parts of India.

Annual Subscription: Rs. 400.00 £ 100.00 $ 150.00; 50% discount admissible to research workers and students and 25% discount to non-research individuals on annual subscription.

Single Copy: Rs. 40.00 £ 10.00 $ 15.00

Payments in respect of subscriptions and advertisements may be sent by cheque, bank draft, money order or postal order marked payable to Publications & Information Directorate, Dr K.S. Krishnan Marg, New Delhi 110 012.

Claims for missing numbers of the journal will be allowed only if received within 3 months of the date of issue of the journal plus the time normally required for postal delivery of the journals and the claim.

AUTHOR INDEX

Acharya Achyuta N 832
Adharani T K 855

Bajaj Rakesh 892
Basheer Ahamed K A 845
Bhattacharya Pabitra K 889

Chatterjee Chinmay 898

Dash Anadi C 824, 832
Dash Neelamadhab 824
Date S K 870
Deshpande S B 870

Elwerfalli Jamal T 881

Garg A N 849, 878
Godbole P D 870
Gupta S K 892

Iyengar T Asha 838

Jai Bhagwan 817
Jain C L 892
Jain Vimal K 861
Joshi N G 878
Jothibai Margret R 865

Kannan S 845
Keerthi C N 855
Khan N H 883
Krishan Lal 817, 892
Kulkarni S P 878
Kureshi R I 883

Lakshmanan Vasanthi 896
Lanjewar R B 849

Mahadevappa D S 838
Mahan Ashok 901
Mehrotra R C 886
Mittal J P 811
Mokal Vijaya K 861
Mukherjee T 811

Nagaraja K S 896
Nanda Rabindra K 832
Nasir Mohd Ibrahim 901

Pal H 811
Palit D K 811
Potdar H S 870
Pradhan Jyotsnamayee 824

Rabindra Reddy P 855

Sankaranarayana Pillai M 865
Shah A 886
Shoukry Abdel F 881
Sikkandar G 845
Singh A 886
Singh Archana 874
Singh Kehar 874
Sivasankaran Nair M 865
Stephen Mary 898
Sudha C 865

Talele Gangadhar G 889
Taqui Khan M M 883
Thillai Arasu P 865

Udupa M R 896

Indian Journal of Chemistry

Sect. A: Inorganic, Bio-inorganic, Physical, Theoretical & Analytical

VOLUME 31A **NUMBER 11** **NOVEMBER 1992**

CONTENTS

Triplet state and semiquinone free radical of 5-methoxyquinizarin: A laser flash photolysis and pulse radiolysis study 811
H Pal, D K Palit, T Mukherjee* & J P Mittal

Thermal and spectral studies on cellulose arylphosphinites in air 817
Jai Bhagwan & Krishan Lal*

Medium effects on the electron-transfer processes: Reduction of aquapentaammineco-balt(III) by hexacyanoferrate(II) in ethyleneglycol-water, ethylene carbonate-water and urea-water media 824
Anadi C Dash*, Neelamadhab Dash & Jyotsnamayee Pradhan

Kinetics and mechanism of acid and base hydrolysis of *cis*-(bioxalato)(imidazole)bis(ethy-lenediamine)cobalt(III) ion: A study of the role of the coordinated imidazole and its anion 832
Anadi C Dash*, Rabindra K Nanda & Achyuta N Acharya

Kinetics and mechanism of oxidation of monosaccharides by sodium-N-bromobenzene-sulphonamide in alkaline medium 838
T Asha Iyengar & D S Mahadevappa*

Kinetics and mechanism of oxidation of γ-oxoacids by acid permanganate . . . 845
G Sikkandar, K A Basheer Ahamed* & S Kannan

Synthesis, electronic, infrared and Mössbauer spectroscopic studies of mixed ligand com-plexes of mono- and bis(N,N′-diethyldithiocarbamato)iron(III) with O,N and S con-taining chelating ligands and their thermal decomposition 849
R B Lanjewar & A N Garg*

Interaction of metal ions with uridine 5′-monophosphate: Existence of possible intramo-lecular interactions 855
P Rabindra Reddy*, T K Adharani & C N Keerthi

Synthesis and spectroscopic studies of di-*s*- and *t*-butyltin(IV) carboxylates . . . 861
Vimal K Jain* & Vijaya B Mokal

Studies on copper(II) and zinc(II) mixed ligand complexes involving some potentially tri-dentate ligands 865
M Sivasankaran Nair*, P Thillai Arasu, R Jothibai Margret, C Sudha & M Sankaranarayana Pillai

Notes

Dielectric characterization of BTO-derived barium titanate ($BaTiO_3$) ceramics . . 870
H S Potdar, S B Deshpande, P D Godbole & S K Date*

Electrochemical studies on zirconium phosphate-kynar composite ion-exchange membrane system 874
Kehar Singh* & Archana Singh

Gamma ray induced decomposition of lanthanide double nitrates with some bivalent cations 878
S P Kulkarni, N G Joshi & A N Garg*

Plastic membrane *p*OH-electrode based on chlorpromazine base 881
Adel F Shoukry* & Jamal T Elwerfalli

Reversible binding of carbon monoxide with Ru(III) aminopolycarboxylic acid complexes 883
M M Taqui Khan*, N H Khan & R I Kureshy

Synthesis and characterization of chloro-acetylacetonato-, and alkoxo-nonaisopropoxodizirconatoiron(III) derivatives 886
A Shah, A Singh* & R C Mehrotra

Synthesis and characterization of homo and hetero trinuclear alkoxides 889
Gangadhar G Talele & Pabitra K Bhattacharya*

Synthesis and characterization of some transition metal picrate complexes with isonicotinic acid hydrazide 892
Rakesh Bajaj, C L Jain, S K Gupta* & Krishan Lal

Tetraoxomolybdato and tetraoxotungstato complexes of iron(II) diimines . . . 896
Vasanthi Lakshmanan, K S Nagaraja & M R Udupa*

Acid hydrolysis of iminodiacetatotetraammine cobalt(III), $[Co(NH_3)_4idaH](ClO_4)_2$ complex 898
Chinmay Chatterjee* & Mary Stephen

Cation exchange chromatographic separation of a number of metal ions in ammonium iodide media 901
Mohd Ibrahim Nasir* & Ashok Mahan

Authors for correspondence are indicated by (*)

VALUABLE BOOKS IN CHEMISTRY

Advanced Inorganic Chemistry	Agarwal, Lal	110.00
Reactions & Reagents	Agarwal, Manivasakam	65.00
Advanced Physical Chemistry	Gurtu, Hemant	140.00
Water Pollution	Kudesia	200.00
Air Pollution	Kudesia	360.00
Industrial Pollution	Kudesia	240.00
Physico-Chemical Examination of Water Sewage and Industrial Effluents	Manivasakam	180.00
Desert Environment	Saxena	250.00
Pollution Everywhere	Kudesia	300.00
Environmental & Biochemistry	Kudesia	125.00
Some Analytical Techniques and Reagents	Lal, Katyal	100.00
Instrumental Methods of Chemical Analysis	Kudesia Sawhney	45.00
Advanced Inorganic Analysis	Subhash-Satish	42.00
Advanced Organic Analysis	Agarwal,Agarwal	40.00
Physical Chemistry Experiments	Kudesia	25.00
I.I.T. Chemistry	Agarwal, Lal	120.00
Chemistry for Engineering & Medical Competitions	Agarwal, Lal	130.00
Numerical Problems in Chemistry	Agarwal, Lal	65.00
Problems in Chemistry	Singh, Verma	60.00
Objective Type Chemistry	Agarwal, Lal	35.00

RR / PP — 92 E - 3

PRAGATI PRAKASHAN
P.B. No. 62, Begum Bridge
Meerut-250 001 (U.P.)

High T_C Superconductors

Special Issue of the Indian Journal of Pure & Applied Physics (Oct - Nov 1992)

To mark The Golden Jubilee of CSIR

Guest Editor	:	**Dr A.V. Narlikar**
Pages	:	**250 (Approx.)**
ISSN	:	**0019 - 5596**
Price	:	**Rs.120.00; $ 28.00; £ 16.00**

This special issue presents 21 original research articles written by eminent experts in the frontier areas of research in high temperature superconductors. It essentially focusses on techniques like crystal growth, X-ray absorption and plasma parameters which are immensely useful in studying the high temperature superconducting systems.

Broadly the topics relate to four categories: (i) theory; (ii) materials and physical properties; (iii) characterization and electronic structures; and (iv) thin films and devices.

This issue would not only provide interesting reading but should be a must for all engaged in R&D in material science, solid state electronics, superconductivity, structural chemistry, device engineering and condensed matter physics.

Orders should be accompanied by Money Order or Demand Draft made payable to "Publications & Information Directorate" and sent to:

Sales & Distribution Officer,
Publications & Information Directorate,
Dr K.S. Krishnan Marg,
New Delhi-110012.

Indian Journal of Chemistry
Vol. 31A, November 1992, pp. 811-816

Triplet state and semiquinone free radical of 5-methoxyquinizarin : A laser flash photolysis and pulse radiolysis study

H Pal, D K Palit, T Mukherjee* & J P Mittal
Chemistry Division, Bhabha Atomic Research Centre, Trombay, Bombay

Received 24 February 1992; accepted 20 July 1992

The triplet(T) state properties like T-T absorption spectra, quantum yield, energy level and decay kinetics of 5-methoxyquinizarin (5-methoxy-1,4-dihydroxy-9,10-anthraquinone ; MQZ) have been investigated in cyclohexane, acetonitrile and isopropyl alcohol using nanosecond laser flash photolysis technique. In isopropyl alcohol, a neutral semiquinone radical is also formed which has been characterised by comparing the long lived transient spectra with the MQZ-semiquinone spectra obtained by pulse radiolysis of MQZ in the same solvent. A relatively small amount of a long lived transient formed in cyclohexane and acetonitrile, along with the triplet state of MQZ, could not be characterised unambiguously, but has been attributed to the semiquinone radical of MQZ, produced by the reaction of the excited states of the quinone with the solvent. The quantum yield of the semiquinone radical in isopropyl alcohol is considerably higher than the triplet quantum yield, showing that both the excited singlet and the triplet states of the quinone probably react with the solvent molecules to form the semiquinone radical. The photophysical properties of the triplet and the semiquinone radical of MQZ have been compared with those of simple 1,4-disubstituted anthraquinones.

Amino and hydroxy substituted 9,10-anthraquinones have long been used as dispersed dyes for colouring synthetic polymer materials[1]. It has been observed that the light fastness of these anthraquinonoid dyes is often hampered by catalytic fading when applied as mixtures. Among several mechanisms suggested[2] for photobleaching, the most popular is the formation of intermediate singlet molecular oxygen by reactions of the triplet states of the anthraquinonoid dyes with ground state triplet oxygen. Hence the ability of bleaching is related to the quantum efficiencies of formation of the triplet states (ϕ_T), which depends upon the nature and position of the substituents in the basic anthraquinone moiety[3-5]. Triplet states of quinones and their derivatives are well known to form semiquinone radicals by abstracting hydrogen atoms from hydrogen donating solvents[6,7]. The anthrasemiquinone radicals are also involved in the photosensitized degradation of textile materials dyed with anthraquinonoid dyes[8]. The photochemistry of quinones also plays an important role in a number of biological processes[9], e.g., the initiation of biological electron transport through light absorption by the quinones.

The triplet state and the semiquinone characteristics of 1,4-amino and hydroxy disubstituted anthraquinones are already reported[5]. In the present work the triplet state and the semiquinone characteristics of MQZ, a 5-methoxy derivative of 1,4-dihydroxy-9,10-anthraquinone, were investigated in different solvents like cyclohexane, acetonitrile and isopropyl alcohol to understand the effect of the additional methoxy group on the excited state characteristics of the substituted quinones.

Materials and Methods

Pure MQZ was kindly donated by Dr J M Bruce of Manchester University, U.K., and was used without further purification. All solvents were of spectroscopic grade from Spectrochem (India) and used without further purification. Anthracene, biphenyl and fluorenone (scintillation grade from J.T. Baker Chemical Co., USA) and perylene (Aldrich) were used as received. All solutions were deoxygenated by bubbling oxygen-free nitrogen (IOLAR grade from Indian Oxygen Ltd.) for about 15 min, using a proper solvent trap prior to the solution.

Ground state absorption spectra were recorded with a Shimadzu UV-160 A spectrophotometer. Nanosecond flash photolysis experiments were carried out using the laser kinetic spectrometer model K 347 (Applied Photophysics, U.K.), the details of which have been described earlier[10]. Pulse radiolysis experiments were conducted with a 7 MeV linear electron accelerator (Ray Technology, U.K.). The details of the pulse radiolysis set up have been described elsewhere[11].

Results and Discussions

Transient absorption spectra and decay kinetics

Time-resolved difference [(transient)-(parent)] absorption spectra produced by KrF excimer laser (248 nm) excitation of MQZ in cyclohexane and isopropyl alcohol are shown in Figs 1 and 2 respectively. In acetonitrile, the time-resolved spectra were qualitatively identical to those in cyclohexane.

The time-resolved spectra in cyclohexane (Fig.1) and acetonitrile indicate that in both the solvents at least two different transients were produced. The optical density values of the long-lived transients were, however, very small in comparison to those of the short-lived transients. The decay of the short-lived transients followed a first order kinetics and the transients have been characterised as the triplet states of MQZ by the usual oxygen quenching and the triplet-triplet (T-T) energy transfer method[12]. The first order decay rate constants (k_T) of the triplets are given in Table 1.

In isopropyl alcohol also, the time-resolved transients absorption spectra clearly revealed the presence of two transient species following the laser excitation. Moreover, the optical density of the long-lived transient was comparatively higher, at least in some wavelength ranges. The short-lived transient in isopropyl alcohol was characterised as the triplet state of the quinones by the usual techniques. The first order decay rate constant (k_T) of the triplet could be determined accurately only at selective wavelength where the overlapping of the spectra of the shorter-lived triplet and longer-lived transient was minimum. The k_T values thus determined at suitable wavelengths are given in Table 1.

The short lifetimes ($=1/k_T$) of the triplet states ($\sim$6 μs) in all the three solvents may be due to the involvement of excited state intramolecular proton

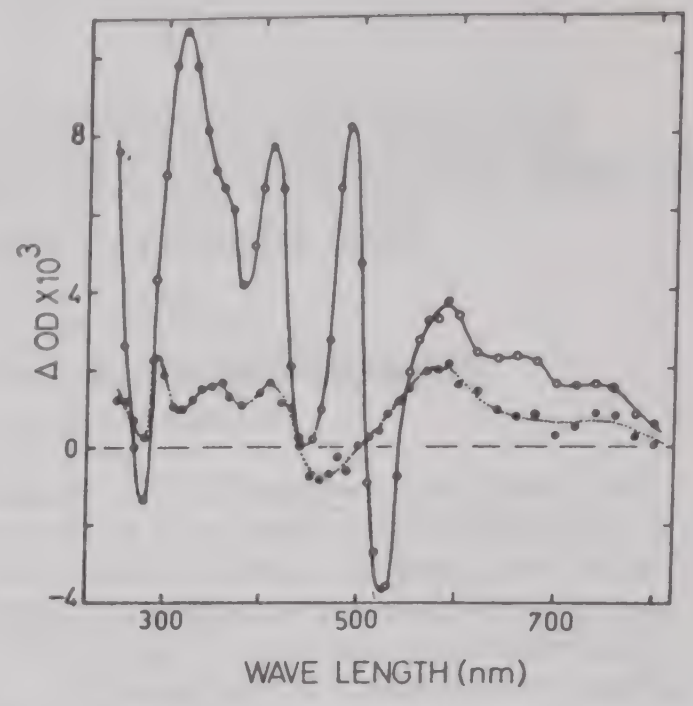

Fig. 1—Time-resolved difference absorption spectra of the transients produced by laser flash photolysis of MQZ in cyclohexane at 0.5 μs (○—○) and 18 μs (●. . . . ●) after the laser pulse

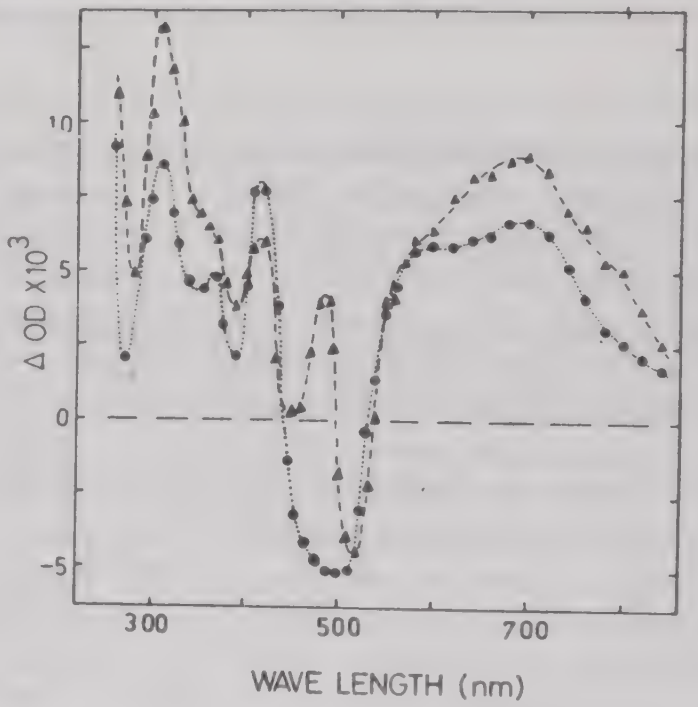

Fig. 2—Time-resolved difference absorption spectra of the transients produced by laser flash photolysis of MQZ in isopropyl alcohol at 0.5 μs (▼--▼) and 18 μs (●...●) after the laser pulse

Table 1—Photophysical characteristics of the triplet state and the semiquinone radical of MQZ in different solvents

(*a*) *Triplet Characteristics:*

Solvent	ϕ_T	$\varepsilon_T(\lambda, nm)$ ($10^4 dm^3 mol^{-1} cm^{-1}$)	k_T ($10^5 s^{-1}$)
Cyclohexane	0.17±0.03	1.6±0.2 (320)	1.8±0.2
Acetonitrile	0.24±0.04	0.7±0.2 (600)	1.5±0.2
Isopropyl alcohol	0.12±0.03	2.2±0.4 (320)	2.5±0.3

(*b*) *Semiquinone Characteristics:*

Solvent	$\phi_{QH^\cdot}$	$\varepsilon_{QH^\cdot}(\lambda, nm)$ ($10^3 dm^3 mol^{-1} cm^{-1}$)	$2k_{QH^\cdot}$ ($10^8 mol^{-1} s^{-1}$)
Isopropyl alcohol	0.20±0.03	4.4±0.3 (600)	6.6±0.3

transfer (ESIPT[13-16]), a likely process as the two hydroxy groups in MQZ are intramolecularly hydrogen-bonded to the two quinonoid oxygens. It was, however, difficult to obtain any direct evidence of ESIPT process in the T_1 state, since the ESIPT is a much faster process than the triplet decay rate. Considering that the ESIPT process is occurring, the triplet state structure of MQZ is most likely to be a rapid equilibrium one of the two proton transferred forms (Scheme 1).

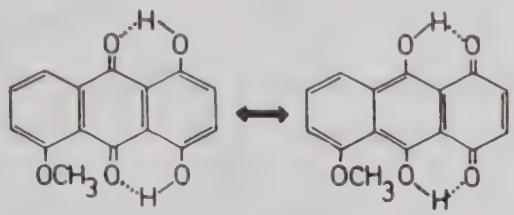

Scheme 1

A careful investigation of the time-resolved spectra of the transients produced in all the three solvents, especially in isopropyl alcohol, revealed that the longer-lived transients were also present immediately after the laser excitation. The longer-lived transient spectra obtained in isopropyl alcohol were qualitatively identical to the absorption spectra of the neutral semiquinone radical of MQZ, obtained by pulse radiolysis study in pure isopropyl alcohol, in the wavelength rage 340-760 nm. The difference absorption spectrum of the semiquinone radical produced by pulse radiolysis of MQZ in isopropyl alcohol is shown in Fig.3. Hence the longer-lived transient produced in isopropyl alcohol by laser flash photolysis was characterised as the neutral semiquinone radical, probably formed by both the triplet ($^3Q_1$) and the excited singlet ($^1Q_1$) states of the quinones abstracting a hydrogen atom from the solvent[5-7,10].

$$^3Q_1\,(^1Q_1) + (CH_3)_2CHOH \rightarrow QH^{\cdot} + (CH_3)_2\dot{C}OH \quad \ldots (1)$$

The isopropyl ketyl radicals (CH3)2ĊOH] thus formed in reaction 1 could also react with the ground state quinones ($^1Q_0$) to produce more semiquinone radicals[5,10].

$$^1Q_0 + (CH_3)_2\,COH \rightarrow QH + (CH_3)_2CO \quad \ldots (2)$$

However, unlike juglone (5-hydroxy-1,4-naphthoquinone)[10] and 1,4-disubstituted-9,10-anthraquinones[5] the reaction 2 was not clearly indicated in the kinetic spectrophotometric traces for MQZ.

The long-lived transient absorption spectra in cyclohexane and acetonitrile were so weak that it was difficult to characterise the species. However, comparing the difference absorption spectrum of this transient (Fig.1) with the corresponding spectrum in

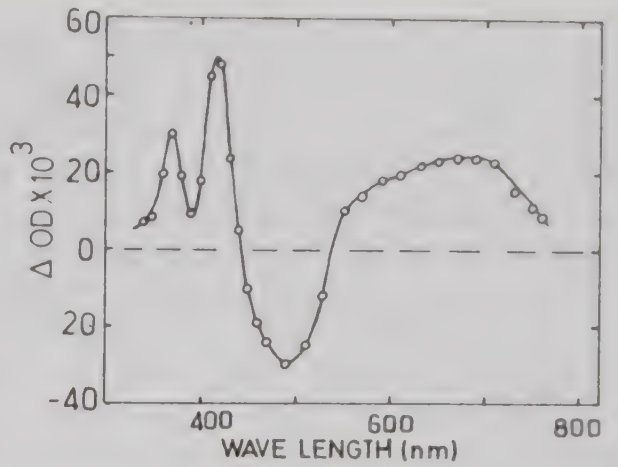

Fig. 3—Difference absorption spectra of the reduced semiquinone radical of MQZ in isopropyl alcohol as obtained by pulse radiolysis experiment. Dose = 9.4 Gy

isopropyl alcohol (Fig.2) and also comparing similar results obtained for 1,4-amino and hydroxy disubstituted 9,10-anthraquinones[5], it can be stated that the long-lived transient produced in these two solvents is the reduced semiquinone radical of MQZ. The latter is formed probably by a hydrogen abstraction reaction similar to reaction 1. The S_1 state of the quinone probably reacts with the solvent molecules of cyclohexane and acetonitrile, which are not normally hydrogen donating solvents.

The semiquinone radicals produced in isopropyl alcohol decayed by a second-order process, attributed to their disproportionation into the parent quinone ($^1Q_0$) and the fully reduced hydroquinone (QH_2),

$$2\dot{Q}H \rightarrow {}^1Q_0 + QH_2 \quad \ldots (3)$$

The second-order decay rate constants of the semiquinone radicals ($2k_{QH^{\cdot}}$), determined by pulse radiolysis in isopropyl alcohol, are given in Table 2.

Triplet energy levels

The energy of the first triplet state (E_T) of MQZ in cyclohexane was determined by triplet-triplet energy transfer method[17]. T-T energy transfer was observed from anthracene (E_T = 176 kJ mol^{-1}) to MQZ, while T-T energy transfer occurred from the latter to perylene (E_T = 151 kJ mol^{-1}). The triplet energy of MQZ was thus estimated to be in the range of 151-176 kJ mol^{-1}. It must be mentioned here that the triplet energy of MQZ is in the same range as those of 1,4-, 1,5- and 1,8- amino and hydroxy disubstituted anthraquinones[5,18]. Thus, the additional methoxy group does not have any significant effect on the triplet state energies of the substituted anthraquinones.

Extinction coefficient (ε_T) *and corrected spectra*

Extinction coefficient for T-T absorption (ε_T) was determined by energy transfer method[19], using XeF

excimer laser (351 nm) as the excitation source, as MQZ has negligible absorption at this wavelength. The composition of the solution was maintained in such a way that at least 90% of the excitation laser light was absorbed by the donor, thus minimising the formation of the acceptor triplet by direct excitation. For cyclohexane and isopropyl alcohol, anthracene triplet ($\varepsilon_T = 6.47 \times 10^4$ dm^3 mol^{-1}cm^{-1} in cyclohexane at 422.5 nm, and $\varepsilon_T = 6.35 \times 10^4$ dm^3 mol^{-1}cm^{-1} in ethyl alcohol at 420 nm[20]) and for acetonitrile, fluoren-9-one triplet ($\varepsilon_T = 6.0 \times 10^3$ dm^{3}mol^{-1}cm^{-1} at 420 nm[20]) was used as the reference donor for extinction coefficient determination. It was assumed that ε_T in ethyl alcohol and isopropyl alcohol will not vary much and it can be considered to be equal within the range of experimental error. In cyclohexane, β-carotene triplet ($\varepsilon_T = 2.4 \times 10^5$ dm^{3}mol^{-1}cm^{-1} at 525 nm[20]) was also used as the reference acceptor for the determination of ε_T of the quinone using KrF laser as the excitation source. β-Carotene is a well known acceptor for determination of extinction coefficient for T-T absorption as its quantum yield for intersystem crossing process ($S_1 \rightarrow T_1$) is zero and the energy level of the lowest excited triplet state is very low (75 kJ mol^{-1})[12]. Necessary corrections were introduced for the decay of the donor triplet by means other than energy transfer mechanism, the formation of the acceptor triplets by direct absorption of the laser light by the acceptor molecules and also for the decay of the acceptor triplet after formation[19]. The ε_T values determined at suitable wavelengths are presented in Table 1. These are the averages of at least five independent measurements, the error bars indicating the maximum fluctuations of the independent measurements.

Once the extinction coefficient was determined at a particular wavelength, the value at any other wavelength was obtained using the relation,

$$\varepsilon_T = \varepsilon_S + \triangle OD_T/[^3Q_1] \quad \ldots (4)$$

where ε_S is the extinction coefficient of the ground state absorption and $\triangle OD_T$ is the observed [(triplet) - (quinone)] difference in optical density at the wavelength of interest and $[^3Q_1]$ is the concentration of the triplet formed, estimated using the experimentally determined ε_T and the difference in optical density at that particular wavelength. Hence the true or absolute T-T absorption spectra were determined by applying Eq.4 to the difference absorption spectra of the triplets in cyclohexane and acetonitrile and they are presented in Fig. 4. It was not possible to determine the true T-T absorption spectra in isopropyl alcohol due to the fact that the difference absorption spectra obtained immediately after the laser pulse could not be assigned to pure triplet but a combination of the triplet and the semiquinone radical formed from the singlet and triplet states, since an appreciable amount of the radical is also formed immediately after the laser pulse, was indicated by the time-resolved spectra and also by the kinetic traces (Fig. 4).

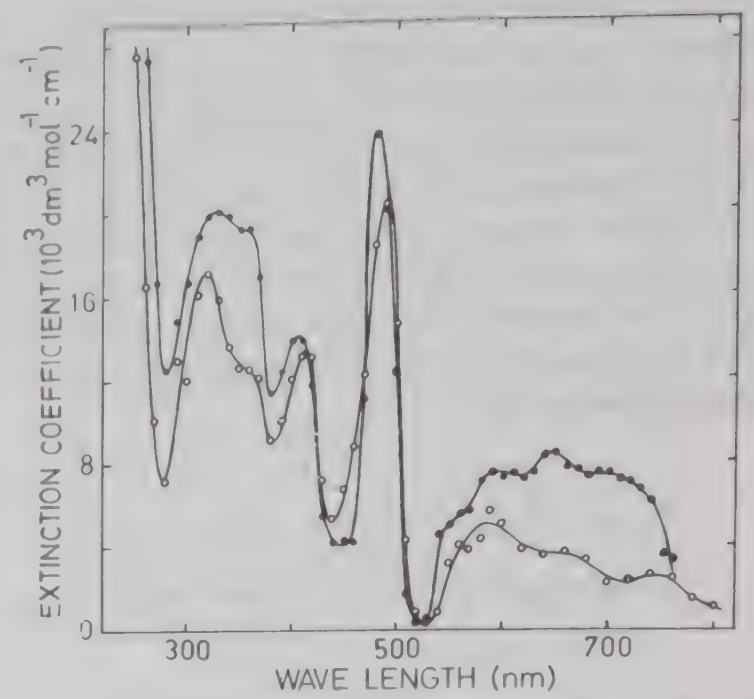

Fig. 4—Corrected T-T absorption spectra of the triplets of MQZ in cyclohexane (○—○) and in acetonitrile (●—●)

Extinction coefficients for the semiquinone radical absorption ($\varepsilon_{QH^\bullet}$) in isopropyl alcohol were determined using pulse radiolysis method. The G-value for semiquinone radical formation ($G_{QH^\bullet}$) was taken to be 5.1 under our experimental condition[5]. Therefore, the extinction coefficient ($\varepsilon_{QH^\bullet}$) at any particulars. wavelength λ was calculated as,

$$\varepsilon_{QH^\bullet} = \varepsilon_S + \frac{\Delta OD_{QH^\bullet} \times \varepsilon_{(SCN)_2^{\bullet-}} \times G_{(SCN)_2^{\bullet-}}}{OD_{(SCN)_2^{\bullet-}} \times G_{QH^\bullet}} \quad \ldots (5)$$

where $\triangle OD_{QH^\bullet}$ is the observed semiquinone-quinone difference in optical density at wavelength λ, $OD_{(SCN)_2^{\bullet-}}$ is the optical density of $(SCN)_2^{\bullet-}$ radicals at 500 nm formed in air-saturated thiocyanate dosimeter solution under an isodose condition, $\varepsilon_{(SCN)_2^{\bullet-}}$ is the extinction coefficient for the $(SCN)_2^{\bullet-}$ radical absorption at 500 nm, taken[21,22] to be 7.1×10^3 dm^{3}mol^{-1}cm^{-1} and $G_{(SCN)_2^{\bullet-}}$ is the G-value of $(SCN)_2^{\bullet-}$ radical formation, taken[21,22] to be 2.9 molecules (100 eV)$^{-1}$. The true absorption spectra of semiquinone radicals were determined by two methods. First, from the difference absorption spectra obtained by pulse radiolysis, applying Eq.5 to correct them. The corrected absorption spectra of the semiquinone radicals of MQZ in isopropyl alcohol thus obtained from pulse radiolysis experiment are shown in Fig.5. In the second method, the extinction coefficient values of the semiquinone radical at a

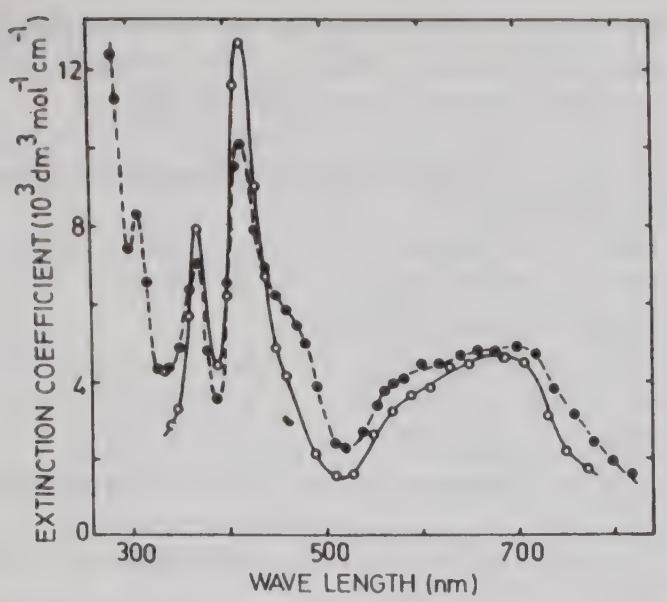

Fig. 5—Corrected semiquinone absorption spectra of MQZ in isopropyl alcohol as obtained from pulse radiolysis (○—○) and from laser flash photolysis experiment (●--●)

suitable wavelength (in the range 600-700 nm, where the parent quinone does not absorb), obtained from pulse radiolysis data, were used to correct the difference absorption spectra of the semiquinone obtained by laser flash photolysis (18 μs after the laser flash, Fig.2), using an equation similar to Eq.4. The corrected semiquinone absorption spectrum thus obtained from flash photolysis experiment is also presented in Fig.5. Comparison of the true semiquinone spectra obtained by the above two methods shows that the peak positions and shapes of the spectra are in good agreement. The little differences in the absolute extinction coefficient values in the wavelength region 380 nm-500 nm may be due to the uncertainty of getting correct values of the extinction coefficient in this wavelength region of high ground state depletion and/or due to the formation of some parmanent products in either of the two techniques.

Quantum yields of triplets and semiquinone radicals

From the known extinction coefficients for T-T and semiquinone radical absorption, it had been possible to determine the singlet to triplet crossing efficiency or triplet quantum yield (ϕ_T) and the quantum yield of semiquinone radical formation ($\phi_{QH^\cdot}$) by the comparative method[23]. For determination of ϕ_T and $\phi_{QH^\cdot}$, the quantum yield of biphenyl triplet in cyclohexane was used as the reference ($\phi_T = 0.84$ and $\varepsilon_T = 4.28 \times 10^4$ $dm^3mol^{-1}cm^{-1}$ at 361.5 nm[23]). For ϕ_T determination the difference in optical density ($\triangle OD_T$), obtained immediately after the laser pulse, was taken at a wavelength where the overlapping of the semiquinone radical absorption with others was minimum. Similarly, for $\phi_{QH^\cdot}$ determination of the difference in optical density, observed about 18 μs after the laser pulse, was taken at a wavelength where the overlapping of the short-lived triplet absorption was minimum. Also, for both the cases, the wavelengths chosen were such that the absorption coefficients of the ground state quinones were either negligible or zero. The values of ϕ_T and $\phi_{QH^\cdot}$ thus obtained are given in Table 1.

Quantum yield of triplet formation for MQZ is somewhat higher than that of 1,4-amino and hydroxy disubstituted anthraquinones[5]. This may be due to the fact that the introduction of the methoxy group in one benzenoid ring of the quinone perturbs the intra-molecular hydrogen bonded structure of the parent 1,4-dihydroxy-9,10-anthraquinone and thus increases its quinone character and consequently the triplet quantum yield.

It is very interesting to note that in the isopropyl alcohol solution the $\phi_{QH^\cdot}$ values are significantly higher than the ϕ_T values. Hence, it is evident that the triplet state was not the only precursor for the semiquinone radical formation. The semiquinone radicals also may have been formed by the reaction of the excited singlet states of the quinones with the solvents, as was also evident from the time-resolved transient absorption spectra. Formation of the semiquinone radicals by the reaction of isopropyl ketyl radicals with the ground state quinones (reaction 2), may also contribute to the higher $\phi_{QH^\cdot}$ values.

The present studies thus indicate that in hydrogen atom donating solvents like isopropyl alcohol, the semiquinone free radicals are formed quite substantially over and above the usual triplet state of the quinone due to the H-abstraction by the latter from the solvent. The singlet excited state of the quinone is also involved as the precursor of the semiquinone radicals in such solvents. A quantitative estimation of the contribution of the excited singlet states to the semiquinone formation has, however, not been possible in the present experimental conditions as the other channels (e.g. reaction of the triplets with the solvent molecules (Eq.1) and the reaction of $CH_3\dot{C}OHCH_3$ radical with the parent quinone (Eq. 2)) of semiquinone formation are not quantitatively separable. In cyclohexane and acetonitrile, a long lived transient is also formed along with the usual triplet state, attributed to be the semiquinone radical of MQZ.

The energy of the lowest triplet state of MQZ is seen to be comparable to those of the 1,4-amino and hydroxy disubstituted 9,10-anthraquinones. The triplet quantum yield of MQZ is, however, relatively higher than those of the latter anthraquinone derivatives.

References

1 Rembold M W & Kramer H E A, *J Soc Dyers and Colorists*, 94 (1978) 141.

2 Asquith R S & Ingham P, *J Soc Dyers Colorists*, 94 (1978) 12 and references therein.

3 Rembold M W & Kramer H E A, *J Soc Dyers Colorists*, 94 (1978) 12 & 96 (1980) 122.

4 Ritter J, Borst H U, Lindner T, Hauser M, Brosig S, Bredereck K, Steiner U E, Kuhn D, Kelemen J & Kramer H E A, *J Photochem Photobiol Å: Chem*, 41 (1988) 227.

5 Palit D K, Pal H, Mukherjee T & Mittal J P, *J Photochem Photobiol A: Chem*, 52 (1990) 375.

6 Bridge N K & Porter G, *Proc Roy Soc A*, 244 (1958) 259.

7 Amouyal E & Bensasson R, *J chem Soc, Faraday Trans* 1, 72 (1976) 1274.

8 McKellar J F, *Radiat Res Rev*, 3 (1971) 141.

9 Bordie A F, in *Biochemistry of quinones*, edited by R A Morton (Academic Press, New York), 1965.

10 Palit D K, Pal H, Mukherjee T & Mittal J P, *J Photochem*, 37 (1987) 95.

11 Priadarsini K I, Naik D B, Moorthy P N & Mittal J P, *Proceedings of the seventh Tihany symposium on radiation chemistry* (Hungarian Chemical Society, Budapest), 1991.

12 Bensasson R V, Land E J & Truscott T G, *Flash photolysis and pulse radiolysis: Contributions to the chemistry, biology and medicine* (Pergamon Press, Oxford), 1983, 14.

13 Smulevich G & Foggi P , *J chem Phys*, 87 (1987) 5657.

14 Smulevich G, Foggi P, Feis A & Marzocchi M P, *J chem Phys*, 87 (1987) 5664.

15 Folm S R & Barbara P F, *J phys Chem*, 89 (1985) 4489.

16 Palit D K, Pal H, Mukherjee T & Mittal J P, *J chem Soc, Faraday Trans*, 86 (1990) 3861.

17 Porter G & Wilkinson F, *Proc Roy Soc A*, 264 (1961) 1.

18 Pal H, Palit D K, Mukherjee T & Mittal J P, *J Photochem Photobiol A: Chem*, 62(1991) 183.

19 Amouyal E, Bensasson R & Land E J, *Photochem Photobiol*, 20 (1974) 415.

20 Carmichael I & Hug C L, *J Phys Chem Ref Data*, 15 (1986) 1 and references therein.

21 Spinks J W T & Woods R J, *An introduction to radiation chemistry* (Wiley, New York), 2nd edition, 1976.

22 Adams G E, Boag J W, Currant J & Michael B D, in *Pulse radiolysis*, edited by M Ebert, J P, Keene, A J Swallow and J M Baxendale (Academic Press, London), 1965, 117.

23 Amand B & Bensasson R, *Chem Phys Lett*, 34 (1975) 44.

Indian Journal of Chemistry
Vol. 31A, November 1992, pp. 817-823

Thermal and spectral studies on cellulose arylphosphinites in air

Jai Bhagwan & Krishan Lal*
Department of Chemistry, Kurukshetra University, Kurukshetra 132 119, India

Received 19 August 1991; revised and accepted 3 April 1992

The thermal behaviour of cellulose and cellulose arylphosphinite samples have been studied using DTA, TG and DTG techniques from ambient temperature to 700°C in dynamic air atmosphere. First exotherms in DTA curves of cellulose arylphosphinite samples attributable to the decomposition process have been found to be lower than that of cellulose. Various kinetic and thermodynamic parameters have been obtained from TG curves using Broido method and transition state theory. For the decomposition stage of cellulose arylphosphinite samples the values of the activation energies are found to be in the range 83-138 kJ mol^{-1} and are lower than that of cellulose (187 kJ mol^{-1}). The EPR signals have given indication of the formation of trapped and stable free radicals in the thermal degradation of cellulose and cellulose arylphosphinite samples. Higher char yields of cellulose arylphosphinite samples as compared to cellulose lead to the conclusion that cellulose arylphosphinites are good flame retardants. A flame-retardancy mechanism for the thermal degradation of cellulose arylphosphinites has been proposed.

Cotton is widely available and the cheapest natural fibre used for clothing. From the consumer's point of view, the fibre should be difficult to ignite, have as low a flame spread as possible, liberate minimum heat, smoke and toxic gases if involved in fire. As cotton contains the highest percentage of cellulose, it will be desirable to modify cellulose, a primary substance of cotton, to make it flame retardant. In view of the above, cellulose arylphosphinites were prepared and the kinetics of thermal degradation were studied from ambient temperature to 700°C in dynamic air using differential thermal analysis (DTA), thermogravimetry (TG) and derivative thermogravimetry (DTG) techniques. Further, the composition of the charred products was studied by IR and EPR spectra of chars obtained at various temperatures.

Materials and Methods

The following samples were selected for the present work: (i) cellulose (from Dassel, West Germany); (ii) cellulose phenylphosphinite; (iii) cellulose *p*-methylphenylphosphinite; (iv) cellulose *p*-chlorophenylphosphinite; and (v) cellulose *p*-bromophenylphosphinite.

Preparation of aryl dichlorophosphines

A mixture of benzene (1.0 mol), PCl_3 (1.0 mol) and anhydrous $AlCl_3$ (0.25 mol) was refluxed for 6 h in nitrogen atmosphere, residual benzene and PCl_3 were distilled. Pyridine (0.25 mol) was dropped in at a temperature below 50°C. Phenyl dichlorophosphine was collected at 100-105°C/13 mm. On the same lines, *p*-methylphenyl dichlorophosphine[1] (110-115°C/10 mm), *p*-chlorophenyl dichlorophosphine[2] (105-115°C/14 mm) and *p*-bromophenyl dichlorophosphine[3] (135-136°C/14 mm) were obtained by mixing appropriate quantities of toluene, chlorobenzene and bromobenzene, respectively, in place of benzene with other reagents.

Preparation of cellulose arylphosphinites

Cellulose phenylphosphinite (II) was prepared by treating cellulose (5.0 g) in pyridine (100 ml) with phenyl dichlorophosphine (12.50 ml) at 115°C for 6 h with constant stirring. Products obtained were filtered, washed first with pyridine and then thoroughly with water and then dried over P_2O_5 *in vacuo* at 80°C. Similarly, cellulose *p*-methylphenylphosphinite, cellulose *p*-chlorophenylphosphinite and cellulose *p*-bromophenylphosphinite were also prepared.

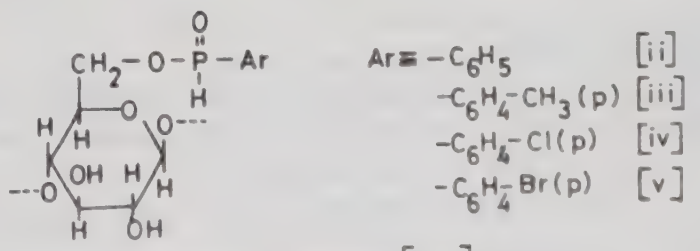

Structures of Samples [ii-v]

Table 1—Elemental analyses data of cellulose arylphosphinite samples

Sample No.	Compound	Per cent			
		P	Cl	Br	N
(i)	Cellulose	—	—	—	—
(ii)	Cellulose phenylphosphinite	4.25	1.0	—	0.27
(iii)	Cellulose *p*-methylphenylphosphinite	4.64	1.04	—	0.35
(iv)	Cellulose *p*-chlorophenylphosphinite	5.01	13.85	—	0.52
(v)	Cellulose *p*-bromophenylphosphinite	5.05	1.20	16.50	0.39

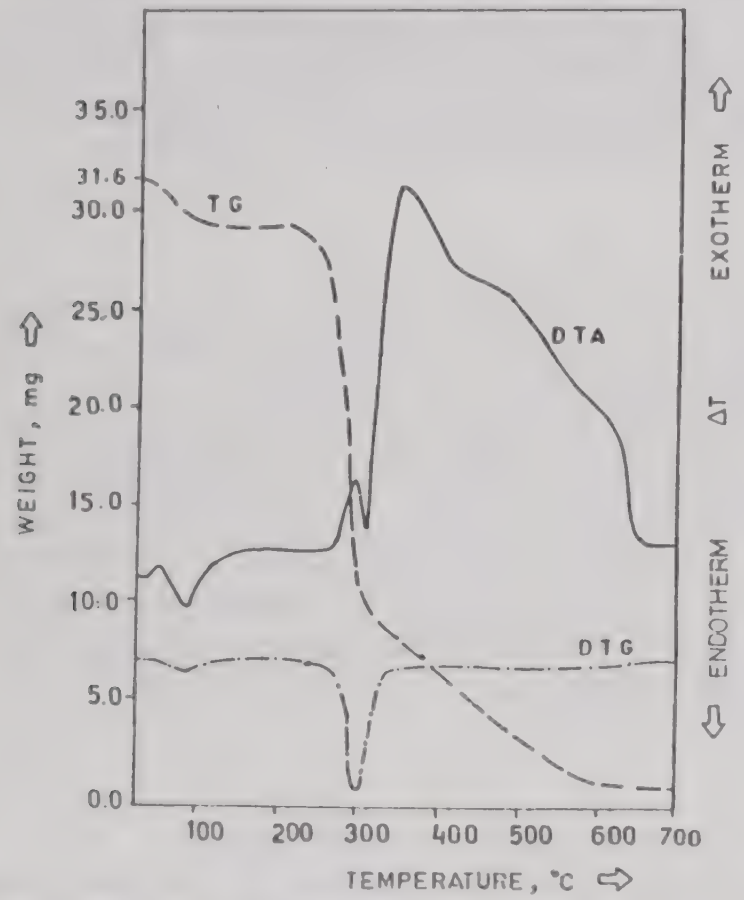

Fig. 1—DTA, TG and DTG curves for cellulose in dynamic air

Elemental analyses

Elemental analyses of phosphorus, nitrogen, chlorine and bromine were carried out by Energy Dispersive X-ray Fluorescence using kevex 3060, retractable Si(Li) detector system. The results are given in Table 1.

Thermal analyses

DTA, TG and DTG curves of samples (i-v) were recorded in dynamic air from ambient temperature to 700°C at the heating rate of 10°C/min using ULAC SINKU-RIKU TGD-5000 RH(P) Model instrument.

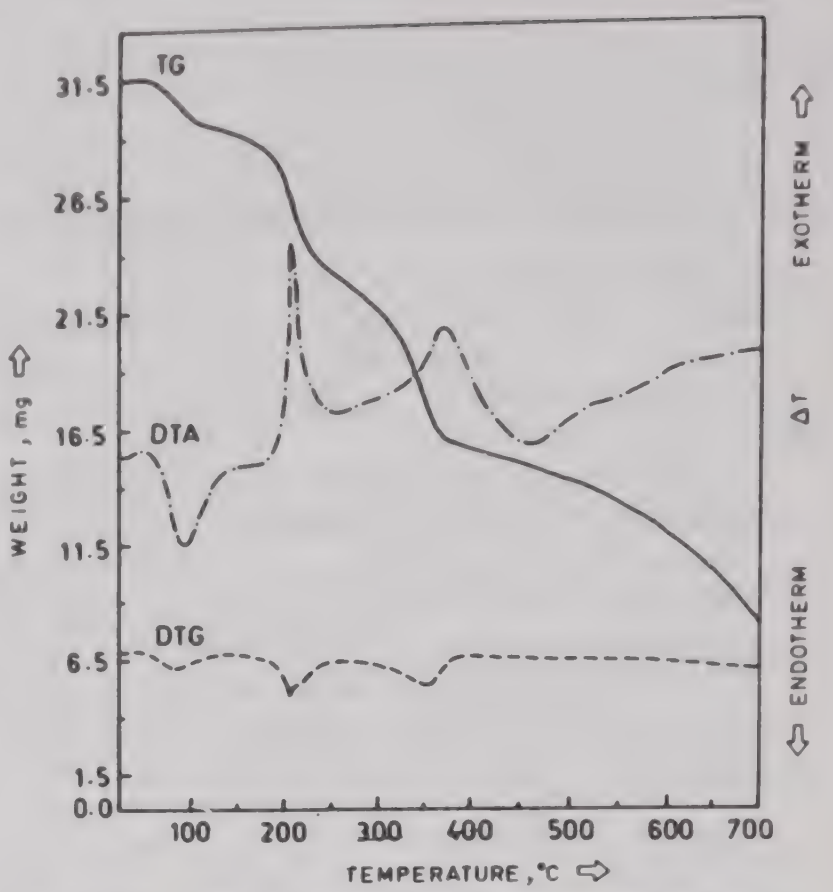

Fig. 2—DTA, TG and DTG curves for cellulose phenylphosphinite in dynamic air

IR spectroscopic studies

IR spectra of cellulose phenylphosphinite (ii) and its chars obtained at different temperatures were recorded by KBr pellet technique using Perkin-Elmer IR spectrophotometer (UK).

EPR studies

EPR spectra of charred samples of cellulose derivatives (ii-v) were recorded on Jeol, Japan, EPR spectrophotometer operating at 9.45 GHz. The 1,1-diphenyl-2-picrylhydrazyl (DPPH) signal was used as a standard for g values.

Results and Discussion

DTA, TG and DTG curves of cellulose (i) and cellulose arylphosphinite samples (ii-v) were recorded in dynamic air and representative plots for cellulose and cellulose phenylphosphinite are shown in Figs 1 and 2. The initiation, maximum and termination peak temperatures for various endotherms and exotherms of DTA of all the samples (i-v) are given in Table 2. DTA curve of each sample shows endotherm below 100°C due to the evolution of sorbed moisture. DTA curve of cellulose shows an endotherm with maximum at 265°C which is due to the dehydration process. This endotherm is followed by a large exotherm at 300°C which is attributed to the decomposition of cellulose leading to the formation and volatilization of products. This exotherm is followed by another exotherm peak centred at 365°C which

Table 2—Description of DTA curves in dynamic air for cellulose and cellulose arylphosphinite samples

Sample No.	Compound	DTA temperature/°C			Nature of peak
		Initiation	Maxima	Termination	
(i)	Cellulose	—	95	150	Endo, large
		185	265	280	Endo, small
		280	300	315	Exo, large
		315	365	645	Exo, broad
(ii)	Cellulose phenyl-phosphinite	—	85	120	Endo, large
		120	165	190	Endo, small
		190	200	240	Exo, sharp
		240	360	410	Exo, large
		440	510	530	Exo, v. small
		530	610	700	Exo, v. small
(iii)	Cellulose *p*-methyl-phenylphosphinite	—	95	115	Endo, large
		115	155	180	Endo, small
		180	205	240	Exo, sharp
		260	350	450	Exo
		480	570	690	Exo, broad
(iv)	Cellulose *p*-chloro-phenylphosphinite	—	95	120	Endo, large
		120	165	190	Endo, small
		190	202	230	Exo, sharp
		310	365	460	Exo, sharp
		500	545	645	Exo, sharp
(v)	Cellulose *p*-bromo-phenylphosphinite	—	90	115	Endo, large
		115	150	185	Endo, small
		185	200	220	Exo, sharp
		310	360	420	Exo, small
		480	555	650	Exo, large

may be attributed to the oxidation of volatile and charred products.

DTA curves of cellulose arylphosphinite samples (ii-v) show endotherms with maxima at 165, 155, 165 and 150°C, respectively, due to dephosphorylation, acid catalyzed dehydration and dehydrohalogenation reactions. Endotherms of the sample (ii-v) are at lower temperatures than that of cellulose (265°C) which indicates that the primary reactions in samples (ii-v) start occurring at lower temperature than that of cellulose. The endotherm in each of the samples (ii-v) is followed by an exotherm with maxima at 200, 205, 202 and 200°C, respectively, which is attributed to the decomposition process. These exotherms are at much lower temperatures than that of cellulose (300°C). Second exotherms of the samples (ii-v) (with maxima at $\simeq$360°C) are due to oxidation of volatile products formed during the decomposition process.

Succeeding this, exotherms with maxima at 510, 570, 545 and 550°C of samples (ii-v), respectively, are due to the oxidation of aliphatic and aromatic components of char residue and are at higher temperature than that of pure cellulose (365°C).

TG curves of cellulose arylphosphinite samples (ii-v) show four significant areas of weight loss, termed as four stages of thermal degradation whereas cellulose shows three stages of thermal degradation. Broido's method[4] is used to evaluate the kinetic parameters from TG curves. Equation 1 is used in this method.

$$\ln(\ln(1/y)) = -\frac{E_a}{R}\cdot\frac{1}{T} + \ln\left[\frac{R}{E_a}\cdot\frac{Z}{\beta}\cdot T_m^2\right] \quad \ldots (1)$$

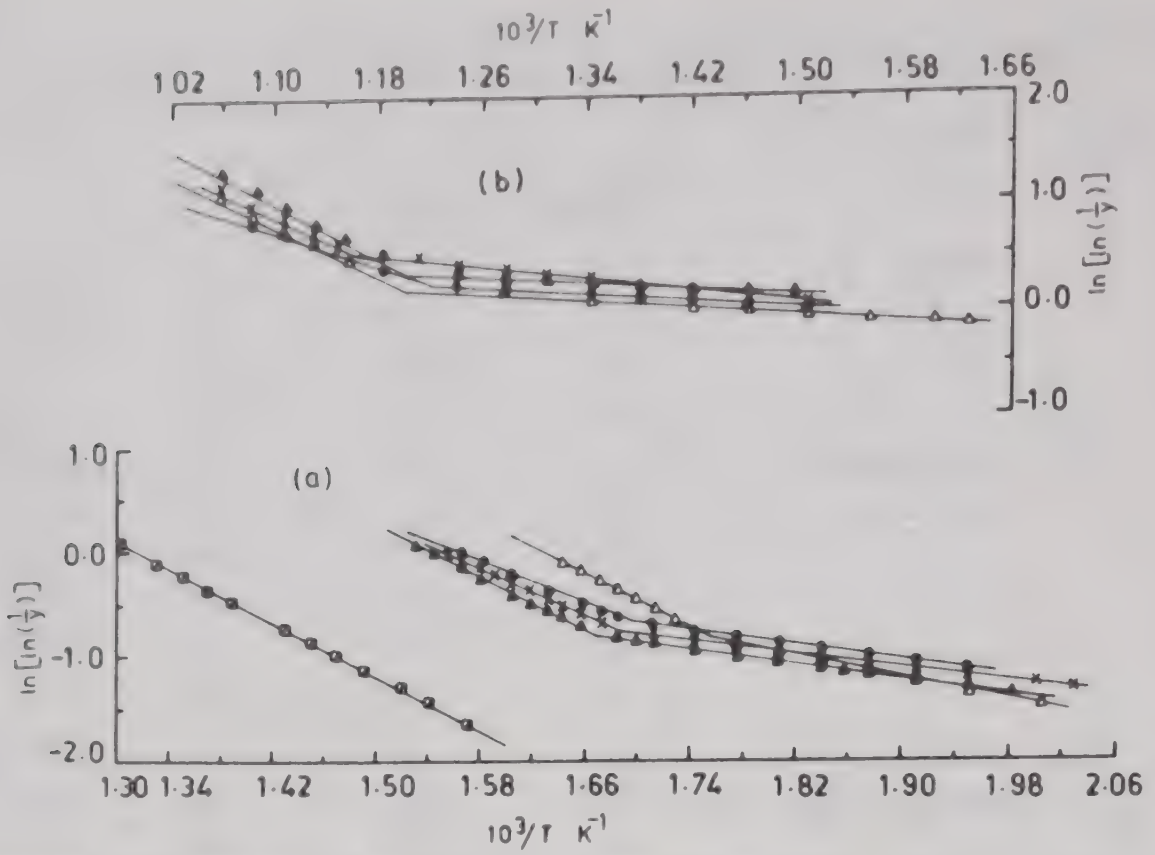

Fig. 3—Plots of ln [ln(1/y)] versus $10^3/T$ using Broido eq. for cellulose [▨], cellulose phenylphosphinite [●], cellulose *p*-methylphosphinite [△], cellulose *p*-chlorophenylphosphinite [▲] and cellulose *p*-bromophenylphosphinite [×] for first stage (a) and second stage (b) of thermal degradation in dynamic air

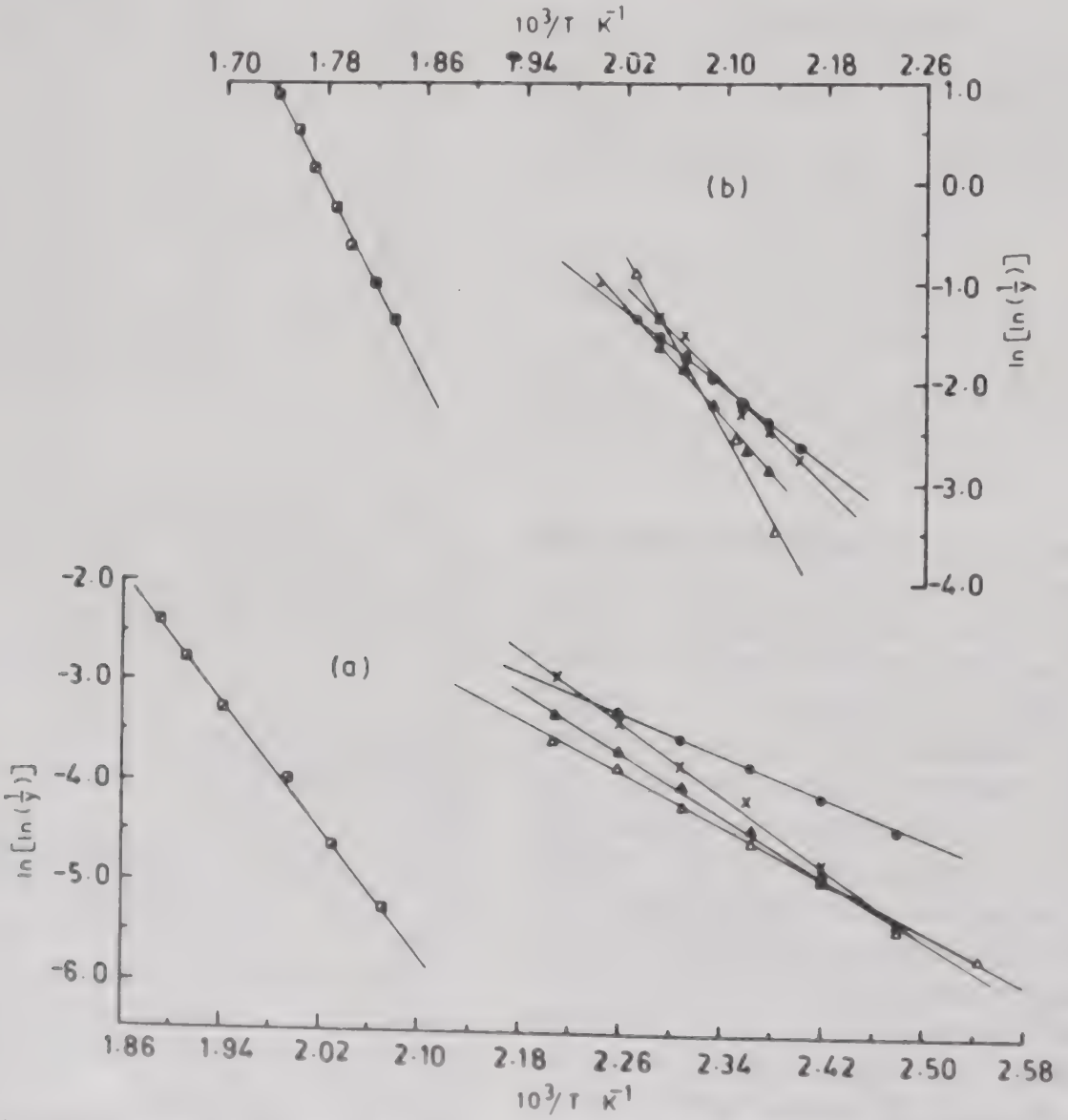

Fig. 4—Plots of ln [ln (1/y)] versus $10^3/T$ using Broido eq. for cellulose [▨], cellulose phenylphosphinite [●], cellulose *p*-methylphosphinite [△], cellulose *p*-chlorophenylphosphinite [▲] and cellulose *p*-bromophenylphosphinite [×] for third stage (a) and fourth stage (b) of thermal degradation in dynamic air

Table 3—Activation energies and frequency factors for all stages of thermal degradation of cellulose and cellulose arylphosphinite samples in dynamic air

Sample No.	Compound	Stage	Weight loss (%)	DTG Maxima (°C)	Temperature range (°C)	E_a (kJ mol^{-1})	Z (s^{-1})
(i)	Cellulose	1st	5.4	80	190-275	132.00	9.00×10^{9}
		2nd	57.6	300	275-340	187.00	2.52×10^{15}
		3rd	26.3		340-600	57.20	15.70
(ii)	Cellulose phenyl-phosphinite	1st	4.9	80	110-190	43.24	20.10
		2nd	14.6	200	190-230	83.95	3.27×10^{5}
		3rd	9.2		230-320	14.73	9.11×10^{-3}
			13.6	350	320-370	43.36	7.86
		4th	8.2		370-540	7.84	1.07×10^{-3}
			17.1		540-700	32.45	0.11
(iii)	Cellulose *p*-methyl-phenylphosphinite	1st	2.2	90	110-190	54.61	315.26
		2nd	12.5	180	190-220	137.14	1.12×10^{12}
		3rd	11.6		220-290	20.95	0.06
			19.4	320	290-340	50.49	53.84
		4th	11.3		340-540	7.48	1.44×10^{-3}
			21.3		540-700	41.37	0.53
(iv)	Cellulose *p*-chloro-phenylphosphinite	1st	3.8	95	110-190	61.82	4.51×10^{3}
		2nd	14.2	205	190-230	112.46	1.93×10^{9}
		3rd	12.5		230-325	14.78	9.69×10^{-3}
			25.0	365	325-390	50.67	29.39
		4th	6.8		390-530	7.10	9.05×10^{-4}
			19.8		530-700	46.10	1.46
(v)	Cellulose *p*-bromo-phenylphosphinite	1st	4.1	90	110-185	66.52	1.63×10^{4}
		2nd	14.4	200	185-220	106.00	5.99×10^{8}
		3rd	9.5		220-310	12.17	3.85×10^{-3}
			24.4	355	310-390	45.66	11.51
		4th	8.6		390-535	9.09	1.66×10^{-3}
			17.4		535-700	37.90	0.39

where, y is the fraction of number of initial molecules not yet decomposed, β is the heating rate and T_m is the temperature at maximum reaction rate. Using Broido equation, plots of ln(ln(1/y)) versus 1/T for various stages of thermal degradation of samples (i-v) were plotted and are shown in Figs 3 and 4. The activation energies and frequency factors (Table 3) have been calculated from slopes and intercepts, respectively, of these plots. Thermodynamic parameters such as ΔS^*, ΔH^* and ΔG^* were calculated using transition state theory[5] and are given in Table 4.

First stage of thermal degradation

This stage corresponds to the endotherms in DTA curves. In all samples (i-v) a weight loss below 100°C, due to the sorbed moisture, also indicated by DTG peaks below 100°C, was neglected. For cellulose, 5.4% weight loss occurs in the temperature range 190-275°C with the activation energy 132 kJ mol^{-1} due to dehydration process. For samples (ii-v), 2-5% weight losses occur in temperature range 110-190°C with the activation energies in the range 43-67 kJ mol^{-1} which are attributed to the acid catalyzed dehydration, deposphorylation and dehydrohalogenation. The temperature range 110-190°C for this stage of samples (ii-v) is much lower than that of cellulose, indicating that the primary degradation reactions in each of the samples (ii-v) start occurring at much lower temperature than that of cellulose.

Second stage of thermal degradation

In cellulose, 57.6% weight loss occurs in the

Table 4—Entropies, enthalpies and free energies of activation for second stage of thermal degradation of cellulose and cellulose arylphosphinite samples in dynamic air

Sample No.	Compound	T_m (K)	ΔS^* (JK^{-1} mol^{-1})	ΔH^* (kJ mol^{-1})	ΔG^* (kJ mol^{-1})	Char yield at 923 K (%)
(i)	Cellulose	578	36.11	182.19	161.31	3.5
(ii)	Cellulose phenyl-phosphinite	483	−160.95	69.93	147.66	32.4
(iii)	Cellulose *p*-methyl-phenylphosphinite	478	−26.47	133.16	145.81	24.5
(iv)	Cellulose *p*-chloro-phenylphosphinite	483	−79.47	108.44	146.16	18.0
(v)	Cellulose *p*-bromo-phenylphosphinite	473	−89.02	102.08	144.16	21.2

temperature range 275-340°C (DTG peak at 300°C) with the activation energy 187 kJ mol^{-1}. For samples (ii-v), 12-15% weight losses occur in the temperature range 185-230°C with activation energies in the range 83-138 kJ mol^{-1}. This stage is assigned to the decomposition process leading to the generation and oxidation of volatile flammable products and corresponds to the first exotherms in DTA curves. The decomposition temperatures of cellulose arylphosphinite samples (ii-v) are found to be lower than that of cellulose. From the data, it is evident that there is no significant difference of the effect of Cl and Br on the decomposition temperature of the samples.

Third stage of thermal degradation

In cellulose, 26.3% weight loss occurs in the temperature range 340-600°C with activation energy 57.20 kJ mol^{-1} due to oxidation of volatile compounds and charred residue. This corresponds to the last exotherm (365°C) in DTA curve of cellulose. For cellulose arylphosphinite samples (ii-v) gradual weight losses in the range 9-13% in the temperature range 220-325°C with activation energies in the range 12-21 kJ mol^{-1}. Further, in the temperature range 290-390°C rapid weight losses occur to the extent of 13-25% with activation energies in the range 43-51 kJ mol^{-1}. This is due to gradual followed by rapid oxidation of volatile products. Rapid weight losses in samples (ii-v) are also substantiated by DTG peaks at 350, 320, 365 and 355°C, respectively. This stage corresponds to the second exotherm in the respective DTA curve of samples (ii-v). The high temperature exotherm also supports the rapid oxidation of volatile products.

Fourth stage of thermal degradation

For cellulose arylphosphinite samples (ii-v), a gradual followed by rapid weight losses to the extent 6-12% (17-20%, rapid weight loss) in the temperature range 340-540°C (530-700°C) with activation energies in the range 7-10 kJ mol^{-1} (32-47 kJ mol^{-1}) occur due to the oxidation and cross-linking of charred residue.

Char yields

Char yields (in weight %) for cellulose and cellulose arylphosphinite samples (ii-v) were calculated from the respective TG curves at 923 K and are listed in Table 4. Char yields of cellulose arylphosphinites are found to be 32.4, 24.5, 18.0 and 21.2%, respectively, which are much higher than that of cellulose (3.5%). A large amount of char is formed at the expense of combustible volatile products of thermal degradation, thus suppressing the combustion. From the above-mentioned results, we conclude that cellulose arylphosphinite samples are good flame retardants.

The values of ΔS^*, ΔH^*, and ΔG^* were calculated at their respective T_m's (temperature where rate of weight loss is maximum) for the decomposition stage (second stage) of cellulose and cellulose arylphosphinites and are given in Table 4. The data shows variations in the values of ΔS^* (-26 to -161 JK^{-1} mol^{-1}), but this variation is compensated by change in ΔH^* values, leading to the almost constant value of ΔG^* (144-148 kJK^{-1} mol^{-1}). This indicates that the basic step involved in the decomposition stage of thermal degradation of all samples (ii-v) is the same.

IR and EPR studies of chars

IR spectra of chars of cellulose phenylphosphinite obtained at different temperatures were recorded. In the IR spectrum of char (prepared at 200°C) of cellulose phenylphosphinite, a band at 2340 (P−H str.) disappears and bands at 1440,

1140, 750, 720 (P−C str.), 1220 (P=O str.), 1160 (C−O−C str.), 1070, 750 (P−O−C str.), 830 (P−O str.) and 700 cm^{-1} (C−Cl str.) nearly disappear and new absorption bands at 1700 (C=O str.) and 1630 cm^{-1} (C=C) appear which indicate that decomposition takes place at this temperature. At 250°C, each characteristic band of cellulose disappears and bands at 2350 (P−H str.), 1440, 760, 720 (P−C str.), 1200 (P=O str.), 1140 (P−C and C−O str.) and 1000 cm^{-1} (P−O−P str.) appear which may be explained due to the formation of dimer of phenylphosphinic acid. Absorption band at 1630 (C=C) shifts to 1600 (C=C, conjugated) indicating that skeletal rearrangement takes place at this temperature. At higher temperature (350°C), absorption bands at 2380 (P−H str., 1700 (C=O str.), 1600 (C=C), 1200 (P=O str.), 1180 (C−O str.) and 1000 cm^{-1} (P−O−P str.) remain which indicate the formation of compounds containing C=O, C−O, C=O and P=O groups. Similar spectra were observed for other cellulose arylphosphinite samples.

EPR spectra of chars of pure cellulose and cellulose arylphosphinite samples were recorded. The values of g factors for all the samples were calculated and found to be constant (2.0086). The relative intensities of EPR spectral lines were calculated by the procedure described by Wertz and Bolton[6] and hence the relative concentration of free radicals of chars of cellulose and its derivatives (ii-v) are found in the ratio 1.0 : 1.6 : 1.1 : 1.2 : 2.3, respectively. The formation of free radicals is associated with char formation[7]. Char yields of cellulose arylphosphinite samples (ii-v) are higher than that of cellulose and also free radical generation in samples (ii-v) is greater than that of cellulose as expected. The bond energy of C−Br bond (280 ± 29 kJ mol^{-1}) is lower than the bond energy of C−Cl bond (397 ± 28 kJ mol^{-1}). Since the C−Br bond is weaker than C−Cl; the C−Br bond will break at a lower temperature than C−Cl bond. Consequently, cellulose *p*-bromophenylphosphinite (v) with weak C−Br bond will generate more free radicals[8] as compared to cellulose *p*-chlorophenylphosphinite (iv).

Mechanism of thermal degradation

In previous studies by mass and IR[9] on cellobiose ester, a model compound, evolution of large quantities of oxides of carbon was indicated which was due to extensive breakdown for pyranose ring. In view of the carboxylic acid formed during the heating of cellobiose ester in mass spectrometry, it might be assumed that this constitutes a principal pathway for the decomposition process. Since there is a β-hydrogen atom available for each acyl group, the elimination of the acid can be represented by Eq. (2).

... (2)

Based on these observations[9-11] it was assumed that during the thermal degradation for cellulose arylphosphinite, initially arylphosphinic acid is released which then alters thermal degradation in such a way that the production of volatile products is minimized. Arylphosphinic acid, on further heating can form dimer which catalyzes the dehydration reactions of cellulose effectively. It can react with cellulose moiety which then breaks down to give water, arylphosphinic acid and unsaturated cellulose analogue and char of repetition of these steps[11].

In cellulose *p*-chlorophenylphosphinite and *p*-bromophenylphosphinite with the side product (chlorodeoxycellulose), the mechanism of thermal degradation is also affected by chlorine and bromine contents. The released HCl/HBr then catalyzes a series of heterolytic reactions, including transglycosylation, dehydration, etherification and other condensation reactions which provide volatile compounds including tarry products. Finally, the homolytic cleavage of the substituents on the carbon chain of condensation products gives carbonaceous char. A similar type of mechanism has been suggested by Shafizadeh *et al.*[12].

References

1 Okon K, Sobezynski J, Sowinski J & Niewielski K, *Biul Wojskowej Akad Tech*, 13 (7/143), 109 (1964); *Chem Abstr*, 62 (1965) 4050g.
2 Kharrasova F M, Gil'm Kamai, Sultanova R B & Matveeva G I, *Zh Obshch Khim*, 37(4), (1967) 902.
3 Karrasova F M, Gil'm Kamai & Shagidullin R R, *Zh Obshch Khim*, 35(11) (1965) 1993.
4 Broido A, *J polym Sci*, Part-2, 7 (1969) 1761.
5 Laidler K J, *Chemical kinetics*, (Tata McGraw-Hill, New Delhi), (1976) 86.
6 Wertz J E & Bolton J R, *Electron spin resonance*, (McGraw-Hill, New York), (1972) 32.
7 Kaur B, Gur I S & Bhatnagar Hari L, *Fire safety J*, 14(3), (1989) 151.
8 Jain R K, Krishan Lal & Bhatnagar Hari L, *J appl polym Sci*, 33 (1987) 247.
9 Jain R K, Krishan Lal & Bhatnagar Hari L, *Cellulose Chem Technol*, 20 (1986) 169.
10 Scotney A, *Eur polym J*, 8 (1972) 163.
11 Lyons J W, *J Fire Flamm*, 1 (1970) 302.
12 Shafizadeh F, Lai Y Z & McIntyre C R, *J appl polym Sci*, 22 (1978) 1183.

Indian Journal of Chemistry
Vol. 31A, November 1992, pp. 824-831

Medium effects on the electron-transfer processes: Reduction of aquapentaamminecobalt(III) by hexacyanoferrate(II) in ethyleneglycol-water, ethylene carbonate-water and urea-water media

Anadi C Dash*, Neelamadhab Dash & Jyotsnamayee Pradhan
Department of Chemistry, Utkal University, Bhubaneswar 751 004

Received 3 January 1992; revised and accepted 15 May 1992

The outer-sphere electron transfer between $Co(NH_3)_5OH_2^{3+}$ and $Fe(CN)_6^{4-}$ which proceeds via precursor ion-pair formation has been investigated in ethylene glycol-water (0-47.6 wt% of EG), ethylene carbonate-water (0-40 wt% of EC) at 20-35°C and in urea-water (0-19.4 wt% of U) at 25°C ($I = 0.50$ mol dm^{-3} $NaNO_3$). The electron transfer rate constant for the ion pair (k, s^{-1}) follows the order $H_2O \sim U\text{-}H_2O < EG\text{-}H_2O \ll EC\text{-}H_2O$. The specific solvent effect on the rate constant for EG-H_2O and EC-H_2O media can be accounted for in the frame work of the Marcus theory by considering the ion solvent dipole interaction in the solvent cospheres of the precursor and the successor ionpairs. Both $\Delta H^{\neq}$ and $\Delta S^{\neq}$ decrease linearly with increase in mole fraction of EC(X_{EC}) while for the EG-H_2O media a broad maximum is discernible in the plot of $\Delta H^{\neq}$ (or $\Delta S^{\neq}$) versus X_{EG} indicating thereby that the solvent structural effects might mediate the activation process.

Our general interest in the mechanistic investigations of inorganic substitution reactions in mixed solvents[1] prompted us to extend studies to redox reactions with a view to examine the effects of solvents variations on such reactions which have been only sparingly investigated[2-6]. It has been suggested that the electronic tails from reacting molecules protruding into the polar medium are strongly affected by the medium[4]. This has a significant role to play on solvent dynamics associated with electron transfer processes. Extensive theoretical treatments[7-9] have quantified the solvent reorganisation contributions towards the energetics of the electron-transfer processes. However, solvent variations may affect the kinetics and energetics of the electron transfer processes, particularly in mixed solvent media, in a complex manner as the physico chemical properties of the mixed solvent media are often quite different from those of the pure solvents or of their ideal mixtures[10-12]. This aspect has been partly addressed by Eldik *et al.*[13] in a recent study of the viscosity dependence of the redox reaction between $(NH_3)_5CoOH_2^{3+}$ and $Fe(CN)_6^{4-}$ in glycerol-water medium which is believed to follow outer sphere mechanism involving the electron transfer within the precursor ion-pair, $[(NH_3)_5CoOH_2^{3+}, Fe(CN)_6^{4-}]$.

We have chosen the $(NH_3)_5CoOH_2^{3+}$-$Fe(CN)_6^{4-}$ redox reaction as its mechanism is well understood[13-15] and report in this work a detailed study of the kinetics and energetics of the reaction in aquo-organic solvent systems using ethyleneglycol (EG), ethylene carbonate (EC), and urea (U) as the cosolvents. The presence of cosolvents, EC[16] and U[17] in water increases the bulk dielectric constant of the medium relative to water while the dielectric constants of EG-H_2O media[18] are lower than that of water. The structuredness of the water-cosolvent system will depend upon the water-cosolvent-solute interactions. All the three cosolvents can also interact with the ionpair, $[(NH_3)_5CoOH_2^{3+}, Fe(CN)_6^{4-}]$, modifying its solvation cosphere. Hence this work extends opportunity to examine the effects of structural perturbations in the bulk solvent and the solvent cospheres of the reactant species on the unimolecular outersphere electron transfer (OSET) process.

Materials and Methods

The complex $[Co(NH_3)_5OH_2](ClO_4)_3$ was prepared as described in literature[19] and its purity checked by analysis of cobalt and UV-visible spectral data which were in agreement with the theoretical values and those reported in literatur,e respectively. The extra pure quality $K_4[Fe(CN)_6].3H_2O$ was recrystallised from water, dessicated over fused calcium chloride, and dried at 110°C in an air oven to convert it to anhydrous form[20]. All other chemicals and solvents were of

analytical reagent grade. Doubly distilled water, the second distillation being made from alkaline $KMnO_4$ in a glass distillation still, was used. Ethylene glycol (AR) was dried over molecular sieve (4Å) and distilled before use. Density measurements were made using specific gravity bottle of 25 cm^3 capacity. The ionic strength of the reaction mixture was adjusted to 0.5 mol dm^{-3} using $NaNO_3$. The redox reaction was followed via formation of $Fe(CN)_6^{3-}$; Na_2H_2EDTA (EDTA = ethylenediaminetetraacetate) was used to prevent formation of $Co_3[Fe(CN)_6]_2$ and dilute acetate buffer was used to limit the drift in *p*H during the reaction resulting from the release of NH_3. These experimental details were similar to those adopted by Eldik *et al.*[13] Further the solutions of $Fe(CN)_6^{4-}$ were prepared every time by adding weighed amount of $K_4[Fe(CN)_6]$ to the reaction medium just before taking the kinetic run to avoid its reaction with oxygen which was considerably slow (reaction time > 40 min)[21].

Instrumentation and measurements

UV-visible absorption spectra were recorded using a JASCO recording spectrophotometer model 7800. An Elico (India) digital *p*H-meter LI120 with combination glass-Ag/AgCl/NaCl (2 mol dm^{-3}) electrode was used for *p*H measurements. The kinetic measurements were made with a fully automated HI-TECH (U.K.) stopped flow spectrophotometer model SF51. The reservoir syringes and the flow module were thermostated by circulating water from a thermostat (C85D) through a cooler (FC 200) supplied by HITECH. The concentration of the aquo complex was 5×10^{-4} or 2.5×10^{-4} mol dm^{-3} and that of $[Fe(CN)_6^{4-}]_T$ varied from 3.0×10^{-3} to 25.0×10^{-3} mol dm^{-3}. The concentrations of $[EDTA]_T$ and $[CH_3COOH]_T=[CH_3COONa]_T$ were maintained at 1.0×10^{-3} and 2.5×10^{-3} mol dm^{-3} respectively. The increase in absorbance of the reaction mixture with time, due to the formation of $Fe(CN)_6^{3-}$, was monitored at 420 nm ($\varepsilon^{420}_{Fe(CN)_6^{3-}}=1023$ dm^3 mol^{-1} cm^{-1})[21] and the pseudo-first order rate constants were calculated by a nonlinear least squares program using an on line Apple II GS P.C.; the relevant computer programme was available to us as ADS_2 soft ware from M/s Hi-Tech Scientific Ltd (U.K.). Each value of k_{obs} reported is the mean from seven to ten replicate runs and its error quoted is the standard deviation. Representative rate data for EC-H_2O system are collected in Table 1.

Viscosity measurements were made at 25°, 30° and 35°C with an Ostwald viscometer; conductivity water was used as the reference medium for calibration. Ionic strength of the mixed solvent media (including 0% of cosolvent) was adjusted to 0.5 mol dm^{-3} with sodium nitrate. The values of η(cp) were calculated using those for conductivity water as reference[22].

Results and Discussion

The outer-sphere electron transfer reaction between $Co(NH_3)_5OH_2^{3+}$ and $Fe(CN)_6^{4-}$ is delineated in Eq. (1) for which the observed pseudo-first order rate constant is given by Eq. (2).

$$Co(NH_3)_5OH_2^{3+} + Fe(CN)_6^{4-} \overset{K}{\rightleftharpoons} [Co(NH_3)_5OH_2, Fe(CN)_6]^- \xrightarrow{k} 5NH_3 + Co^{2+} + H_2O + Fe(CN)_6^{3-} \quad ..(1)$$

$$k_{obs} = kK[Fe(CN)_6^{4-}]/(1+K[Fe(CN)_6^{4-}]) \quad ..(2)$$

The k_{obs} versus $[Fe(CN)_6^{4-}]$ plots for all solvent systems at all temperatures were nonlinear consistent with Eq. (2) (refs 13-15). Values of the rate constant (k) and the equilibrium constant (K) for the precursor ion-pair calculated from the intercepts and gradients of the plots of k_{obs}^{-1} versus $[Fe(CN)_6^{4-}]_T^{-1}$ using the weighted least squares procedure[23] are collected in Table 2. Values of k for the fully aqueous medium agree with the same reported by Eldik *et al.*[13] The values of the ion-pair equilibrium constant reported by them are, however, higher than those reported by us (see footnote a of Table 2) which may be due to different ionic medium used. The medium effect on the equilibrium constant is rather small as compared to the same on the rate constant k. However, large errors associated with the values of K and its small variation with changing nonaqueous solvent component of the mixed solvent media do not warrant further interpretation of the mdium effect on the ion pairing process.

The rate data (k, s^{-1}) (see Table 2) depict substantial medium effect on the OSET reaction, the effect being strongly dependent on the nature of the cosolvent. Variation of the rate constant with molefraction of the cosolvent is linear. The rate constant increases in the order urea < ethyleneglycol < ethylene carbonate for a given value of X_{org} (see Fig. 1). The solvent acceleration reported by Eldik *et al.*[13] for glycerol-water media is smaller than for ethyleneglycol media.

The viscosity dependence of the rate constant, k, at all temperatures is essentially linear. Typical plots of k versus η at 25° are presented in Fig. 2. However, a linear least squares analysis

Table 1—Representative rate data for electron transfer reaction between $(NH_3)_5CoOH_2^{3+}$ and $Fe(CN)_6^{4-}$ in ethylene carbonate-water media[a]

20.0 ± 0.1°C		25.0 ± 0.1°C		30.0 ± 0.1°C		35.0 ± 0.1°C	
10^3 C[b] (mol dm^{-3})	10^2 k_{obs} (s^{-1})	10^3 C[b] (mol dm^{-3})	10^2 k_{obs} (s^{-1})	10^3 C[b] (mol dm^{-3})	10^2 k_{obs} (s^{-1})	10^3 C[b] (mol dm^{-3})	10^2 k_{obs} (s^{-1})
			9.1 wt % EC (X_{EC} = 0.020)				
3.57	3.16 ± 0.06	2.89	6.65 ± 0.02	3.71	13.7 ± 0.1	3.62	27.1 ± 0.8
5.36	4.36 ± 0.09	4.77	9.35 ± 0.20	5.66	19.8 ± 0.5	5.62	39.2 ± 1.4
7.69	5.60 ± 0.08	6.98	11.5 ± 0.3	7.71	24.7 ± 0.7	7.77	50.8 ± 0.8
12.6	7.09 ± 0.12	11.2	15.4 ± 0.2	12.6	29.9 ± 0.3	12.6	66.5 ± 1.7
14.1	7.44 ± 0.16	13.2	16.6 ± 0.3	—	—	—	—
18.1	7.83 ± 0.17	16.1	17.5 ± 0.3	17.8	33.9 ± 0.8	17.7	71.6 ± 1.7
20.2	8.15 ± 0.21	18.3	18.4 ± 0.3	20.3	35.5 ± 0.9	20.4	70.3 ± 2.1
25.1	8.42 ± 0.11	22.9	19.6 ± 0.2	25.6	37.0 ± 0.9	25.6	81.2 ± 2.3
			16.7 wt % EC (X_{EC} = 0.0393)				
3.62	5.38 ± 0.16	3.02	10.8 ± 0.3	3.55	22.0 ± 0.4	3.61	45.9 ± 1.1
6.13	7.09 ± 0.21	4.47	14.8 ± 0.2	5.34	31.0 ± 0.3	5.41	62.3 ± 0.4
7.72	9.94 ± 0.21	6.38	18.0 ± 0.3	7.69	40.4 ± 0.9	7.69	79.9 ± 1.0
12.7	11.3 ± 0.2	10.2	23.0 ± 0.6	12.4	47.1 ± 1.0	12.4	103 ± 1
14.3	12.0 ± 0.2	12.6	25.5 ± 0.2	14.9	52.6 ± 1.4	14.9	110 ± 3
18.0	12.8 ± 0.2	14.8	26.5 ± 0.3	18.0	54.9 ± 1.0	17.9	113 ± 3
20.3	13.3 ± 0.3	16.8	27.6 ± 0.5	20.3	54.5 ± 1.9	20.2	117 ± 2
25.2	13.5 ± 0.3	21.1	29.8 ± 0.5	25.5	58.6 ± 1.7	25.4	123 ± 4
			28.6 wt % EC (X_{EC} = 0.0757)				
3.49	11.7 ± 0.1	—	—	3.29	49.7 ± 0.9	3.55	99.4 ± 1.8
5.16	18.0 ± 0.2	5.29	29.8 ± 0.5	5.65	73.5 ± 1.2	5.63	146 ± 4
7.50	20.8 ± 0.3	7.86	37.3 ± 0.8	7.56	83.7 ± 1.5	7.46	168 ± 2
12.4	23.7 ± 0.3	12.1	45.8 ± 0.9	12.7	96.3 ± 1.3	12.7	191 ± 5
14.6	25.0 ± 0.5	14.9	51.4 ± 0.9	14.2	99.2 ± 1.4	14.7	197 ± 5
17.7	25.9 ± 0.2	17.6	54.1 ± 0.9	17.8	103 ± 2	17.6	202 ± 4
20.2	27.1 ± 0.5	20.5	55.3 ± 0.7	20.1	105 ± 3	20.2	208 ± 5
25.1	27.7 ± 0.5	25.4	58.9 ± 1.0	25.3	110 ± 3	25.3	224 ± 3
			40.6 wt % EC (X_{EC} = 0.1226)				
3.35	22.8 ± 0.6	3.29	33.7 ± 0.5	3.66	96.7 ± 4.2	3.66	186 ± 4
5.98	32.5 ± 0.4	5.25	47.9 ± 0.8	5.99	131 ± 2	5.95	258 ± 3
7.70	34.5 ± 0.3	7.60	57.6 ± 1.4	7.36	140 ± 3	7.41	279 ± 3
12.7	32.7 ± 0.6	12.2	68.9 ± 1.4	12.6	135 ± 2	12.6	266 ± 4
15.6	37.0 ± 1.0	14.7	73.9 ± 1.0	15.6	152 ± 5	15.0	282 ± 11
17.6	38.7 ± 0.5	17.5	79.9 ± 1.5	17.6	156 ± 1	17.7	304 ± 8
21.2	40.0 ± 0.9	20.3	81.2 ± 1.3	20.0	159 ± 2	20.1	306 ± 5
24.8	42.6 ± 0.9	25.3	83.7 ± 1.5	24.8	175 ± 5	24.9	331 ± 6

(a) I = 0.50 mol dm^{-3} ($NaNO_3$); $[Co(NH_3)_5OH_2^{3+}]_T$ = (2-5) × 10^{-4}, $[EDTA]_T$ = 1 × 10^{-3}, $[CH_3CO_2H] = [CH_3CO_2Na]$ = 2.5 × 10^{-3} mol dm^{-3}, pH = 4.6 ± 0.1

(b) $C = [Fe(CN)_6^{4-}]_T$.

Table 2—Values of k and K as a function of solvent composition at various temperatures and the activation parameters for the OSET reaction[a]

Wt % of organic cosolvent	X_{org}	Temp. °C (±0.1°C)	$10^2 k$, (s^{-1})	K, ($dm^3\ mol^{-1}$)	$\Delta H^{\neq}$ ($kJ\ mol^{-1}$)	$\Delta S^{\neq}$ ($JK^{-1}\ mol^{-1}$)
0		20.0	6.20 ± 0.23	109 ± 4	120 ± 7	+ 144 ± 23
		25.0	11.9 ± 0.6	131 ± 10		
		30.0	33.4 ± 0.8	78.3 ± 2.1		
		35.0	67.8 ± 0.3	92.5 ± 5.7		
			U-H_2O			
9.1	0.029	25.0	12.2 ± 0.2	98.8 ± 1.6		
19.4	0.067		11.7 ± 0.4	83.2 ± 4.6		
			EG-H_2O			
10.0	0.031	20.0	7.87 ± 0.23	97.8 ± 5.3	112 ± 7	+ 119 ± 24
		25.0	19.4 ± 0.5	117 ± 5		
		30.0	36.7 ± 1.6	95.9 ± 4.9		
		35.0	79.3 ± 5.9	95.1 ± 8.1		
19.9	0.067	20.0	9.89 ± 0.17	137 ± 2	119 ± 3	+ 143 ± 10
		25.0	23.5 ± 0.4	130 ± 4		
		30.0	48.6 ± 0.4	106 ± 12		
		35.0	108 ± 6	96.6 ± 7.2		
30.0	0.110	20.0	10.2 ± 0.2	208 ± 9	124 ± 8	+ 159 ± 29
		25.0	30.5 ± 2.0	142 ± 9		
		30.0	60.9 ± 2.7	107 ± 7		
		35.0	117 ± 6	146 ± 12		
39.9	0.161	20.0	14.9 ± 0.4	259 ± 22	109 ± 9	+ 112 ± 31
		25.0	36.9 ± 0.4	199 ± 6		
		30.0	70.5 ± 2.2	184 ± 13		
		35.0	140 ± 7	210 ± 22		
47.9	0.210	20.0	21.2 ± 0.6	224 ± 19	105 ± 5	+ 100 ± 15
		25.0	48.3 ± 1.0	199 ± 8		
		30.0	85.2 ± 2.5	273 ± 28		
		35.0	192 ± 5	189 ± 11		
			EC-H_2O			
9.1	0.020	20.0	11.8 ± 0.5	110 ± 7	113 ± 4	+ 126 ± 13
		25.0	27.7 ± 0.5	108 ± 3		
		30.0	58.5 ± 2.6	83.2 ± 3.6		
		35.0	116 ± 10	98.3 ± 8.6		
16.7	0.039	20.0	17.4 ± 0.7	143 ± 15	109 ± 6	+ 113 ± 21
		25.0	41.9 ± 0.8	120 ± 4		
		30.0	81.7 ± 0.6	112 ± 11		
		35.0	191 ± 8	90.6 ± 5.1		
28.6	0.076	20.0	36.3 ± 2.5	150 ± 10	94 ± 3	+ 67 ± 10
		25.0	80.0 ± 1.5	113 ± 2		
		30.0	136 ± 4	190 ± 6		
		35.0	275 ± 15	188 ± 10		

(contd)

Table 2—Values of k and K as a function of solvent composition at various temperatures and the activation parameters for the OSET reaction[a]—*Contd*

Wt % of organic cosolvent	X_{org}	Temp. °C (±0.1°C)	$10^2 k$ (s^{-1})	K ($dm^3 mol^{-1}$)	$\Delta H^{\neq}$ (kJ mol^{-1})	$\Delta S^{\neq}$ (JK $^{-1}$ mol^{-1})
40.6	0.123	20.0	48.8 ± 4.7	239 ± 23	85 ± 8	+39 ± 27
		25.0	110 ± 2	140 ± 5		
		30.0	180 ± 5	382 ± 11		
		35.0	362 ± 18	40. ± 21		

[a] $10^2 k$, s^{-1} (K, $dm^3 mol^{-1}$) = 12.7 ± 1.0 (213 ± 13) at 25°C,
I = 1.0 mol dm^{-3} ($NaClO_4$), $\Delta H^{\neq}$ = 102 ± 5 kJ mol^{-1},
$\Delta S^{\neq}$ = 79 ± 15 JK^{-1} mol^{-1} Eldik *et al.*[13] reported for aqueous medium.

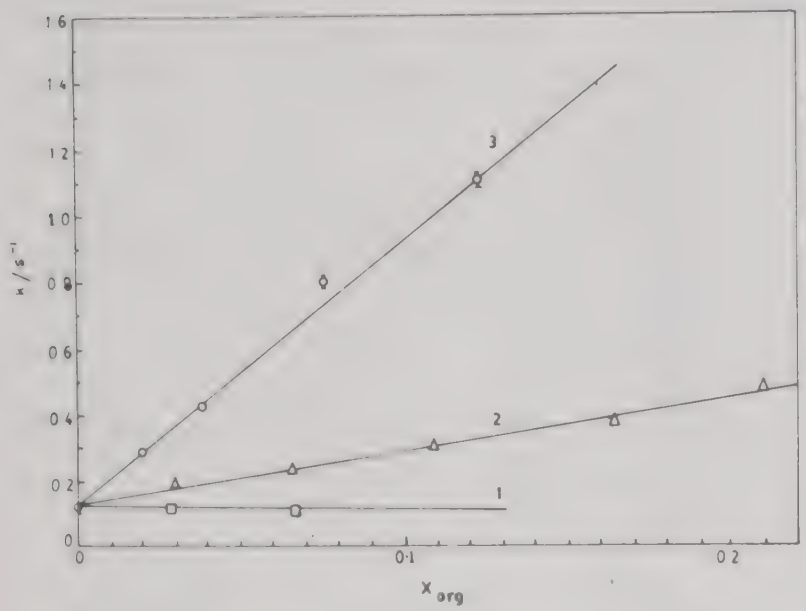

Fig. 1—Variation of the rate constant (k, s^{-1}) with mole fraction (X_{org}) of cosolvent at 25°C (1) U-water, (2) EG-water, (3) EC-water

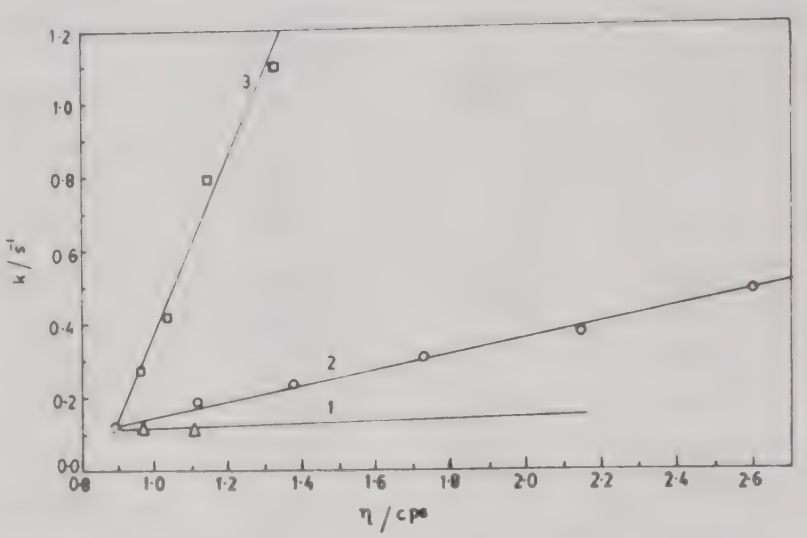

Fig. 2—Variation of the rate constant (k, s^{-1}) with viscosity (η, cps) of the medium at 25°C. (1) U-water, (2) EG-water, (3) EC-water

($k = 1 + b\eta$) indicates that the values of the zero viscosity limit rate constant (a) at all temperatures (20-35°C) are negative or zero for EC-water and EG-water media respectively in contrast with the observations of Eldik *et al.*[13] reported for glycerol-water media. For U-water, k is virtually independent of η. It is further worth noting that k increases 9 fold at 25°C for EC-water when η increases only marginally i.e. from 0.9 to 1.2 cps. Under similar conditions, the increase in k is less than 2 fold for EG-water and 1.5 fold for glycerol-water media[13] respectively. Hence specific solvent effect on the electron transfer processes is evident. Recently Abbott and Rusling[24] dealt with the solvent effects on electron transfer kinetics. A multiparameter linear free energy correlation between the rate constants and solvent acidity, basicity and polarizability for pure solvent media based on Taft[25-27] model was found to be satisfactory. Lack of relevant solvatochromic parameter (π^*), acidity and basicity data for the mixed solvent media used in this work precludes attempting such a correlation.

The outer sphere electron transfer reaction within the preassembled ion-pair may be treated as an intramolecular process for which Marcus theory[8,28] predicts the free energy correlation as given in Eq. (3)

$$\Delta G^{\neq} = \lambda/4 + \Delta G^{0/2} + \Delta G^{0^2}/4\lambda \quad \ldots (3)$$

where λ is reorganisational energy parameter, $\Delta G^{\neq}$ is the free energy of activation of the ion pair for the OSET process and ΔG^0 is the free energy change associated with the conversion of the precursor ionpair $(IP)_1$ to its successor $(IP)_2$ (see Eq. 4). The dissociation of the latter (i.e. $(IP)_2$) to the final products is considered to be a fast process.

$$(NH_3)_5CoOH_2^{2+}, Fe(CN)_6^{4-} \overset{\Delta G^0}{\rightleftharpoons} (IP)_1 \rightarrow (NH_3)_5CoOH_2^{2+}, Fe(CN)_6^{3-} \quad \ldots (4)$$
$$(IP)_2$$

The electron transfer process within the ionpair may be split into three parts such as (i) a partial reorientation of the solvent molecules in the cosphere of the precursor ion-pair (IP_1) to form the transition state, (ii) a fast electron transfer step, and (iii) another reorientation of the solvent molecules to form the solvated successor ionpair (IP_2). The specific interaction, between the solvent molecules and the ionpairs (IP_1, IP_2) will be important in the first and the third steps while for the fast electron transfer step the electronic polarizability of the solvent molecules solvating the transition state will be one important parameter owing to the Frank Condon restrictions[24]. Thus the solvent dependence of $\Delta G^{\neq}$ may be attributed to the variation of ΔG^0 and the solvent components of λ ($\lambda_{overall} = \lambda_{internal} + \lambda_{solvent}$) with solvent composition. It may be further noted that the dielectric constant of the media used in this study vary only marginally {D_s = 78-82 (EC-water)[16], 78-88 (U-water)[17] and 78-66 (EG-water)[18]}, and the overall charges of the precursor and the successor ionpairs are also the same. Hence the Born contribution to $\lambda_{solvent}$ and ΔG^0 based on DCM theory[8,24] may be taken to be virtually constant for different media used. Assuming that $\lambda_{solvent}$ and the ion-dipole interaction[29] component of ΔG^0 vary linearly with the mean polarizability (α_s) and mean dipole moment (μ_s) of the solvent molecules in the cosphere of the transition state and the precursor/successor ionpairs and combining the limiting form[30] of Eq. (3) with the transition state equation, $k = x(k_B T/h)\, e^{-\Delta G^{\neq}/RT}$ (x, the electronic transmission coefficient is ~ 1)[13] the solvent dependence of k can be given by Eq. (5):

$$\ln k_s = \ln k_w + (A\Delta\mu + B\Delta\alpha) X_{org} \quad \ldots (5)$$

where k_s, k_w denote rate constant in mixed solvent and in water respectively, $\Delta\alpha = \alpha_{org} - \alpha_w$ and $\Delta\mu = \mu_{org} - \mu_w$, A and B are constants. Equation (5) further assumes that $\alpha_s = X_w\alpha_w + X_{org}\alpha_{org}$ and $\mu_B = X_w\mu_w + X_{org}\mu_{org}$ and the solvent compositions in the cospheres of the transition state, and the ionpairs are the same as that of the bulk phase. The least squares plots of ln k_s versus $\Delta\mu X_{org}$ ($\Delta\mu$ = 3.036 D and 0.446 D for EC-H_2O and EG-H_2O respectively) at 20-35°C are linear (see Fig. 3, corr. coeff = 0.92-0.94) despite the fact that $\Delta\alpha$ (10^{-30} m^3) for EC-H_2O (=5.2) and EG-H_2O (=4.3) are comparable[31]. Hence the rate dependence on solvent composition for EC-water and EG-watermedia is rationalised in terms of ion-dipole model of solvation (i.e. $B\Delta\alpha \ll A\Delta\mu$). However, it is important

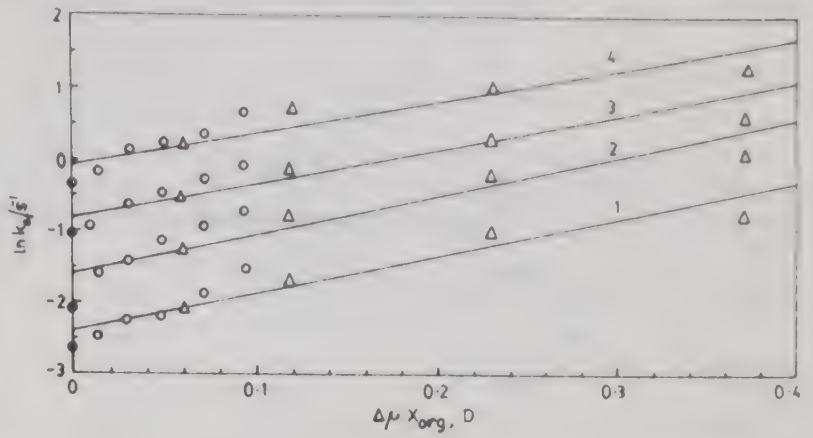

Fig. 3—ln k_s (s^{-1}) versus $\Delta\mu$ X_{org}, D plots (see Eq. 5) at 20° (1), 25° (2), 30° (3) and 35°C (4); ⊙-EG-water, △-EC-water

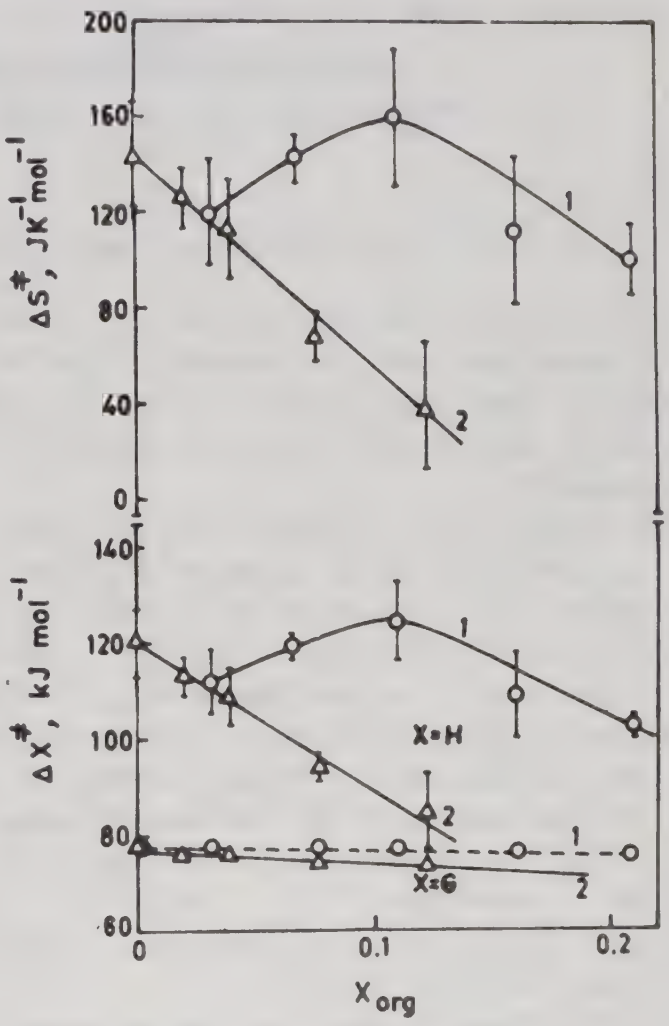

Fig. 4—Variation of $\Delta X^{\neq}$ (*H*, *G*) kJ mol^{-1} and $\Delta S^{\neq}$, JK^{-1} mol^{-1} with molefraction (X_{org}) of the cosolvents ⊙-EG-water, △-EC-water

to note that ion-dipole interactions for the ionpairs (IP_1 and IP_2), the potential hydrogen bond donor and acceptor species, will be mediated by the H-bonding effects in the solvent systems used. The urea-water system stands out as an exception to this interpretation as there was virtually no rate mediating effect of urea despite the fact that its dipole moment (μ_u = 4.56D) is comparable to that of ethylene carbonate. It is known that the ability of urea to stabilise large Ph_4As^+ is insignificant compared to alcohols[32]. In the present case for the ionpair, {$(NH_3)_5CoOH_2^{3+}$, $Fe(CN)_6^{4-}$} carrying net charge of −1 presumably the same situation

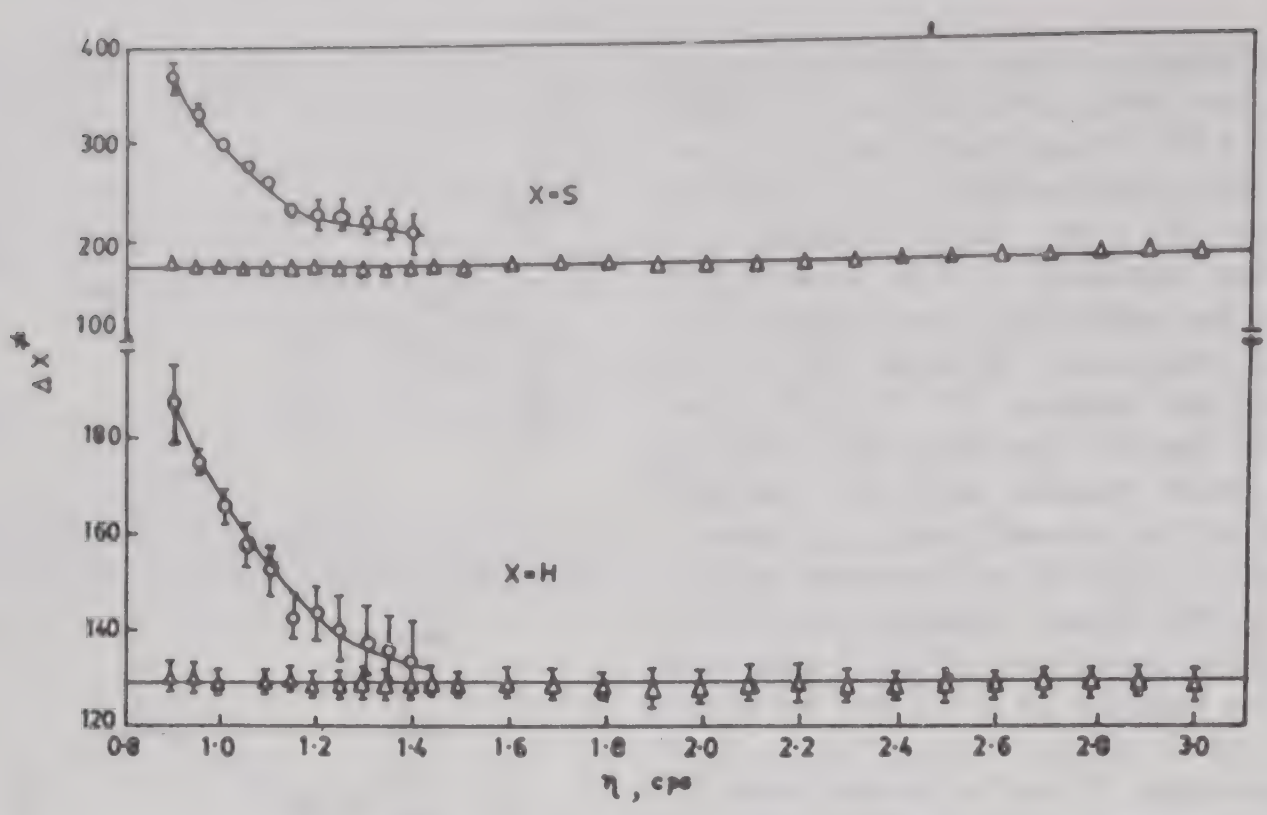

Fig. 5—Viscosity dependence of $\Delta H^{\neq}$ (kJ mol^{-1}) and $\Delta S^{\neq}$ (JK^{-1} mol) ⊙-EC-water, △-EG-water

prevails. It can be said that the effects of solvation of the initial state and the transition state of the ionpairs by molecules of urea are virtually compensated by the solvent structural effects due to this cosolvent.

The values of the activation enthalpy and entropy reported by us for aqueous medium compare with those reported by Sasaki *et al.*[15] ($\Delta H^{\neq} = 115$ kJ mol^{-1}, $\Delta S^{\neq} = 122$ JK^{-1} mol^{-1} at $I = 0.1$ mol dm^{-3}) but are marginally at variance with those reported by Eldik *et al.*[13] (see footnote of Table 2). The electron transfer within the ionpair is associated with the substantial values of $\Delta S^{\neq}$ which compares with the difference of the aqueous entropies of $Fe(CN)_6^{3-}$ and $Fe(CN)_6^{4-}$ $\{\bar{S}^0_{aq}[Fe(CN)_6^{3-}] - \bar{S}^0_{aq}[Fe(CN)_6^{4-}} = 153$ JK^{-1} mol^{-1} at 25°C$\}$ (ref. 33).

It is important to note that the activation enthalpy ($\Delta H^{\neq}$) linearly decreases with solvent composition for EC-H_2O media from 120 ± 7 to 84 ± 8 kJ mol^{-1} in the range of $X_{EC} = 0$-0.123, while for EG-H_2O media a broad maximum is displayed around $X_{EG} = 0.11$ (see Fig. 4). Similar behaviour is exhibited in $\Delta S^{\neq}$ versus composition plots. In contrast with this $\Delta G^{\neq}$ shows only small dependence on X_{org} indicating thereby that the effects of solvent on $\Delta H^{\neq}$ and $\Delta S^{\neq}$ are mutually compensatory and the solvent compositions hardly affect the activation free energy.

The activation parameters ($\Delta H^{\neq}$, $\Delta S^{\neq}$) were also calculated at different values of viscosities of the mixed solvent media by the same procedure as adopted by Eldik *et al.*[13] Strikingly a completely different trend in the variation of $\Delta H^{\neq}$ or $\Delta S^{\neq}$ with η emerged (see Fig. 5). Noteworthy is the fact that while both $\Delta H^{\neq}$ and $\Delta S^{\neq}$ were virtually independent of η in the range 0.9-3.0 cps for EG-water media these parameters decreased non-linearly with increasing η in a much smaller range ($0.9 \leq \eta$, cps ≤ 1.4) for EC-water media. This behaviour is in contrast with the observed increasing trend of $\Delta H^{\neq}$ and $\Delta S^{\neq}$ with increasing viscosity for glycerol-water media[34]. The effects of solvents on the activation parameters are mutually compensatory as $\Delta H^{\neq}$ versus $\Delta S^{\neq}$ plot is linear accomodating all data points for EG-H_2O and EC-H_2O media.

Acknowledgement

We are thankful to the Department of Science and Technology, Government of India, for generous funding to procure the HI-TECH SF 51 stopped flow spectrophotometer with accessories. N D and J P are thankful to the CSIR, New Delhi, and UGC, New Delhi for senior research fellowships.

References

1 Dash A C & Pradhan J, *J chem Soc Faraday Trans*, 1, 85 (1989) 2797; Dash A C & Dash N, *Int J chem Kinet*, 21 (1989) 101; Dash A C & Pradhan J, *Indian J Chem*, 29A (1990) 379.
2 Prow W F, Garmostani S K & Farina R D, *Inorg Chem*, 20 (1981) 1297.
3 Kajer A M & Ulstrup J, *Inorg Chem*, 18 (1979) 3624.
4 Kajer A M & Ulstrup J, *Inorg Chem*, 25 (1986) 644.
5 Lewis N A & Ray A M, *Inorg Chem*, 23 (1984) 3698.
6 Van Eldik R, *Inorg Chem*, 21 (1982) 2501.

7 Marcus R A, Zwolinski B J & Eyring H, *J phys Chem*, 58 (1954) 432.

8 Marcus R A, *J chem Phys*, 56 (1956) 863; Marcus R A, *Ann Rev Phys Chem*, 15 (1967) 155; Taube H, *Advan inorg Chem Radiochem*, 1 (1959) 1.

9 Marcus R A, *J phys Chem*, 90 (1986) 3466.

10 Marcus Y, *Ion solvation* (John Wiley, New York) (1985).

11 Blandamer M J, *Adv phys Org Chem*, 14 (1977) 247.

12 Blandamer M J & Burgess J, *J chem Soc Rev*, 4 (1975) 55.

13 Krack I & Van Eldik R, *Inorg Chem*, 28 (1989) 851.

14 Gaswick D & Haim A, *J Am chem Soc*, 93 (1971) 7347.

15 Saski Y, Endo K, Nagasawa A & Saito K, *Inorg Chem*, 25 (1986) 4845.

16 D'Aprano A, *Gazz Chim Ital*, 104 (1974) 91; D'Aprano A, Goffredi M & Triolo R, *Electro Chim Acta*, 21 (1976) 139.

17 Wyman J, *J Am chem Soc*, 55 (1933) 4116.

18 Akerlof G, *J chem Soc*, 54 (1932) 4125.

19 Splinter R S, Harris S J & Tobis R S, *Inorg Chem*, 7 (1968) 898.

20 Vogel A I, *A text book of quantitative inorganic analysis*, (ELBS and Longmans Green, London) (1962) pp 320.

21 Al Shatti N, Lappin A G & Sykes A G, *Inorg Chem*, 20 (1981) 1466.

22 *Hand book of chemistry and physics*, (CRC Press, Boca Raton, Florida) (1980) F-51.

23 The weight of k_{obs}^{-1} was taken to be $[\sigma(k_{obs})/k_{obs}^2]^{-2}$.

24 Abbot A P & Rusling J F, *J phys Chem*, 94 (1990) 8910.

25 Taft R W, Abboud J L M, Kamlet M J & Abraham M H, *J sol Chem*, 14 (1985) 153.

26 Kamlet M J, Abboud J L M, Abraham M H & Taft R W, *J org Chem*, 48 (1983) 2877.

27 Kamlet M J, Abboud J L M & Taft R W, *J Am chem Soc*, 99 (1977) 8325.

28 Earley J E, in *Progress in inorganic chemistry* (Wiley Interscience, New York) (1970) vol 13, p 253.

29 Bockris J O'M & Reddy A K N, *Modern electrochemistry* (Plenum, New York) (1977) vol 1, Chapt 2.

30 Equation (3) is linearized to the form $\Delta G^{\neq} = \lambda/4 + \Delta G^0/2$ assuming $4\lambda \gg (\Delta G^0)^2$.

31 Reference (10), pp 139, 140.

32 Das K & Kundu K K, *J sol Chem*, 8 (1979) 189.

33 Reference (10), pp 109.

34 $\Delta H^{\neq}$, kJ mol^{-1} ($\Delta S^{\neq}$, JK^{-1} mol^{-1}) = 95 ± 2 (55 ± 6), 104 ± 1 (88 ± 4) and 116 ± 4 (130 ± 12) at $\eta = 0$, 1 and 3 cps respectively[13].

Indian Journal of Chemistry
Vol. 31A, November 1992, pp. 832-837

Kinetics and mechanism of acid and base hydrolysis of *cis*-(bioxalato)(imidazole)bis(ethylenediamine)cobalt (III) ion: A study of the role of the coordinated imidazole and its anion

Anadi C Dash*, Rabindra K Nanda & Achyuta N Acharya
Department of Chemistry, Utkal University, Bhubaneswar 751 004

Received 31 January 1992; revised and accepted 11 May 1992

The aquation and base hydrolysis of *cis*-$[(en)_2(imH)CoC_2O_4H]^{2+}$ (imH = imidazole) have been investigated in 1.0 mol dm^{-3} (ClO_4^-), ionic strength. The aquation of the complex at $[H^+] = 0.50$-1.0 mol dm^{-3} (60°C) proceeds via spontaneous and H^+ catalysed paths, $k_{obs} = k_{H_2O} + K_H[H^+]$, with $k_{H_2O} = (1.2 \pm 0.2) \times 10^{-6} s^{-1}$ and $k_H = (3.2 \pm 0.4) 10^{-6}$ $dm^3 mol^{-1} s^{-1}$. In the range $[OH^-]_T = 0.010$-1.0 mol dm^{-3} and 15-35°C, the complex exists in doubly deprotonated form, *cis*-$[(en)_2Co(im)C_2O_4]$ and the pseudo-first order rate constant fits the relationship, $k_{obs} = k_0 + k_1[OH^-] + k_2[OH^-]^2$. The rate constants ($k_0$, k_1, and k_2) and the associated activation parameters ($\Delta H^{\neq}$ and $\Delta S^{\neq}$) are reported. Comparison of k_0 and k_{H_2O} shows that imidazolate anion (im^-) has stronger σ-bonded labilisation of Co − O bond relative to imidazole. Base hydrolysis in 50% D_2O medium results in rate acceleration relative to aqueous medium, and $k_{obs} = k_1[OH^-]_T$ is obeyed at $[OH^-]_T = 0.050$-0.70 mol dm^{-3} (30°C).

The aquation and base hydrolysis of carboxylato amine cobalt (III) complexes have been extensively investigated in our laboratories and elsewhere[1,2]. One of the salient features of such studies is the duality of mechanism i.e. Co − O and C − O bond breaking. The Co − O bond breaking mechanism is most common for carboxylato amine cobalt (III) complexes. However, the acyl clevage (C − O bond breaking) mechanism has been shown to occur in the acid and base hydrolysis of oxalato-, trifluoroacetato- and trichloroacetato-pentaamminecobalt (III) complexes[3,4]. In these cases the Co(III)-bound carboxylate function is believed to be activated by the strongly electron-withdrawing substituents making the acyl carbon susceptible to nucleophilic attack by OH^- and by H_2O under further activating influence of H^+ in the proton catalysed path of hydrolysis. Interestingly the base hydrolysis of these complexes at high $[OH^-]$ conforms to two path ways, one first order in $[OH^-]$ i.e. the conventional SN_1CB path, and the other second order in $[OH^-]$ involving C − O bond breaking as depicted in Scheme 1.

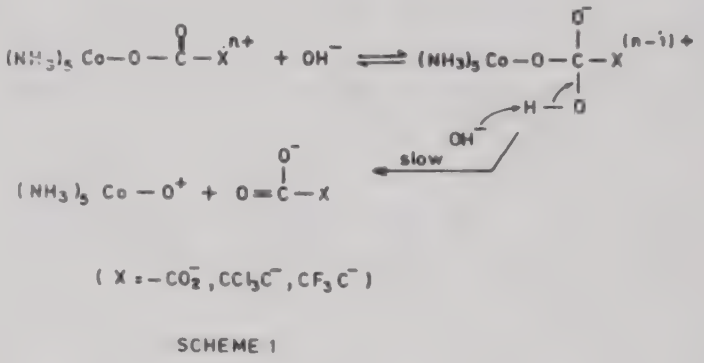

SCHEME 1

In this paper we report the kinetics of acid and base catalysed hydrolysis of *cis*-(bioxalato)(imidazole)bis(ethylenediamine)cobalt (III), a complex not reported earlier in the literature. The overall charge of this substrate can be varied from +2 to 0 due to the deprotonation of the free end of the half bonded oxalate and N − H deprotonation of the coordinated imidazole. Based on the enthalpies of formation of imidazolate/imidazole (im^-/imH) complexes of $(CN)_5Fe^{2-}$ (ref. 5), ferrimyoglobin$^+$ (ref. 6) and cobalamin$^+$ (ref. 7), it has been suggested that imidazolate is a better σ-donor than imidazole. This has greatly aroused interest in the study of the chemical labilities of the metal ion centres coordinated to the imidazolate ligand as imidazole is a ubiquitous ligand in the biological domain. As a sequel to our studies we examine here the specific effect of the coordinated imidazole or its imido base on the rate and mechanism of replacement of oxalate from the cobalt (III) centre.

Materials and Methods

cis-(Hoxalato)(imidazole)bis(ethenediamine)cobalt (III) perchlorate was prepared staring from the *cis*-(chloro)(imidazole)bis(ethylenediamine)cobalt (III) perchlorate[8]. The chloro complex was heated at 60.0°C with moist Ag_2O·AgCl and excess Ag_2O

were filtered off. The solution was treated with excess of oxalic acid (10%), *p*H adjusted to 4 and concentrated to a small bulk. The red coloured crystals appeared on cooling in an ice bath which were filtered out. The complex, dissolved in minimum volume of warm water (60°C), was reprecipitated on adding 70% $HClO_4$ and cooling the content in an ice bath. It was collected on a glass filter, washed successively with absolute alcohol and diethyl ether and stored over fused calcium chloride, {Found: Co, 11.1; $C_2O_4^{2-}$, 16.8; C, 19.9; H, 4.20; N, 14.6%. Calculated for $[Co(en)_2(imH)CoC_2O_4H](ClO_4)_2 \cdot H_2O$: Co, 11.0; $C_2O_4^{2-}$, 16.6; C, 20.2; H, 3.9; N, 15.7%. λ_{max}, nm (ε_{max}, $dm^3mol^{-1}cm^{-1}$); 490 (100); 350 sh (133) in 0.1 mol dm^{-3} $HClO_4$}.

The IR spectrum of $[(en)_2(imH)CoC_2O_4H)(ClO_4)_2 \cdot H_2O$ in KBr phase shows absorption bands at 1765, 1660, 1595 and 1390 cm^{-1}. The bands at 1765 and 1660 cm^{-1} may be ascribed to the free carboxyl group and the carboxylate group bound to cobalt (III) respectively[9,10].

The NMR spectrum of the complex in D_2O (TMS external reference) displayed peaks at δ (ppm) −7.30, −7.60 and −8.20 integrating to 1:1:1 indicating the presence of the coordinated imidazole[11]. A doublet at δ (ppm) −2.73 and −2.83 integrating totally for $8 \cdot CH_2$ protons of the two ethylenediamine ligands is clearly indicative of the *cis* configuration of the complex[11,12]. Analar grade chemicals were used. Solutions were prepared in freshly prepared doubly distilled water. Dowex 50W-X8 resin (20-50 mesh) (H^+-form) was used for ion exchange experiments. D_2O (purity >99.4%) was received from BARC, Trombay, India.

A JASCO 7800 recording spectrophotometer was used for UV-visible spectral measurements. The C, H, N analysis, NMR and IR measurements were made at CDRI (Lucknow) India.

Kinetics

The rates of acid and base hydrolysis of the complex were followed by conventional titrimetric procedure involving titrations of the liberated oxalate at a given time by standard $KMnO_4$ ($N/50$) after removing the unreacted cobalt (III) complex and its cobalt (III) product by Dowex 50W-X8 cation exchange resin in acid form, as described earlier[13]. The pseudo-first order rate constants were calculated from the $\log(V_\infty - V_t)$ versus time plots where V_t and V_∞ stand for the permanganate titre values at time t and for the complete reaction respectively. The rate constants (k_{obs}) reported (see Table 1) are average of duplicate runs. The rates of base hydrolysis in (50% D_2O) medium (30.0°C) and in aqueous medium (30°C, 35°C) were also studied spectrophotometrically in the thermostated cell compartment of the JASCO 7800 spectrophotometer. The reaction was monitored at 310 nm at which the oxalato cobalt (III) complex was the predominant absorbing species. The decrease in absorbance with time due to the decay of the complex was followed. The pseudo-first order rate constants were calculated from the linear plots of $\log(D_t - D_\infty)$ versus t(s) where, D_t and D_∞ denote the absorbance of the reaction mixture at time t and for completion of the reaction respectively.

Results and Discussion

Dissociation constants of *cis*-$[(en)_2(imH)CoC_2O_4H]^{2+}$

Figure 1 depicts the *p*H sensitivity of the absorbance of the complex. This is due to the deprotonation of the free caboxyl group and the coordinated imidazole (Eqs 1 and 2). The absorbance data of the complex (see Fig. 1) at 290 nm in varying $[HClO_4]_T$ and at 330 nm in the *p*H range 9.93-11.64 were used to calculate respectively the dissociation constant of the free carboxyl group and the N−H group of imidazole bound to cobalt (III) by the pyridine N− as reported earlier[13]. We obtained $pK_1 = 2.28 \pm 0.15$ and $pK_2 = 10.4 \pm 0.1$ (at 28°C and $I = 1.0$ mol dm^{-3}) which compare satisfactorily with the values of the dissociation constants of the half bonded bioxalate group in $N_5CoC_2O_4H^{2+}$ [$N_5 = 5NH_3$, (ref. 13) $(en)_2(NH_3)$ (ref. 9), α-(trien)(NH_3) (ref. 14)] and that of coordinated imidazole in *cis*-$[Co(en)_2(imH)X]^{2+}$ ($X = Cl^-$, NH_3^-, NCS^-, $C_6H_4(O)(OH)CO_2^-$[11,12(b),15], ferrimyoglobin (imH)(ref. 6), cobalamin $(imH)^+$ (ref. 7) and $(NH_3)_5Co(imH)^{3+}$ (ref. 16) when the overall charges of the substrates and the effect of the ionic strength on the dissociation constant are taken into account. It is evident here that coordination enhanced the pK_{NH} of imidazole by a factor of ~ 3.8 units ($pK_{NH} = 14.44$ at 25°C, $I = 1.0$ mol dm^{-3} for free imidazole in aqueous medium)[6].

$$cis\text{-}[Co(en)_2(imH)C_2O_4H]^{2+} \overset{K_1}{\rightleftharpoons} cis\text{-}[Co(en)_2(imH)C_2O_4]^{+} + H^{+} \quad \ldots (1)$$

$$cis\text{-}[Co(en)_2(imH)C_2O_4]^{+} \overset{K_2}{\rightleftharpoons} cis\text{-}[Co(en)_2(im)C_2O_4] + H^{+} \quad \ldots (2)$$

Acid hydrolysis

The rate of acid hydrolysis of *cis*- $[(en)_2(imH)CoC_2O_4H]^{2+}$ is extremely slow at room tempera-

Table 1—Rate data for base hydrolysis of *cis*-$[(en)_2(imH)CoC_2O_4H]^{2+}$, $[complex]_T = 1.9 \times 10^{-3}$ mol dm^{-3}, $I = 1.0$ mol dm^{-3}

$[OH]_T$/mol dm^{-3}	$10^5 k_{obs}$ (s^{-1})							
	15.0 ± 0.1°C		25.0 ± 0.1°C		30.0 ± 0.1°C		35.0 ± 0.1°C	
	k_{obs}	k_{calc}	k_{obs}	k_{calc}	k_{obs}	k_{calc}	k_{obs}	k_{calc}
0.010	—	—	1.29 ± 0.06	1.28	1.9 ± 0.10	1.94	3.20 ± 0.22	3.13
0.025	1.05 ± 0.04	1.07	1.85 ± 0.08	1.89	4.0 ± 0.4	3.8	7.15 ± 0.32	7.36
0.050	1.36 ± 0.06	1.32	2.96 ± 0.21	2.95	7.10 ± 0.6	6.9	15.5 ± 1.0	14.6
0.10	1.87 ± 0.1	1.86	5.3 ± 0.2	5.3	14.3 ± 0.9	14.0	30.5 ± 1.2	29.8
0.20	3.22 ± 0.21	3.11	11.8 ± 1.0	10.6	29.8 ± 1.0	30.1	61.2 ± 2.3	63.4
0.30	4.63 ± 0.31	4.5	16.2 ± 1.3	16.7	48.3 ± 2.0	49.2	100 ± 4.8	101
0.40	6.2 ± 0.4	6.25	22.9 ± 1.1	22.7	69.8 ± 5.0	71.1	145 ± 4[b]	143
0.50	7.8 ± 0.2	8.0	31.0 ± 1.9	31.5	95.3 ± 3.2	96.0	192 ± 6[b]	189
0.60	10.0 ± 0.3	9.9	40.1 ± 0.5	40.3	122 ± 5[b]	124	242 ± 8[b]	240
0.70	11.9 ± 1.0	12.1	49.3 ± 2.3	50.0	158 ± 8[b]	156	292 ± 10[b]	293
0.80	14.6 ± 1.2	14.5	62.3 ± 2:3	60.4	192 ± 8[b]	188	354 ± 12[b]	353
0.90	18.3 ± 1.2	17.1	73.1 ± 4.0	71.8	223 ± 10[b]	224	412 ± 15[b]	416
1.0	20.1 ± 0.8	19.8	—	—	—	—	—	—
$10^5 k_0$ (s^{-1})	0.86 ± 0.03		1.04 ± 0.05		1.22 ± 0.06		1.49 ± 0.13	
$10^5 k_1$ (dm^{3}mol^{-3}s^{-1})	9.6 ± 0.5		40.0 ± 1.6		119 ± 3		275 ± 6	
$10^5 k_2$ (dm^{6}mol^{-2}s^{-1})	9.5 ± 0.9		43.5 ± 3.0		145 ± 5		209 ± 10	

(a) error quoted for k_{obs} is average deviation of the mean from duplicate runs, values of k_{obs} at $[OH^-]_T \leq 0.025$ mol dm^{-3} are observed upto 20 – 40% of the reactions.

(b) rate constants quoted were measured spectrophotometrically.

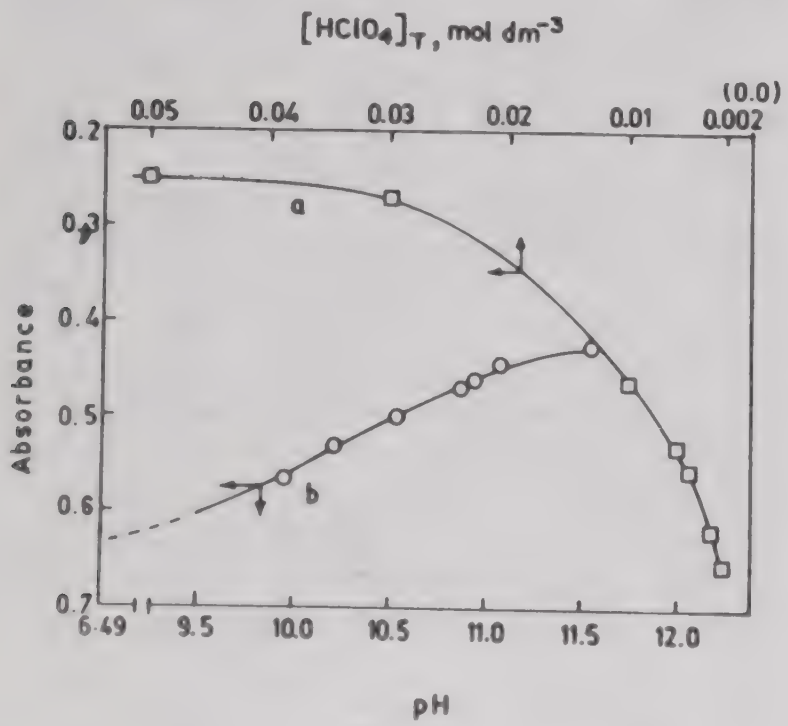

Fig. 1—Plot of absorbance of *cis*-$[Co(en)_2(imH)C_2O_4]^{2+}$ as a function of *p*H

(a) $[HClO_4]_T = 0.002$-0.05 mol dm^{-3}, $[complex]_T = 2.90 \times 10^{-4}$ mol dm^{-3}, and λ, nm = 290 nm

(b) *p*H = 9.93-11.64 (*n*-propyl amine buffer), $[complex]_T = 9.0 \times 10^{-4}$ mol dm^{-3}; λ, nm = 330 nm, Cell path = 10 mm, temp = 28°C and $I = 1.0$ mol dm^{-3}

ture even at high acidity. The pseudo-first order rate constants (k_{obs}) measured at 60°C and $[H^+]_T = 0.5$-1.0 mol dm^{-3} ($I = 1.0$ mol dm^{-3}) vary linearly with $[H^+]$ (Fig. 2) and fit Eq. (3)

$$k_{obs} = k_{H_2O} + k_H[H^+] \quad \ldots (3)$$

which is consistent with the operation of the spontaneous and H^+ catalysed aquation of the bioxalate complex [see Eqs (4) and (5)].

$$(en)_2(imH)CoC_2O_4H^{2+} + H_2O \xrightarrow{k_{H_2O}} (en)_2(imH)CoOH_2^{3+} + HC_2O_4^- \quad \ldots (4)$$

$$(en)_2(imH)CoC_2O_4H^{2+} + H^+ + H_2O \xrightarrow{k_H} (en)_2(imH)CoOH_2^{3+} + H_2C_2O_4 \quad \ldots (5)$$

values of $k_{H_2O} = (1.2 \pm 0.2) \times 10^{-6}$ s^{-1} and $k_H = (3.2 \pm 0.4) \times 10^{-6}$ dm^{3}mol^{-1}s^{-1} may be compared with the analogous data for *cis*-$[(en)_2Co(NH_3)C_2O_4H]^{2+}$ ($k_{H_2O} = (4.9 \pm 0.2)10^{-6}$ s^{-1}, $k_H = (8.0 \pm 0.4) \times 10^{-6}$ dm^{3}mol^{-1}s^{-1} at 60°C, $I = 1.0$ mol dm^{-3})[9]. It is evident that relative to NH_3, imidazole slows down the aquation of the bioxalato complex in the spontaneous and the acid catalysed paths by factors of 4 and 2.5 respectively under

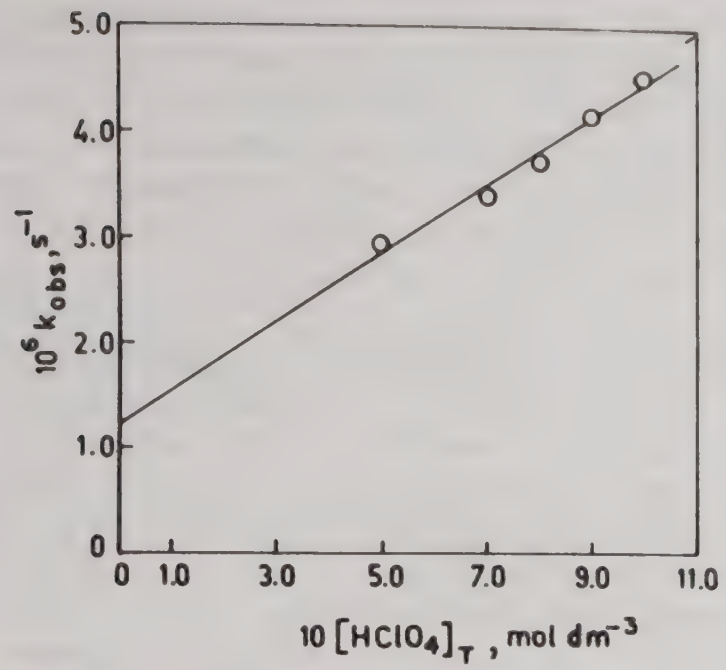

Fig. 2—Plot of k_{obs} (s^{-1}) versus $[H^+]_T$ (mol dm^{-3}) at 60°C, $I = 1.0$ mol dm^{-3}, $[complex]_T = 1.9 \times 10^{-3}$ mol dm^{-3}

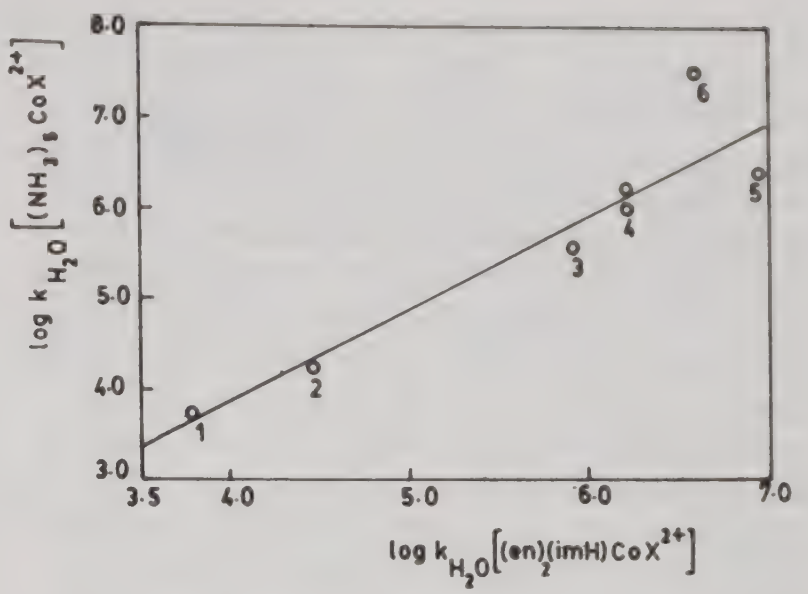

Fig. 3—Plot of log $k_{H_2O}\{(NH_3)_5CoX^{2+}\}$ versus log k_{H_2O} $\{(en)_2(imH)CoX^{2+}\}$ at 60°C; (1)—Br^-, (2)—Cl^-, (3)—$C_2O_4H^-$, (4)—$HSal^-$, (5)—N_3^- and (6)—NCS^-

comparable conditions. It is very unlikely that the mechanism of substitution at the cobalt (III) centre involved in the spontaneous and acid catalysed aquation paths will be altered on replacing NH_3 by imidazole. The plot of log $k_{H_2O}[(NH_3)_5CoX^{2+}]$ versus log k_{H_2O}[*cis*-$(en)_2Co(imH)X^{2+}$] at 60°C using the available rate data[8,11,15,17] (after extrapolation/intrapolation) (see Fig. 3) is linear with slope = 1.03 ± 0.2 (corr. coeff = 0.93). Such a linear free energy correlation with unit slope conforms to the Langford's dissociative interchange mode of aquation of the substrates, *cis*-$[Co(en)_2(imH)X]^{2+}$, in the spontaneous aquation path as it is valid for the acidopentaamminecobalt (III), $(NH_3)_5CoX^{2+}$, species[18,19].

Base hydrolysis

The base hydrolysis of the title complex was studied at $[OH^-]_T = 0.010$-1.0 mol dm^{-3} and 15-35°C ($I = 1.0$ mol dm^{-3}). Rate data are collected in Table 1. Under this condition the complex will exist in the doubly deprotonated form, *cis*-$[(en)_2(im)CoC_2O_4]$ with net charge zero. k_{obs} versus $[OH^-]_T$ plots extrapolated to finite intercept at $[OH^-]_T = 0$ and increased nonlinearly with increase in $[OH^-]_T$. The rate data were fitted to Eq. (6) with $[OH^-] = [OH^-]_T - 2[complex]_T$ (corrections being made for the deprotonation of NH and CO_2H groups) and

$$k_{obs} = k_0 + k_1[OH^-] + k_2[OH^-]^2 \quad \ldots (6)$$

the values of k_0, k_1 and k_2 were calculated by a nonlinear least squares program which minimized the sum of the weighted residuals $\Sigma W(k_{calc} - k_{obs})^2$ ($W = [1/\sigma(k_{obs})^2]$). The calculated values of k_0, k_1 and k_2 reproduced the rate constants satisfactorily (see k_{calc} in Table 1).

The validity of Eq. (6) is consistent with the reaction sequence shown in Scheme 2 for which k_0 is the spontaneous aquation rate constant of the imidazolato complex, *cis*-$[Co(en)_2(im)C_2O_4]$ and k_1, k_2 denote its base hydrolysis rate constants via $[OH^-]$ and $[OH^-]^2$ dependent paths respectively. It is interesting to note that the spontaneous aquation rate constant of the imidazolato species (k_0) is weakly sensitive to temperature (see Table 1). Large negative values of $\Delta S^{\neq}$ in this path discounts the possibility of stereochemical change in this path. However, by way of comparison of the values of k_0 at 15-35°C with that of k_{H_2O} at 60°C, it turns out that imidazolate ion (im^-) has a greater σ-bonded labilising effect on the Co − O bond relative to imidazole. This is also reflected in the low value of $\Delta H^{\neq}$ for the k_0 path. The strong labilising action of imidazolate was also observed earlier in the aquation reaction of *cis*-$[(en)_2(imH)CoX]^{2+}$ ($X = Cl^-$, Br^-, N_3^-, NCS^-, $C_6H_4(OH)CO_2^-$)[8,11,15]. However, values of the rate constants and the activation parameters, $\Delta H^{\neq}$ and $\Delta S^{\neq}$, (see Table 2) for the second order base hydrolysis of *cis*-$[(en)_2(im)CoC_2O_4]$, *cis*-$[(en)_2(NH_3)CoC_2O_4]^+$, and *cis*-$[(NH_3)_5CoC_2O_4]^+$ are comparable with each other. The conventional SN_1CB mechanism involving Co − O bond breaking is believed to oper-

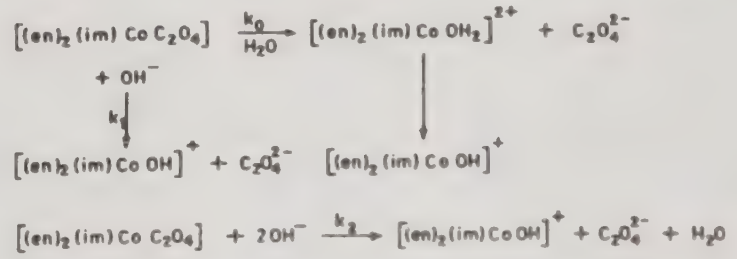

SCHEME 2

ate in the second order base hydrolysis path for $(NH_3)_5CoC_2O_4^+$ (ref. 4) and *cis*-$[(en)_2(NH_3)CoC_2O_4]^+$ (ref. 9). This leads us to believe that the second order base hydrolysis of the imidazolato complex occurring via $[OH^-]$ dependent path (k_1) involved conventional conjugate base mechanism[17]. Since the conjugate base is produced by the NH deprotonation of the coordinated ethylenediamine, a low value of k_1 for the imidazolato complex compared to the same for the corresponding NH_3 complex (Table 2) is consistent with less favourable conjugate base equilibria for the imidazolato complex, indeed a pK_{NH} perturbation effect[17,20], which offsets the expected higher reactivity of the conjugate base, *cis*-$[(en)_2(H)(im)CoC_2O_4]^-$ as compared to the same for the analogous NH_3 complex (*cis*-$[(en)_2(NH_3)CoC_2O_4]^+$) from electrostatic grounds. It is further interesting to note that the labilising action of the bound imidazolate anion (im) and the reduced charge of the complex did not prevent $[OH^-]^2$ dependent path (i.e. the third order base catalysed path) (see Scheme 1). It is worth mentioning that the imidazolato complex is more susceptible to base hydrolysis via acyl cleavage path relative to $(NH_3)_5CoC_2O_4^+$ (see Scheme 1). This indicates that the nucleophilicity of the acyl carbon of the bound carboxyl group is little reduced by the presence of the coordinated imidazole.

Further evidence in favour of the acyl cleavage mechanism stems from our observation that the base hydrolysis reaction is accelerated in 50% (D_2O+H_2O) medium. Similar observation was also made by Dash and Dash[14] in the base hydrolysis of α-*cis*-(trien)$(NH_3)CoC_2O_4^+$. It is interesting to note that k_{obs} versus $[OH^-]_T$ plot for 50% (D_2O+H_2O) medium at 30°C is linear passing virtually through origin (intercept = $(2.5\pm1.4)\times10^{-5}$) (see Fig. 4) indicating thereby that both the third order base hydrolysis path (k_2) and the spontaneous aquation path of the imidazolato complex slowed down to the extent not being observable. The second order base hydrolysis was, however, markedly accelerated in D_2O+H_2O medium ($k_1=(22.6\pm3.3)\times10^{-4}$ $dm^3mol^{-1}s^{-1}$ at 30°C, $I=1.0$ mol dm^{-3} in 50% D_2O+H_2O; $k_1(D_2O+H_2O)/k_1(H_2O)=1.88$). It is known that the aquation and base hydrolysis of the halogeno amine cobalt (III) complexes, N_5CoX^{2+} ($X=Cl^-$, Br^-), for which the rate limiting step is Co−X bond breaking are retarded by D_2O[21-24]. The observed solvent isotope effect on the k_1 path might indicate that in addition to the conventional amido conjugate base mechanism there might be acyl cleavage mechanism operative in the k_1 path in which OD^- acts as a better nucleophile than OH^- for the attack at the acyl carbon and resulting tetrahedral intermediate releases oxalate without $OH^-(OD^-)$ assistance. However, the deprotonation of the resulting tetrahedral intermediate by OD^- and OH^- either by an equilibrium step or by a concerted mechanism is considerably less favoured in D_2O+H_2O medium than in fully aqueous medium resulting in the disappearance of the k_2 path under the experimental condition.

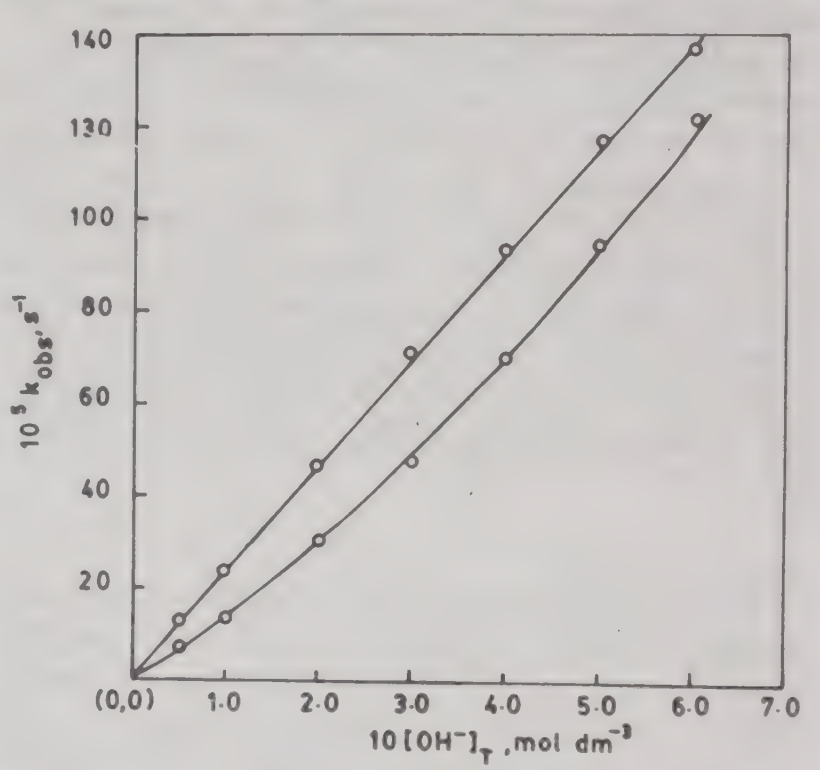

Fig. 4—Plot of k_{obs} (s^{-1}) versus $[OH^-]_T$ (mol dm^{-3}) at 30°C, $I=1.0$ mol dm^{-3}, (1) 50% (D_2O+H_2O) medium; (2) aqueous medium

Table 2—Comparative listing of the rate constants and activation parameters for the k_1 and k_2 paths for related complexes at 30.0°C, $I=1.0$ mol dm^{-3}

Complex	$10^3 k_1$ ($dm^3mol^{-1}s^{-1}$)	$\Delta H^{\neq}$ (kJ mol^{-1})	$\Delta S^{\neq}$ ($JK^{-1}mol^{-1}$)	$10^3 k_2$ ($dm^6mol^{-2}s^{-1}$)	$\Delta H^{\neq}$ (kJ mol^{-1})	$\Delta S^{\neq}$ ($JK^{-1}mol^{-1}$)	Ref
$(NH_3)_5CoC_2O_4^+$	0.62	132	99	0.11	99	10	4
cis-$[(en)_2Co(NH_3)C_2O_4]^+$	2.75	125±5	120±15	—	—	—	9
cis-$[(en)_2Co(im)C_2O_4]^a$	1.19(0.03)	126±8	116±28	1.45(0.05)	115±20	79±66	(This work]

(a) For the spontaneous aquation path (k_0), $\Delta H^{\neq}=15.2\pm2.3$ kJ mol^{-1}, $\Delta S^{\neq}=-289\pm7$ $JK^{-1}mol^{-1}$

Acknowledgement

This work was supported by a research grant from the Department of Science and Technology, Govt. of India. A N A is thankful to the DST, for a junior research fellowship.

References

1 House D A, *Cord Chem Rev*, 23 (1977) 223.
2 Pradhan G C, Nanda R K & Dash A C, *Transition met Chem*, 14 (1989) 309.
3 Andrade C, Jordan R B & Taube H, *Inorg Chem*, 9 (1970) 711.
4 Angerman S & Jordan R B, *Inorg Chem*, 6 (1967) 1376.
5 Johnson C R, Shepherd R E, Marr B, O'Donnell S & Dressick W, *J Am chem Soc*, 102 (1980) 6227.
6 George P, Hanania G I H, Irvine D H & Aber-Issu I, *J chem Soc*, (1964) 5689.
7 Hanania G I H & Irvine D H, *J chem Soc*, (1964) 5694.
8 Dash A C & Mohapatra S K, *J chem Soc (Dalton Trans)*, (1977) 246.
9 Dash A C & Nanda R K, *J inorg nucl Chem*, 36 (1974) 2071.
10 Rao C N, *Chemical application of infrared spectroscopy*, (Academic Press, New York) (1963); Nakamota K, *Infrared spectra of inorganic and coordinaton compounds* (Wiley, New York) 1963; Svatos G F, Sweeny D M, Mizushima S, Corran C & Quagliano J V, *J Am chem Soc*, 79 (1957) 3313.
11 Dash A C, Mohanty B & Mohapatra S K, *Indian J Chem*, 23A (1984) 312.
12 (a) Hay R W & Piplani D P, *J chem Soc (Dalton Trans)*, (1978) 556; (b) Hay R W, Tajik M & Norman P R, *J chem Soc (Dalton Trans)*, (1979) 636; (c) Lantzke J R & Watts D W, *Aust J Chem*, 20 (1967) 35.
13 Dash A C & Nanda R K, *Inorg Chem*, 13 (1974) 655.
14 Dash A C & Dash M S, *J inorg nucl Chem*, 43 (1981) 2873.
15 Dash A C & Mohanty B, *Transition met Chem*, 5 (1980) 183.
16 Harrowfield J mac B, Noris V & Sargeson A M, *J Am chem Soc*, 98 (1976) 7282.
17 Basolo F & Pearson R G, *Mechanism of inorganic reactions: A study of metal ion complexes in solution* (Wiley, New York) 2nd edn (1968) p 164.
18 Langford C H, *Inorg Chem*, 4 (1965) 265.
19 Haim A, *Inorg Chem*, 9 (1970) 426.
20 Dash A C, Pradhan J & Dash N, *J chem Soc (Daltaon Trans)* (1991) 1843.
21 Chan S C & Leh F, *J chem Soc (A)*, (1967) 2010.
22 Zipp S G & Madan S K, *Inorg Chem Acta*, 23A (1972) 6.
23 Dash A C & Pradhan J, *J chem Soc Faraday Trans*, 85 (1989) 2797.
24 Adamson A W & Basolo F, *Acta Chem Scand*, 9 (1955) 1261.

Indian Journal of Chemistry
Vol. 31A, November 1992, pp. 838-844

Kinetics and mechanism of oxidation of monosaccharides by sodium-N-bromobenzenesulphonamide in alkaline medium

T Asha Iyengar & D S Mahadevappa*
Department of Studies in Chemistry, University of Mysore, Manasagangothri, Mysore 570 006, India

Received 21 October 1991; revised and accepted 3 June 1992

Kinetic studies of the oxidation of D-fructose, D-glucose, D-galactose, D-mannose, D-xylose, D-ribose, D-lyxose and L-arabinose by bromamine-B (sodium-N-bromobenzene sulphonamide, BAB) have been carried out in alkaline medium at 30°. The reaction shows a zero order dependence on $[BAB]_0$ and fractional orders in $[sugar]_0$ and $[HO^-]_0$. The rates tend to level off at higher $[sugar]_0$ and $[HO^-]_0$. Variation in ionic strength of the medium, and the addition of benzene sulphonamide, Cl^- and Br^- ions do not alter the rate while lowering the dielectric constant of the medium increases the rate slightly. Solvent isotope and proton-inventory studies have been made. Enolization rate coefficients and activation parameters for the rate limiting step have been determined from Michaelis-Menten type of plots. A probable scheme for the oxidation of monosaccharides through a common intermediate, 1,2-enediol has been proposed.

Oxidation of monosaccharides by metal ions[1,2] has received some attention but information on the oxidation of aldo and ketohexoses and pentoses by halogens[3] is scanty. Agrawal and Mushran[4] oxidised several monosaccharides by chloramine-T (CAT) in alkaline medium and we have reported on the kinetics of oxidation of hexoses[5] and pentoses[6] by chloramine-B (CAB) in alkaline medium. It was therefore of interest to study the oxidation of sugars by bromamine-B (BAB) and make a preliminary comparison of the oxidative behaviour of the chlorine and bromine analogues. The present paper reports the kinetics and mechanism of oxidation of D-fructose, D-glucose, D-galactose, D-mannose, D-xylose, D-ribose, D-lyxose and L-arabinose by BAB in alkaline medium at 30°C.

Materials and Methods

Bromamine-B ($C_6H_5SO_2NBrNa$, 1.5 H_2O) was prepared by the literature method[7] and recrystallised from hot water. The available bromine was determined by iodometry (28.0%) and the compound[8] was further characterised by its IR (in KBr, on a Carl-Zeiss UR-10 IR spectrophotometer) and FT-NMR ^{13}C spectra (in D_2O on a Bruker WH 270-MHz NMR spectrometer).

Aqueous solutions of BAB were prepared, standardized by the iodometric method and preserved in amber coloured bottles to prevent its photochemical deterioration.

Pure samples of D-fructose (John Baker, USA), D-glucose (Ranbaxy, India), D-mannose (SRL, India), D-xylose and D-ribose (Loba Chemie), D-lyxose (Sigma) and L-arabinose (CRL, Bombay) and other analar grade chemicals were used. Fresh solutions of sugars were prepared using triply distilled water whenever required. A concentrated solution of $NaClO_4$ was used to maintain the ionic strength at a high constant value.

Heavy water (99.2% deuterium) was supplied by the Bhabha Atomic Research Centre, Trombay.

Kinetic measurements

The reactions were carried out in glass stoppered boiling tubes coated black on the outside to eliminate photochemical effects. The oxidant, alkali, $NaClO_4$ and H_2O (constant total volume) and sugar solution taken separately were thermostated for 30 min. at 30°. The reaction was initiated by the rapid addition of substrate solution to the mixture and its progress was monitored by iodometric determination of unconsumed BAB in aliquots of the mixture at regular intervals of time. The reaction was monitored for two half-lives. Rate constants calculated were reproducible within ± 3%.

Regression analysis of experimental data to obtain regression coefficient *r* and standard deviation *s* of the points from the regression line, was performed on an EC-72 statistical calculator.

Stoichiometry and product analysis

Reaction mixture containing sugar, NaOH and excess BAB was equilibrated for 48 hr at 30°. The excess oxidant was determined iodometrically. The stoichiometry was as shown in Eq. (1):

$$C_nH_{2n}O_n + PhSO_2NBrNa + H_2O \rightarrow C_nH_{2n}O_{n+1} + PhSO_2NH_2 + Na^+ + Br^- \quad \ldots (1)$$

Table 1—Effect of reactant concentrations on the rate of oxidation of monosaccharides at 30° $[HO^-]_0 = 2.0 \times 10^{-2}$ mol dm^{-3}, $I = 0.5$ mol dm^{-3}

10^3 [BAB]$_0$ (M)	10^2 [S]$_0$ (M)	$10^5 k_s$ (mol dm^{-3} min^{-1})							
		D-Fru	D-Glu	D-Gala	D-Man	D-Xyl	D-Rib	D-Lyx	L-Ara
0.5	1.0	17.95	4.65	3.14	2.15	5.09	3.20	—	1.54
1.0	1.0	18.85	4.60	2.96	2.19	5.48	3.42	2.10	1.60
1.5	1.0	18.46	4.62	3.13	2.19	5.25	3.00	2.23	1.50
2.0	1.0	17.84	4.71	3.15	2.20	5.25	2.98	2.16	1.55
3.0	1.0	18.65	5.02	3.13	2.15	4.99	2.72	2.20	1.48
1.5	0.5	10.90	2.86	1.83	1.47	2.86	1.74	1.22	0.86
1.5	1.5	22.64	5.68	4.42	2.63	6.67	4.29	3.15	2.12
1.5	2.0	25.26	6.77	5.32	2.88	8.24	5.53	4.00	2.85
1.5	2.5	30.50	7.64	6.09	3.28	9.33	6.36	4.75	3.47
1.5	4.0	34.80	8.95	7.00	3.68	10.92	7.53	5.48	3.72
1.5(a)	1.0	18.52	4.62	3.13	2.20	5.25	3.0	2.25	1.52
1.5(b)	1.0	18.40	4.60	3.16	2.16	5.28	3.04	2.28	1.50
1.5(c)	1.0	18.45	4.66	3.20	2.28	5.30	3.01	2.22	1.48
1.5(d)	1.0	18.50	4.70	3.13	2.26	5.30	3.03	2.26	1.52

(a) $I = 1.0$ mol dm^{-3}, (b) [BSA] $= 6.0 \times 10^{-3}$, mol dm^{-3}, (c) $[Cl^-] = 1.0 \times 10^{-2}$ mol dm^{-3}, (d) $[Br^-] = 1.0 \times 10^{-2}$ mol dm^{-3}.

Table 2—Effect of $[NaOH]_0$ on the rate of reaction at 30° $[BAB]_0 = 1.5 \times 10^{-3}$ mol dm^{-3}, $[S]_0 = 1.0 \times 10^{-2}$ mol dm^{-3}, $I = 0.5$ mol dm^{-3}

10^2 [NaOH]$_0$	$10^5 k_s$ (mol dm^{-3} min^{-1})							
	0.5	1.0	1.5	2.0	2.5	3.0	4.0	5.0
D-Fructose	4.79	9.89	14.0	18.46	21.0	22.83	24.74	25.20
D-Glucose	1.42	2.71	3.72	4.62	5.38	6.35	7.50	7.92
D-Galactose	0.71	1.67	2.53	3.13	3.89	4.62	5.12	5.46
D-Mannose	0.67	1.23	1.75	2.19	2.63	2.95	3.38	3.48
D-Xylose	1.33	2.63	4.2	5.25	6.77	7.78	8.40	8.70
D-Ribose	0.69	1.54	2.31	3.00	3.6	4.06	4.82	4.93
D-Lyxose	0.60	1.29	1.82	2.23	2.89	3.31	3.75	3.83
L-Arabinose	0.44	0.90	1.23	1.50	2.0	2.4	2.55	2.70

Here n = 6 for D-glucose, D-galactose and D-mannose and n = 5 for D-xylose, D-ribose, D-lyxose and L-arabinose.

Oxidation of D-fructose is represented by Eq. (2):

$$C_6H_{12}O_6 + 2PhSO_2NBrNa + 2H_2O \rightarrow C_5H_{10}O_6 + HCOOH + 2PhSO_2NH_2 + 2Na^+ + 2Br^- \quad \ldots (2)$$

Benzenesulphonamide (BSA), formed was extracted into ether and then detected ($R_f = 0.88$) by TLC (2:2:1 light petroleum-chloroform-1-butanol) with iodine as the detecting agent. The aldonic acids were identified by literature procedures[5,6]. Formic acid was determined by the chromotropic acid procedure, after reducing it with magnesium powder in the presence of acid.

Results

The reaction was studied at several initial [reactants]. With the [sugar] in large excess, plots of $[BAB]_0$-[BAB] versus time were linear ($r > 0.9978$, $s \leq 0.03$) passing through the origin indicating zero order dependence on $[BAB]_0$. Further, the zero order rate constants (k_s) remained constant (Table 1) confirming the fact that oxidation of sugars stops at the stages indicated by Eqs (1) and (2).

The rate increased with $[sugar]_0$ and plot of log k_s versus log $[S]_0$ was linear ($r > 0.9925$, $s \leq 0.02$) with a fractional slope, indicating fractional order in $[S]_0$.

At constant $[BAB]_0$ and $[S]_0$, the rate increased with increase in $[HO^-]$. A plot of log k_s versus log $[HO^-]$ is linear ($r > 0.9965$, $s \leq 0.03$) with a fractional slope except in the cases of galactose, xylose, and

Table 3—Kinetic and thermodynamic parameters for the oxidation of monosaccharides by BAB

Substrate	Ea (kJ mol^{-1})	$\Delta H^{\neq}$ (kJ mol^{-1})	$\Delta S^{\neq}$ (JK^{-1} mol^{-1})	$\Delta G^{\neq}$ (kJ mol^{-1})	log A
D-Fructose	95.5 (95.1)	93.0 ± 0.0 (92.5 ± 0.0)	−44.3 ± 0.4 (−4.3 ± 0.3)	106.5 ± 0.05 (93.8 ± 0.1)	10.5 (12.6)
D-Glucose	100.4 (89.2)	97.9 ± 0.0 (86.7 ± 0.2)	−39.4 ± 0.3 (−35.0 ± 0.4)	109.9 ± 0.3 (97.4 ± 0.10)	10.8 ± 0.01 (11.0 ± 0.03)
D-Galactose	93.6 (109.9)	91.1 ± 0.1 (107.3 ± 0.1)	−64.6 ± 0.3 (33.6 ± 0.8)	110.8 ± 0.4 (97.1 ± 0.3)	9.4 ± 0.01 (14.6 ± 0.02)
D-Mannose	100.5 (107.7)	97.9 ± 0.1 (105.2 ± 0.1)	−45.9 ± 0.5 (18.7 ± 0.5)	112.0 ± 0.3 (99.5 ± 0.4)	10.4 ± 0.06 (13.8 ± 0.05)
D-Xylose	98.2 (97.2)	95.7 ± 0.1 (94.7 ± 0.1)	−45.4 ± 0.0 (−4.4 ± 0.1)	109.6 ± 0.07 (96.0 ± 0.1)	10.4 ± 0.01 (12.6 ± 0.02)
D-Ribose	107.2 (77.5)	104.6 ± 0.01 (75.0 ± 0.01)	−20.4 ± 0.01 (−71.1 ± 0.1)	110.9 ± 0.03 (96.7 ± 0.1)	11.7 ± 0.02 (9.1 ± 0.01)
D-Lyxose	110.5 (82.5)	107.9 ± 0.1 (79.9 ± 0.1)	−12.1 ± 0.1 (−55.3 ± 0.1)	111.6 ± 0.03 (96.8 ± 0.1)	12.2 ± 0.02 (9.9 ± 0.03)
L-Arabinose	103.8 (98.4)	101.3 ± 0.1 (95.9 ± 0.1)	−36.4 ± 0.2 (−6.7 ± 0.2)	112.4 ± 0.08 (97.9 ± 0.10)	10.9 ± 0.05 (12.5 ± 0.03)

Values in parentheses refer to the activation parameters for the rate limiting step obtained from the plot of log k_2 versus 1/T.

Table 4—Proton inventory plots for the oxidation of D-glucose D-xylose by BAB in H_2O-D_2O mixtures at 30°

Atom fraction of deuterium (n)	$10^5\ k_s$ (mol dm^{-3} min^{-1})	
	D-glucose	D-xylose
0.000	4.62	5.25
0.245	4.89	5.50
0.495	5.49	5.78
0.744	6.11	6.02
0.882	6.65	6.33

$[BAB]_0 = 1.5 \times 10^{-3}$ mol dm^{-3}, $[S]_0 = 1 \times 10^{-2}$ mol dm^{-3}, $[HO^-]_0 = 2.0 \times 10^{-2}$ mol dm^{-3}, $I = 0.5$ mol dm^{-3}.

ribose where the orders were nearly unity. At higher $[HO^-]$, the rate levels off (Table 2).

Addition of the reaction product, benzenesulphonamide, and Br^- or Cl^- ions had negligible influence on the rate of reaction (Table 1). The rate of oxidation of sugars was unaltered when ionic strength (I) of the medium was changed using $NaClO_4$ solution (Table 1). When the solvent composition was varied by adding methanol (0-30% v/v), the reaction rate increased with methanol content of the medium. A plot of log k_s versus 1/D where D is the dielectric constant of medium was linear ($r > 0.9978$, $s \leq 0.04$) with a positive slope.

The rate of oxidation of sugars was studied at different temperatures in the range 298-313 K, and the Arrhenius plot, log k_s versus 1/T was linear ($r > 0.9978$, $s \leq 0.02$).The activation parameters, E_a, $\Delta H^{\neq}$, $\Delta S^{\neq}$, $\Delta G^{\neq}$ and log A were calculated for the composite reaction (Table 3).

Solvent isotope studies were conducted in pure D_2O for D-glucose and D-xylose. Values of $(k_s)_{D_2O}$ were 6.63×10^{-5} mol dm^{-3} min^{-1} and 6.33×10^{-5} mol dm^{-3} min^{-1} as compared to $(k_s)_{H_2O} = 4.62 \times 10^{-5}$ and 5.25×10^{-5} mol dm^{-3} min^{-1} leading to the solvent isotope effect, $(k_s)_{H_2O}/(k_s)_{D_2O}$ of 0.70 and 0.83 respectively for D-glucose and D-xylose. Proton inventory studies were made for these probes in H_2O-D_2O mixtures (Table 4, Fig. 1).

Addition of reaction mixtures to acrylamide did not initiate polymerization of the monomer confirming the absence of free radical species in the mixture.

Discussion

Investigations of Bishop and Jennings[9], Morris *et al.*[10] and Hardy and Johnston[11] have shown that identical equilibria exist in aqueous solutions of N-metallo-N-haloarylsulphonamides of the general formula RNXNa (R = *p*-$CH_3C_6H_4SO_2$- or $C_6H_5SO_2$- and X = Cl or Br). Bromamine-B behaves like a strong electrolyte in aqueous solution[11] and the anion is protonated in acidic solutions.

In aqueous alkaline medium, BAB exists in the following equilibria:

$$PhSO_2NBr^- + H_2O \overset{K_b}{\rightleftharpoons} PhSO_2NBrH + HO^- \quad \ldots (3)$$

$$K_b = 7.10 \times 10^{-10} \text{ at } 25°C$$

$$PhSO_2NBrH + HO^- \rightleftharpoons PhSO_2NH_2 + BrO^- \quad \ldots (4)$$

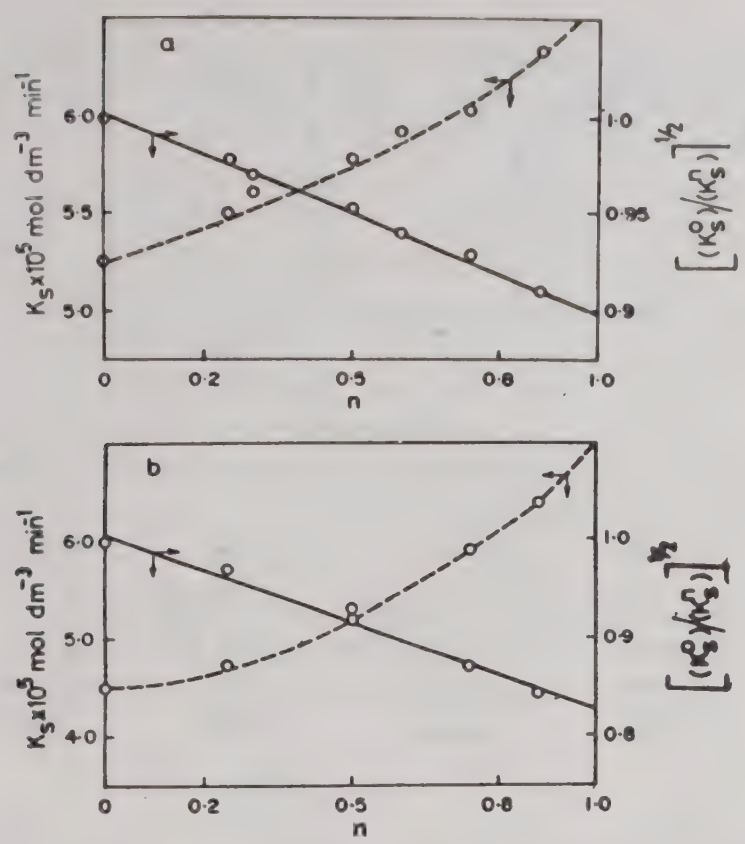

Fig. 1—Proton inventory plots for the oxidation of (a) D-xylose and (b) D-glucose by BAB in H_2O-D_2O mixtures at 303K. ($[BAB]_0 = 1.5 \times 10^{-3}$ mol dm^{-3}, $[S]_0 = 1.0 \times 10^{-2}$ mol dm^{-3}, $[HO^-]_0 = 2.0 \times 10^{-2}$ mol dm^{-3}, I = 0.5 mol dm^{-3} and temp. = 30°C).

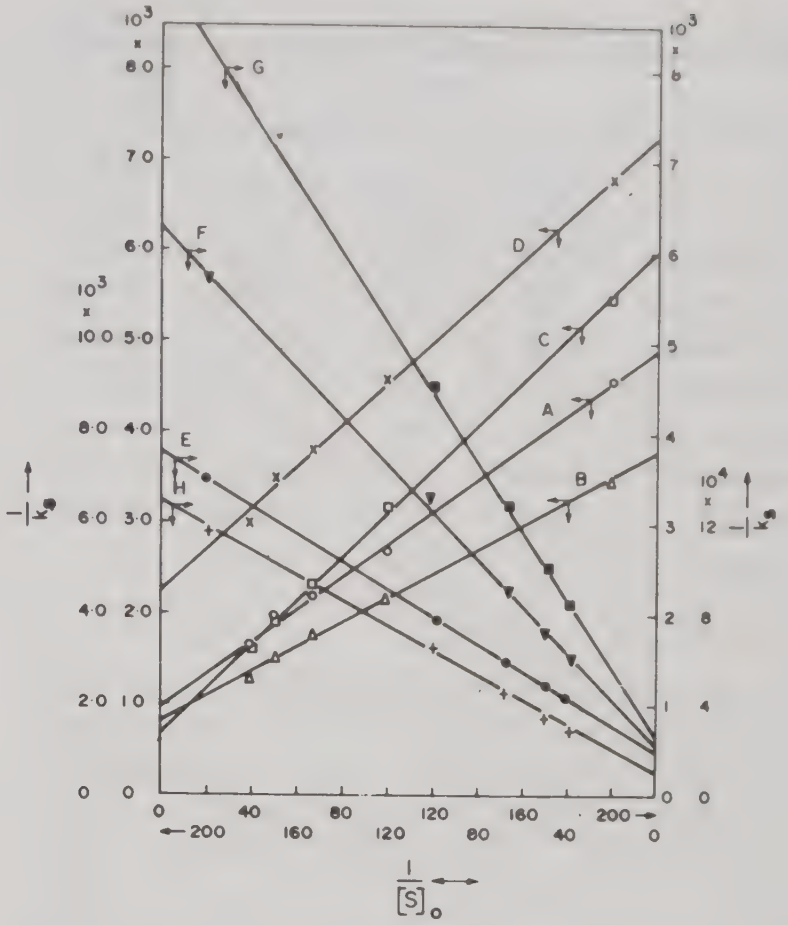

Fig. 2—Plots of $1/k$ versus $1/[S]_0$, ($[BAB]_0 = 1.5 \times 10^{-3}$ mol dm^{-3}, $[HO^-]_0 = 2.0 \times 10^{-2}$ mol dm^{-3}, $I = 0.5$ mol dm^{-3} and temp. = 30°.)

In the present investigations, the rate of oxidation of sugars exhibits a zero order dependence on $[BAB]_0$ indicating that the oxidant is involved in a fast step of the reaction sequence after the rate limiting step. Under these conditions the kinetic information alone would not throw light on the reactive oxidant species. However Eq. 3 involves a base retarding step which is not observed experimentally. The anion $PhSO_2NBr^-$, which is in higher concentrations in alkaline solutions could be the likely oxidising species for the sugars. Further confirmation of the zero order dependence in $[BAB]_0$ is obtained, as the reaction product, benzenesulphonamide has no effect on the rate indicating that it is not involved in a pre-equilibrium.

Since the rate of reaction is dependent on $[sugar]_0$ and $[HO^-]_0$, the preliminary step of the mechanism involves an interaction between the reducing sugar molecule (S) and HO^- forming an enediol anion ($\bar{E}_1$) which is subsequently oxidised by BAB in a fast step. Since the hexoses and pentoses show similar kinetics, Eqs 5-7 are proposed for the oxidation of sugars by BAB in alkaline medium:

$$S + HO^- \underset{k_{-1}}{\overset{k_1}{\rightleftharpoons}} Y \quad \ldots (5)$$

$$Y \xrightarrow[\text{slow}]{k_2} E_1^- + H_2O \quad \ldots (6)$$

$$E_1^- + PhSO_2NBr \xrightarrow[\text{fast}]{} \text{Products} \quad \ldots (7)$$

Scheme 1

Assuming Michaelis-Menten type of kinetics with $[S]_0 = [S] + [Y]$ and $[HO^-]_0 = [HO^-] + [Y]$ and steady state conditions for the intermediate Y[12],

$$\frac{-d[S]}{dt} = \frac{-d[BAB]}{dt}$$

$$= k_s = \frac{k_2 k_1 [S]_0 [HO^-]_0}{k_1[S]_0 + k_1[HO^-]_0 + (k_{-1} + k_2)} \quad \ldots (8)$$

Rate law (8) is in agreement with the experimental findings. The rate is linear at lower concentrations of S and HO^- when $k_1\{[S]_0 + [HO^-]\} < k_{-1} + k_2$ and becomes independent at higher concentrations of these species, under the conditions, $k_1\{[S]_0 + [HO^-]\} > k_{-1} + k_2$. Equation (8) can be transformed into Eq. (9):

$$1/k_s = \frac{[k_{-1} + k_2]}{k_1 k_2 [S]_0 [HO^-]_0} + \frac{1}{k_2[HO^-]_0} + \frac{1}{k_2[S]_0} \quad \ldots (9)$$

Double reciprocal plots, $1/k_s$ versus $1/[S]_0$ and $1/k_s$ versus $1/[HO^-]_0$ were linear with intercepts ($r > 0.9964$, $s \leq 0.03$, Fig. 2) and values of k_2 were calculated.

Evaluation of activation parameters for the rate limiting step

The enediol anion (E_1) is formed as shown in Eq. 6 and evidence for its formation was obtained by

Table 5—Enediol anion formation constants k_2 at different temperatures

Substrate	$10^3\ k_2\ (min^{-1})$			
	298	303	308	313 K
D-Fructose	13.78	25.28	49.47	85.43
D-Glucose	3.81	6.17	10.99	21.40
D-Galactose	3.10	7.16	15.57	23.17
D-Mannose	1.44	2.22	5.72	10.73
D-Xylose	5.54	10.93	20.02	36.67
D-Ribose	5.47	8.79	14.32	24.57
D-Lyxose	5.03	8.05	13.20	25.27
L-Arabinose	2.52	5.36	10.42	16.62

UV spectroscopy[13]. Keeping $[HO^-]_0$ and $[BAB]_0$ constant, $[S]_0$ was varied at several temperatures in the range of 298-313 K. The value of k_2 was calculated from the double reciprocal plot, $1/k_s$ versus $1/[S]_0$ at each temperature (Table 5). The Arrhenius plots of log k_2 versus 1/T were linear ($r > 0.9900$, $s \leq 0.07$) and from the slope, the energy of activation E_a for the rate limiting step was calculated (Table 3).

A probable mechanistic picture of oxidation of aldoses by BAB is shown in Scheme 2(a). At low [alkali], the sugar molecule is converted into 1,2-enediol, (Lobry de Bryun-Alberda Van Ekenstein reaction). The enediol formed in the rate limiting step is subjected to an electrophilic attack by the positive halogen of the species $PhSO_2\bar{N}Br$. Elimination of benzenesulphonamide anion followed by HBr results in a ketene which on hydrolysis forms the aldonic acid. In the case of D-fructose, the 1,2.-enediol (Scheme 2(b)) formed is transformed into a ketoaldehyde which is converted into a 2,3-enediol (E_2^-). The latter is subjected to an electrophilic attack by the second molecule of oxidant to produce formic acid and ketene. The latter hydrolyses to give arabonic acid.

Absence of ionic strength effect on rate precludes the involvement of two ions in the rate sequence. The positive dielectric effect where the rates are enhanced in solvents of lower dielectric constant (methanol-water mixtures) can be explained if the transition state (TS) is less polar than the initial state, because although TS has the same overall charge it is spread over a larger volume. Highly polar solvents destabilize such transition states relative to the initial state while it is anticipated that the rates increase in non-polar solvents which are expected to stabilize[14] the TS.

Solvent isotope studies in D_2O have shown that rates are higher in D_2O medium. For a fast pre-equilibrium proton transfer, it is generally expected from

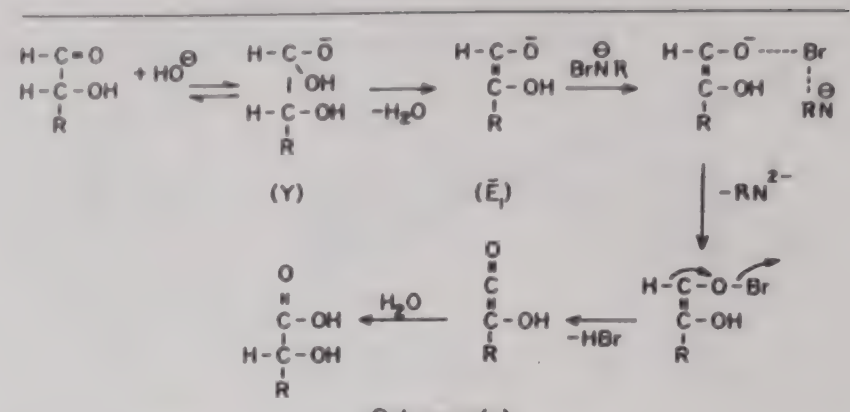

Scheme 2—A possible oxidation mechanism for (a) pentoses and aldohexoses and (b) D-fructose.

a knowledge of electrophilicities of H_3O^+ and D_3O^+ ions and nucleophilicities of HO^- and OD^-, that k_{D_2O}/k_{H_2O} is 2-3 since D_3O^+ and OD^- are stronger acid and stronger base than H_3O^+ and HO^- ions[15]. Hamill and Lamer[16] and Maron and Lamer[17] observed a slight decrease in rate in D_2O medium for the mutarotation of glucose and isomerization of nitromethane respectively, although a proton transfer is shown in these reactions. A similar observation is made in the oxidation of dimethyl sulphoxide by chloramine-T in acid medium[18]. It is concluded that the ratio of dissociation constants of the proto and deutero acids depends only on the ratio of their dissociation constants and is completely

independent of their rates of association. Further, a rapid exchange of sulphoxide hydrogens with D_2O to form DMSO-d_6 is invoked to explain the rate decrease in D_2O medium. In the present investigations, a rapid O−H/O−D exchange cannot be ruled out[19] and formation of the enediol anion from the deuterated sugar molecule involves a substantial primary isotope effect, $k_H/k_D > 1$ because of the O−H and O−D bond scissions in H_2O and D_2O respectively. The latter can compensate for the increase in inverse solvent isotope effect, with the net result that $(k_s)_{D_2O}/(k_s)_{H_2O}$ is considerably less than the expected value of 2-3.

The dependence of rate constant (k_s^n) on n, the atom fraction of deuterium in a solvent mixture of H_2O and D_2O is given by Eq. (10), (refs 20, 21).

$$(k_s^n)/(k_s^0) = \frac{\prod_{\pi_i}^{TS}(1 - n + n\phi_i)}{\prod_{\pi_j}^{RS}(1 - n + n\phi_j)} \quad \ldots (10)$$

where ϕ_i and ϕ_j are the isotopic fractionation factors for isotopically exchangeable hydrogen sites in the transition state and reactant state respectively. If it is assumed that the reaction proceeds through a single transition state, with two exchangeable protons as in the intermediate Y, (Scheme 1), Eq. (10) can be transformed into Eq. (11):

$$\{(k_s^0)/(k_s^n)\}^{1/2} = [1 + n(\phi_j - 1)] \quad \ldots (11)$$

Plots of $\{(k_s^0)/(k_s^n)\}^{1/2}$ versus n are linear [($r > 0.9925$, $s \leqslant 0.01$, Fig. 1(a), (b))] with slope $= (\phi_j - 1)$ from which ϕ_j, the fractionation factor of HO^- ion can be calculated. The values so obtained[22] are 0.80 and 0.85 respectively with glucose and xylose. Hence the formation of a single transition state with with the active participation of HO^- ion is indicated in the present studies.

A constancy of $\Delta G^{\neq}$ values (Table 3) indicates the operation of a common mechanism for the oxidation of sugars by BAB. Further, plot of $\Delta H^{\neq}$ versus $\Delta S^{\neq}$ was linear (Table 3) from which the isokinetic temperature β was 348 K. The relation was found to be genuine by the Exner criterion[23] where log $k_{2(303K)}$ versus log $k_{2(313K)}$ was linear and the value of β was 364 K. Since the value of β is above the experimental temperature (303K) it can be concluded that the reactions are enthalpy controlled.

Relative rates of oxidation and enolization

Since a common mechanism is operative, a relative comparison of the rates of oxidation of sugars by BAB is desirable. If the values of standard zero order rate constants (k_s) are taken into consideration, (Table 1), then D-xylose and D-fructose have the highest rates while L-arabinose and D-mannose react slowly among the two classes of sugars respectively. Contrary to general expectations[5,6,24], the rates of oxidation of pentoses are not higher than those of hexoses. This might be due to the strict zero order dependence of rate on $[BAB]_0$ observed since the resulting enediol anion is oxidised by BAB in a fast step and k_s is a composite quantity which includes several constants. A similar trend is observed in the comparison of enolization rate co-efficients k_2 (from Table 5), except for a reversal of rates between D-glu and D-gal. Isbell and coworkers[24] in their tritium exchange experiments have observed the rate sequence: fru > glu > gal > man and rib > lyx > xyl > ara. DeWit *et al.*[13] studied the behaviour of monosaccharides in aqueous alkaline solution through UV absorption spectroscopy by monitoring the 310 nm band. The rates of enediol formation are fru > glu > gal > man and xyl > ara > rib. Gleason and Barker[25] noted that the rate of oxidation of pentoses by oxygen in presence of alkali is dependent on the medium. In dilute KOH solution the relative rate was, xyl > rib > ara > lyx, while in the presence of 0.5 mol dm^{-3} sodium carbonate, the sequence was, rib > lyx > xyl > ara. However, using the published pK_a values of the pentoses, relative rates for the oxidation in carbonate system was calculated as xyl > rib > lyx > ara. This is also the order found in the present investigations. The differences found between this work and the rate sequence reported by earlier workers could be possibly due to medium effects and/or formation of 1,2-enediols either in the E or Z forms. Isbell and co-workers[24] propose that aldoses and ketoses generally yield mixtures of Z- and E-enediols, the proportions of which differ from sugar to sugar. In the present work, a perusal of $\Delta S^{\neq}$ values for the rate limiting step (Table 3) may indicate the formation probability of E- or Z-isomer.

We believe that the trend reflects the probability of E-enediol formation, which is more stable than the Z-isomer. The probability is greatest with D-ribose while D-galactose has the least tendency to form the *trans* isomer. It appears in general that with the exception of D-glucose, the probability of E-enediol formation in the case of pentoses, is greater than that of hexoses.

Comparison of the rates of oxidation of sugars by BAB and CAB

Oxidation of hexoses[5] and pentoses[6] by chloramine-B (CAB) in alkaline medium indicates a rate law of the type, rate $= k[CAB]_0\,[S]_0\,[HO^-]$ which

amounts to the involvement of oxidant in a rate limiting step. Substantial primary salt, solvent isotope and dielectric effects were noticed. But in the present oxidation studies it is seen that enolization is rate limiting and the sugar molecule is oxidized by BAB in a fast step. It has been observed that oxidations are generally faster with the bromine analogue[26,27]. This has been rationalised in terms of the differences in electrophilicity of halonium cations, Cl^+ and Br^+ which are the reactive species in these reactions[28] and is also partly due to the moderate differences in the Van der Waal's radii of bromine and chlorine.

The oxidation of monosaccharides, thus, takes place via the intermediate formation of an enediol anion of the sugar, in alkaline medium, suggesting an intramolecular rearrangement in the sugar molecule prior to oxidation. The relative rates of enolization of the monosaccharides could depend upon the configuration of the isomers which yield *cis* and *trans* enediols in varying proportions, and also on the experimental conditions employed such as concentration and nature of alkali used and temperature. Further, the operation of $\Delta 2$ instability factors due to dipole interactions cannot be discounted although the significance of these factors is not very apparent. The faster rate of oxidation of fructose is possibly due to an easy attack on the two active primary H atoms at C-1 when compared to a single active H at C-2 of aldoses. We observe that aldohexoses as a group react more slowly than the pentoses, except L-arabinose which seems to have the enolization rate slower than D-glucose and D-galactose. A large group on C-5 of the aldohexose possibly retards the tendency of the sugar to enolize. So the rate determining step in the oxidation reaction seems to be the rate of enolization brought about by the catalytic action of alkali.

Acknowledgement

The award of a senior research fellowship to TAI from the UGC, New Delhi is acknowledged.

References

1 (a) Sen Gupta K K, Gupta S N & Basu S W, *Carbohydr Res*, 71 (1979) 75; 72 (1979) 139; 80 (1980) 223.
(b) Virtanen P O I, Lindroos R, Oirkarinen E & Vasukari J, *Carbohydr Res*, 167 (1987) 29.

2 (a) Singh S V, Saxena O C & Singh M P, *J Am chem Soc*, 92 (1970) 537.
(b) Singh M P, Singh A K & Tripathi V, *J phys Chem*, 82 (1978) 1222.

3 (a) Isbell H S & Pigman W W, *J Res Natl Bur Standards*, 18 (1937) 141.
(b) Isbell H S, *Chem Ind* (1961) 593; *J Res Natl Bur Standards*, 66A (1962) 233.
(c) Ingles O G & Israel G C, *J chem Soc*, (1948) 810.

4 Agrawal M C & Mushran S P, *J Chem Soc* (1973) 762.

5 Iyengar T A, Puttaswamy & Mahadevappa D S, *Carbohydr Res*, 197 (1990) 119.

6 Iyengar T A, Puttaswamy & Mahadevappa D S, *Carbohydr Res*, 204 (1990) 197.

7 Ahmed M S & Mahadevappa D S, *Talanta*, 27 (1980) 669.

8 Gowda B T & Mahadevappa D S, *Microchem J*, 28 (1983) 374.

9 Bishop E & Jennings V J, *Talanta*, 1 (1985) 197.

10 Morris J C, Salazar J A & Wineman M A, *J Am chem Soc*, 70 (1948) 2036.

11 Hardy F E & Johnston J P, *J chem Soc, Perkin Trans* 2 (1973) 742.

12 Laidler K J, *Chemical kinetics* (Tata McGraw Hill, Bombay 1965) p. 441.

13 DeWit G, Kieboom A P G & Van Bekkum H, *Carbohydr Res*, 74 (1979) 157.

14 Connors K A, *Reaction mechanisms in organic analytical chemistry* (Wiley, New York) p. 75.

15 Collins C J & Bowman N S, *Isotope effects in chemical reactions* (Van Nostrand-Reinhold, New York) (1970) p. 267.

16 Hamill W H & Lamer V K, *J chem Phys*, 4 (1936) 395.

17 Maron S H & Lamer V K, *J Am chem Soc*, 61 (1939) 692.

18 Mahadevappa D S, Jadhav M B & Naidu H M K, *Int J chem Kinet*, 11 (1979) 261.

19 Isbell H S & Pigman W W, in *Advances in carbohydrate chemistry*, edited by R S Tipson & D Horton (Academic Press, New York) 24 (1969) 82.

20 Albery W J & Davies M H, *J chem Soc, Faraday Trans*, 68 (1972) 167.

21 Gopalakrishnan G & Hogg J L, *J org Chem*, 50 (1985) 1206.

22 (a) Kresge A J & Allred A L, *J Am chem Soc*, 85 (1963) 1541.
(b) Gold V & Grist S, *J chem Soc, Perkin Trans* 2 (1972) 89.

23 Exner O, *Coll Czech Chem Commun*, 29 (1964) 1094.

24 Isbell H S, Frush H L, Wade C W R & Hunter C E, *Carbohydr Res*, 9 (1969) 163.

25 Gleason W B & Barker R, *Can J Chem*, 49 (1971) 1425.

26 Ruff F & Kucsman A, *J chem Soc, Perkin Trans* 2, (1982) 1075.

27 Naidu H M K, Yamuna B & Mahadevappa D S, *Indian J Chem*, 26A (1987) 114.

28 Puttaswamy, Mahadevappa D S & Rangappa K S, *Bull chem Soc*, Japan, 62 (1989) 3343.

Indian Journal of Chemistry
Vol. 31A, November 1992, pp. 845-848

Kinetics and mechanism of oxidation of γ-oxoacids by acid permanganate

G Sikkandar & K A Basheer Ahamed*
Post Graduate Department of Chemistry, Jamal Mohamed College, Tiruchirapalli 620 020
and
S Kannan
School of Sciences, Indira Gandhi National Open University, Maidan Garhi, New Delhi 110 068

Received 16 August 1990; revised 30 January 1992; accepted 10 March 1992

Kinetics of oxidation of unsubstituted and substituted γ-oxoacids by acid permanganate in aqueous acetic acid medium have been studied at high and low $[H_3O^+]$. At high $[H_3O^+]$, the reaction is first order each in [oxoacid], $[MnO_4^-]$ and $[H_3O^+]$. At low $[H_3O^+]$, the reaction is zero order in $[MnO_4^-]$ and first order each in $[H_3O^+]$ and the [oxoacid]. Variation in ionic strength of the reaction medium has no significant effect on the rate of oxidation. But the rate of the reaction is enhanced by lowering the dielectric constant of the reaction medium. Electron-releasing substituents in the aromatic ring accelerate the reaction rates and electron-withdrawing substituents retard them. The value of the reaction constant (ρ) at 303 K (at $[H_3O^+] = 1\,M$) obtained from the Hammett's plot is -1.49 (corr. coeff. = 0.998). A mechanism consistent with the observed results has been suggested and the related rate laws deduced. Activation parameters have been computed.

Kinetics of oxidation of a variety of organic compounds by permanganate have been studied extensively[1-3]. But there is meagre information about the oxidation of γ-oxoacids and the present report incorporate the results of the title investigation.

Materials and Methods

The parent γ-oxoacid, namely, 4-oxo-4-phenylbutanoic acid and the phenyl substituted γ-oxoacids were prepared by the Friedel-Crafts acylation of the substituted benzenes with succinic anhydride[4]. All the chemicals used were Analar grade. Potassium permanganate was used as such and acetic acid was distilled over chromic oxide before use. Perchloric acid was used as a source of hydrogen ions and sodium perchlorate was added to maintain the ionic strength constant. Sodium fluoride was added as a complexing agent to suppress the autocatalysis common in permanganate oxidations[5].

The kinetics of the reaction was followed titrimetrically by standard iodometric procedure. A large excess of oxoacid was taken as compared to permanganate concentration.

Product analysis and stoichiometry

The reaction mixture of γ-oxoacid and permanganate was allowed to remain together till the completion of the reaction and the product was found to be the corresponding benzoic acid which was characterised by m.p. and co-IR spectra. The stoichiometric results obtained indicate that one mole of the oxoacid required 2.8 mole of permangante for oxidation.

$$5C_6H_5-CO-CH_2-CH_2-CO_2H + 14MnO_4^- + 42H^+ \rightarrow 5C_6H_5CO_2H + 15CO_2 + 31H_2O + 14Mn^{2+}$$

Results and Discussion

A scrutiny of the kinetic data reveals the following

(i) At $[H_3O^+] = 1$ mol dm^{-3}, the reaction shows first order dependence on $[MnO_4^-]$ as shown in Table 1 over the initial $[MnO_4^-]$ concentration range of 1.0×10^{-3} to 5.0×10^{-3} mol dm^{-3}.

(ii) At $[H_3O^+] = 0.04$ mol dm^{-3}, the reaction shows zero order dependence on $[MnO_4^-]$ as shown in Table 2.

(iii) The variation of the rate constant at 1 mol dm^{-3} $[H_3O^+]$ for various [oxoacid] is given in Table 1. The second order rate constant obtained by dividing the observed rate constant by [oxoacid] is found to be constant which indicates that the reaction is first order in [oxoacid].

(iv) Rate measurements in solutions of different $[HClO_4]$ in the range 0.5 to 2.0 mol dm^{-3} (as shown in Table 1) indicate that the reaction is first order in $[H_3O^+]$. The plot of log k_{obs} against log $[H_3O^+]$ is

Table 1—Oxidation of γ-oxoacid, 4-oxo-4-phenylbutanoic acid by acid permanganate

$[NaClO_4] = 5 \times 10^{-2}$ mol dm^{-3}; $[NaF] = 5 \times 10^{-2}$ mol dm^{-3}; Solvent = HOAc (30% v/v); temp. = 303 K

$10^3[KMnO_4]$ (mol dm^{-3})	10^2[oxoacid] (mol dm^{-3})	$[H^+]$ (mol dm^{-3})	$10^5 k_1$ (s^{-1})
1.0	2.0	1.0	6.90
2.0	2.0	1.0	6.85
3.0	2.0	1.0	6.82
4.0	2.0	1.0	6.84
5.0	2.0	1.0	6.83
2.0	1.0	1.0	3.41
2.0	3.0	1.0	10.23
2.0	4.0	1.0	13.71
2.0	5.0	1.0	17.13
2.0	3.0	0.5	5.32
2.0	3.0	1.25	12.80
2.0	3.0	1.5	16.12
2.0	3.0	2.0	20.16

Table 2—Oxidation of 4-oxo-4-phenylbutanoic acid by acid permanganate at $[H_3O^+] = 0.004$ mol dm^{-3}

$[NaF] = 0.05$ mol dm^{-3}; $[H_3O^+] = 0.04$ mol dm^{-3}; Solvent = 50% HOAc; temp. = 303 K
$[NaClO_4] = 0.05$ mol dm^{-3}; [oxoacid] $= 4.0 \times 10^{-2}$ mol dm^{-3}

$10^3[KMnO_4]$ (mol dm^{-3})	10^5 (first order rate constant) (s^{-1})	$10^3 \times$ (Zero order rate constant) (mol dm^{-3} s^{-1})
2.0	1.65	3.365
3.0	1.017	3.358
4.0	0.640	3.349

linear with unit slope revealing that the reaction is first order in $[H_3O^+]$ in the above $[H_3O^+]$ range.

(v) The change in the polarity of the medium has a marked effect on the reaction rate. As acetic acid percentage is increased three times, the reaction rate also increases by about three times. For instance under the conditions:

[Oxoacid] $= 0.025$ mol dm^{-3},

$[MnO_4^-] = 2.0 \times 10^{-3}$ mol dm^{-3}

$[H^+] = 1.0$ mol dm^{-3}; $[NaClO_4] = 0.05$ mol dm^{-3}

$[NaF] = 0.05$ mol dm^{-3} and T = 303 K, the rate constant increases from $6.90 \times 10^{-5} s^{-1}$ to $18.61 \times 10^{-5} s^{-1}$ for the parent oxoacid when acetic acid percentage increases from 20% to 60%. The trend in the rate observed may be due to more than one factor. It may be attributed to the lowering of dielectric constant of the medium which favours reactions involving protonation. Further, the enolisation of the oxoacid may be catalysed by acetic acid and this may also contribute to rate enhancement.

A mechanism has been proposed involving the attack of permanganic acid on the enol form of the substrate in the rate determining step. The protonation of permanganate ion leads to the formation of permanganic acid[6,7]. The enolisation is proposed to be the necessary step prior to the oxidation of the substrate; the above two are assumed following the mechanism suggested for acid catalysed permanganate oxidation of ketones[8,9]. The mechanism is given in Scheme 1.

The reaction involves two protons, one for the formation of $HMnO_4$ and another for the enolisation of the oxoacid. Hence, the reaction could be expected to exhibit second order dependence on $[H_3O^+]$. But the experimental results indicate (a) first order dependence only on $[H_3O^+]$ whether the mineral acid concentration is high or low, (b) first order dependence only on [oxoacid] again at high and low mineral acid concentration and (c) first order dependence on $[MnO_4^-]$ at high mineral acid concentration and zero order dependence on $[MnO_4^-]$ at low mineral acid concentration.

These results can be explained using the limiting conditions of high and low $[H_3O^+]$ as follows

$$-\frac{d}{dt}[MnO_4^-] = \frac{k_2 k_3 k_4 [H_3O^+][X][HMnO_4]}{(k_{-2}k_{-3}[H_3O^+] + k_4(k_{-2} + k_3)[HMnO_4])} \quad \ldots(7)$$

At high mineral acid concentration $k_{-2}k_{-3}[H_3O^+] > k_4(k_{-2} + k_3)[HMnO_4]$.

Hence Eq. 7 simplifies to the form,

$$-\frac{d}{dt}[MnO_4^-] = \frac{k_2 k_3 k_4 [H_3O^+][X][HMnO_4]}{k_{-2}k_{-3}[H_3O^+]}$$

$$= \frac{k_2 k_3 k_4 [X]}{k_{-2}k_{-3}}[HMnO_4]$$

$$\text{i.e. } -\frac{d}{dt}[MnO_4^-] = \frac{k_2 k_3 k_4 [X][MnO_4^-][H_3O^+]}{k_{-2}k_{-3}K_a} \quad \ldots(8)$$

where the dissociation constant of $HMnO_4$,

$$Ka = \frac{[MnO_4^-][H_3O^+]}{[HMnO_4]}$$

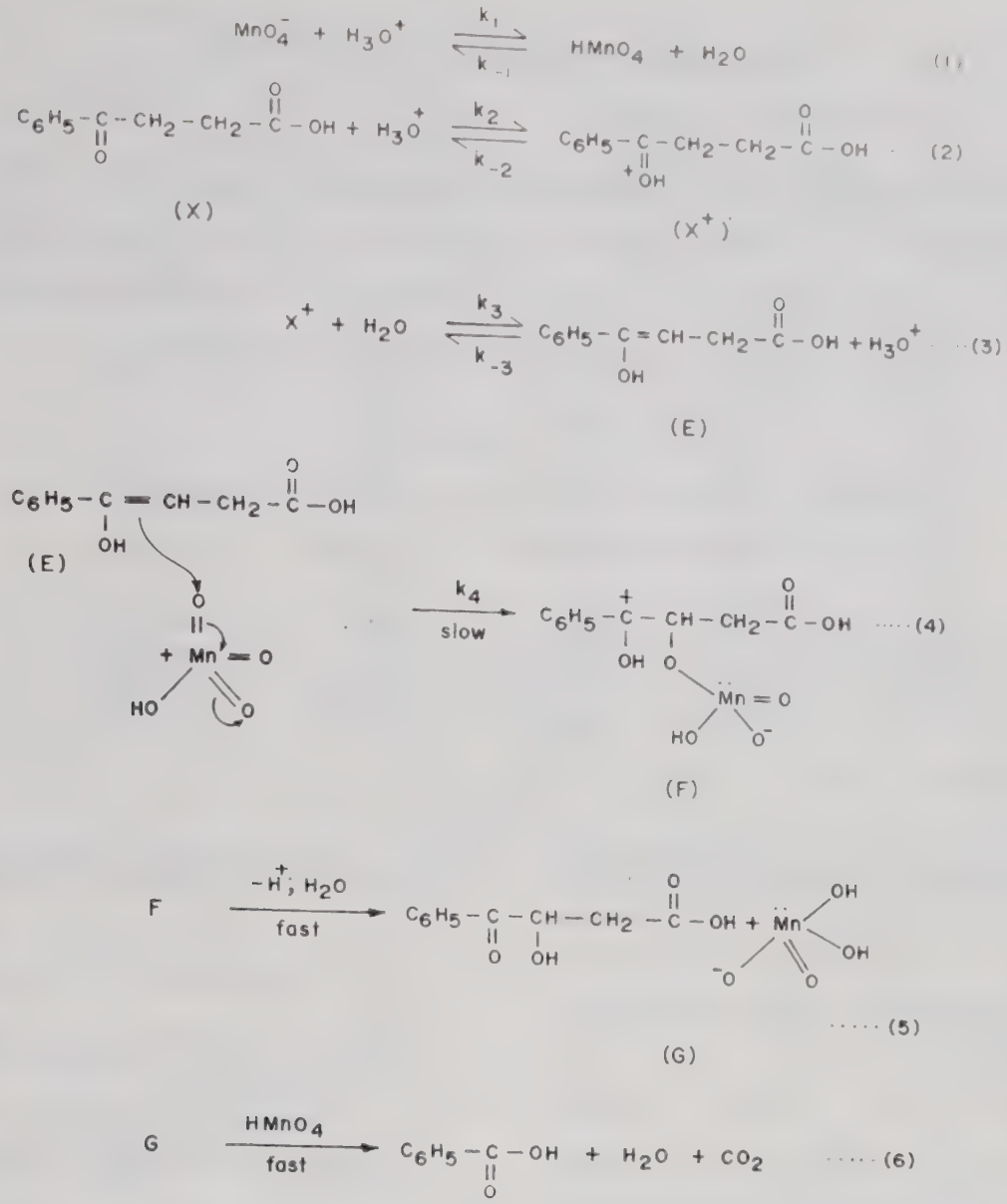

Scheme 1

Hence observed rate constant at high

$$[H_3O^+] = \frac{k_2 k_3 k_4}{k_{-2} k_{-3} K_a} \qquad \ldots(9)$$

At lower mineral acid concentration,

$$k_4(k_{-2} + k_3)[HMnO_4] > k_{-2} k_{-3}[H_3O^+]$$

Hence Eq. 7 becomes,

$$-\frac{d}{dt}[MnO_4^-] = \frac{k_2 k_3 k_4 [H_3O^+][X][HMnO_4]}{k_4(k_{-2} + k_3)[HMnO_4]}$$

$$= \frac{k_2 k_3}{(k_{-2} + k_3)}[H_3O^+][X] \qquad \ldots(10)$$

Possibly under conditions of lower acidity enol removal (step 4) is faster than enol formation (step 3) and at higher acidity conditions, the enol removal is less rapid than its formation. Such a difference in order with respect to oxidant concentrations under the conditions of high and low $[H_3O^+]$ has been reported[10,11] in the oxidation of cyclohexanone by $IrCl_6^{2-}$ and tris-2,2′-bipyridylruthenium(III) ion.

Again in step 4, Mn^{VII} is reduced to Mn^{V} as hypomanganate ester (F) and this is followed by its hydrolysis to form the α-hydroxy ketone (G) which undergoes further oxidation. The formation of hypomanganate is believed to be a reaction intermediate in the acid medium permanganate oxidation of many organic and inorganic compounds[12].

The observed rate constant under high $[H_3O^+]$ is of composite nature as shown in Eq. 9. Consequently the observed ρ value is also dependent on k_2, k_3, k_4, k_{-2} and k_{-3}. No attempt has been made to resolve the ρ value into its components. Special mention needs to be made about the enolisation (step 3) of the substrate. In the bromination of the title compounds for which enolisation is the rate determining step it has been reported that ρ value is −0.75 (ref. 13).

The order of reactivity is: *p*-methoxy > *p*-ethoxy > *p*-methyl > *p*-ethyl > H > *p*-phenyl > *p*-chloro > *p*-bromo > *m*-nitro. The Hammett plot is linear with a slope giving ρ = −1.49 at 303 K.

Table 3—Rate constants and activation parameters

[oxoacid] = 2.0×10^{-2} mol dm^{-3}; [$KMnO_4$] = 2.0×10^{-3} mol dm^{-3};
[H^+] = 1.0 mol dm^{-3}; [NaF] = 0.05 mol dm^{-3}
Solvent = HOAc (30% v/v); [$NaClO_4$] = 0.05 mol dm^{-3}

Substituent	$10^5 k_1$ (s^{-1})				$\Delta H^{\neq}$ (KJ mol^{-1})	$-\Delta S^{\neq}$ (JK^{-1}mol^{-1})
	303	313	323	333 K		
H	6.85	12.94	25.24	45.82	51.17	123.49
– *p*-C_6H_5	6.64	12.88	24.04	44.77	51.37	123.04
– *p*-Cl	3.32	7.43	13.52	24.04	52.43	119.86
– *p*-Br	3.03	6.78	11.51	20.94	53.67	116.40
– *m*-NO_2	0.66	1.48	3.90	6.04	61.41	96.42
– *p*-C_2H_5	12.05	20.94	39.91	66.23	45.77	136.53
– *p*-CH_3	12.91	24.05	44.77	70.96	45.64	136.38
– *p*-OC_2H_5	17.02	28.25	52.61	93.55	45.51	134.51
– *p*-OCH_3	19.10	30.27	56.37	102.57	44.90	135.58

The activation parameters evaluated (Table 3) indicate negative entropy of activation. The value of isokinetic temperature is found to be 425 K. This is in close agreement with the value obtained from the plot of $\Delta H^{\neq}$ against $\Delta S^{\neq}$.

Acknowledgement

The authors thank the authorities of Jamal Mohamed College, Tiruchirapalli for providing facilities.

References

1 Ladbury J W & Cullis C P, *Chem Rev*, 58 (1958) 403.
2 William A Waters, *Q Rev Chem Soc*, 12 (1958) 277.
3 Marigangaiah N P & Banerji K K, *Austr J Chem*, 29 (1976) 1939.
4 Fadnavis N W & Bagavant G, *Indian J Chem*, 17B (1979) 518.
5 Barter R N & Littler J S, *J chem Soc (B)*, (1967) 205.
6 Nath P & Banerji K K, *Bull chem Soc Japan*, 42 (1969) 2038.
7 Littler J S, Quick G R & Wozniak D, *J chem Soc, Perkin Trans*, 2 (1980) 657.
8 Shorter J & Hinshelwood C N, *J chem Soc*, (1962) 3425.
9 Marigangaiah, Mathur P N & Banerji K K, *Indian J Chem*, 14A (1976) 85.
10 Littler J S, Celil R & Easton G, *J chem Soc (B)*, (1970) 626.
11 Audsley A J, Littler J S & Quick G R, *J chem Soc, Perkin(II)*, (1980) 557.
12 Cotton F A & Wilkinson G, *Adv inorg Chem*, (John Wiley) 1988, p. 707; Greenwood N N & Earnshaw A, *Chemistry of the elements* Pergamon Press, Oxford), 1984, p. 1222.
13 Banumathi K, M.Phil dissertation, Bharathidasan University, (1987).

Indian Journal of Chemistry
Vol. 31A, November 1992, pp. 849-854

Synthesis, electronic, infrared and Mössbauer spectroscopic studies of mixed ligand complexes of mono- and bis(N, N′-diethyldithiocarbamato) iron(III) with O, N and S containing chelating ligands and their thermal decomposition†

R B Lanjewar & A N Garg*

Department of Chemistry, Nagpur University, Nagpur 440 010

Received 11 February 1992; revised and accepted 15 May 1992

Two series of mixed ligand complexes of the general formulae $Fe(dtc)_2L$ and $Fe(dtc)L_2$ where L = acetylacetone, 8-hydroxyquinoline, glycine, 1,10-phenanthroline, phenylalanine and thiomalic acid and dtc = N, N′-diethyldithiocarbamate have been synthesized and characterized by elemental analysis, electronic and infrared spectra. Room temperature Mössbauer spectra of the complexes exhibit doublet with $\delta = 0.40\text{-}0.85$ mms^{-1} and $\Delta E_Q = 0.21\text{-}1.64$ mms^{-1}. Magnetic moments of the complexes are in the range 3.74-5.78 B.M. suggesting equilibrium between high spin ⇌ low spin crossover. Thermogravimetric studies suggest stability of the complexes upto 200°C after which they decompose in a single or two steps with 16.8-55.0% residue at 800°C. None of the complexes is volatile.

Sulphur donor ligands are well known for their anticancer, antiviral and antifungal activities as well as widespread industrial applications in vulcanization of rubber[1,2]. Dithiocarbamate is a unique ligand as it can coordinate to the metal ion both as a uni- and bidentate ligand[3]. Martin and White[4] synthesized a novel series of five coordinate iron(III) complexes $[Fe(S_2CNR_2)_2X]$ (X = Cl, Br, I) with square pyramidal geometry and spin state $S = 3/2$. Raynor[5] reported Mössbauer spectral studies of $Fe(NO)(S_2CNEt_2)_2$ and estimated 4s electron population. Korecz *et al.*[6] studied Mössbauer spectra of several iron dioxime mixed ligand complexes and determined the effect of ligand exchange on the electronic structure. Octahedrally coordinated iron(III) complexes may exist in two distinct spin states depending on the nature of ligand. Ewald *et al.*[7] and Hall and Hendrickson[8] suggested electronic spin state equilibrium between the high spin ($^6A_{1g}$) and low spin ($^2T_{2g}$) states in $[Fe(S_2CNR_2)_3]$. Detailed infrared, magnetic and electron paramagnetic resonance studies have suggested that both the $^2T_2$ and $^6A_1$ states are very vibronic with a flipping rate of 10^{10} s^{-1}.

In this paper we report the synthesis of mixed ligand complexes of Fe(III) diethyldithiocarbamate with other bidentate ligands containing O, N, and S donors such as acetylacetone (acac), glycine (gly), phenylalanine (phalan), 1,10-phenanthroline (phen), thiomalic acid (thiomal) and 8-hydroxyquinoline (ox). Their Mössbauer, infrared and electronic spectral studies were carried out to investigate the spin behaviour and bonding characteristics. Also thermal decomposition of the complexes was studied.

Materials and Methods

All the chemicals used were of AR or GR grade. Organic solvents were purified before use.

Preparation of complexes

Mixed ligand complexes of Fe(III) diethyldithiocarbamate with other bidentate ligands were prepared as per methods suggested by Kanungo *et al*[9]. Ethanolic solution of iron(III) chloride (GR, S. Merck), sodium diethyldithiocarbamate (LR, BDH) and the respective ligands L were mixed in 1 : 2 : 1 and 1 : 1 : 2 mole ratios respectively. The ligands chosen were L = acetylacetone (AnalaR, BDH), glycine, phenylalanine (Fluka AG, Switzerland), 1,10-phenanthroline (GR, E. Merck), thiomalic acid and 8-hydroxyquinoline (Sisco Chem.). The resultant contents were stirred for 1 hr at room temperature. Coloured compounds separated out which were filtered, washed with water, absolute ethanol and ether. These were dried *in vacuo* over $CaCl_2$.

†Partly presented at the 25th Annual Convention of Chemists, Calcutta, Dec. 23-27, 1988, Abstract No. ING(G)-40.

Physical measurements

Mössbauer spectra were recorded using a constant acceleration transducer driven Mössbauer spectrometer in conjunction with a PC based 1 k Multichannel Analyzer (Nucleonix, Hyderabad). A 5 mCi $^{57}Co(Rh)$ source (procured from the Isotope Group, BARC, Bombay) was used. All the spectra were recorded at room temperature and computer fitted with Lorentzian line shape as described earlier[10]. The spectrometer was calibrated using natural iron foil. Sodium nitroprusside dihydrate (SNP) was used as standard for isomer shift measurements.

Infrared spectra (4000-400 cm^{-1}) were recorded in KBr medium on a Perkin-Elmer 157 IR spectrophotometer. Thermogravimetric Analyzer System Model TGS-2 and Thermal Analysis Data Station TADS-3600 at a heating rate of 12°C min^{-1}. Magnetic moments were determined from magnetic susceptibility measurements using Gouy balance and $Hg[Co(SCN)_4]$ as the standard. Reflectance spectra were recorded using a Shimadzu Model UV-240 spectrophotometer employing MgO as the reference standard.

Table 1—Analytical data of the iron(III) mixed ligand diethyldithiocarbamate complexes

Complex	Found (calcd) %			
	C	H	S	Fe
$Fe(dtc)_2(acac)$	39.28	5.87	28.56	12.69
	(39.91)	(5.98)	(28.38)	(12.38)
$Fe(dtc)(acac)_2$	44.45	5.49	16.12	12.57
	(44.79)	(5.97)	(15.92)	(12.89)
$Fe(dtc)_2(ox)$	46.23	5.63	25.85	11.15
	(45.98)	(5.24)	(25.81)	(11.26)
$Fe(dtc)(ox)_2$	56.43	4.17	13.05	11.20
	(56.11)	(4.47)	(13.00)	(11.35)
$Fe(dtc)_2(gly)$	34.12	5.68	30.48	12.80
	(33.81)	(5.63)	(30.05)	(13.11)
$Fe(dtc)(gly)_2$	30.65	4.90	18.20	15.90
	(30.69)	(5.11)	(18.19)	(15.87)

where acac = acetylacetone; ox = 8-hydroxyquinoline; gly = glycine (H_2NCH_2COOH); other complexes were characterized on the basis of Fe and S analysis only.

Results and Discussion

All the complexes are black or dark grey coloured solids and are stable under normal atmospheric conditions. Analytical data of C, H, S and Fe for the six complexes with acetylacetone (acac), oxime (ox) and glycine (gly) are given in Table 1. For other complexes only Fe and S analyses were done and respective molecular formulae were confirmed. Typical reflectance spectra of the mixed ligand complexes with 1,10-phenanthroline (phen), phenylalanine (Phalan) and thiomalic (thiomal) acid are shown in Fig. 1. Room temperature Mössbauer spectra of all the complexes exhibit well resolved doublet. Typical Mössbauer spectra of phenylalanine complexes of both types are shown in Fig. 2. Mössbauer parameters and magnetic moments of the complexes are listed in Table 2.

Tris(N,N′-diethyldithiocarbamato)iron (III), $Fe(dtc)_3$, has trigonally distorted octahedral geometry with six sulphur donor atoms surrounding central iron(III)[11]. When one or two dtc ligands are substituted with other bidentate ligands containing O−O, O−N, N−N or O−S donor atoms it will still be an octahedral geometry except that larger distortions are expected. Such complexes are of great interest because of comparable ligand field stabilization energy (Δ) and mean pairing energy ($\bar{p}$) of the *d* electrons[9]. As a first approximation, neglecting distortion in oc-

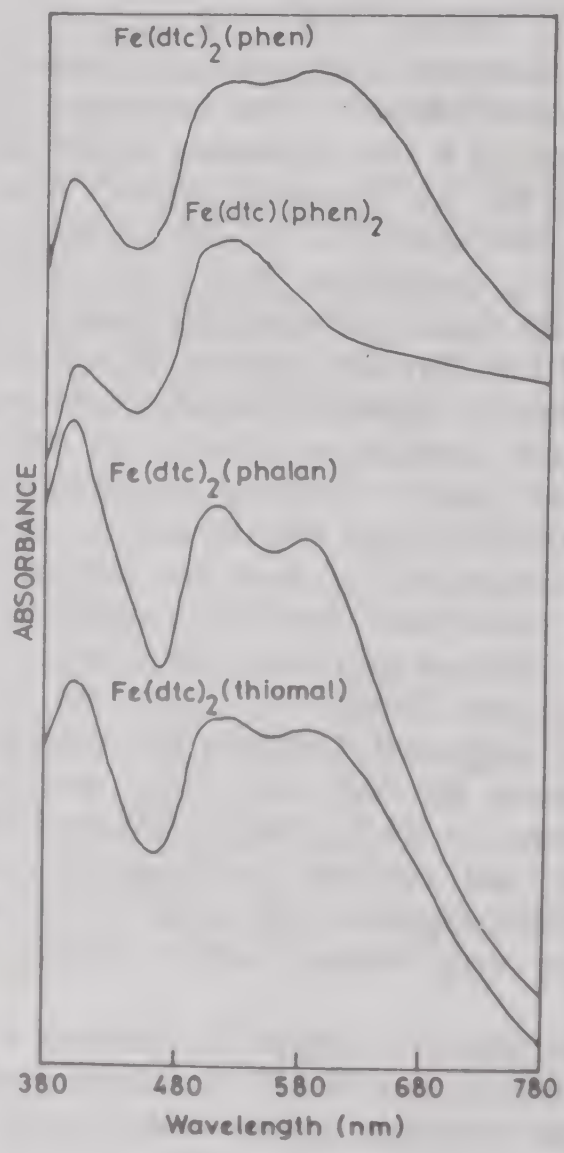

Fig. 1—Electronic reflectance spectra of mixed ligand iron(III) dithiocarbamate complexes

Table 2—Mössbauer parameters and magnetic moment data of mixed ligand iron(III) diethyldithiocarbamates at room temperature

No.	Complex	Isomer shift δ (mms^{-1})	Quadrupole splitting ΔE_Q (mms^{-1})	Magnetic moment μ_{eff} (B.M.)
I	$Fe(dtc)_2(acac)$	0.69	0.23	4.21
II	$Fe(dtc)(acac)_2$	0.74	0.23	3.79
III	$Fe(dtc)_2(ox)$	0.72	0.21	5.78
IV	$Fe(dtc)(ox)_2$	0.67	0.24	5.50
V	$Fe(dtc)_2(gly)$	0.69	0.23	5.80
VI	$Fe(dtc)(gly)_2$	0.68	0.23	3.74
VII	$Fe(dtc)_2(phen)$	0.60	0.74	4.73
VIII	$Fe(dtc)(phen)_2$	0.48	0.37	5.36
IX	$Fe(dtc)_2(Phalan)$	0.62	0.22	5.61
X	$Fe(dtc)(Phalan)_2$	0.46	1.02	5.53
XI	$Fe(dtc)_2(thiomal)$	0.85	1.24	5.14
XII	$Fe(dtc)(thiomal)_2$	0.40	1.64	4.75

where phen = 1, 10-phenanthroline, Phalan = phenylalanine [$C_6H_5CH_2CH(NH_2)COOH$] and thiomal = thiomalic acid [$HOOC.CH_2CH(SH)COOH$].

tahedral geometry and considering only ideal O_h symmetry, electronic configurations in high and low spin states would be $t_{2g}^3e_g^2$ ($^6A_{1g}$) and $t_{2g}^5e_g^0$ ($^2T_{2g}$). The Tanabe-Sugano diagram for a d^5 ion in an octahedral field shows that the spin state of the ground state should change from $^6A_{1g}$ to $^2T_{2g}$ when $\Delta \geqslant \bar{p}$. The two states have effective paramagnetic moments 5.9 B.M. and 2.3 B.M. respectively[12,13]. We have observed magnetic moments for various mixed ligand chelate complexes in the range 3.74-5.80 B.M. It is further observed that magnetic moments of $Fe(dtc)_2L$ are somewhat higher (4.21-5.80 B.M.) compared to those for $Fe(dtc)L_2$ type complexes which show magnetic moments in the range 3.74-5.50 B.M. except for L = 1,10-phenanthroline. For some complexes, viz., $Fe(dtc)_2(gly)$, $Fe(dtc)(phen)_2$, $Fe(dtc)_2(phalan)$, $Fe(dtc)(phalan)_2$ and $Fe(dtc)_2(thiomal)$, μ_{eff}, values correspond to high spin state ($S = 5/2$) while for others these correspond to low spin ($S = 3/2$) state. Mitchell and Parker[14] have suggested that low magnetic moments can not be explained by interactions between iron atoms and most probable explanation would be the change of spin state. Kanungo *et al.*[9] have also observed similar trends and suggested that intermediate magnetic moments may be due to spin pairing of one of the electron resulting in $S = 3/2$. For other complexes, however, high spin state seems to be formed.

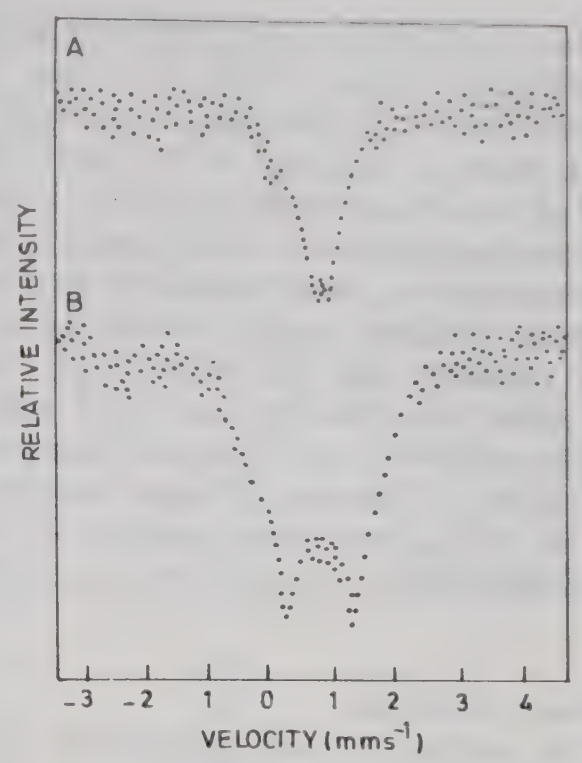

Fig. 2—Room temperature Mössbauer spectra of (A) $Fe(dtc)_2L$ and (B) Fe(dtc)L, where L = phenylalanine

Electronic and infrared spectra

Electronic spectra of the dithiocarbamate complexes are characterized by intense absorptions attributed to both internal transitions in the ligand and metal to ligand ($d_\pi \rightarrow p_\pi$) and ligand-to-metal charge transfer[13]. Ewald *et al.*[7a] have shown that spectral features of dithiocarbamate complexes suggest definite trends in populations of $^6A_{1g}$ and $^2T_{2g}$ states by modifications of ligand. Also, band intensities change markedly with change in population of the two states. Reflectance spectra of the complexes exhibit three bands (Fig. 1) of varying intensities at 15,000, 19,500 and 25,000 cm^{-1} corresponding to $^6A_{1g} \rightarrow {}^4T_{1g}'$, $^6A_{1g} \rightarrow {}^4T_{2g}$ and $^6A_{1g} \rightarrow {}^4T_{1g}$, ^4E_g respectively. It is observed that the band at ~25,000 cm^{-1} is sharp and less symmetric in most complexes. Also, the band at ~20,000 cm^{-1} is a shoulder type and less intense. The third band at ~15,000 cm^{-1} appears as a broad shoulder in all cases. An intense band in UV region at ~38,000 cm^{-1} is also observed. Therefore, a distorted octahedral geometry is expected for all the complexes.

Kellner *et al.*[15] attempted to detect the ligand bonding type from the solid state vibrational spectra. Chatt *et al.*[16] suggested resonance structures on the basis of an intense band in the region 1550-1480 cm^{-1} due to C—N stretching vibration. We have observed a characteristic band due to $\nu(C{=}S)$ at 980 ± 20 cm^{-1} suggesting the bidentate nature of the dithiocarbamate ligand. However, according to literature[17] two or three bands are expected in the region 1500-1400

cm^{-1} due to ν(C⎓N) of the dithiocarbamate and other bidentate ligand (C⎓N) in oxime, 1, 10-phenanthroline, etc. vibrations. A medium broad to weak band is observed at 350 cm^{-1} due to ν(Fe-S) of the dithiocarbamate ligand. Hutchinson *et al.*[18] have suggested it to be a ligand band partially coupled to a metal dependent motion. Besides these principal bands, several other bands due to bonding with Fe [ν(Fe-N) at 300-220 cm^{-1}; ν(Fe-O) at 300-230 cm^{-1} and ν(Fe-S) of thiomalic acid at 310 cm^{-1}] are also observed. No other significant differences were observed between IR frequencies corresponding to one or two chelating ligands except slight intensity difference.

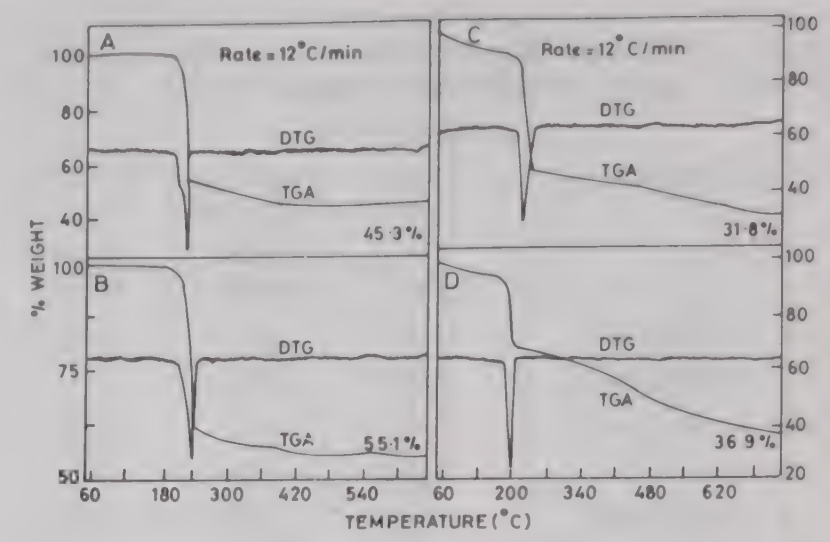

Fig. 3—A comparison of TGA and DTG plots of (A) $Fe(dtc)_2L$ and (B) $Fe(dtc)L_2$, L=acetylacetone with (C) $Fe(dtc)_2L$ and (D) $Fe(dtc)L_2$, L=thiomalic acid

Mössbauer parameters

All the complexes show quadrupole doublets with $\Delta E_Q = 0.21\text{-}1.64$ mms^{-1} and $\delta = 0.40\text{-}0.85$ mms^{-1} (w.r. to sodium nitroprusside dihydrate as standard). All the isomer shift (δ) values are characteristic of high spin state of iron(III) except in a few cases where these are slightly lower and fall in the borderline[19,20] category. This may be partly due to pairing of one of the electrons but this cannot be generalised.

Since the zz-component of the electric field gradient tensor at the iron nucleus is zero for the high spin state, a single absorption line is expected. On the other hand well defined quadrupole splitting is expected for the low spin state ($^2T_{2g}$). On the basis of observed ΔE_Q values, all the complexes can be divided into two groups; first group of eight complexes have ΔE_Q values 0.21-0.37 mms^{-1} which are comparable with that for tris(N, N′-diethyldithiocarbamato)iron(III). In an exhaustive study, Fiddy *et al.*[21] have reported $\Delta E_Q = 0.25$ mms^{-1} for $Fe(dtc)_3$ at room temperature. Second group of four complexes show ΔE_Q values 0.74-1.64 mms^{-1}. It suggests that the substitution by other ligands in $Fe(dtc)_3$ does not always cause a greater distortion in the axial symmetry of the complex. Larger ΔE_Q values are observed for both the thiomalic acid complexes. $Fe(dtc)_2$(phen) and $Fe(dtc)$(phalan)$_2$ show somewhat middle order values of 0.74 and 1.02 mms^{-1} respectively. It seems that with thiomalic acid, ligand having S and O donor atoms, geometrical distortion is maximum presumably due to its large ring size. With other ligands, however, the geometry is not distorted further as evidenced by almost similar ΔE_Q values.

Thermal decomposition studies

Thermal decomposition of metal dithiocarbamates has been a subject matter of detailed investigations[22-25]. It is reported that decomposition proceeds via the formation of metal thiocyanate as intermediate which may ultimately yield metal sulphide and/or oxide[22]. Typical TGA plots of the mixed ligand complexes with acetylacetone and thiomalic acid are shown in Fig. 3. Thermogravimetric data along with DTG peak temperatures and the possible end products are listed in Table 3. In all cases decomposition starts at or after 200°C confirming the absence of water molecules. In the case of both the thiomalic acid complexes, however, decomposition starts at 50°C which may possibly be due to evolution of H_2S.

In most cases decomposition process is fast with single DTG peak though in some cases two peaks have also been observed. On the basis of constant weights at the end, all the complexes can be divided into three groups. First group of complexes yield residue with about 20% wt. at 550-600°C. It may correspond to the formation of Fe_2S_3 or $Fe(SCN)_3$. Second group of three complexes yield 31-39% wt. at 750°C. Third group of complexes with acetylacetone as secondary ligand yield ~ 50% wt. at 500°C. In case of both oxime complexes 51.6% residual wt. is obtained at 800°C with continued decomposition. It seems that one or two ligand molecules are lost and during this process CO_2 (from COOH group) or H_2S (in case of thiomalic acid complex) is lost without affecting Fe-S bond.

A comparison of the decomposition patterns of the two series of complexes in Fig. 3 and thermogravimetric data for all the complexes in Table 3 shows distinct difference between their constant wt. temperatures and residual weights. None of the mixed ligand complexes are volatile[28]. D'As-

Table 3—Thermogravimetric data of the mixed ligand iron(III) diethyl dithiocarbamate chelate complexes

No.	Initial Decomp. temp. (°C)	DTG peak (°C)	Decomp. process	Const. Wt. temp (°C)	Final Wt. (%)	Remarks
I	200	220	Fast, single stage	500	45.3	loss of one ligand of each type
II	200	240	Fast, single stage	550	55.0	loss of 2 acac ligands
III	200	240, 320	Fast, two stage	700	51.6	loss of 1 dtc and
IV	200	200, 240	Slow, two stage	cont. decrease 800 cont. decrease	51.5	possible decomposition of oxime ring
V	200	220, 270	Fast, two stage	550	19.5	Fe_2O_3/Fe_2S_3
VI	200	220, 270	Fast, two stage	550	17.4	"
VII	200	220, 270	Fast, two stage	600	19.4	"
VIII	200	220, 270	Fast, two stage	600	20.6	"
IX	200	220, 280	Fast, slow, two stages	560	16.8	"
X	200	230	Fast, single stage	750 cont decrease	39.3	loss of 2 Phalan ligands
XI	50	230	Fast, single stage	720	31.8	loss of one dtc and CO_2
XII	50	200	Fast, single stage	720	36.9	loss of one ligand of each type

cenzo and Wendldent[26] and Cardwell *et al.*[27] have reported $Fe(dtc)_3$ to be completely volatile. However, our studies do not confirm these observations[28]. It is further observed that the complexes of acetylacetone and 8-hydroxyquinoline are not decomposed completely (constant wt. 45-55%). On the other hand maximum decomposition occurs for the mixed ligand complexes of glycine and 1, 10-phenanthroline. It means that the nature of bidentate ligands is playing an important role in the thermal stability of these complexes. In a recent study of some dithiocarbamate complexes, Muthuswamy and Venkappayya[25b] have suggested the inorganic residue to be a mixture of oxide, sulphate and/or sulphide. Our studies do support this suggestion but for a few complexes only. Probably a detailed product identification by gas chromatography is essential for these investigations.

Acknowledgement

Our sincere thanks are due to the CSIR, New Delhi for financial assistance and the award of SRF to RBL. We are also thankful to the Directors of RSIC, Lucknow for elemental analysis and IR spectra and to RSIC, Nagpur for TGA studies.

References

1 Thorn G D & Ludwig R A, *The dithiocarbamates and related compounds* (Elsevier, New York) 1962.
2 Jorgensen C K, *Inorganic complexes* (Academic Press, London) 1983, 131.
3 Hill J O & Magee R J, *Rev inorg Chem*, 4 (1981) 141.
4 Martin R L & White A H, *Inorg Chem*, 6 (1967) 712.
5 Raynor J B, *J inorg nucl Chem*, 33 (1971) 735.
6 Korecz L, Saghier A A, Varhelyi Cs & Burger K, *Acta chim Acad Sci Hung*, 101 (1979) 27.
7 (a) Ewald A H, Martin R L, Sinn E & White A H, *Inorg Chem*, 4 (1969) 1837.
(b) Ewald A H, Martin R L, Russo I G & White A H, *Proc Roy Soc*, A280 (1964) 235.
8 Hall G R & Hendrickson D N, *Inorg Chem*, 15 (1976) 607.
9 Kanungo B K, Pradhan B & Ramarao D V, *J Indian chem Soc*, 59 (1982) 329.
10 Lanjewar R B & Garg A N, *Bull chem Soc Japan*, 64(1991) 2502.
11 Willemse J, Crass Steggarda J A & Keijzerss C P, *Structure and Bonding*, 28 (1976) 83.
12 Barefield E K, Busch D H & Nelson S M, *Quart Rev*, 22 (1968) 457.
13 Martin R L & White A H in *Transition metal chemistry*, Edited by R L Carlin (Marcel Dekker Inc, New York) 4 (1968) 113.
14 Mitchell P C H & Parker D A, *J chem Soc Dalton Trans*, (1976) 1821.
15 Kellner R, Nikolov G S & Trendafilova N, *Inorg chim Acta*, 84 (1984) 233.
16 Chatt J, Duncanson L A & Veranzi L M, *Nature*, 177 (1956) 1042; *Suomen Kemi*, 29B (1956) 75.

17 Nakamoto K, *Infrared and Raman spectra of inorganic and coordination compounds*, 4th Edn, (John Wiley and Sons, New York), 1986, 246.

18 Hutchinson B, Neil P, Finkelstein A L & Takemoto J, *Inorg Chem*, 20 (1981) 2000.

19 Gutlich P, Link R & Trautwein A, *Mössbauer spectroscopy and transition metal chemistry*, (Springer-Verlag, Berlin), 1978.

20 Dickson D P E & Berry F J, *Mössbauer spectroscopy* (Cambridge University Press, Cambridge), 1986.

21 Fiddy J M, Hall I, Grandjean F, Russo U & Long J G, *Inorg Chem*, 26 (1987) 4138.

22 Sharma A K, *Thermochim Acta*, 104 (1986) 339.

23 Annuar B, Hill J O & Magee R J, *Thermochim Acta*, 8 (1974) 1974.

24 Kaushik N K, Bhusan B & Sharma A K, *Thermochim Acta*, 76 (1984) 345; *Transit met Chem*, 9 (1984) 250; *Thermochim Acta*, 93 (1985) 105.

25 (a) Venkappayya D & Brown D H, *Indian J Chem*, 12 (1974) 838.
(b) Muthuswamy S & Venkappayya D, *J Indian chem Soc*, 64 (1987) 571.

26 D'Ascenzo A & Wendlendt W W, *J inorg nucl Chem*, 32 (1970) 2431.

27 Cardwell T J, Dessarro D J & Uden F C, *Anal chim Acta*, 85 (1976) 415.

28 Lanjewar R B, *Ph.D. Thesis*, Nagpur University, Nagpur 1991.

Indian Journal of Chemistry
Vol. 31A, November 1992, pp. 855-860

Interaction of metal ions with uridine 5′-monophosphate: Existence of possible intramolecular interactions

P Rabindra Reddy*, T K Adharani & C N Keerthi
Department of Chemistry, Osmania University, Hyderabad 500 007, India

Received 5 August 1991; revised and accepted 14 April 1992

Interaction of Cu^{2+}, Ni^{2+}, Zn^{2+}, Co^{2+}, Mg^{2+}, Ca^{2+}, La^{3+}, Pr^{3+}, Nd^{3+}, Gd^{3+} and Dy^{3+} with 5′-uridine monophosphate (5′-UMP) as the primary ligand and glycine (gly), histidine (histi) and histamine (hista) as secondary ligands in 1 : 1 and 1 : 1 : 1 ratio has been investigated potentiometrically at 35°C and 0.10 M (KNO_3) ionic strength. The stability constants of binary (1 : 1) and ternary (1 : 1 : 1) systems are compared to assess the influence of charge of the metal ions and the nature of secondary ligands on the structure and stabilities of these complexes. The stabilisation of the ternary complexes is measured in terms of $\Delta \log K$ which is the difference between the stabilities of binary and ternary complexes in solution. Based on geometry of metal-5′-UMP complexes, coordination number of the metal ions concerned and the steric factors, it has been concluded that O(4) is also involved in coordination in addition to the known phosphate binding in binary complexes. However, in ternary systems only phosphate is involved in metal coordination.

Nucleic acid-protein interactions constitute one of the important natural interactions. Therefore, a study of these interactions at monomer level is worthwhile as they provide good models for these biological interactions. In the present study we have investigated the interactions of 5′-uridine monophosphate (5′-UMP) with Cu^{2+}, Ni^{2+}, Zn^{2+}, Co^{2+}, Mg^{2+}, Ca^{2+}, La^{3+}, Pr^{3+}, Nd^{3+}, Gd^{3+} and Dy^{3+} in the absence and presence of secondary ligands glycine, histidine and histamine to assess the influence of secondary ligands on the structure and stability of 1 : 1 metal-5′-UMP complexes.

Earlier work in solution of 5′-UMP relates to the study of its interaction with Cu^{2+} (ref. 1, 2) and Mn^{2+} at neutral *p*H by NMR spectroscopy[3]. It was concluded, based on preferential line broadening, that in addition to phosphate coordination there is some metal ion-base interaction. Similar observations were made earlier in the case of Mg^{2+} complexes[4]. However, earlier potentiometric studies[5,6] did not confirm the metal ion-base interactions though studies with 5′-UTP showed a lowering in the *pK* value for N(3) in the presence of Cu^{2+} (ref. 7).

A more clear picture on the bonding modes of 5′-UMP emerged from the X-ray crystallographic data, though it conflicted with the solution studies. For example, Goodgame *et al.*[8] have shown in the case of Co^{2+}: 5′-UMP system that only phosphate is involved in metal coordination. Fischer and Bau[9] have reached the same conclusions with a ternary system. Aoki[10] and other workers[11] confirmed bonding by phosphate only in Cd^{2+} complexes.

Recent studies involving the preparation and characterization of Ni^{2+} (ref. 12) and Cr^{3+} (ref. 13) complexes at neutral *p*H indicate direct bonding through phosphate group with additional interaction with base through C(4)O. The non-involvement of N(3) in metal coordination when there is a metal ion-base interaction may be due to the presence of a proton at this site under the experimental conditions employed. However, CH_3Hg^{2+} is shown to bind exclusively to N(3) of the base[14-16].

Thus, it is clear that so far no attempt has been made to study the metal ion interaction with 5′-UMP in the basic region where N(3)-H dissociates making the site competitive with other potential binding sites in the ligand for metal coordination.

Therefore, it was thought important to investigate the metal ion interaction with 5′-UMP both in binary and ternary systems in the *p*H range 4.5-10 to identify the binding modes which are highly *p*H dependent. We have extended these studies to trivalent lanthanons to verify the effect of size and charge of the metal ions on the stability of these complexes. The structures of primary and secondary ligands are depicted in Chart 1 for ready reference.

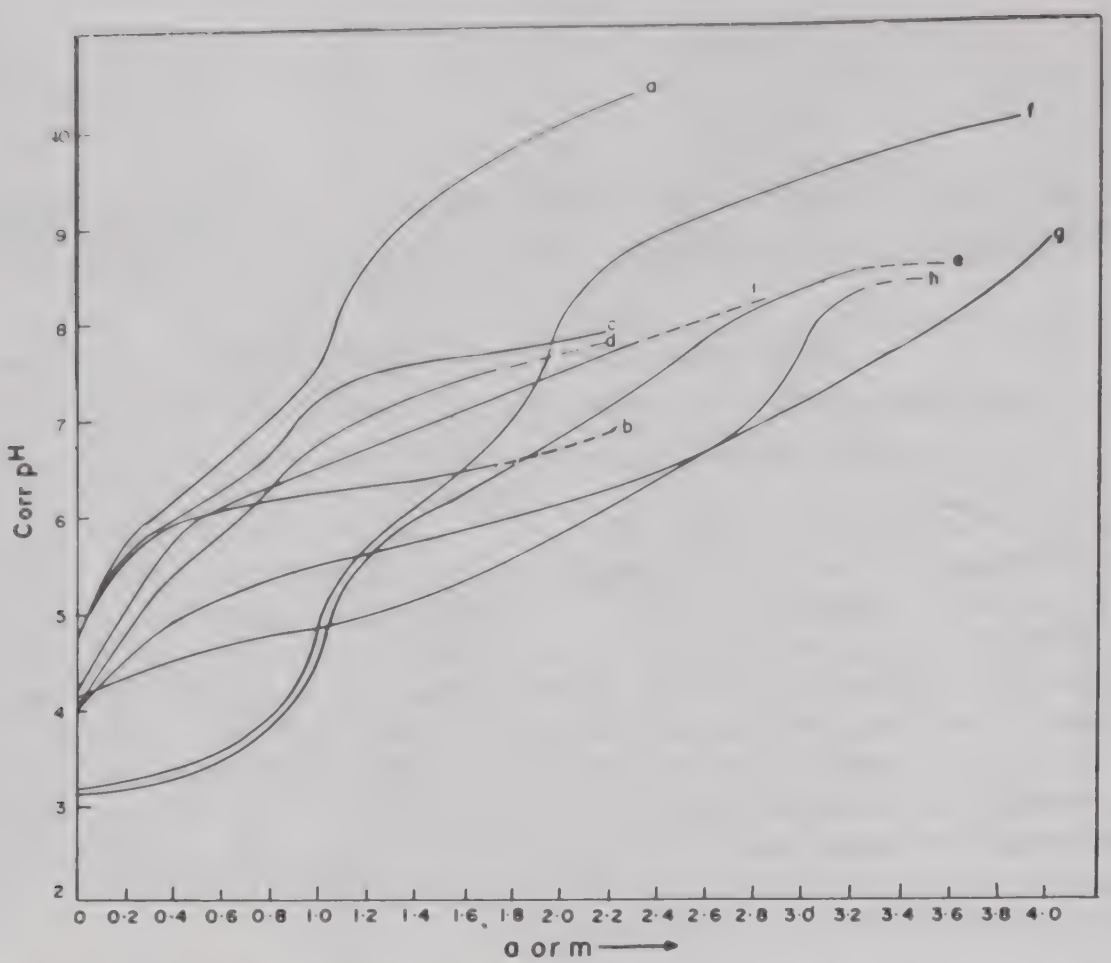

Fig. 1—Potentiometric titration curves for the interaction of 5′-UMP with bivalent and trivalent metal ions both in binary (1 : 1) and ternary (1 : 1 : 1) system at 35 ± 0.1°C $I = 0.10$ M (KNO_3) [(a) Free 5′-uridine monophosphate; (b) Cu(II) : 5′-UMP (1 : 1); (c) Zn(II) : 5′-UMP (1 : 1); (d) La(III) : 5′-UMP (1 : 1); (e) Ni(II) : 5′-UMP : glycine (1 : 1 : 1); (f) Mg(II) : 5′-UMP : glycine (1 : 1 : 1); (g) Cu(II) : 5′-UMP : histamine (1 : 1 : 1); (h) Co(II) : 5′-UMP : histidine (1 : 1 : 1); (i) La(III) : 5′-UMP : histidine (1 : 1 : 1)].

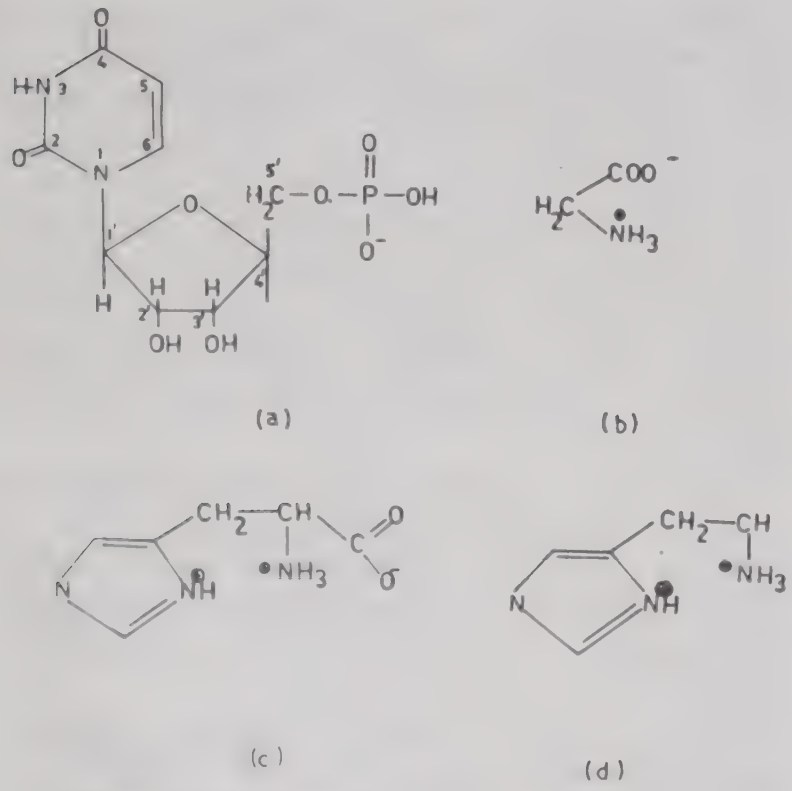

Chart 1—(a) 5′-Uridine monophosphate; (b) glycine; (c) histidine; and (d) histamine.

Table 1—Ionisation constants* of ligands

[Temp. = 35 ± 0.1°C; $\mu = 0.10$ M (KNO_3)]

Ligand	pK_a	pK_{2a}	pK_{3a}
5′-UMP	0.7**	6.34	9.53
Glycine	2.33	9.75	—
Histidine	6.00	9.00	—
Histamine	5.87	9.63	—

*The constants are accurate to ± 0.05 pK units.
**From reference 21.

Materials and Methods

5′-Uridine monophosphate (5′UMP), glycine (gly), histidine (histi) and histamine (hista) were obtained from Sigma Chemical Co. (USA). Transition and alkaline earth metal ions were of AR grade and all rare earth oxides were of Johnson Mathey's spectral grade.

The experimental method consisted of potentiometric titration of metal ions and 5′UMP in the absence and presence of secondary ligands glycine, histidine and histamine in 1 : 1 and 1 : 1 : 1 ratios respectively at 35 ± 0.1°C with standard NaOH solution. The ionic strength was maintained constant by using 0.10 M (KNO_3) as the supporting electrolyte and relatively low concentrations of ligand and metal ion (1×10^{-3} M). During the course of the titrations a stream of nitrogen was passed over the solution to eliminate the adverse effect of atmospheric carbon dioxide,

Table 2—Stability constants* of binary and ternary complexes of M(II) and 5′-UMP with glycine, histidine and histamine (1 : 1 : 1) systems

[Temp. = 35 ± 0.1°C; μ = 0.10 *M* (KNO_3)]

Metal ion	M^{2+} : 5′UMP (1 : 1)			M^{2+} : 5′UMP : gly			M^{2+} : 5′UMP : histi			M^{2+} : 5′UMP : hista		
	K^{M}_{ML}	$K^{M}_{M(HL)}$	$K^{M(HL)}_{ML}$	$K^{M(HA)}_{MAL}$	$K^{M(HA)}_{M(HA)HL}$	$K^{M(HA)HL}_{MAL}$	K^{M}_{MAL}	$K^{M}_{MA(HL)}$	$K^{M}_{M(HA)HL}$	K^{M}_{MAL}	$K^{M}_{MA(HL)}$	$K^{M}_{M(HA)HL}$
Cu(II)	6.57	—	—	13.51	—	—	15.77	—	—	15.86	—	—
Ni(II)	—	2.18	3.97	12.34	—	—	—	13.43	—	—	11.02	—
Zn(II)	—	2.23	4.94	12.92	—	—	—	11.33	—	—	10.70	—
Co(II)	—	2.06	3.87	11.32	—	—	—	11.66	—	—	10.94	—
Mg(II)	—	1.80	2.44	—	2.07	6.71	—	—	7.12	—	—	6.50
Ca(II)	—	1.70	2.30	—	2.04	6.69	—	—	7.05	—	—	6.42

*The constants are accurate to ± 0.06 log *K* units

Table 3—Stability constants* of binary and ternary complexes of M(III) and 5′-UMP with glycine, histidine, histamine (1 : 1 : 1) systems

[Temp. = 35 ± 0.1°C; μ = 0.10 *M* (KNO_3)]

Metal ion	M^{3+} : 5′-UMP (1 : 1)		M^{3+} : 5′-UMP : gly (1 : 1 : 1)	M^{3+} : 5′-UMP : histd (1 : 1 : 1)	M^{3+} : 5′-UMP : histm (1 : 1 : 1)
	$K^{M}_{M(HL)}$	$K^{M(HL)}_{ML}$	$K^{M(HA)}_{M(HA)HL}$	$K^{M}_{M(HA)HL}$	$K^{M}_{M(HA)HL}$
La(III)	3.59	5.47	3.64	8.35	7.72
Pr(III)	3.65	5.80	3.91	8.62	7.91
Nd(III)	3.78	5.94	3.98	8.73	8.05
Gd(III)	3.89	6.05	4.00	8.92	8.12
Dy(III)	4.33	6.29	4.52	9.06	8.49

*The constants are accurate to ± 0.06 log *K* units.

other experimental datails can be found elsewhere[17].

Calculations

For the calculation of stability constants of bivalent and trivalent ternary systems suitable material balanced equation were set up and solved with the help of computer program BEST[18]. However, it was noticed that different types of interactions were observed with the metal ions under investigation.

The constants for transition metal-5′-UMP-glycine, histidine and histamine systems were calculated using equations from ref. 19. For Mg(II), Ca(II) and lanthanide systems the equations described in ref. 20 were used.

Experiments were conducted at three different concentrations to assess the influence of concentration on stabilities. Since there was no appreciable change in the stabilities it was assumed that the probability of formation of species other than those described above is remote. The possible hydrolysis of free metal ion over the experimental *p*H range was ruled out by performing independent metal ion titrations and comparing the curves with those obtained for binary systems. Species distribution curves were generated using computer program BEST.

Results and Discussion

(*a*) *Metal* : *5′-UMP* : *glycine* (1 : 1 : 1) *system*

The mixed ligand titration curve for Ni^{2+} system (Fig. 1e) shows an inflection at m = 1 followed by a buffer region and a precipitate around m = 3.5. In the buffer region m = 0-1, only 1 : 1 (metal : glycine) complex formation takes place. (The stability constant obtained in this buffer region is found to be similar to that of a simple 1 : 1 binary constant). The behaviour of rest of the metal ions was similar in this buffer region. Thus, the ternary complex formation takes place only after m = 1. Accordingly, it was assumed that the simultaneous dissociation of two protons takes place. Cu^{2+}, Zn^{2+} and Co^{2+} behaved in a similar manner. The constants were calculated taking the ex-

Table 4—Δ log K^* values for various metal-ligand (1 : 1 : 1) systems in solution

[Temp. = 35 ± 0.1°C; μ = 0.10 M (KNO_3)]

Metal ion	M : 5′-UMP : gly (1 : 1 : 1)		M : 5′-UMP : histi (1 : 1 : 1)	M : 5′-UMP : hista (1 : 1 : 1)
Cu(II)	—		−0.82	−0.95
Ni(II)	—		+2.83	+2.48
Zn(II)	—		+2.75	+2.36
Co(II)	—		+2.82	+2.60
Mg(II)	+0.27	+0.95	+2.02	+1.40
Ca(II)	+0.34	+0.94	+1.91	+1.28
La(III)	+0.05		+1.35	+1.02
Pr(III)	+0.26		+1.49	+1.08
Nd(III)	+0.20		+1.47	+1.03
Gd(III)	+0.19		+1.68	+1.15
Dy(III)	+0.19		+0.97	+0.68

*The values are calculated taking appropriate binary constants of secondary ligands from reference 26.

perimental points far below the precipitation region[19]. In the case of Cu^{2+} system the constant $K_{MAL}^{M(HA)}$ was computed in the entire buffer region.

However, Mg^{2+} (Fig. 1f) and Ca^{2+} show an additional inflection at m = 2 followed by a buffer region. The constant $K_{M(HA)HL}^{M(HA)}$ was computed in the buffer region m = 1-2 (ref. 20).

For M^{3+} : 5′-UMP : glycine systems, an inflection was obtained at m = 1 followed by a precipitate at m = 1.8. The probability of formation of various complexes $K_{MAL}^{M(HA)}$, $K_{MA(HL)}^{M(HA)}$, $K_{ML(HA)}^{M(HA)}$, $K_{M(HA)HL}^{M(HA)}$ was assumed and based on comparison with binary data, *p*H range, behaviour of similar hard metal ions and species distribution curves it was confirmed that the last probability is the most predominant one.

(b) Metal : 5′-UMP : histidine/histamine (1 : 1 : 1) system

It was assumed, based on titration curve of Cu^{2+} : 5′-UMP : histamine (Fig. 1g), that a simultaneous release of protons takes place and the constant K_{MAL}^{M} was calculated[19]. Cu^{2+} forms similar complexes with histidine also.

The mixed ligand titration curve of Co^{2+} : 5′-UMP : histidine (Fig. 1h) shows an inflection at m = 3. Solid phase appears after this inflection. The constant $K_{MA(HL)}^{M}$ was computed in the buffer region m = 0-3[19]. Ni^{2+} and Zn^{2+} systems showed similar behaviour. The behaviour of these metal ions was similar with histamine also.

The mixed ligand titration curves of Mg^{2+} and Ca^{2+} show an inflection at m = 2 followed by precipitation. The formation of protonated complex $K_{M(HA)HL}^{M}$ was assumed in the region m = 0-2.

In (Fig. 1i) is given the titration curve of La^{3+} : 5′-UMP histidine. A precipitate appeared around m = 2 for all the trivalent ternary systems. The formation of $K_{M(HA)HL}^{M}$ was assumed based on similar reasons as cited in section (a).

The *pK* values of 5′-UMP and various secondary ligands are presented in Table 1.

The stability constants of binary (1 : 1) M^{2+} : 5′-UMP complexes are listed in Table 2. The protonated constants are in fair agreement with the recently reported values[21]. However, the normal 1 : 1 metal : 5′-UMP constants are reported for the first time. Further, the protonated constants are comparable with the corresponding constants of metal phosphate complexes[21] indicating exclusive phosphate interactions in this buffer region. X-ray crystallographic studies also support this view[8]. However, the data for the normal 1 : 1 complexes suggest the possibility of an intramolecular interaction. This is contrary to the literature reports[21] (i.e., intramolecular interactions are absent in pyrimidine nucleotides). When the stability constants of the corresponding (M-RibMP)[21], (M-Uridine)[19] and (M-UMP) systems are compared, it is found that the (M-UMP) constants are comparable neither to (M-uridine) nor to (M-RibMP) constants. Had there been no intramolecular interactions in 5′UMP, the data would have been close to (M-RibMP) data if only phosphate binding is envisaged or to (M-uridine) data if only base binding is involved. Therefore, it is proposed that an intramolecular interaction exists in these systems. Then the question arises about the possible binding modes in the molecule. In basic medium the N(3) site is deprotonated

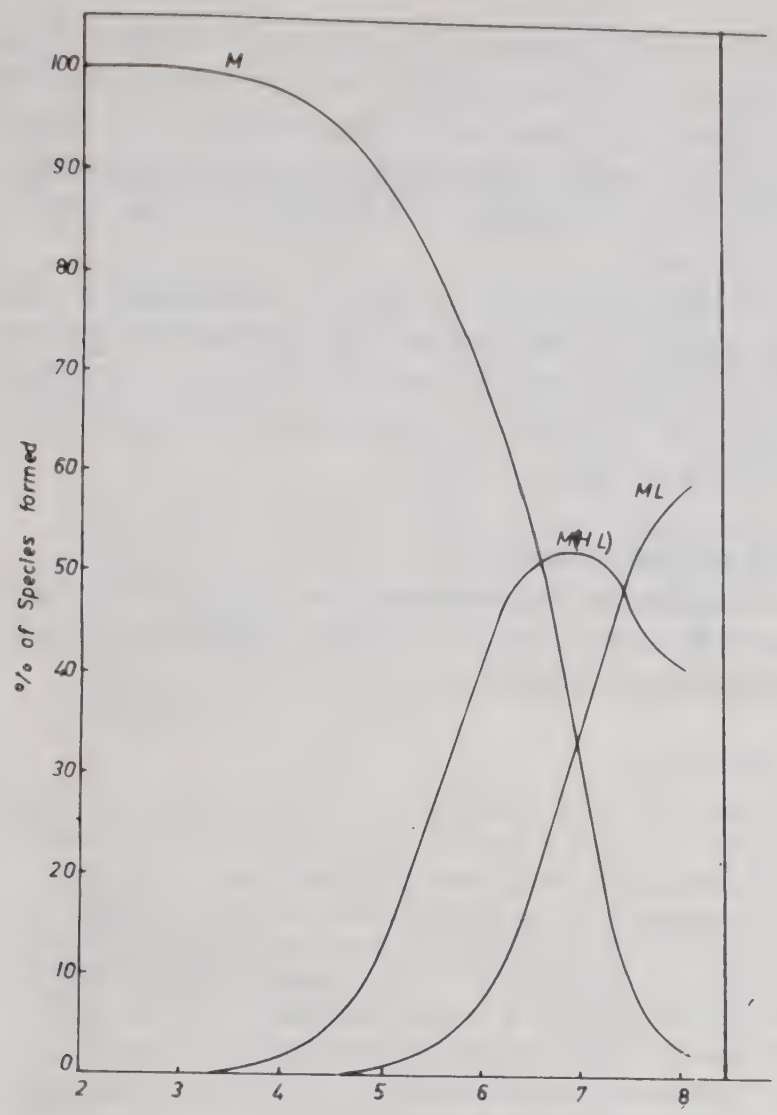

Fig. 2—Species distribution curve of La^{3+} : 5'-UMP (1 : 1) binary system

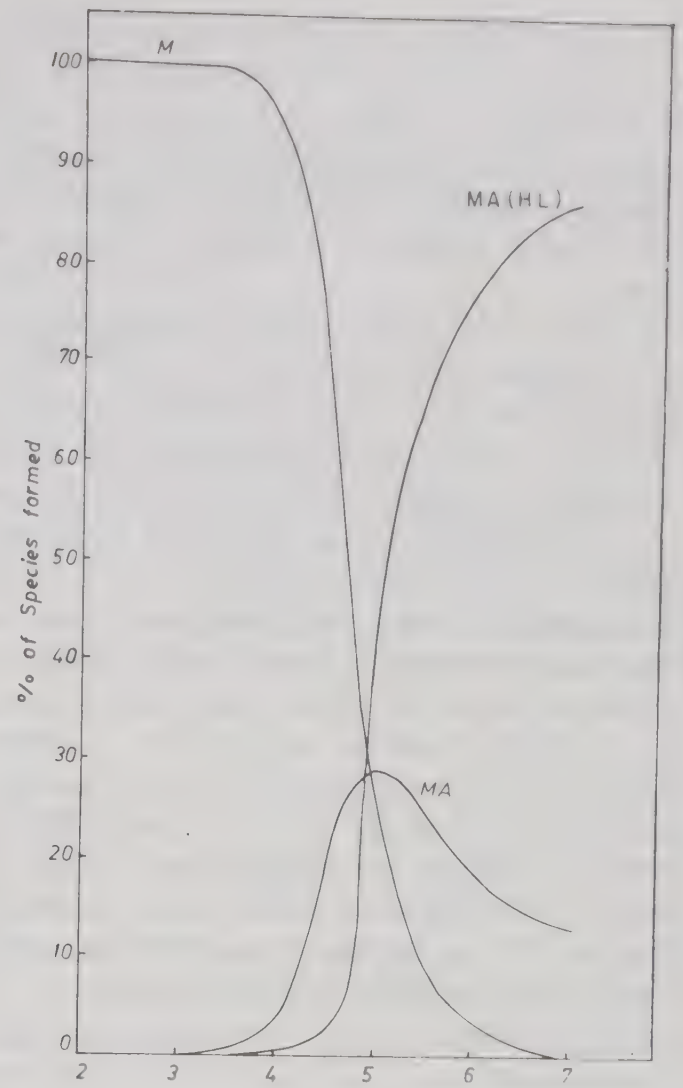

Fig. 3—Species distribution curve of Ni^{2+} : 5'-UMP : histidine (1 : 1 : 1) system

consequently a metal ion can bind to N(3) or O(4). However, O(4) may be preferred over N(3) because of its high charge density. Since there is no evidence of metal ions forming simultaneous innersphere complexes with nucleotide monophosphates there exists a possibility of phosphate involvement through a water molecule in addition to O(4) coordination. Similar observations were made earlier[12,13].

The stability constants pertaining to the interaction of trivalent lanthanons and 5'-UMP are presented in Table 3. It can be seen from the table that the stability constants of 1 : 1 M^{3+} : 5'-UMP are greater than those of the corresponding bivalent metal ions. This may be due to the higher value of charge/radius ratio of the former metal ions. The higher ratio of lanthanons permits a closer approach of ligands and better electrostatic interaction resulting in the greater stability of these complexes. This is further reflected in their species distribution curves. The species distribution curve of La^{3+} : 5'-UMP (Fig. 2) shows the formation of the complex to the extent of 52%; in contrast, only 40% of the species formed with the bivalent metal ions suggesting that the lanthanons bind more effectively with phosphate group. This is in agreement with the known view that lanthanides bind exclusively to phosphate group in 5'-UMP[22]. In the basic region the data suggest that there is an additional interaction with base moiety of 5'-UMP. Based on the conclusions reached in the case of lanthanide : uracil complex[23], it is inferred that these metal ions coordinate through phosphate oxygens with an additional interaction of O(4) through bridged water molecules.

The ternary constants of various systems are given in Tables 2 and 3. It can be seen from the tables that different types of complexes are formed in the case of both bivalent and trivalent metal ions. This specificity does not confine to any particular metal ion or ligand but varies with metal ion to metal ion and ligand to ligand.

The closeness in the ternary stability constants of Cu^{2+} : 5'-UMP : histidine/histamine systems suggests that histidine is acting like histamine. The corresponding $\Delta \log K$ values (the $\Delta \log K$ is the difference between the binary and ternary constants) are presented in Table 4. The negative

Δ log K values indicate the amount of destabilization in ternary systems. This suggests that the 5′UMP is bonded through the base moiety along with indirect phosphate chelation as the direct phosphate involvement would have resulted in the positive Δ log K values as it favours stacking interactions.

Ni^{2+}, Zn^{2+} and Co^{2+} form monoprotonated ternary complexes whereas Mg^{2+} and Ca^{2+} form diprotonated complexes with histidine and histamine. In these cases the experimental *p*H range was restricted to neutral *p*H owing to the formation of a precipitate in the region of base *pK*. Therefore, in the above systems the 5′-UMP coordinates only through the phosphate group in addition to the secondary ligand binding. This is clearly evident from the species distribution curve of Ni^{2+} : 5′-UMP : histidine system (Fig. 3) where the formation of the protonated complex reaches a maximum of 85% at *p*H 7. This type of interaction favours stacking as base moiety is free to stack with the imidazole moieties of the histidine or histamine. This is further reflected in the positive Δ log K values of these systems (Table 4).

However, different types of complexes have been observed in the case of M^{2+} : 5′-UMP : glycine systems resulting in the evaluation of Δ log K values only for Mg^{2+} and Ca^{2+}. These values are positive though lower in magnitude compared to those for histidine and histamine systems, which indicates that the ternary complex formation is favoured due to less steric hindrance and the participation of mixed N/O donor atoms.

These specific and selective interactions were also observed in case of trivalent lanthanons. The trivalent lanthanons form diprotonated ternary complexes with 5′-UMP and histidine or histamine, similar to those observed in the case of Mg^{2+} and Ca^{2+} ternary complexes. This suggests that the mode of bonding is similar in these systems, i.e., 5′-UMP coordinates only through phosphate. This is in accord with the HSAB[24] principle.

However, the differences in the magnitude of the Δ log K values observed are due to the differences in the stabilities of binary[25] and ternary complexes of respective bivalent and trivalent metal ions.

The Δ log K values for the M^{3+} : 5′-UMP : glycine system are less positive compared to those for histidine and histamine system. This is in line with the expected interactions of glycine, histidine and histamine ligands where the latter two are known to participate in stacking interactions, thus enhancing the stability of the ternary complexes.

Finally, it is clear from this investigation that the metal ion interaction with pyrimidine nucleotides is highly *p*H dependent and also varies with metal ion to metal ion and ligand to ligand indicating their high specificity.

Acknowledgement

The financial assistance from the UGC, New Delhi [Scheme No. F. 12-87/84 (SR-III)], is gratefully acknowledged.

References

1 Berger N A & Eichorn G L, *Biochemistry*, 10 (1971) 1857.
2 Kotowycz G, *Can J Chem*, 52 (1974) 924.
3 Kotowycz G & Suzuki O, *Biochemistry*, 12 (1973) 3434.
4 Sari J C & Belaich J P, *J Am chem Soc*, 95 (1973) 7491.
5 Tu A T & Friederich C G, *Biochemistry*, 7 (1968) 4367.
6 Sigel H & Scheller K H, *Eur J Biochem*, 138 (1984) 291.
7 Sigel H, *J Am chem Soc*, 97 (1975) 3209.
8 Cartwright B A, Goodgame D M L, Jeeves I & Skapski A C, *Biochim Biophys Acta*, 477 (1977) 195.
9 Fischer B E & Bau R, *Inorg Chem*, 17 (1978) 27.
10 Aoki K, *J chem Soc Chem Commun*, (1979) 589.
11 Aoki K & Saenger W, *J chem Soc Dalton Trans*, (1984) 1401.
12 Fiol J J & Terron A, *Inorg chim Acta*, 125 (1986) 159.
13 Fiol J J & Terron A, *Polyhedron*, 5 (1986) 1125.
14 Chrisman R W, Mansy S, Peresie H J, Ranade A, Berg T A & Tobias R S, *Bioinorg Chem*, 7 (1977) 245.
15 Mansy S, Wood T E, Sprowles J C & Tobias R S, *J Am chem Soc*, 96 (1974) 1762.
16 Moller M R, Bruck M A, Conner T O', Armatis (Jr) F J, Knolinski E A, Kottmair N & Tobias R S, *J Am chem Soc*, 102 (1980) 4589.
17 Rabindra Reddy P, Harilatha Reddy M & Venugopal Reddy K, *Inorg Chem*, 23 (1984) 974.
18 Motekaitis R J & Martell A E, *Can J Chem*, 60 (1982) 2403.
19 Rabindra Reddy P & Sudhakar K, *Indian J Chem*, 29A (1990) 1182.
20 Rabindra Reddy P & Malleshwar Rao V B, *J chem Soc Dalton Trans*, (1986) 2331.
21 Massoud S S & Sigel H, *Inorg Chem*, 27 (1988) 1447.
22 Mansy S & Tobias R S, *Inorg Chem*, 14 (1975) 287.
23 Gross D S, Simpkins H, Bubienko E & Borer P N, *Arch Biochem Biophys*, 219 (1982) 401.
24 Pearson R G, *J Am chem Soc*, 85 (1963) 3533.
25 Rabindra Reddy P & Malleshwar Rao V B, *Inorg chim Acta*, 125 (1986) 191.
26 Rabindra Reddy P & Malleshwar Rao V B, *Polyhedron*, 4 (1985) 1603.

Indian Journal of Chemistry
Vol. 31A, November 1992, pp. 861-864

Synthesis and spectroscopic studies of di-*s*- and *t*-butyltin(IV) carboxylates

Vimal K Jain* & Vijaya B Mokal
Chemistry Division, Bhabha Atomic Research Centre,
Trombay, Bombay 400 085

Received 10 March 1992; revised 20 April 1992;
accepted 18 June 1992

Di-*s*- and *t*-butyltin(IV) carboxylates, $[Bu^x_2Sn(OOCAr)_2]$ (x = sec. or tert.; Ar = C_6H_5, C_6H_4OMe-2, 2-C_4H_3O, 2-C_4H_3S, 2-C_5H_4N, 2-C_9H_6N and 2-$C_4H_3N_2$) have been prepared and characterized. Carboxylate moiety acts in a bidentate fashion either by coordination through both the oxygen atoms in an asymmetrical manner or chelating through nitrogen in case of ligands containing nitrogen heterocycles. Spectroscpic data (IR and NMR) suggest that these compounds adopt a six-coordinate configuration in solution.

Organotin(IV) carboxylates are widely used as biocides and in industry as homogeneous catalyst for polyurethane and RTV silicon polymerization[1-4]. The central tin atom in these molecules is surrounded by the *n*-alkyl or aryl group(s) and the carboxylate ligand which may have various functionalities[5]. Subtle variations in these groups (both R and the carboxylate ligand) lead to diverse structural forms which may even show various deformations in a given coordination polyhedron. Despite extensive investigations on organotin carboxylates little attention has been focused on the compounds containing sterically demanding alkyl groups on tin[6]. In this paper we report the synthesis of di-*s*- and *t*-butyltin(IV) carboxylates.

Materials and Methods

Benzoic acid, 2-methoxybenzoic acid (*o*-anisic acid), 2-furancarboxylic acid, 2-thiophenecarboxylic acid, pyridine-2-carboxylic acid, pyrazinecarboxylic acid and 2-quinoline carboxylic acid were products of Fluka or Aldrich. Bu^s_2SnO and Bu^t_2SnO were prepared in the laborataory[7]. The solvents were purified and dried under nitrogen atmosphere by standard methods. IR spectra were recorded as nujol mulls using CsI optics on a Perkin-Elmer 7738 spectrophotometer. The ^1H, $^{13}C\{^1H\}$ and $^{119}Sn\{^1H\}$ NMR spectra were recorded on a Varian FT-80A NMR spectrometer operating at 79.542, 20.00 and 29.63 MHz respectively. Chemical shifts are reported in ppm from internal chloroform peak (δ7.26 ppm for ^1H and 77.0 ppm for ^{13}C) and external 33% Me_4SN in C_6D_6 for ^{119}Sn. Microanalyses were performed by the Analytical Chemistry Division of this research centre, and tin was estimated as tin oxide. Melting points were determined in a capillary and are uncorrected.

Preparation of Bu^s_2SnO $(OOC\text{-}C_6H_4OMe\text{-}2)_2$]

To a benzene suspension of Bu^s_2SnO (0.96 g, 3.86 mmol) was added a benzene solution of 2-methoxybenzoic acid (1.17 g, 7.70 mmol). The mixture was refluxed for 3 hr. The water formed during the reaction was removed azeotropically with a Dean and Stark assembly. The clear solution thus obtained was stripped off *in vacuo*. The residue was recrystallized from hot acetone to give colourless crystals of $[Bu^s_2Sn(OOC\text{-}C_6H_4OMe\text{-}2)_2]$ in 70% yield. All other complexes were prepard in a similar manner and were recrystallized from acetone, benzene-hexane or dichloromethane-hexane. Pertinent data for these compounds are given in Table 1.

Results and Discussion

Reactions of dibutyltin oxides with aromatic carboxylic acids in 1:2 stoichiometry in refluxing benzene afforded complexes of the type $[Bu^x_2Sn(OOCAr)_2]$ (x = sec. or tert.; Ar = C_6H_5, C_6H_4OMe-2, 2-C_4H_3O, 2-C_4H_3S, 2-C_5H_4N, 2-$C_4H_3N_2$, 2-C_9H_6N). These are colourless crystalline solids, soluble in common organic solvents.

IR spectra and the NMR data of the complexes containing nitrogen heterocyclic residue (Ar = 2-C_5H_4N, 2-C_9H_6N, 2-$C_4H_3N_2$) were different from other carboxylates. The assignment of IR bands of these complexes has been made by comparison with the *IR spectra of Bu^x_2SnO and the corresponding free acid. The complexes containing nitrogen hetrocycles displayed two or three bands in the region* 1580-1670 cm^{-1} (ν_{as} COO), indicating the presence of free carbonyl group. However, other complexes exhibited a band in the region 1580-1610 cm^{-1} (ν_{as} COO) suggesting bidentate carboxylate group. The

Table 1—M.P., Analyses, IR and ^{1}H NMR data for dibutyltin(IV) carboxylates

Complex	M.P. (°C)	% Analyses, found (Calcd.)				νCO cm^{-1}	^{1}H NMR Data*
		C	H	N	Sn		
$Bu^s_2Sn(FuO)_2$	87-88	47.1 (47.5)	5.4 (5.3)	—	25.9 (26.1)	1610(m)	1.10 (t, 7Hz, MeCH), 1.47 (d, 7Hz, Me), 1.80 (m, CH_2); 2.20 (m, CH-Sn); 6.56 (d, d 1.7 and 4Hz); 7.31 (m); 7.63 (m).
$Bu^t_2Sn(FuO)_2$	164-165	46.5 (47.5)	5.3 (5.3)	—	25.9 (26.1)	1615(m), 1595(m)	1.42 (s, Bu^t, ^3J(Sn-H) 122Hz); 6.47(d,d); 7.23(br); 7.55(br)
$Bu^s_2Sn(Thio)_2$	125-127	44.8 (44.3)	4.2 (4.9)	—	23.9 (24.4)	1580(m)	1.05 (t, 7Hz, MeC-); 1.40 (d, 7Hz, Me); 1.80(m); 2.20(m); 7.05 (m); 7.50 (d,d), 7.80 (d,d)
$Bu^t_2Sn(Thio)_2$	207-208	45.5 (44.3)	5.2 (4.9)	—	24.4 (24.4)	1595(m)	1.42 (s, Bu^t, ^3J(Sn-H) 121Hz); 7.08(m), 7.51(m), 7.84(d,d)
$Bu^s_2Sn(AA)_2$	133-135	53.4 (53.8)	6.1 (6.0)	—	21.8 (22.2)	1610(s)	1.08 (t, 7Hz, CH_3C); 1.48 (d, 7Hz, Me); 1.85(m); 2.20(m); 3.90 (s, OMe); 6.85-7.95(m)
$Bu^t_2Sn(AA)_2$	87-88	53.5 (53.8)	6.1 (6.0)	—	22.7 (22.2)	1595(m)	1.45 (s, Bu^t, ^3J(Sn-H) 120Hz); 3.86 (s, OMe); 6.92-7.80(m)
$Bu^s_2Sn(Benz)_2$	53-54	54.9 (55.6)	6.1 (5.9)	—	25.0 (25.0)	1605(s)	1.11 (t, 7H, MeC); 1.58 (d, 7Hz, Me); 1.85(m); 2.22(m); 7.40-7.62(m); 8.14-8.26(m)
$Bu^t_2Sn(Benz)_2$	156-157	56.1 (55.6)	6.3 (5.9)	—	24.8 (25.0)	1610(s)	1.41(s, Bu^t, ^3J(Sn-H) 120Hz); 7.48-8.18(m)
$Bu^s_2Sn(pyra)_2$	198-200	44.1 (45.1)	5.0 (5.0)	11.5 (11.7)	24.9 (24.8)	1665(m) 1610(m) 1575(w)	1.04(t, 7Hz, Me-C); 1.32(d, 7Hz, Me); 1.75(m); 1.16(m); 8.89, 8.97 (5,6-H, pyra); 9.62 (H-3, pyra)
$Bu^t_2Sn(pyra)_2$	166-167	44.9 (45.1)	5.2 (5.0)	11.5 (11.7)	24.5 (24.8)	1675(m) 1625(w) 1580(w)	1.41(s, Bu^t, ^3J(Sn-H) 125 Hz); 8.78(d, 1Hz, 5 and 6-H pyra); 9.46 (d, 1Hz, 3-H pyra)
$Bu^s_2Sn(Qun)_2$	148-149	57.8 (58.2)	5.2 (5.2)	4.6 (4.8)	20.3 (20.6)	1665(m) 1610(w) 1595(w)	1.05(t, 7Hz, MeC); 1.45(d, 7Hz, Me); 1.80(m); 2.20(m) 7.60-8.60(m) ring protons
$Bu^t_2Sn(Qun)_2$	201-202	58.8 (58.2)	5.6 (5.2)	4.8 (4.8)	20.4 (20.6)	1660(s) 1620(w) 1595(w)	1.39(s, Bu^t, ^3J(Sn-H) 124Hz); 7.68-8.35(m)
$Bu^s_2Sn(pic)_2$	140-142	50.2 (50.3)	5.7 (5.5)	5.7 (5.9)	24.7 (24.9)	1655(vs) 1610(s) 1595(s)	0.95(t, 7Hz, Me-C); 1.15(d, 7Hz, Me), 1.60(m, br); 2.05(br); 7.60(t), 8.05(t); 8.45(d), 8.90(d)
$Bu^t_2Sn(pic)_2$	198-199	50.7 (50.3)	5.8 (5.5)	5.8 (5.9)	25.0 (24.9)	1670(s) 1665(m) 1655(m) 1600(m)	1.13(s, Bu^t, ^3J(Sn-H) 125Hz); 7.50(m), 8.00(m), 8.40(d), 8.70(d)

* s = singlet; d = doublet; t = triplet; d,d = doublet-doublet; m = multiplet; br = broad

absorption bands in the regions 515-560 (usually weak) and 425-500 cm^{-1} (absent in the spectra of the corresponding free ligand) were tentatively assigned to ν(Sn-C) and ν(Sn-O) respectively[8-10].

The ^{1}H NMR spectra exhibited expected peak multiplicities and integration. The Bu^s_2Sn(IV) compounds displayed a doublet for 2-methyl group and a triplet and a multiplet for the ethyl group. The >CH-Sn proton resonances appeared as a multiplet. The Bu^t_2Sn(IV) complexes showed a singlet with $^3J(^{119}Sn\text{-}^1H)$ for the methyl protons of the Bu^t group at δ ~ 1.4 ppm, except $[Bu^t_2Sn(OOCC_5H_4N\text{-}2)_2]$ for which a singlet at δ1.13 ppm was observed. The magnitude of $^3J(^{119}Sn\text{-}^1H)$ for these complexes varies between 120 and 125 Hz and is in agreement with the values reported for di-*t*-tutyltin(IV) compounds[6,11]. The ^3J(Sn-H) value is much greater from the ^2J(Sn-H) observed in analogous dimethyltin(IV) compounds.

Table 2—$^{13}C\{^1H\}$ and $^{119}Sn\{^1H\}$ NMR data for dibutyltin(IV) carboxylates in $CDCl_3$

Complex[a]	δ $^{119}Sn\{^1H\}$ in ppm	$^{13}C\{^1H\}$ NMR data				
		butyltin carbons			ligand carbons	
		C-1[b]	methyl	ethyl	carbonyl	ring carbons
$[Bu^s_2Sn(FuO)_2]$	−170.5	42.2	16.3	27.0,14.1	166.6	144.6(C-2), 118.7(C-3), 111.7(C-4), 146.3(C-5)
$[Bu^t_2Sn(FuO)_2]$	−195.4	46.6	29.6	—	166.3	144.9(C-2), 118.8(C-3), 111.8(C-4), 146.4(C-5)
$[Bu^s_2Sn(Thio)_2]$	−180.6	42.1 (545)	16.5	27.2,14.2	170.8	132.8(C-2), 133.9(C-3), 127.7(C-4), 134.2(C-5)
$[Bu^t_2Sn(Thio)_2]$	−207.6	46.5	29.7	—	170.3	132.8(C-2), 134.2(C-3,5), 127.8(C-4)
$[Bu^s_2Sn((AA)_2]$	−187.5	41.1	16.5	27.2,14.1	175.5	55.7(OMe), 120.2(C-1), 158.9(C-2), 111.6(C-3), 133.1(C-4), 119.7(C-5), 132.0(C-6)
$[Bu^t_2Sn(AA)_2]$	−215.2	45.3	29.6	—	175.1	55.7(OMe), 120.5(C-1), 158.7(C-2), 111.7(C-3), 132.9(C-4), 119.7(C-5), 131.7(C-6)
$[Bu^s_2Sn(Benz)_2]$	−188.6	41.8 (560)	16.8	27.5,14.4	175.7	133.1(C-1), 130.5(C-2,6), 128.3(C-3,4,5)
$[Bu^t_2Sn(Benz)_2]$	−215.4	45.4	29.5	—	174.9	132.5(C-1), 130.1(C-2,6), 127.9(C-3,4,5)
$[Bu^s_2Sn(pyra)_2]$	—	44.4	16.9	27.3,14.4	167.6	142.9(C-2), 147.7(C-3), 148.3(C-5), 142.3(C-6)
$[Bu^t_2Sn((pyra)_2]$	−236.8	47.5	29.7	—	169.3	143.3(C-2,6), 147.0(C-3), 147.8(C-5)
$[Bu^s_2Sn((Qun)_2]$	−245.6	43.7	16.6	27.1,13.8	168.6	149.2,145.1,138.7,130.6 129.2,128.3,127.9,121.3
$[Bu^t_2Sn(Qun)_2]$	−252.1	47.7	29.8	—	170.3	148.7,146.0,137.8,130.2, 129.1,128.2,127.5,121.4
$[Bu^s_2Sn(pic)_2]$	−347.1	43.0	16.7	27.1,14.0	165.6	147.9(C-2),127.2(C-3), 140.5(C-4),125.6(C-5), 146.2(C-6)
$[Bu^t_2Sn(pic)_2]$	−374.3	45.1 (681)	30.0	—	165.6	147.4(C-2),127.0(C-3), 140.3(C-4),125.2(C-5), 145.6(C-6)

[a] FuO = 2-furan carboxylate; Thio = 2-thiophene carboxylate; AA = 2-methoxy benzoate; Benz = benzoate; pyra = 2-pyrazine carboxylate; Qun = 2-quinoline carboxylate, pic = 2-pyridine carboxylate

[b] values in parantheses are $^1J(^{119}Sn\text{-}^{13}C)$ in Hz

Although the magnitude of ^2J(Sn-H) in dimethyltin(IV) compounds has been correlated with the coordination number of tin[12], the ^3J(Sn-H) is seemingly unaffected by the coordination number of tin.

The ^{13}C NMR spectra of these complexes exhibited single resonances for the chemically equivalent carbon atoms of butyltin and ligand moities. The C-1 carbon resonance of the butyl group attached to tin showed ligand dependence, while the methyl and ethyl carbon resonances are little affected. The carbonyl carbon resonance is deshielded in all the derivative on complexation.

The ^{119}Sn NMR spectra of these complexes showed a single resonance in the region δ-170.5 to -374.3 ppm. The observed signals are considerably shielded from the corresponding di-*n*-butyltin(IV) compounds for which skew-trapezoidal planar geometry has been established[13]. Shielding is greater for Bu^t_2Sn(IV) complexes than that for the corresponding Bu^s_2Sn(IV) carboxylates. This is consistent with the fact that for a series of organotin compounds the ^{119}Sn chemical shift moves to lower frequency as the electron releasing power of the alkyl group on tin increases. As is evident from Table 2 nature of the ligand also influences the ^{119}Sn NMR shifts. The chemical shifts for furoic,

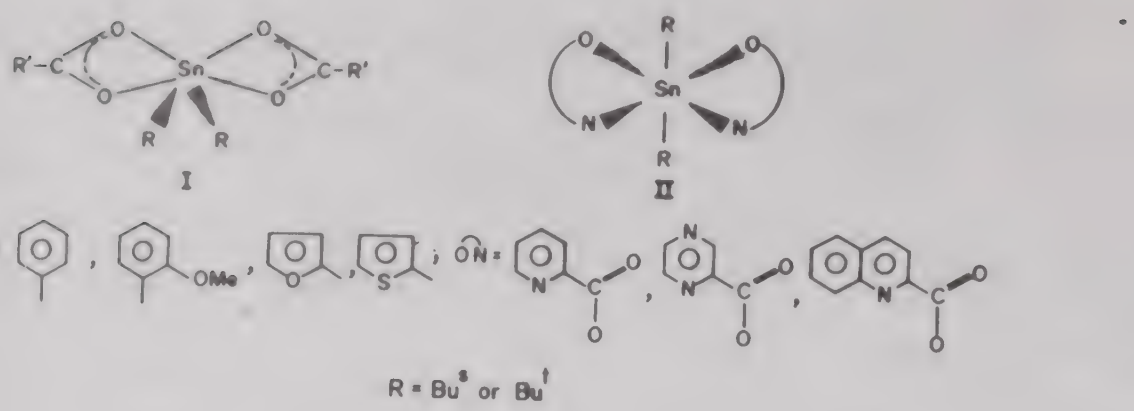

thiophenic, anisic or benzoic acid complexes appear in one region while those for picolinic acid complexes are most shielded. The signals for pyrazine and 2-quinoline carboxylic acids complexes lie in between these two regions. The *n*-alkyl complexes of the former series of ligands have now been shown to adopt an octahderal geometry with asymmetrically chelated carboxylate groups[10,13-15] (**I**) while the picolinate complexes are polymeric in the solid state[16] but monomeric in solution[17] with $\widehat{ON}$ chelation. The spetroscopics data of $Bu^s_2Sn(IV)$ and $Bu^t_2Sn(IV)$ complexes are comparable to the data for analogous di-*n*-alkyltin(IV) compounds and, therefore, can be interpreted in terms of octahedral structures with chelating carboxylate group and $\widehat{ON}$ chelation (**II**). The presence of a free carbonyl band in the IR spectra of the complexes of pyrazine and quinoline carboxylic acids suggests that these complexes also have structures similar to picolinic acid derivatives.

Acknowledgement

We thank Dr J P Mittal, Head, Chemistry Division for his interest in the work and the Analytical Chemistry Division for microanalyses. The DAE is thanked for the award of a Junior Research Fellowship to VBM.

References

1 Davies A G & Smith P J, *Comprehensive Organometallic Chemistry*, edited by G Wilkinson, F G A Stone & E W Abel (Pergamon Press, Oxford), Vol.2, 1982; Harrison P G, *Chemistry of Tin* (Blackie, London), 1989; Evans C J & Karpel S, *J organomet Chem Lib*, 16 (1985); Omae I, *J organomet Chem Lib*, 21 (1989).

2 Otera J, Yano T & Okawara R, *Organometallics*, 5 (1986) 1167.

3 Molloy K C, Purcell T G, Quill K & Nowell I W, *J organomet Chem*, 267 (1984) 237: Molloy K C, Quill K & Nowell I W, *J chem Soc (Dalton Trans)*, (1987) 101.

4 Nakanishi M & Tsuda A, *Japan Pat*, 15690 (1964) [*CA*, 62 (1965) 6513b]; M & T International, B V Neth, Applied, 7312329 (1974) [*CA*, 81 (1974) 91732b].

5 Maeda Y & Okawara R, *J organomet Chem*, 10 (1967) 247; Sandhu G K, Boparai N S & Sandhu S S, *Synth React inorg met-org Chem*, 10 (1980) 535; Crowe A J, Hill R, Smith P J, Brooks J S & Formstone R, *J organomet Chem*, 204 (1981) 47; Sandhu G K, Gupta R, Sandhu S S & Parish R V, *Polyhedron*, 4 (1985) 81; Sandhu G K, Gupta R, Sandhu S S, Parish R V & Brown K, *J Organomet Chem*, 279 (1985) 373; Lockhart T P, Manders W F & Holt E M, *J Am chem Soc*, 108 (1986) 6611; Lockhart T P, Calabrese J C & Davidson F, *Organometallics*, 6 (1987) 2479; Narula S P, Bharadwaj S K, Sharma H K, Mairesse G, Barbier P & Nowogrocki G, *J chem Soc Dalton Trans*, (1988) 1719; Sandhu G K, Sharma N & Tiekink E R T, *J organomet Chem*, 403 (1991) 119.

6 Dietzel S, Jurkschat K, Tzshach A & Zschunke A, *Z anorg allg Chem*, 537 (1986) 163.

7 Mokal V B & Jain V K, *J organomet Chem* (submitted).

8 Perruzzo V, Plazzogna G & Taglivini G, *J organomet Chem*, 40 (1972) 121.

9 Sandhu G K & Verma S P, *Polyhedron*, 6 (1987) 587.

10 Visalakshi R, Jain V K & Rao G S, *Spectrochim Acta*, 43A (1987) 1235; Parulekar C S, Jain V K, Das T K and Tiekink E R T, *J organomet Chem*, 387 (1990) 163; Vatsa C, Jain V K, Das T K & Tiekink E R T, *J organomet Chem*, 396 (1990) 9; Vatsa C, Jain V K & Das T K, *Main Group Met Chem*, 13 (1990) 279; Vatsa C, Jain V K, Das T K & Tiekink E R T, *J organomet Chem*, 408 (1991) 157.

11 Gielen M & Topart J, *Bull Soc Chim Belg*, 84 (1975) 13; Otera J, Yano T & Kusakabe K, *Bull chem Soc Japan*, 56 (1983) 1057.

12 Lockhart T P, Manders W F & Zuckerman J J, *J Am chem Soc*, 107 (1985) 4546.

13 Tiekink E R T, *Appl organomet Chem*, 5 (1991) 1.

14 Tiekink E R T, *J organomet Chem*, 408 (1991) 323.

15 Vatsa C, Jain V K, Das T K & Tiekink E R T, *J organomet Chem*, 410 (1991) 135.

16 Lockhart T P & Davidson F, *Organometallics*, 6 (1987) 2471.

17 Vatsa C, Jain V K & Das T K, *Indian J Chem*, 30A (1991) 451.

Indian Journal of Chemistry
Vol. 31A, November 1992, pp. 865-869

Studies on copper(II) and zinc(II) mixed ligand complexes involving some potentially tridentate ligands

M Sivasankaran Nair*, P Thillai Arasu & R Jothibai Margret
Department of Chemistry, Manonmaniam Sundaranar University, St. Mark's Road, Schaffter Hall, Palayamkottai 627 002
and
C Sudha & M Sankaranarayana Pillai
Department of Chemistry, S T Hindu College, Nagercoil 629 002

Received 11 October 1991; revised 15 January 1992; accepted 17 March 1992

The computer-based analysis of the *p*H titration data obtained in the M – A – B[M = Cu(II)/Zn(II); A = L-aspartic acid (aspt) and iminodiacetic acid (imda) and B = DL – 2, 3-diaminopropionic acid (dapa), DL-2, 4-diaminobutyric acid (daba), and DL-Ornithine (Orn)] mixed ligand systems show the presence of mixed species of the types $MABH_2$, MABH and/or MAB in addition to the various binary species due to ligands A and B. The modes of binding of ligands in various species are discussed on the basis of the results obtained.

In our laboratories, investigations on the binary and mixed ligand complex systems containing diaminocarboxylic acids are being carried out for quite sometime[1-5]. The present paper reports the complexometry involved in the Cu(II) and Zn(II) mixed ligand systems containing L-aspartic acid (aspt) and iminodiacetic acid (imda) as the primary ligands (A) and DL-2, 3-diaminopropionic acid (dapa), DL-2, 4-diaminobutyric acid (daba) and DL-ornithine (Orn) as the secondary ligands (B). All the studies have been carried out by *p*H titrimetry at 37°C and ionic strength of 0.15 ($NaClO_4$).

Materials and Methods

All the measurements were carried out as described earlier[5]. The stock solutions of the metal perchlorate were prepared and estimated as described earlier[2,3]. All the ligands used were Fluka product of Puriss quality. Computations have been made with the aid of SCOGS Computer program[10] on a CYBER 180/830A computer. The results obtained for the ternary systems are given in Tables 2 and 3. The binary stability constants[1,5-9] under the present experimental conditions (Table 1) have been kept as non-refinable parameters during the computation of stability constants of ternary complexes. The charges of all the complexes reported in this paper are omitted for clarity.

Results and Discussion

The mixed ligand complex species of stoichiometry MABH and MAB have been detected in the Cu(II) - aspt(A) - dapa, daba and Orn(B) and Zn(II) - aspt(A) - dapa and Orn(B) systems. The Cu(II) - imda(A) - dapa(B) and Zn(II) - imda(A) - dapa(B) systems showed the presence of $MABH_2$ and MABH types of mixed species. Only the MAB type of mixed ligand species have been found to be present in the Cu(II) - imda(A) - daba(B), Zn(II) - aspt(A) - daba(B), and Zn(II) - imda(A) - Orn(B) systems. The Cu(II) - imda (A) - Orn(B) system showed the presence of MABH type of species. The $MABH_2$, MABH and MAB types of mixed species have been found to be present in the Zn(II) - imda(A) - daba(B) system. The various binary species accounted due to ligands A and B are given in Table 1.

Stability and structure of MABH and $MABH_2$ types of ternary species

The log K^{CuA}_{CuABH} values obtained in the Cu(II) - aspt(A)-dapa, daba and Orn(B) and also in the Cu(II) - imda(A) - dapa and Orn(B) mixed ligand systems follow the trends of log β_{CuBH} values obtained in the respective Cu(II) - dapa, daba or Orn(B) binary systems (Table 1). Similarly the log K^{ZnA}_{ZnABH} values obtained in the Zn(II) - aspt(A) - dapa and Orn(B) and also in the Zn(II) - imda(A) - dapa and daba(B) systems follow the trends of the respective log β_{ZnBH} values (Table 1). This suggests that the extra proton in the MABH type of species in the Cu(II) and Zn(II) ternary systems resides with the dapa, daba or Orn secondary ligand. In the

Table 1—Stability constants of Cu(II) Zn (II) complexes of aspt, imda, dapa, daba and Orn binary systems [Temp. = 37°C μ = 0.15 $NaClO_4$]

Parameters	Copper (II)					Zinc (II)				
	aspt[a]	imda[b]	dapa[c]	daba[c]	Orn[c]	aspt[d]	imda[e]	dapa[f]	daba[f]	Orn[f]
$\log \beta_{HB}$	9.27(3)	9.11(2)	9.37(2)	9.93(2)	10.22(1)					
$\log \beta_{H_2B}$	12.87(5)	11.80(1)	15.98(3)	18.02(4)	18.85(2)					
$\log \beta_{H_3B}$	14.82(9)	13.56(4)	17.37(5)	19.88(6)	20.99(4)					
$\log \beta_{MBH}$	—		15.37(4)	16.99(3)	17.67(2)	—	—	13.61(4)	14.22(4)	14.56(2)
$\log \beta_{MB}$	9.46(9)	10.48(9)	10.61(4)	10.94(3)	—	5.71(4)	7.00(1)	—	—	6.69(3)
$\log \beta_{MB_2H_2}$	—	—	30.16(5)	32.92(4)	34.32(3)	—	—	25.70(3)	27.04(16)	27.83(11)
$\log \beta_{MB_2H}$	—	—	25.32(6)	26.89(4)	26.12(6)	—	18.17(5)	—	21.47(4)	—
$\log \beta_{MB2}$	17.02(9)	16.32(8)	20.18(5)	19.15(6)	—	9.65(8)	12.39(2)	13.70(2)	13.44(4)	—

aspt and imda become the primary ligand A in the ternary systems.
[a]Ref: 6 [b]Ref: 7 [c]Ref: 1 [d]Ref: 9 [e]Ref: 8 [f]Ref: 5.

Table 2—Stability constants of Cu(II) - aspt/imda(A) - dapa, daba and Orn(B) mixed ligand systems [Temp. = 37°C, μ = 0.15 $NaClO_4$]

	Cu(II) - aspt(A) - B systems			Cu(II) - imda(A) - B systems		
	Ligands B			Ligands B		
	dapa	daba	Orn	dapa	daba	Orn
$\log \beta_{CuABH_2}$	—	—	—	29.49(3)	—	—
$\log \beta_{CuBH}$	24.02(9)	25.30(5)	25.80(5)	24.38(3)	—	25.22(3)
$\log \beta_{CuAB}$	18.74(3)	19.04(4)	17.57(4)	—	21.04(3)	—
$pK^{H}_{CuABH_2}$	—	—	—	5.11	—	—
pK^{H}_{CuABH}	5.28	6.26	6.23	—	—	—
$\log K^{CuBH}_{CuABH_2}$	—	—	—	4.12	—	—
$\log K^{CuBH}_{CuABH}$	8.65	8.31	8.13	9.01	—	7.55
$\log K^{CuA}_{CuABH}$	14.56	15.84	16.34	13.90	—	14.74
log Q	14.65	15.37	15.58	15.01	—	15.00
$\Delta \log K_{CuABH}$	−0.61	−1.42	−1.33	−1.47	—	−2.93
$\log X_{CuABH}$	0.68	0.66	0.26	2.28	—	−0.20
$\log K^{CuA}_{CuAB}$	9.28	9.58	8.11	—	10.56	—
$\log K^{CuB}_{CuAB}$	8.13	8.10	—	—	10.10	—
$\Delta \log K_{CuAB}$	−1.33	−1.36	—	—	−0.38	—
$\log X_{CuAB}$	0.28	1.91	—	—	5.58	—

MBH, MB_2H_2 or MB_2H types of species in the Cu(II)/Zn(II) - dapa, daba or Orn(B) binary systems, it has been shown that the extra proton is attached with the terminal amino group of the respective ligands. The same should be the site of protonation in the MABH mixed species in the above ternary systems. The log Q values ($\log Q = \log \beta_{MABH} - \log \beta_{HB}$) obtained in the above ternary systems (Tables 2 and 3) compare well with the values expected for the glycine-like mode of binding of the protonated secondary ligands with the metal ion and these values follow the trends of ($\log \beta_{H_3B} - \log \beta_{HB}$) as expected based on the basicity of the secondary ligands. However, in the Cu(II) - imda(A) - dapa(B), and Zn(II) - aspt(A) dapa(B) systems, the log Q values obtained (Tables 2 and 3) are comparable or slightly higher than those values in the corresponding Orn secondary ligand mixed systems, though the parameter ($\log \beta_{H_3B} - \log \beta_{HB}$) is lesser for dapa as compared to that of Orn. Similarly, the log Q value obtained (Table 3) in the Zn(II) - imda(A) - dapa(B) system is slightly higher than that obtained in the Zn(II) - imda(A) - daba(B) system, though ($\log \beta_{H_3B}$ - $\log \beta_{HB}$) is lesser for dapa as compared to that for daba. These trends suggest that the MABH types of ternary species in the dapa secondary ligand mixed systems cited above have higher stability compared to the corresponding Orn or daba secondary ligand mixed systems. This may be accounted by considering one more structure for the

Table 3—Stability constants of Zn(II) - aspt/imda(A) - dapa, daba and Orn(B) mixed ligand systems [Temp. = 37°C, μ=0.15 $NaClO_4$]

	Zn(II) - aspt(A) - B systems			Zn(II) - imda(A) - B systems		
	Ligands B			Ligands B		
	dapa	daba	Orn	dapa	daba	Orn
$\log \beta_{ZnABH_2}$	—	—	—	24.01(3)	24.65(2)	
$\log \beta_{ZnABH}$	19.23(2)	—	19.74(5)	18.91(3)	19.28(2)	—
$\log \beta_{ZnAB}$	11.70(9)	11.73(2)	12.28(2)	—	14.04(2)	12.54(5)
$pK^{H}_{ZnABH_2}$	—	—	—	5.10	5.37	—
pK^{H}_{ZnABH}	7.53	—	7.46	—	5.24	—
$\log K^{ZnBH}_{ZnABH_2}$	—	—	—	10.40	10.43	—
$\log K^{ZnBH}_{ZnABH}$	5.62	—	5.18	5.30	5.06	—
$\log K^{ZnA}_{ZnABH}$	13.52	—	14.03	11.91	12.28	—
log Q	9.86	—	9.52	9.54	9.35	—
$\Delta \log K_{ZnABH}$	−0.09	—	−0.53	—	—	—
$\log X_{ZnABH}$	3.11	—	2.00	−0.27	−0.87	—
$\log K^{ZnA}_{ZnAB}$	5.99	6.02	6.57	—	7.04	5.54
$\log K^{ZnB}_{ZnAB}$	—	—	5.59	—	—	5.85
$\Delta \log K_{ZnAB}$	—	—	−0.12	—	—	
$\log X_{ZnAB}$	0.05	0.37	—	—	2.25	

MABH species in the dapa secondary ligand system where the proton is attached with the α-amino group of dapa and the metal-ligand binding is between the terminal amino and carboxylato groups.

The log K^{CuBH}_{CuABH} values obtained in the Cu(II) - aspt(A) - dapa, daba and Orn(B) systems (Table 2) are higher than those expected for the glycine - like mode of binding of aspt demonstrating the tridentate nature of aspt in its CuABH species. The same parameter obtained in the Cu(II) - imda(A) - dapa(B) system bears favourable comparison with the log K^{Cu}_{CuA} value (Table 1) in the Cu(II) - imda(A) binary system after giving due allowance for the statistical considerations, indicating that imda should bind the metal in a tridentate manner in its CuABH type of species. However, in the Cu(II) - imda(A) - Orn(B) mixed system, the above parameter is slightly lower than the log K^{Cu}_{CuA} value in the Cu(II) - imda(A) binary system suggesting that imda binds the metal through its imino and one of the carboxylato groups. A similar argument in the case of ZnABH species in the Zn(II) - aspt(A) - dapa and Orn(B) systems show that the primary ligand (aspt) binds the metal in a tridentate manner, while in the ZnABH type of species in the Zn(II) - imda(A) - dapa and daba(B) systems, the primary ligand (imda) binds the metal in a bidentate manner.

The Δlog *K* and log *X* values[5] calculated for the CuABH type of species in most of the title systems do not deviate much from the statistical values demonstrating less preference for the formation of

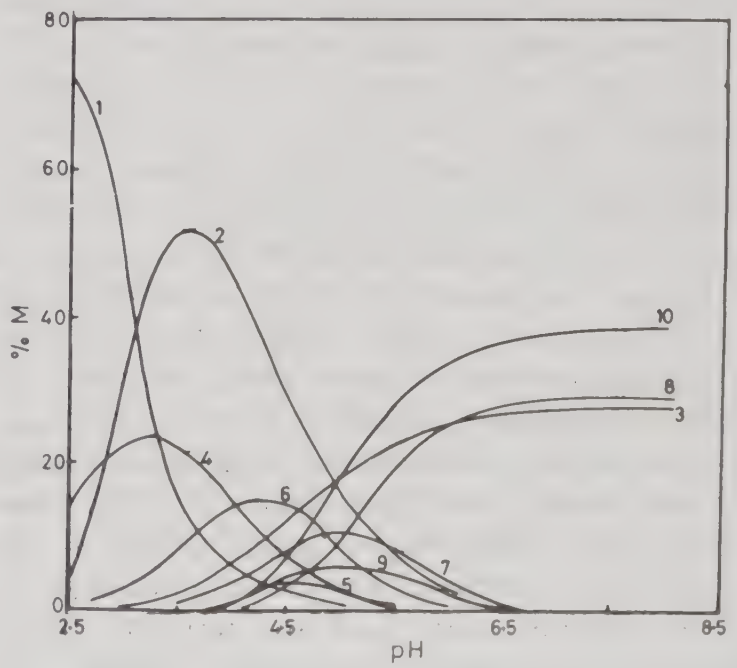

Fig. 1—Distribution curve for the Cu(II) - aspt(A) - dapa(B) ternary system ($C_M = C_A = C_B = 0.003$). (1) metal ion (M = Cu) (2) MA, (3) MA_2, (4) MBH, (5) MB (6) MB_2H_2 (7) MB_2H, (8) MB_2, (9) MABH and (10) MAB

ternary species compared to the binary analogues. The same trends have also been reflected in the species distribution plots, where the percentage of the total metal ion in the form of CuABH type of species has not reached the statistically expected of 50% of the total metal ion. As shown in the distribution plot of Cu(II) - aspt(A) - dapa(B) system (Fig. 1) about 5% of the total metal has been found to be present in the form of CuABH type of species. The computer calculations excluding this species in this system has not improved the statistical

fit. In most of the Zn(II) mixed ligand systems reported here, the $\Delta \log K$ and $\log X$ values obtained for the ZnABH species (Table 3) are higher than the statistical values indicating their enhanced stabilities. In the species distribution plots, appreciable amounts of the total metal ion have been found to be present in the form of ZnABH species. The $\Delta \log K_{MABH}$ values in the Cu(II) - imda(A) Orn(B) and Zn(II) - imda(A) - dapa and daba(B) systems have not been computed because the $\log \beta_{MA}$ value for the bidentate binding of imda with the Cu(II) and Zn(II) are not available,i.e.,in the above ternary systems, the primary ligand (imda) binds the metal in a bidentate manner, while $\log \beta_{MA}$ values in the Cu(II)/Zn(II) - imda(A) systems reported in Table 1 are those for the tridentate binding of the ligands.

The $MABH_2$ type of species have been detected in the Cu(II) - imda(A) - dapa(B) ad Zn(II) - imda(A) - dapa and daba(B) ternary systems. It may be inferred that of the two protons in this species, one would reside with the imda primary ligand and the other would be attached with the respective secondary ligands. The $pK^{H}_{CuABH_2}$ value of 5.11 in the former system suggests that the imino group of the imda ligand should be protonated. In case, this proton is attached with the carboxylato groups of this ligand, this parameter should be below 2.7 log units, because the pK_a values for the two carboxylato groups and imino group are 2.69, 1.76 and 9.11 respectively. Similarly from the $pK^{H}_{ZnABH_2}$ values in the latter two systems, it may be concluded that one proton should be attached with the imino group of the imda primary ligand (Table 3). As outlined above the second proton in all the above systems should reside with the terminal amino group of the respective secondary ligands. The parameters $\Delta \log K$ and $\log X$ values could not be computed for the $MABH_2$ type of species in the above three systems, because the stability constant data for some of the binary constants are not available (Table 1). In all the above three systems, appreciable amounts of the metal ion have been found to be present in the form of this species. It was observed that about 54% of the total Cu(II) has been found to be present in its form at *p*H 3.2 in a 1:1:1 solution of Cu(II), imda and dapa. In the Zn(II) - imda(A) - dapa(B) system, ~34% of the total metal ion has been found to be present in its form at a *p*H of 5.02 and in the corresponding daba secondary ligand system, ~40% of the total metal ion has been found to be present in its form in the same *p*H region.

Stability and structure of MAB type of ternary species

The $\log K^{CuA}_{CuAB}$ values obtained in the Cu(II) - aspt(A) - dapa and daba(B) systems (Table 2) are higher than those expected for the glycine - like or diamine - like modes of binding of dapa and daba secondary ligands, indicating the terdentate mode of binding of these ligands in their CuAB ternary species. However, this parameter obtained in the Cu(II) - aspt(A) - Orn(B) system is comparable to the value expected for the glycine - like mode of binding of Orn secondary ligand in its CuAB species. But in the corresponding Zn(II) mixed ligand system, $\log K^{ZnA}_{ZnAB}$ value of 6.57 is comparable to the $\log K^{Zn}_{ZnB}$ value of 6.69 in the Zn(II) - Orn(B) binary system suggesting that Orn binds Zn(II) in a tridentate manner in its ZnAB ternary species. Such a comparison is not possible in the case of dapa and daba secondary ligand systems because the $\log K^{Zn}_{ZnB}$ values in the Zn(II) - dapa and daba(B) binary systems are not available (Table 1). However, from the trends in the $\log \beta_{ZnAB}$ values given in Table 3 in these systems, it may be inferred that the dapa and daba secondary ligands should be terdentate in their ZnAB species. By following the same type of arguments in the Cu(II) - imda(A) - daba(B) system and Zn(II) - imda(A) daba and Orn(B) systems, it may be concluded that imda binds both Cu(II) and Zn(II) in a terdentate manner, while in presence of Orn, imda binds Zn(II) in a bidentate manner.

The $\Delta \log K$ and $\log X$ values[11] obtained in the Cu(II) - aspt(A) - dapa and daba (B) systems do not deviate much from the statistical values. However, the percentage distribution plots show that the amount of metal ion present in the form of CuAB type of species in all the above systems are well above the statistically expected value of 50% of the total metal ion (Fig. 1) in the case of Cu(II) - aspt(A) dapa(B) system. The above two parameters obtained in the Cu(II) - imda(A) - daba(B) system is more positive than the corresponding statistical value indicating the marked stabilities of the CuAB species. In a 1:1:1 solution of Cu(II), imda and daba, about 98% of the total metal ion has been found to be present in the form of CuAB species in the *p*H range of 7.2 to 7.6. The $\Delta \log K$ value obtained for the ZnAB species in the Zn(II) - aspt(A) - Orn(B) system is more positive compared to the corresponding statistical value indicating its higher stability. This parameter could not be calculated in the Zn(II) - imda(A) - daba(B) and

Orn(B) systems because log K^{Zn}_{ZnB} value is not available in the Zn(II) - daba(B) system and this parameter is not available for the bidentate binding of Orn in the Zn(II) - Orn(B) binary system. The log X_{ZnAB} values obtained in the Zn(II) - aspt(A) - dapa and daba(B) systems do not indicate the marked stabilities for the ZnAB species compared to the ZnA_2 and ZnB_2 binary species. However, this parameter obtained in the Zn(II) - imda(A) - daba(B) system is more positive compared to the statistical value, demonstrating marked stability for the ternary complex species. The maximum amount of the metal ion found to be present in the form of ZnAB species is ~59% in the Zn(II) - aspt(A) - dapa(B) system and 18% in both the Zn(II) - aspt(A) - daba and Orn(B) systems in the *p*H range of 7.2. The respective amounts of ZnAB species found to be present in the Zn(II) - imda(A) -daba and Orn(B) systems are 80% and 15% of the total metal ion in the *p*H range of 7.5.

References

1 Nair M S & Santappa M, *J chem Soc Dalton Trans*, (1981) 992; (1982) 561.

2 Nair M S, Chalapathy K V, Santappa M & Murugan P K, *Inorg Chem*, 21 (1982) 2418; ibid 21 (1982) 142.

3 Nair M S, Sivasankar B & Rengaraj K, *Indian J Chem* 26A (1987) 52.

4 Nair M S, Manickam S T D, Arasu P T & Natarajan C, *Proc Indian Acad Sci (Chem Sci)*, 102 (1990) 731.

5 Nair M S, Pillai M S & Ramalingam S K, *J chem Soc Dalton Trans*, (1986) 1.

6 Nair M S, Chellam E, Arasu P T & Natarajan C, *Indian J Chem*, 29A (1990) 1233.

7 Thavaseeli J E, *M Phil Dissertation*, Madurai Kamaraj University 1989.

8 Rajathirumoni P,*M Phil Dissertation*, Madurai Kamaraj University 1990.

9 Sudha C, *M Phil Dissertation*, Madurai Kamaraj University 1990.

10 (a) Sayce I G, *Talanta*, 15 (1968) 1397; 18 (1971) 653.
(b) Sayce I G & Sharma V S, *Talanta*, 19 (1972) 831.

11 Sigel H, *IUPAC coordination chemistry*-20 edited by D Banerjea (Pergamon Press, Oxford), 1980, p 27.

Indian Journal of Chemistry
Vol. 31A, November 1992, pp. 870-873

Notes

Dielectric characterization of BTO-derived barium titanate ($BaTiO_3$) ceramics†

H S Potdar, S B Deshpande, P D Godbole & S K Date*
Physical Chemistry Division, National Chemical Laboratory, Pune 411 008, India

Received 12 March 1992; accepted 15 May 1992

Ultrafine barium titanate (BT) powders, produced by controlled pyrolytic decomposition of 'BTO' (precipitated by a novel chemical route) in air at 700°C/5 hr, are sintered in the form of pellets at 1250°/4 hr to get ceramic compacts with density ≈ 91%. These compacts show nearly uniform microstructure with average grain size ≈ 4.00 μm, dielectric constant (ε_{RT}) = 1250, ε_{max} (T = 121°C) ≈ 7600 and tan δ = 1.5×10^{-2}.

The preparation of stoichiometric submicron size ceramic powders[1] at low temperatures using chemical methods is an area of considerable interest and technological significance. The synthesis of electronic materials having high dielectric constant[2,3] and low dielectric loss (e.g. $BaTiO_3$) is of particular importance for the manufacture of capacitors and sensors.

Three low temperature methods[4] have been reported for the preparation of barium titanate in the literature. These are: (1) sol-gel process[5], (2) modified alkoxide synthesis[6] and (3) chemical coprecipitation[7]. In sol-gel and modified alkoxides routes, controlled hydrolysis reactions of metal alkoxides have been used to prepare monodispersed oxide powders of controlled size and shape. During the hydrolysis of mixed (Ba & Ti) precursors, two main problems are encountered: (i) irregular chemical bonding with two metals and (ii) heterogeneous polycondensation. In addition, the starting chemicals are costly.

To overcome these difficulties, we have reported a simple chemical method[8] to precipitate a molecular precursor, namely $BaTiO(C_2O_4)_2.4H_2O$ (BTO), using water soluble salts — barium acetate and potassium titanyl oxalate. The well characterized 'BTO' precipitate was further converted to submicron (0.2 μm) size spherical stoichiometric BT powders by pyrolytic decomposition in air in the temperature range 550°-700°C. Resulting BT powders were characterized using various techniques.

The primary objective of the present investigation is to further characterize BT in the form of sintered ceramic compacts for dielectric/ferroelectric properties. The temperature dependence of dielectric constant (ε) and loss factor (tan δ) support strongly the formation of high quality BT powders and compacts.

Experimental

The detailed experimental procedure adopted during the present studies is summarized in a processing flow-chart (Fig.1).

The well-characterized potassium-free (conc. < 10 ppm) dry precipitate of 'BTO' was calcined in air at 700°C/5 hr to obtain stoichiometric BT powders. These powders were then cold-pressed into discs (diameter = 20 mm, thickness = 2 mm) at a pressure of 5 tons/sq. inch with 2% PVA binder. The discs were sintered as a stack of four pieces in air at 1250°C/4 hr. The furnace was then allowed to cool at its natural cooling rate.

XRD and SEM techniques were used to identify crystalline phases and microstructure in the final ceramic BT ccompacts.

The sintered compacts were then lapped up to 0.5 mm thickness with fine emery powder paste. These

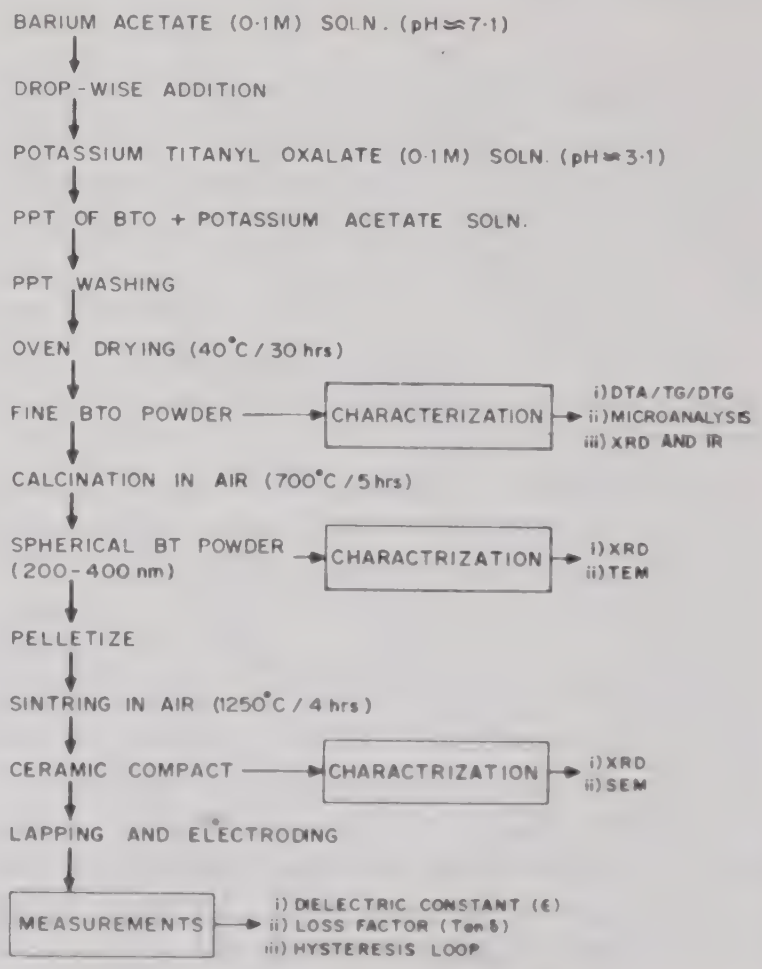

Fig. 1 Processing flow-chart

† NCL Comm. No.5283.

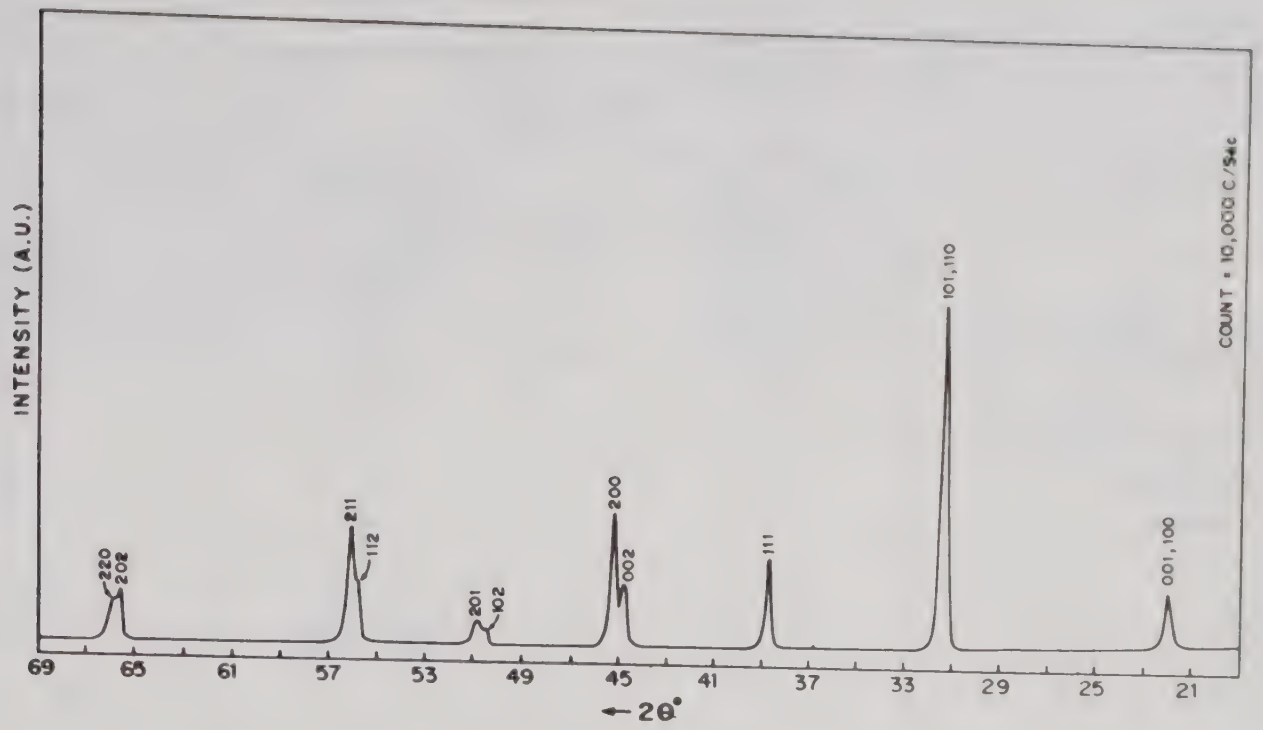

Fig. 2—XRD of sintered BT ceramic disc

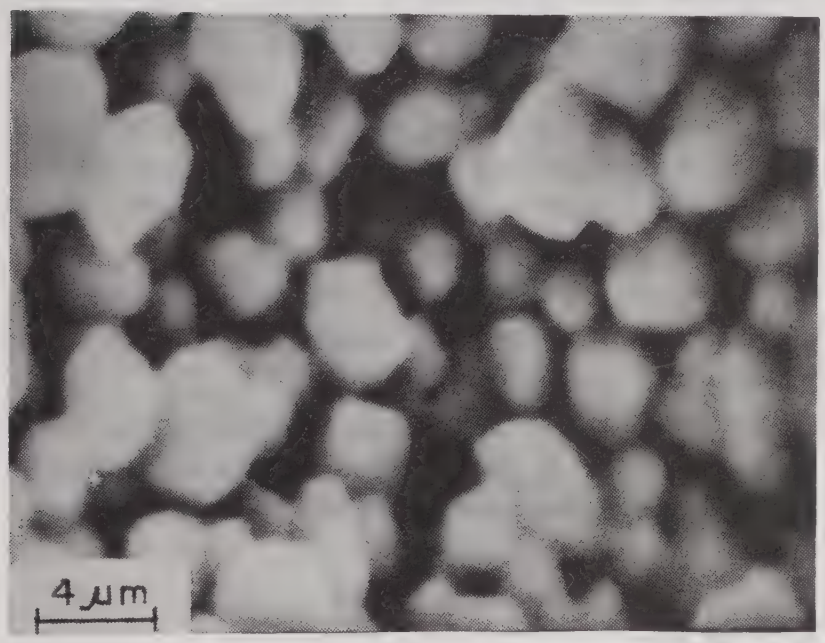

Fig. 3—SEM of sintered BT ceramic disc

lapped compacts were coated with conducting silver paint on both sides and fired in air at 600°C/2 hr to cure the paint.

Dielectric measurements were done employing a commercial LCR bridge at 1 kHz frequency. The temperature dependence of dielectric constant (ε) and loss factor (tan δ) were studied to estimate the Curie temperature (T_c, °C). Finally the values of the spontaneous polarization (P_s), coercive field (E_c) and break down voltage (E_b) were determined from hysteresis-loop measurements using a (home-built) Sawyer-Tower circuit[9].

Results and discussion

The pressed pellets of these powders showed green density ≈ 60%, which increased after sintering at 1250°C/4 hr, to density (5.5 g/cm³) ≈ 91% of theoretical density of BT.

Fig. 2 shows the XRD plot of a sintered ceramic

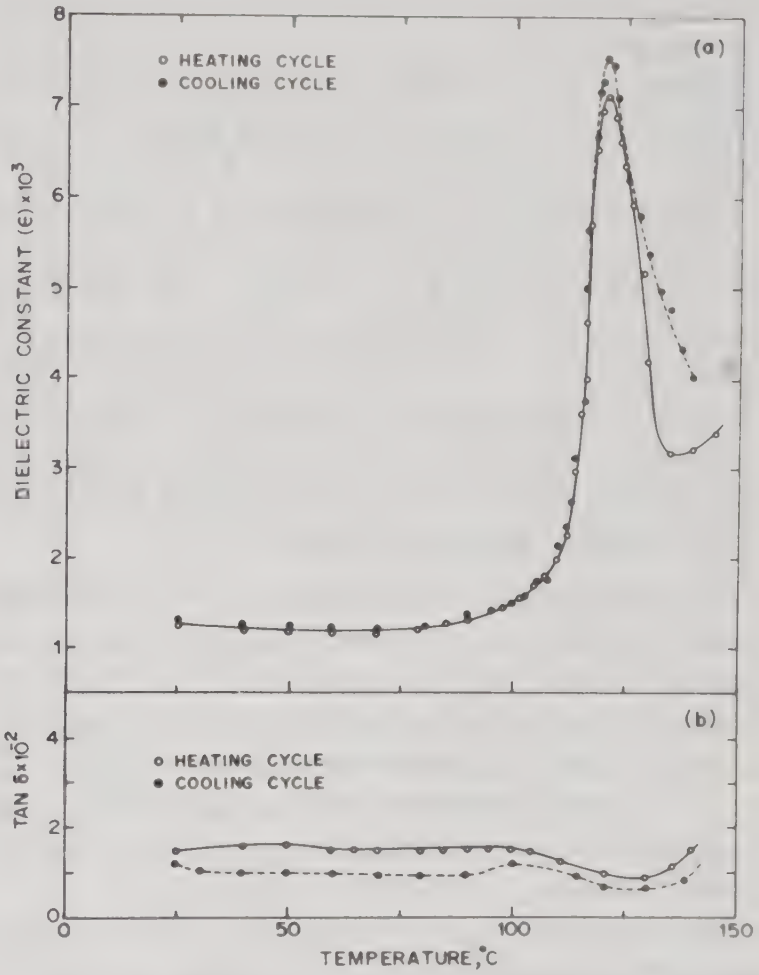

Fig. 4—Temperature dependence of dielectric constant (ε) (a) and tan δ (b)

disc. The distinct separation between reflections of the (002, 200) planes is also clearly seen in Fig.2. The lattice parameters of the unit cell are, $a = 3.99$°A, $c = 4.026$°A with c/a ratio = 1.009. These values match well with reported data[10] for the tetragonal phase of BT. Furthermore, no extra lines are observed corresponding to any additional phases of the Ba-Ti-O system.

Fig. 3 shows the microstructure developed during sintering-cycle of the green pellet. It shows (i) nearly

Table 1—Comparison of data on ceramic BT compacts

Parameter	Standard data		Present work
	Single crystal (Ref.19,20)	Polycrystalline (Ref.19,21)	
Structure	Tetragonal	Tetragonal	Tetragonal
Axial ratio (c/a)	1.01	1.01	1.009
Relative density (g/cm^3)	100%	98%	91%
Curie temp. (°C)	121	121-130	121
Spontaneous polarization P_s (μc/cm^2)	26	14.6	7.8
Coercive field (E_c) Kv/cm	1.00	2.5	4.4
Electric strength Kv/cm	120	> 50	25
Dielectric constant (ε)			
(i) Room temp.	2000	1400-2100	1250
(ii) Curie temp.	> 10,000	7500-10,000	7600
Dielectric loss (tan δ)	5×10^{-2}	1.0×10^{-2}	1.5×10^{-2}

uniform microstructure with well-defined grains, (ii) average grain size ≈ 4 μm and (iii) presence of pores resulting in low densification. The average grain diameter D was determined by the linear intercept method[11] using the correction by Mendelson[12].

After confirming the formation of proper ohmic contacts on the BT ceramic discs, the DC-resistivity was found to be 2.16×10^{10} Ω −cm. At room temperature (T = 30°C), dielectric constant (ε_{RT}) = 1250 with tan δ = 1.5% were obtained at 1 kHz frequency. These values of the dielectric parameters are comparable with the reported values on polycrystalline BT ceramics synthesized by various other chemical synthesis routes[13-18].

The temperature dependence of the dielectric constant (ε) and tan δ was measured using heating and cooling cycles. .Fig.4a shows that the dielectric constant (ε) is nearly constant up to 95 ± 1°C and then increases rapidly to a maximum value of ≈ 7200 at 121 ± 1°C. It drops down to 4000 around 140°C. The temperature corresponding to ε_{max} (T_c) is ≈ 121°C. During cooling cycle, the nature of the ε vs T behaviour was found to be similar to that observed during heating cycle with ε_{max} = 7600 at T_c = 121 ± 1°C. The temperature dependence behaviour of tan δ was the same during heating and cooling cycles with tan δ values ≈ 1.2-1.5 × 10^{-2} (Fig.4b).

The values of ε_{max} during heating and cooling cycles are lower than the reported values of ε_{max} (> 10,000) for best ceramic samples reported in the literature[17]. The lower value of ε_{max} is attributed to poor densification (≈ 91%) and related microstructure. Experiments are in progress to improve the microstructure using further modification in processing procedures.

Electroded BT discs gave well-defined hysteresis-loops, when placed in a Sawyer-Tower circuit. The estimated values of spontaneous polarization (P_s), coercive field (E_c) and break down voltage (E_b) are tabulated along with reported data on single crystals[19,20] and polycrystalline[19,21] BT compacts for comparison (Table 1).

The observed values are comparatively smaller in magnitudes due to the lower sintered density resulting in poor microstructure.

Attempts to control processing parameters during various stages of chemical synthesis to improve further dielectric performance parameters are underway.

Conclusions

Ceramic processing of ultrafine BT powders (made from BTO precursor) via a novel chemical route resulted in good ceramic compacts exhibiting better performance parameters.

Acknowledgement

We are thankful to Mr. M V Kuber and Dr.(Mrs.) A Mitra for their help in recording XRD and SEM micrograph of dense BT compacts.

References

1 Phule P P, Raghavan S & Risbud S H, *J Am ceram Soc*, 70 (1987) C108.
2 Phule P P & Risbud S H, *Advan ceram Mater*, 3 (1988) 183.
3 Phule P P & Risbud S H, *J mater Sci*, 25 (1990) 1169.
4 Bernier J C (preprint).
5 Hench L & Ulrich D R (Editors), *Science of ceramic chemical processing*) (Wiley-Interscience, New York), 1986.
6 Phule P P & Risbud S H, *Mater Sci Eng*, B3 (1989) 241.
7 Clabaugh W S, Swigbard E M & Gilchrist R, *J Res Natl Bur Std*, US56 (1956) 298.

8 Potdar H S, Singh P, Deshpande S B, Godbole P D & Date S K, *Mater Lett*, 10(1) (1990) 112.
9 Sawyer C B & Tower C H, *Phys Rev*, 35 (1930) 269.
10 ASTM Card No.5-0626 for $BaTiO_3$.
11 Fullman R L, *Trans AIME (USA)*, 197 (1953) 447.
12 Mendelson M I, *J Am ceram Soc*, 52 (1969) 443.
13 Phule P P & Risbud S H, in *Better ceramics through chemistry*, Vol.3, edited by C J Brinker, D R Clark & D R Ulrich (Materials Research Society, Pittsburgh) 1988, 275.
14 Mostaghaci & Brook R J, *J mater Sci*, 21 (1986) 3575.
15 Mazdiyasni K S & Brown L M, *J Am ceram Soc*, 59 (1972) 633.
16 Maurice A K & Buchanan R C, *Ferroelectrics*, 74 (1987) 61.
17 Mazdiyasni K S, *Bull Am ceram Soc*, 53(4) (1984) 591.
18 Godbole P D, Deshpande S B, Date S K, Navathey R & Ogale S B, *Ferroelectrics*, 102 (1990) 91.
19 Jaffe B, Cook (Jr) W R & Jaffe H, in *Piezoelectric ceramics* (Academic Press, New York), 1971.
20 *Landolf - Bornstein Series* (New) (Springer-Verlag, Berlin), Vol III/169, 1981.
21 Subbarao E C, in *Solid state chemistry*, edited by C N R Rao (Marcel Dekker Inc., New York), 1974.

Indian Journal of Chemistry
Vol. 31A, November 1992, pp. 874-877

Electrochemical studies on zirconium phosphate-kynar composite ion-exchange membrane system

Kehar Singh* & Archana Singh
Department of Chemistry, University of Gorakhpur, Gorakhpur

Received 20 January 1992; revised and accepted 2 April 1992

Zirconium phosphate obtained through chemical combination has been dispersed in kynar for the preparation of ion-exchange membrane. Hydrodynamic and electrodriven permeation studies alongwith membrane potential measurements have been carried out to ascertain suitability of this composite membrane system for accomplishing separations.

Membranes based on inorganic ion-exchange materials have been focus of attention because of their ability to withstand impairment in functional activity and stability towards temperature, ionizing radiation, oxidizing and acid media[1-4]. Zirconium phosphate membrane in particular have been investigated for application in electrodialysis separations and fuel cells[5-7]. In the present note we report, preparation and characterization of zirconium phosphate-kynar composite ion-exchange system to assess its suitability for accomplishing electrodriven membrane separations[8] from membrane conductance and membrane potential measurements using sodium chloride and magnesium chloride solutions.

Experimental

For the preparation of ion-exchange zirconium phosphate, equimolar solutions of zirconium sulphate and disodium hydrogen phosphate (both E. Merck) were mixed under constant agitation and heated at 80-85°C for two hrs. The precipitate thus obtained was separated by filtration, washed and dried. A desired quantity of the finely ground zirconium phosphate thus obtained was dispersed in 20% kynar solution in N,N′-dimethyl acetamide (CDH). Uninterrupted stirring of the mixture for about two hours resulted in a homogeneous slurry. This slurry was spread on a clean dried glass plate, allowed to dry at 70°C for one hr and immersed in distilled water to detach the membraneous film formed.

A piece of zirconium phosphate membrane was fixed in a glass cell schematically shown in Fig. 1. It was equilibrated with 1 *M* sodium chloride or magnesium chloride to convert it to appropriate ionic form. Solutions of unequal concentrations were then kept on the two sides of the membrane and membrane potential measured using the electrochemical set-up,

$$\text{SCE}\,||\,\underset{(C_1)}{\text{Solution}}\,|\,\text{Membrane}\,|\,\underset{(C_2)}{\text{Solution}}\,||\,\text{SCE}$$

The solutions were renewed before measurements (|| denotes KCl salt bridge and SCE, the saturated calomel electrode). A Systronics digital multimeter (model HIL 2161) was used for potential measurements.

For pressure driven and electrodriven membrane permeation studies, experimental setup reported earlier[9,10] was used. For conductance measurements potential difference across the membrane was applied in steps using Hindustan Powertronic INC power supply. These potentials were measured using saturated calomel electrodes. Corresponding current measurements were carried out with HIL (model 2161) digital multimeter using silver-silver chloride electrodes.

Results and discussion

The rate at which pressure driven permeation through a porous membrane takes place is given by

$$(J_v)_{\Delta\phi=0} = \frac{n\pi r^4}{8\eta l} \cdot \Delta P \qquad \ldots (1)$$

So that hydrodynamic permeability

$$\frac{(J_v)_{\Delta\phi=0}}{\Delta P} = \frac{n\pi r^4}{8\eta l} \qquad \ldots (2)$$

In view of non uniformity of pores, a membrane, for the purpose of description of its permeation characteristics, is considered to be associated with an average pore radius, r. l denotes membrane thickness. ΔP and $\Delta\phi$ respectively denote the difference of pressure and potential acting across the membrane, η is coefficient of viscosity of the solution and n denotes the number of pores in the membrane.

Hydrodynamic permeability and membrane conductance data obtained using sodium chloride and magnesium chloride solutions are presented in Fig. 2. $(J_v/\Delta P)_{\Delta\phi=0}$ and $(I/\Delta\phi)_{\Delta P=0}$ values obtained from these curves alongwith equivalent pore radius values obtained using the permeability and conductance data as earlier reported[11] are given in Table 1.

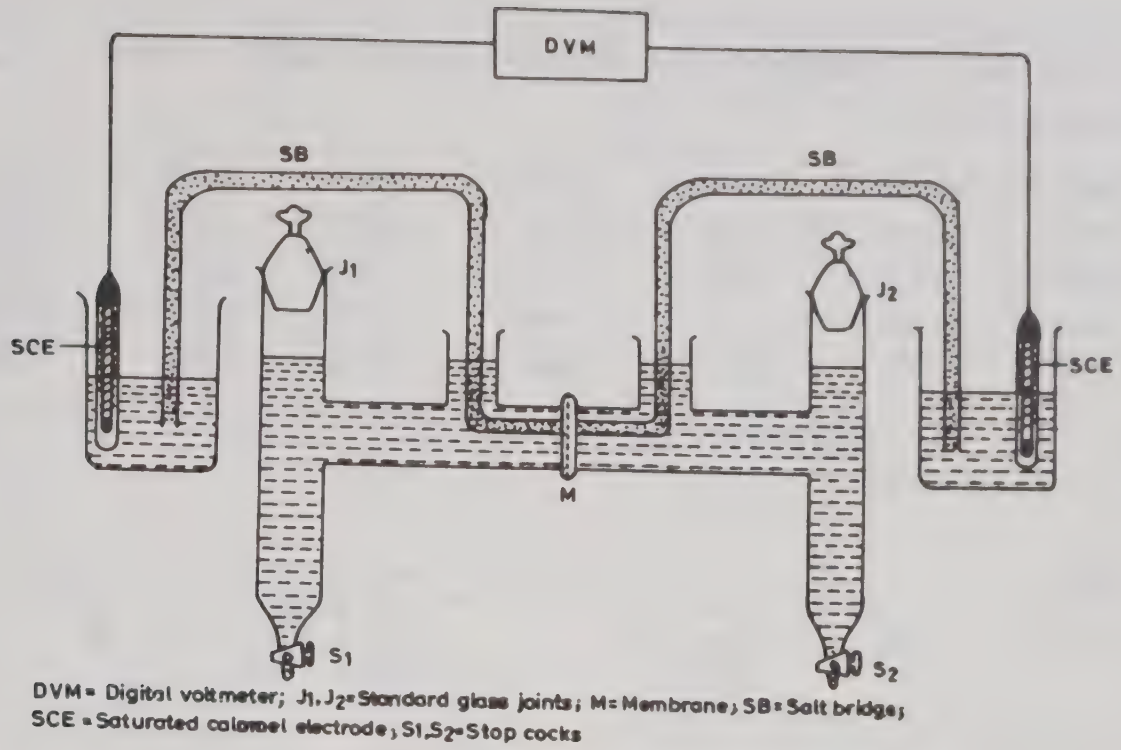

Fig. 1—Experimental set up for membrane potential studies

Table 1—Permeability and conductivity values

Electrolyte	Concentration	$\left(\frac{J_v}{\Delta P}\right)_{\Delta\phi=0}$	$\left(\frac{I}{\Delta\phi}\right)_{\Delta P=0}$	r
	(M)	($cm^5\ sec^{-1}\ dyne^{-1}$)	(ohm^{-1})	(cm)
Sodium chloride	0.005	5.0×10^{-9}	4.2×10^{-5}	0.94×10^{-4}
Magnesium chloride	0.005	4.7×10^{-9}	1.0×10^{-4}	0.60×10^{-4}

Table 2—Membrane potential values at fixed C

Concentration (M)		Membrane Potential (mV)		Activity coefficient			
C_1	C_2	NaCl	$MgCl_2$	f_1		f_2	
				NaCl	$MgCl_2$	NaCl	$MgCl_2$
0.001	0.009	11.20	26.20	0.9673	0.8904	0.9105	0.7458
0.002	0.008	8.13	22.33	0.9541	0.8543	0.9139	0.7561
0.003	0.007	5.60	13.71	0.9432	0.8277	0.9183	0.7653
0.004	0.006	3.25	6.42	0.9366	0.8065	0.9243	0.7777
0.005	0.005	0.00	0.00	0.9303	0.7317	0.9303	0.7317

It is seen that under comparable experimental conditions membrane equivalent pore radius, when sodium chloride is used as permeant, is significantly larger than that for magnesium chloride. This indicates relatively enhanced deswelling of the membrane matrix i.e., increase in the void volume of the membrane when it is kept equilibrated with sodium chloride solution.

Membrane potential data obtained using sodium chloride and magnesium chloride solutions are summarized in Table 2. Mean concentration was kept fixed at 0.05 M in both the cases. Figure 3 shows that these data are consistent with the equation[12]

$$(\Delta\phi)_{I=0} = 2.303\,(2\bar{t}_+ - 1)\,\frac{RT}{F}\log\frac{a_2}{a_1} \qquad \ldots (3)$$

where $\bar{t}_+$ denotes transport number of the cation in the membrane phase. The transport number values obtained from the slopes of the curves given in Fig. 3 were found to be $\bar{t}_+ = 0.665$ for Na^+ and

Table 3—Permselectivity values at different concentrations $\Delta C = 0.008\ M$

concentration (M)	Membrane potential (mV)		$\bar{t}_+$		t_+		P_s	
	NaCl	$MgCl_2$	NaCl	$MgCl_2$	NaCl	$MgCl_2$	NaCl	$MgCl_2$
0.005	17.2	26.40	0.653	0.730	0.3925	0.3763	0.4288	0.5683
0.010	14.15	18.21	0.802	0.912	0.3928	0.3762	0.6744	0.8589
0.015	10.90	11.01	0.853	0.889	0.3910	0.3761	0.7586	0.8220
0.020	07.55	06.42	0.857	0.800	0.3902	0.3760	0.7654	0.6583

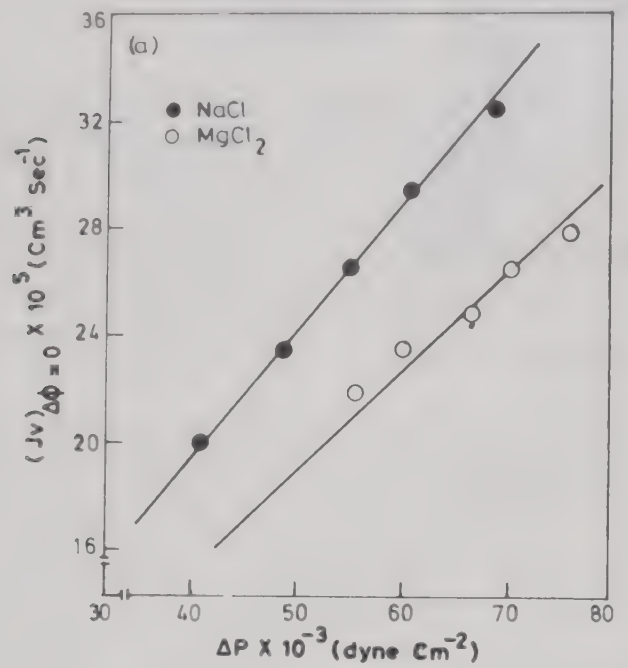

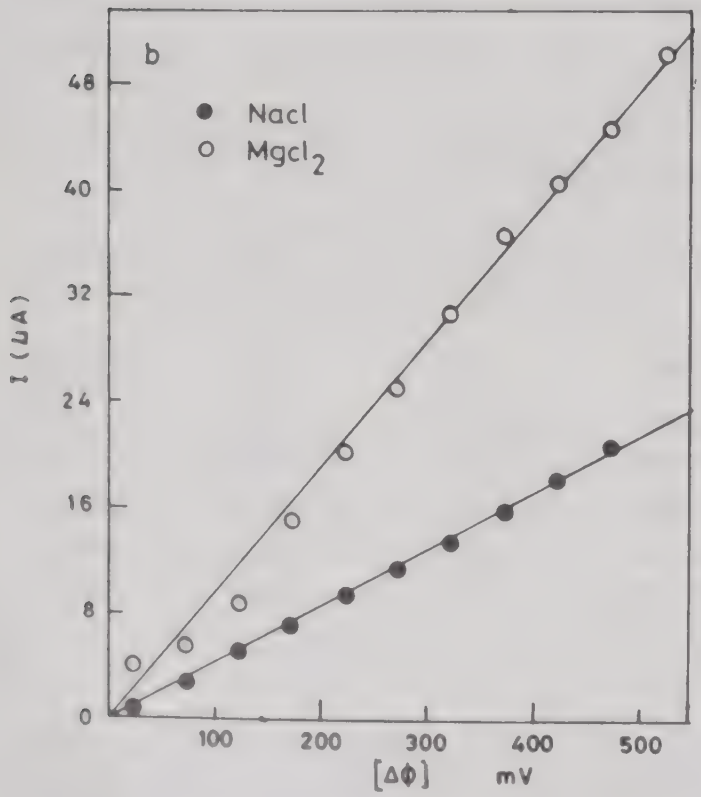

Fig. 2—(a) Variation of hydrodynamic flux with applied pressure difference (b) Membrane conductance data (●—NaCl; ○—$MgCl_2$)

$\bar{t}_+ = 0.809$ for Mg^{++}. Activity coefficients needed for this purpose were estimated using the relationship[13]

$$\log f = -\frac{A(Z_+ Z_-) I^{1/2}}{1 + BaI^{1/2}} \quad \ldots (4)$$

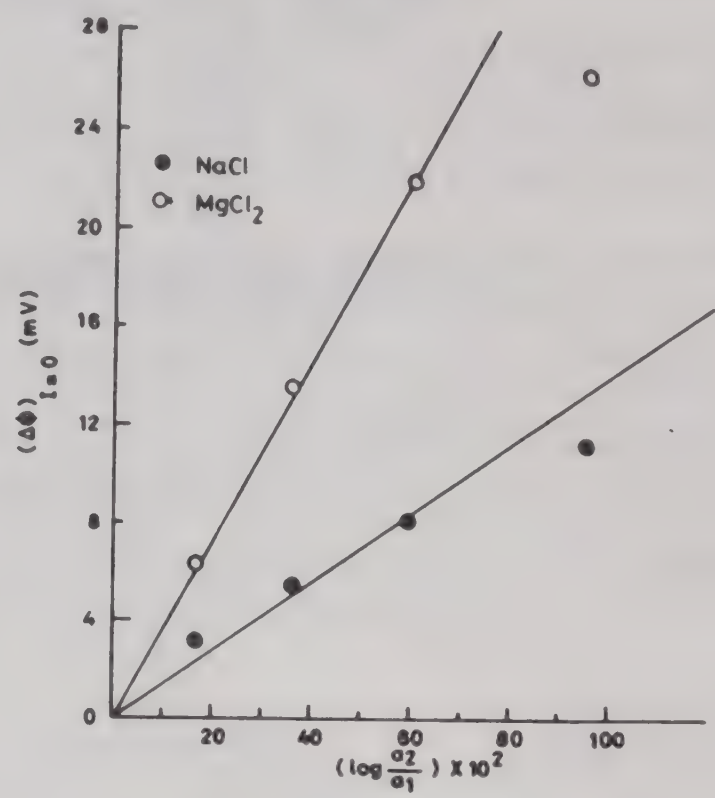

Fig. 3—Test of the validity of Eq. (6) (●—NaCl; ○—$MgCl_2$)

where $A = 0.5161$, $B = 0.3301 \times 10^8$ and $a = 6$ Å.

Membrane ionic transport numbers are expected to depend on mean concentrations of the solutions. Membrane potentials alongwith the transport number values estimated using equation (3) are included in Table 3. In both the cases transport numbers are lowered with increase in concentration. This trend may be attributed to deswelling of the membrane matrix when concentration is increased.

The relative ease with which a counterion migrates through a charged membrane is expressed in terms of permselectivity defined as[14]

$$P_s = \frac{\bar{t}_+ - t_+}{1 - t_+} \quad \ldots (5)$$

Permselectivity values obtained using Eq. 5 are summarised in Table 3 alongwith ionic transport numbers needed for its calculation.

An important membrane electrochemical parameter is fixed charged density. According to Tasaka *et al.*[15,16], membrane potential may be expressed

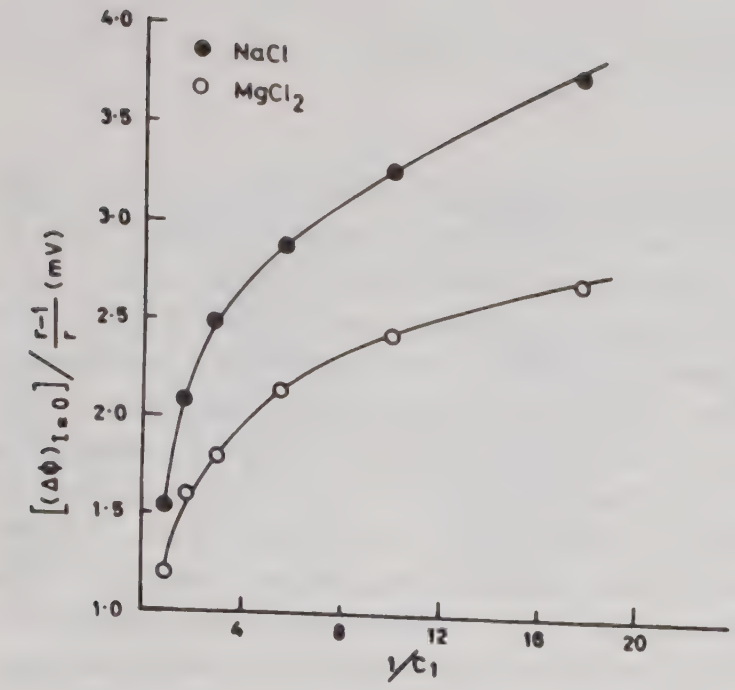

Fig. 4—Estimation of fixed charge density according to Eq. (6) (●—NaCl; ○—$MgCl_2$)

in terms of fixed charge density at higher concentrations by the following relationship:

$$\left\{\frac{\Delta\phi}{\left(\frac{\gamma-1}{\gamma}\right)}\right\}=\frac{RT}{F}\left(\frac{\phi x}{2}\right)\frac{1}{C'} \qquad \ldots (6)$$

C' = lower concentration; and $\gamma=\frac{C_2}{C_1}$. This relationship has been used for the estimation of fixed charge density using membrane potential data included in Fig. 4. In these studies the ratio $\frac{C_2}{C_1}$ was kept fixed at 2. The ϕx values are found to be 8.6×10^{-3} litre/mol and 2.6×10^{-3} litre/mol when membrane is in a state of equilibration with sodium chloride and magnesium chloride solutions respectively. The foregoing procedure assumes fixed charge density to be independent of concentration. This is very unlikely in view of the possibility of alteration in the character of the membrane with change in electrolytic environment.

To conclude it may be stated that the zirconium phosphate kynar composite membrane investigated above is not suitable from the point of view of electrodriven membrane separations because of its permselectivity being somewhat low.

Acknowledgement

The authors thank the CSIR, New Delhi for financial assistance.

References

1 Amphlett C B, *Inorganic ion exchanger* (Elsevier, Amsterdam) 1964.
2 Clearfeld A, Nancollas G H & Blessing R H, *Ion exchange and solvent extraction*, Vol. V, edited by J A Marinsky, V Manius (Marcel Dekker, New York) 1973.
3 Alberti G, Casicola M, Constantino U & Levi G, *J membr Sci*, 3 (1975) 179.
4 Clearfeld A, *Preparation and characterization of material*, edited by J M Honig & C N R Rao (Academic Press) 1984.
5 Dravnicks A & Brigman J I, *Chem Eng News*, 39 (1961) 42.
6 Hamlen R P, *J electrochem Soc*, 109 (1962) 7546.
7 Brigman J I & Braman R S, *J colloid Sci*, 20 (1965) 913.
8 Zelman A, Walsh D, Wayt H & Gisser D, *Desalination*, 25 (1978) 253.
9 Rastogi R P, Singh K, Kumar Raj & Shaba Ram, *J membr Sci*, 6 (1981) 181.
10 Rastogi R P, Singh K & Singh J, *J phys Chem*, 49 (1975) 2574.
11 Singh K, Srivastava V N & Chandra M, *J non-equilib Thermodyn*, 6 (1981) 181.
12 Lakshminarayanaiah N, *Membrane electrodes* (Academic Press, New York) 1976, p. 64.
13 Lakshminarayanaiah N, *Equations of membrane biophysics* (Academic Press, New York).1987, p. 73.
14 Lakshminarayanaiah N, *Equations of membrane biophysics* (Academic Press, New York) 1987, p. 118.
15 Tasaka M, Aoki N, Kondo Y & Nagasawa M, *J phys Chem*, 79 (1975) 1307.
16 Tasaka M & Wada C, *J membr Sci*, 6 (1980) 171.

Indian Journal of Chemistry
Vol. 31A, November 1992, pp. 878-880

Gamma ray induced decomposition of lanthanide double nitrates with some bivalent cations

S P Kulkarni,(Ms) N G Joshi & A N Garg*
Department of Chemistry, Nagpur University, Nagpur 440 010

Received 20 January 1992; revised and accepted 8 June 1992

The gamma ray induced decomposition of double nitrates of Pr and Gd with Mg^{2+}, Co^{2+} and Zn^{2+} has been studied over a wide absorbed dose range upto 640 kGy at room temperature. Also, the radiolytic decomposition of Nd, Sm and dy double nitrates with Mg^{2+} and Zn^{2+} has been investigated at an absorbed dose of 205 kGy. The $G(NO_2^-)$ values depend on the absorbed dose, nature of the lanthanide ion and the bivalent outer cation. The $G(NO_2^-)$ value for all the lanthanide double nitrates at an absorbed dose of 205 kGy follow the order Mg^{2+}, $Co^{2+} > Zn^{2+}$. The double nitrates with Mg^{2+} exhibit $G(NO_2^-)$ values at same dose in the order $Nd^{3+} \simeq Gd^{3+} > Sm^{3+} > Pr^{3+} > La^{3+} > Dy^{3+} > Ce^{3+}$ whereas for Zn^{2+} salts the order is changed to $Ce^{3+} > Nd^{3+} \simeq Sm^{3+} > Gd^{3+} \simeq Pr^{3+} > La^{3+}$.

The radiation induced decomposition of inorganic nitrates has been studied by several workers[1-3]. Johnson[2] extensively reviewed the work on alkali metal nitrates and the effect of various parameters. The interaction of gamma photons with solid inorganic nitrates leads to the formation of NO_2^- and molecular oxygen as the stable products[1]. $[NO_2^-]$ and $G(NO_2^-)$ are affected by several factors such as the absorbed dose, the free space volume in the crystal lattice, the lattice energy[4], water of crystallization[5], the nature of the outer cation[6], the nature and amount of additives such as oxides[7], halides[8], sulphates[8,9] and carbonates[9]. Bleany *et al.*[10] have identified NO_2 in gamma irradiated solid rare earth double nitrates. Earlier, we have studied the radiolytic decomposition of double nitrates of La and Ce with some mono- and bivalent double cations in the solid state[11]. The present study deals with the radiolysis of Pr and Gd double nitrates of Mg^{2+}, Co^{2+} and Zn^{2+} over a dose range upto 640 kGy and of Nd, Sm and Dy with Mg^{2+} and Zn^{2+} at an absorbed dose of 205 kGy.

Experimental

All nitrate salts and other chemicals were of AR or high purity grade. All solutions were prepared in doubly distilled water. The double nitrate salts were prepared by slow evaporation of a mixture of aqueous solutions containing the bivalent and trivalent (lanthanide) nitrates in 3:2 mole ratio. Fully grown, well shaped crystals were separated from the mother liquor, dried on the filter paper and stored in an evacuated desiccator over fused $CaCl_2$. The formation of double salts was confirmed be elemental analysis. The crystals were finely ground in an agate mortar and irradiated in an unsealed Corning glass tube at a dose rate of 0.92 kGy h^{-1} in a Cobalt-60 Gamma chamber-900 procured from BARC, Bombay. The dose rate was assayed using a Fricke dosimeter, $G(Fe^{3+}) = 15.6$ and an alanine dosimeter[12]. Actual gamma dose was corrected by using the mass energy absorption coefficients[13] for the individual elements. $[NO_2^-]$ was estimated spectrophotometrically by the modified Shinn's method of diazotization[14,15]. Absorbances were measured either on a Beckman model DU-2 and/or Shimadzu model UV-240 spectrophotometer, at $\lambda_{max} = 540$ nm.

Results and Discussion

$[NO_2^-]$ and $G(NO_2^-)$ values of the lanthanide double nitrates with the general formula $3M^{II}(NO_3)_2.2Ln^{III}(NO_3)_3.24\,H_2O$ (where $M^{II} = Mg^{2+}$, Co^{2+}, Zn^{2+} and $Ln^{III} = Pr^{3+}$, Nd^{3+}, Sm^{3+}, Gd^{3+} and Dy^{3+}) at 205 kGy in solid state at room temperature, are listed in Table 1. Gamma rays induce decomposition of inorganic nitrates into NO_2^- and O_2 through intermediate species[2,3] like NO_3^-*, NO_3^-**, NO_3, NO_3^{2-} etc. Interaction of primary species is affected

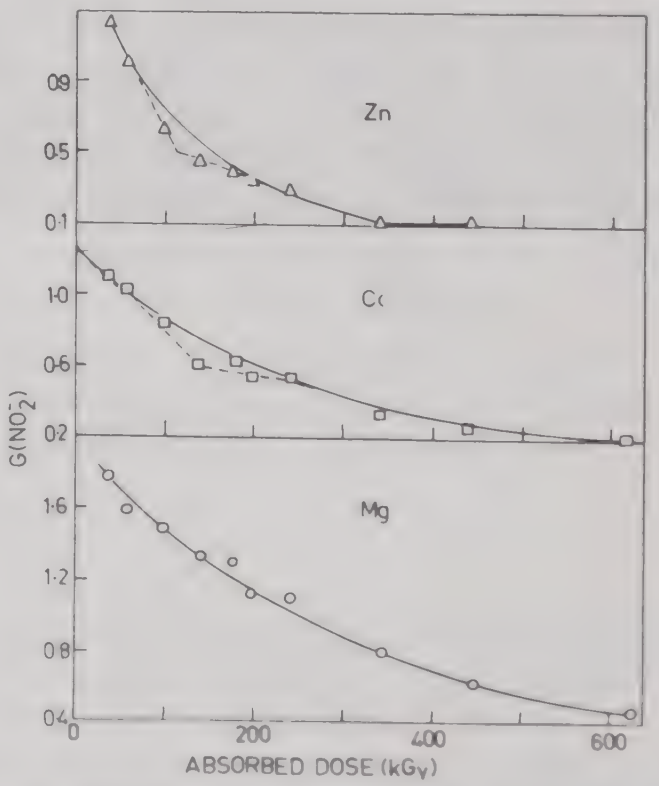

Fig. 1—Dependence of $G(NO_2^-)$ on absorbed dose in praseodymium double nitrates with Mg^{2+}(○),Co^{2+}(□) and Zn^{2+}(△)

Table 1—Concentration of NO_2^- and $G(NO_2^-)$ for radiolytic decomposition of double nitrates of lanthanides with bivalent cations at an absorbed dose of 205 kGy at room temperature

M^{II}	Mg^{2+}		Co^{2+}		Zn^{2+}	
Ln^{III}	$[NO_2^-]$, μg/g or ppm	$G(NO_2^-)$	$[NO_2^-]$, μg/g or ppm	$G(NO_2^-)$	$[NO_2^-]$, μg/g or ppm	$G(NO_2^-)$
Ln^{3+}(*)	1036±38	1.05±0.04	426±16	0.43±0.02	212±10	0.22±0.01
Ce^{3+}(*)	906±35	0.91±0.03	658±22	0.67±0.02	610±21	0.62±0.02
Pr^{3+}	1051±40	1.11±0.04	502±20	0.54±0.02	326±12	0.35±0.02
Nd^{3+}	1236±52	1.32±0.05	—	—	518±18	0.53±0.02
Sm^{3+}	1196±45	1.23±0.05	—	—	514±20	0.53±0.02
Gd^{3+}	1266±56	1.31±0.06	1162±40	1.21±0.05	363±15	0.38±0.02
Dy^{3+}	951±30	0.98±0.03	—	—	—	—

(*) From ref. 11 for comparison.

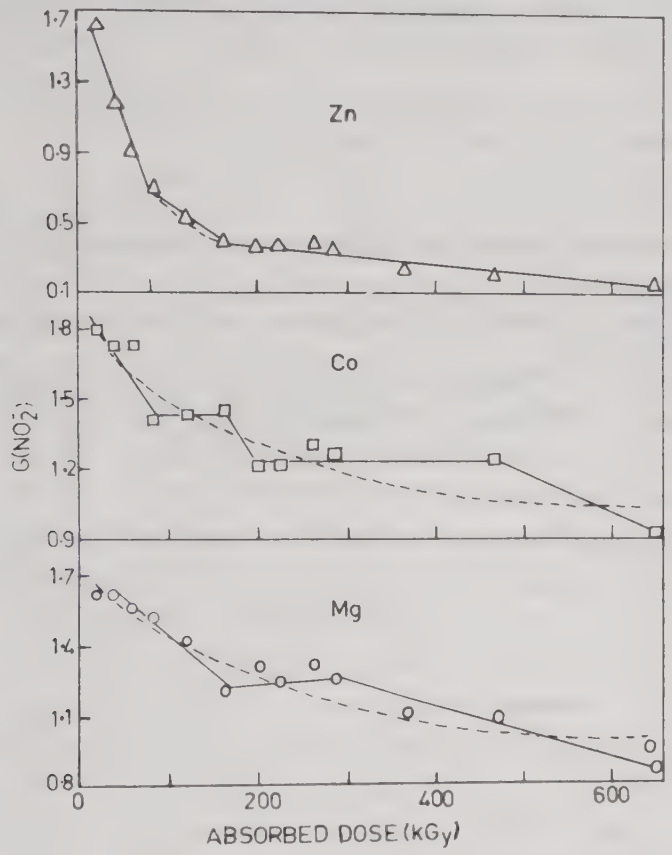

Fig. 2—Plot of $G(NO_2^-)$ vs absorbed dose in gadolinium double nitrates with Mg^{2+} (○), Co^{2+} (□) and Zn^{2+} (△)

by factors such as the absorbed dose, free space volume in the crystal lattice, lattice energy, nature of cation, water of crystallization etc. which in turn affects the production of NO_2^- and hence $G(NO_2^-)$ as well.

(i) *Effect of absorbed dose*—In order to investigate the effect of absorbed dose, radiolysis of Pr and Gd double nitrates was studied over a dose range up to 640 kGy. It has been observed that $[NO_2^-]$ increases with absorbed dose upto a certain limit and then somewhat levels off due to radiation annealing. Further, the dose at which $[NO_2^-]$ levels off is lower for Zn-double nitrate (50 kGy) compared to that for Co and Mg (200 kGy) salts. Variation of $G(NO_2^-)$ with absorbed dose in Figs 1 and 2 is rather complex though approximately smooth variation can also be visualized. On the basis of these plots for Pr double nitrates in Fig. 1, one could identify three dose regions; low, medium and high. In the low dose region (< 200 kGy) $G(NO_2^-)$ decreases rapidly and almost linearly. In the medium dose range (150-400) kGy the decrease is again linear but it becomes slow. At still higher doses the rate of decrease further slows down or becomes constant. In case of Gd double nitrates also the $G(NO_2^-)$ values decrease rapidly and almost linearly below 150 kGy beyond which the rate of decrease becomes slow (Fig. 2). Large variations of $G(NO_2^-)$ in Zn-Gd nitrate (1.7 to 0.1) and Mg-Pr nitrate (1.8 to 0.4) are particularly significant. Perhaps some structural changes may be more prominent in this particular case[11] and a detailed investigation is required.

(ii) *Bivalent cation*—The radiolytic decomposition of double nitrates of La, Ce, Pr and Gd with Mg^{2+}, Co^{2+} and Zn^{2+} at 205 kGy shows that $G(NO_2^-)$ values follow the order $Mg^{2+} > Co^{2+} > Zn^{2+}$ (Table 1). Crystal structure studies of $3Mg(NO_3)_3 2Ce(NO_3)_3.24H_2O$ by Zalkin *et al.*[16] have suggested that the salt may be formulated as $[Mg(H_2O)_6]_3.[Ce(NO_3)_6]_2.6H_2O$. Since double nitrate salts of lanthanides with bivalent cations form an isomorphous series[17], these may be represented by a general formula, $[M^{II}(H_2O)_6]_3.[Ln^{III}(NO_3)_6]_2.6H_2O$ where $M^{II} = Mg^{2+}$, Co^{2+}, Zn^{2+} and $Ln^{III} = La^{3+}$, Ce^{3+}, Pr^{3+}, Nd^{3+}, Sm^{3+}, Gd^{3+}, Dy^{3+}. Therefore, for a given Ln^{III} ion, except for M^{II} other factors such as absorbed dose, crystal structure, number of water molecules and their arrangement in the crystal lattice remain unchanged. Hence one can conclude that $G(NO_2^-)$ values decrease with the increase in ionic radius of the bivalent cation. A similar observation has been made for Mg, Co and Zn nitrates.

(iii) *Trivalent(lanthanide)ion*—A perusal of data in Table 1 suggests that for a given M^{2+} ion, the nature of Ln^{III} ion also affects the radiolytic decomposition[18]. $G(NO_2^-)$ values of the Mg double salts at 205 kGy decrease in the order $Nd^{3+} \simeq Gd^{3+} > Sm^{3+} > Pr^{3+} > La^{3+} > Dy^{3+} > Ce^{3+}$ whereas for Zn-salts the order is changed to $Ce^{3+} > Nd^{3+} \simeq Sm^{3+} > Gd^{3+} \simeq Pr^{3+} > La^{3+}$. This change in the order may possibly be attributed to the combined effects of bivalent and trivalent outer cations. It may be noted that ionic radius of Mg^{2+} is 0.65 Å whereas that of Zn^{2+} is 0.74Å. This may lead to different free space volume in the crystal lattice and hence the change in G-values.

Further, a comparison of $G(NO_2^-)$ values of the double nitrates with those of the corresponding bivalent and trivalent nitrates at 205 kGy shows that, in general, $G(NO_2^-)$ for a given double salt lies in between those for the corresponding trivalent and bivalent nitrates. This is in accordance with our earlier observations[11] for double nitrates of La^{3+} and Ce^{3+} with some bivalent cations.

Acknowledgement

Thanks are due to the UGC, New Delhi for financial support. Our sincere thanks are due to the Director, USIC for providing irradiation facilities. One of us (SPK) thanks Shri R.R. Kulkarni, Prinicipal, Adarsha Science College, Dhamangaon for encouragement.

References

1 Cunningham J, *J phys Chem*, 67 (1963) 1771.
2 Johnson E R, *The radiation induced decomposition of inorganic molecular ions* (Gordon and Breach, New York), 1970.
3 Muhammad D & Maddock A G, *J chem Soc Faraday Trans I*, 74 (1978) 919.
4 Kulkarni S P & Garg A N, *Indian J chem*, 23A (1984) 712.
5 Parwate D V & Garg A N, *J radioanal nucl Chem Lett*, 85 (1984) 203.
6 Kulkarni S P & Garg A N, *J radioanal nucl Chem Articles*, 98 (1986) 65.
7 Patil S F & Bedekar A G, *Int J Radiat Phys Chem*, 29 (1987) 121.
8 Kulkarni S P & Garg A N, *Int Radiat Phys Chem*, 32 (1988) 609.
9 Kulkarni S P, Batra R J & Garg A N, *Radiat effects and defects in solids*, 113 (1990) 315.
10 Bleany B, Hayes W & Llewellyn P M, *Nature*, 179 (1957) 140.
11 Kulkarni S P & Garg A N, *Int J Radiat Phys Chem*, 38 (1991) 39.
12 Gupta B L, Bhat R M, Narayan G R & Nilekani S R, *Int J Radiat Phys Chem*, 26 (1985) 647.
13 Hubbel J H, *Int J appl Radiat Isot*, 33 (1982) 1269.
14 Shinn M B, *Ind Engng Chem Analyt Edn*, 13 (1941) 33.
15 Kershaw N F & Chamberlin N S, *Ind Engng Chem Analyt Edn.*, 14 (1942) 312.
16 Zalkin A, Forrester J D & Templeton D H, *J chem Phys*, 39 (1963) 2881.
17 Addison C C & Sutton D, *Progr Inorg Chem*, 8 (1967) 226.
18 Joshi N G & Garg A N, *Indian J chem*, 31A (1992) 184.

Indian Journal of Chemistry
Vol. 31A, November 1992, pp. 881-882

Plastic membrane *p*OH-electrode based on chlorpromazine base

Adel F Shoukry* & Jamal T Elwerfalli
Department of Chemistry, Faculty of Science,
University of Garyounis, Benghazi, Libya

Received 21 October 1991; accepted 26 May 1992

A new hydroxyl-ion selective poly(vinyl chloride)-membrane electrode based on chlorpromazine base in the presence of sodium tetraphenyl borate has been prepared with dioctylphthalate as a plasticizer. The performance characteristics of the electrode have been studied. It exhibits a good Nernstian response at room temperature, over a relatively wide range of hydroxyl ion concentrations and is highly selective toward a large number of inorganic anions.

Hydronium and hydroxyl ions are among the most important species in chemistry of aqueous solutions. The *p*H/*p*OH frequently determine the course and rate of many reactions. The glass electrode has been the most commonly used sensor to indicate degrees of acidity or alkalinity in aqueous electrolytes. In recent years there has been an increasing interest in utilizing other types of *p*H-electrodes using plastic[1,2] or metal oxide[3,4] membranes. The plastic type has the advantages that their construction is very easy and they are cheaper. Moreover micro electrodes of either conventional or wire coated types can be prepared. In a previous work[5], a plastic membrane hydroxyl ion-selective electrode was constructed and used for the determination of ionisation constants of sparingly soluble organic bases. The electroactive ionophore of the membrane was a nitron-8-hydroxyquinoline-5-sulphonate ion-associate. In the present work a new *p*OH-electrode is constructed, based on incorporating chlorpromazine base as the anion exchanger in plasticized PVC membrane Chlorpromazine (CP) is an antipsychotic drug[6] among the phenothiazine family; it is easily available and not expensive. This represents an advantage of the present sensor over the previously reported electrode[5].

Experimental

All reagents were of analytical grade. Chlorpromazine base (CP) was prepared from the protonated salt by treating with NaOH solution. Sodium tetraphenylborate (NaTPB)(Aldrich), Poly(vinyl chloride) of high molecular weight (Aldrich) and dioctylphthalate (DOP)(Fluka) were used. Potentiometric measurements were carried out using a Phillips digital *p*H/mV meter type PW 9409.

Construction of the electrode

The membrane and the electrode were constructed according to the method of Moody and Thomas[7]. Powdered PVC (100 mg), CP (45 mg), NaTPB (70 mg) and DOP plasticizer (120 mg) were dissolved in about 5 ml tetrahydrofurane. The membrane was cast on a Petri dish of 7 cm diameter and was formed as the solvent evaporated at room temperature. Punched circular membranes of 5 mm diameter were gluded to a polyethylene cap attached to a 10 cm long glass tube. The electrode body was filled with 10^{-2} *M* NaCl solution in which a Ag/AgCl wire was immersed. The electrode was preconditioned for 2 hr in distilled water.

The potentiometric cell used was as follows: Ag, AgCl/internal filling solution/membrane/test solution/KCl salt bridge/saturated calomel electrode. To construct the calibration graphs, suitable aliquots of a standard NaOH solution was added to 50 ml 10^{-6} *M* NaOH solution, at room temperature, so as to cover the concentration range $10^{-6} - 10^{-1}$ *M* NaOH. The sensor and calomel electrodes were immersed in this solution and the emf value was recorded after each addition and plotted versus *p*OH. The selectivity coefficient, $K^{pot}_{OH,J}$, were evaluated by the separate solutions method[8] in which the following Eq. (1) was applied

$$\log K^{pot}_{OH,J} = (E_2 - E_1)/S + \log[OH^-] - \log[J^{Z-}]^{1/Z} \quad \ldots (1)$$

where E_1 is the electrode potential in 10^{-3} *M* NaOH solution and E_2 is the potential of the electrode in 10^{-3} *M* solution of interferent, J^{Z-}.

Results and discussion

The ion-specific behaviour of glass electrodes is largely determined by the cation-exchange equilibria established between the sites R of the glass phase (e.g. $(SiO_{3/2})O^-$ or $(AlO_2)^-$) and the external solution. The origin of response in the present membrane (PVC 29.8%, DOP 35.8%, NaTPB 21% and CP 13.4%) is most likely an anion-exchange equilibrium at the membrane/solution interfacial junction. Conditioning the electrode by soaking in water leads to adsorption of water molecules at the surface of the lipophilic Brönsted base, chlorpromazine B, incubated in the plasticized PVC network.

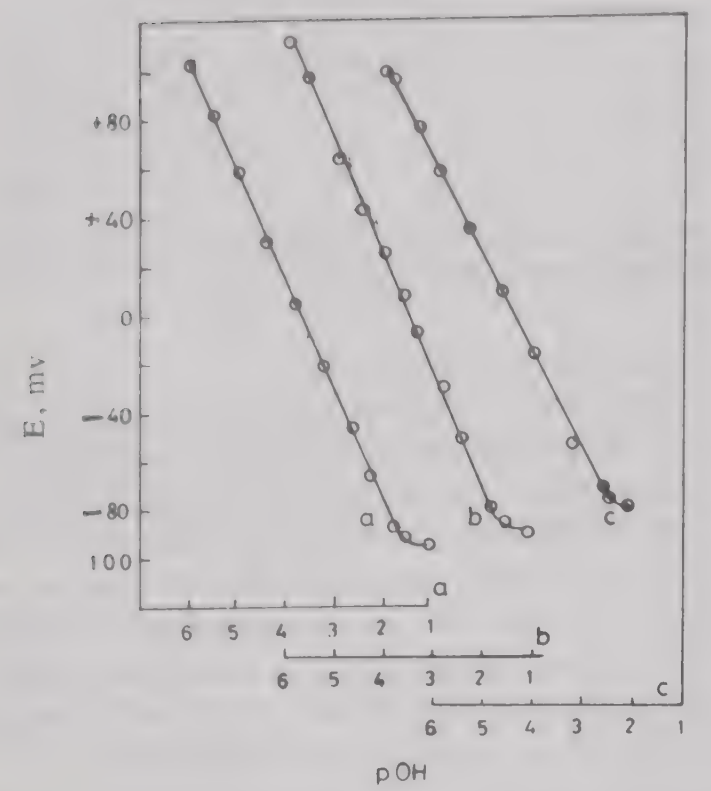

Fig. 1—Calibration graphs of *p*OH-electrode obtained at different soaking time: (a) 1 day; (b) 6 days; and (c) 30 days.

$$B + H_2P \overset{\text{soaking}}{\rightleftharpoons} BH^+ OH^-$$

The resulting ion-pair acts as the anion-exchanger of the electrode. Presoaking the electrode for 24 h in distilled water was found sufficient for the formation of an active hydrated layer at the solid-solution interface of the membrane as the electrode exhibited instantaneous response for the hydroxyl ions over the concentration range ($10^{-1.5}-10^{-6}$ *M*), Fig. 1a. The response time was 5 sec and slope of calibration graph was 48 mV/decade. After 6 days of continuous soaking the rectilinear concentration range of the electrode had not changed significantly. It was $2.5\times10^{-2}-10^{-6}$ *M* (Fig. 1b) while the slope of the calibrated graph increased to 51 mV/decade and the response time remained constant at 5 sec. Up to 17 days the aforementioned electrode characteristics were almost the same. Longer soaking of the elctrode decreased gradually the slope of the calibration graph to only 41 mV/decade after one month. This decrease in slope was associated with gradual increase in the response time to about 20 sec and constancy in the useable concentration range. The above results revealed that the electrode should be kept in a closed vessel and stored in a refrigerator while not in use in order to avoid leaching of the electroactive ingredient into the bathing solution[9]. Trials to use plasticized membrane free from NaTPB in constructing OH^--responsive electrode was not successful; calibration graphs of bad characteristics were obtained which were most probably due to high resistance of the membrane.

Table 1—Selectivity coefficient, $K^{pot}_{OH,J}$, for OH-responsive electrode using the separate solution method

Interferent	$K^{pot}_{OH,J}$	Interferent	$K^{pot}_{OH,J}$
Cl^-	1.4×10^{-5}	SO_4^{2-}	3.1×10^{-6}
Br^-	1.1×10^{-5}	$S_2O_3^{2-}$	2.8×10^{-6}
I^-	1.2×10^{-5}	$B_4O_1^{2-}$	2.5×10^{-4}
TPB^-	1.8×10^{-3}	$C_2O_4^{2-}$	1.2×10^{-5}
CH_3COO^-	2.0×10^{-5}	PO_4^{3-}	2.5×10^{-6}
NO^{3-}	1.0×10^{-5}		

Selectivity of the electrode

The influence of various anions on the OH-electrode was investigated; the selectivity coefficients being determined by the separate solution method (Table 1). None of the investigated species were found to interfere as shown by the very small values of $K^{pot}_{OH,J}$. This reflects a very high selectivity of investigated electrode for the hydroxyl ion.

References

1 Kosonen P O, *Finn chem Lett*, 2-3 (1978) 86.
2 Erne D, Ammann D & Simon W, *Chimia*, 33 (1979) 88.
3 Niedrach L W, *J Electrochem Soc*, 127 (1980) 2122.
4 Hitchman M L & Ramanathan S, *Analyst*, 113 (1988) 35.
5 Shoukry A F & Ibrahim H, *J Electroanal Chem*, 272 (1989) 79.
6 Kaiser C & Settler P E, in Wolff M E, Editor, Burger's Medicinal Chemistry, Fourth Edition (Wiley, New York) 1981, Part 111, Chapter 56.
7 Moody G J & Thomas J D R, in Freiser H, Editor, Ion Selective Electrodes in Analytical Chemistry (Plenum Press, New York) 1978, Chapter 4, pp. 287.
8 Shoukry A F, Badawy S S & Issa Y M, *Anal Chem*, 59 (1987) 1078.
9 Shoukry A F, Badawy S S & Farghali R A, *Anal Chem*, 60 (1988) 2399.

Indian Journal of Chemistry
Vol. 31A, November 1992, pp. 883-885

Reversible binding of carbon monoxide with Ru(III) aminopolycarboxylic acid complexes

M M Taqui Khan*, N H Khan & R I Kureshy
Discipline of Coordination Chemistry & Homogeneous Catalysis, Central Salt & Marine Chemicals Research Institute
Bhavnagar 364 002

Received 7 October 1991; revised and accepted 30 June 1992

The reversible binding of carbon monoxide to the complexes [Ru^{III}(EDTA-H)(H_2O)] **1** and [Ru^{III}(PDTA-H)(H_2O)] **2** have been studied in aqueous solution at *p*H = 5 by spectrophotometric and electrochemical studies. The equilibrium constant for carbonylation, K_{CO} was evaluated at 10°, 25° and 40°C. The thermodynamic parameters, $\Delta H°$, $\Delta G°$ and $\Delta S°$ for the carbonylation of the complexes **1** and **2** have been evaluated. The complex [Ru(PDTA-H)(CO)] **4** is more stable than the complex [Ru(EDTA-H)(CO)] **3** in solution.

Understanding the role, the protein plays in regulating the binding of small ligands to hemoproteins continues to be a topic of active interest[1-4]. Recently attention has been focussed on the discrimination of the heme cavity between small ligand such as CO and O_2, thereby affecting their relative binding affinities[5-9]. In order to understand the role of the steric effect on the discrimination reaction in hemoproteins a series of model porphyrins were designed and synthesized[6-10].

Carbonyl complexes of ruthenium, osmium, rhodium and iridium in lower oxidation states are partly stabilized by CO to give rise to cluster formation[11,12]. Some *p*H-dependent kinetic and equilibrium studies of these metal carbonyl complexes were also reported in nonaqueous[13] and aqueous media[14,15]. Reaction of $RuCl_3.xH_2O$ with CO in acidic medium was studied in solution by IR technique[14]. Taqui Khan *et al.*[16] studied the rate of formation of the carbonyl species [Ru(EDTA-H)(CO)] by stopped flow method. No systematic attempt has, however, been made to evaluate the equilibrium constant for carbonylation in aqueous solution. In this paper we report the reversible binding of CO to [Ru(EDTA-H)(H_2O)] **1** and [Ru(PDTA-H)(H_2O)] **2** in aqueous medium at *p*H 5. The factors influencing the CO affinity were also evaluated in terms of thermodynamic parameters $\Delta H°$, $\Delta G°$ and $\Delta S°$ for the formation of these complexes in solution.

Experimental

$RuCl_3xH_2O$ was obtained from Johnson Matthey, ethylenedinitrilotetraacetic acid (EDTA-H) and propylenedinitrilotetraacetic acid (PDTA-H) were purchased from Aldrich. Doubly distilled deionized water was used for solution formation of the complexes. Carbon monoxide was prepared by the reaction of sodium formate with concentrated H_2SO_4 and purified by passing through a tower of KOH pellets. The complexes [Ru(EDTA-H)(H_2O)][17] and [Ru(PDTA-H)(H_2O)][18] were prepared by reported procedure and characterized by elemental analysis.

Physical measurements

The spectrophotometric measurements were carried out on Shimadzu UV/visible 160 spectrophotometer equipped with a temperature controller TCC-240A. Matched 10 or 2 mm cells were used to record the spectra. Cyclic voltammogram, D.C. and differential pulse polarogram were recorded on a PAR electrochemical system 174, equipped with a precision x-y recorder and model 173 galvanostat as described earlier[19]. Ag/AgCl was used as reference electrode with 0.1 *M* $NaClO_4$ as supporting electrolyte.

CO uptake measurements

In order to evaluate the equilibrium constant for carbonylation K_{CO} by UV/visible spectrophotometry, the solutions of aquo species [Ru(EDTA-H)(H_2O)] **1** and [Ru(PDTA-H)(H_2O)] **2** were prepared in the concentration of $5 \times 10^{-4} M$ at *p*H = 5 in doubly distilled water. The chloro complexes immediately underwent aquation in solution to form the aquo species [Ru(EDTA-H)(H_2O)] **1** and [Ru(PDTA-H)(H_2O)] **2**. Solutions of complexes **1** and **2** were saturated with CO by varying the concentration of CO in the range 1:1, 1:2 and 1:3 with respect to the degassed doubly distilled water. The wavelength of maximum absorbance (λ_{max}) at 386-390 nm for carbonyl complexes was found by passing CO through the solution of the complexes **1** and **2** and recording the spectra. For each concentration, the spectrum was recorded immediately at 10°, 25° and 40° and a constant value of absorbance was noted. The solubility of CO was also measured separately in water at different temperatures. The reaction of the complexes with CO may be written as:

$$Ru^{III}L(H_2O) + CO \leftrightharpoons Ru^{III}(L)(CO) + H_2O$$

$$K_{CO} = \frac{[Ru^{III}L(CO)]}{[Ru^{III}(L)(H_2O)][CO]}$$

L = EDTA-H; PDTA-H

Table 1—Thermodynamic parameters and equilibrium constant for CO binding in Ru(III) aminopolycarboxylic acid complexes in aqueous medium

Complexes	Temp. °C	log K_{CO}	$\Delta H°$ (kJ mol^{-1})	$\Delta G°$ (25°) (kJ mol^{-1})	$\Delta S°$ (25°) (J deg^{-1} mol^{-1})
1 [Ru(EDTA-H)(H_2O)	10	2.80 ± 0.2			
	25	2.65 ± 0.3	−28 ± 1	−15.1 ± 0.5	−43 ± 4
	40	2.31 ± 0.1			
2 [Ru(PDTA-H)(H_2O)]	10	3.01 ± 0.1			
	25	2.73 ± 0.02	−30 ± 1	−15.5 ± 0.5	47 ± 4
	40	2.45 ± 0.1			

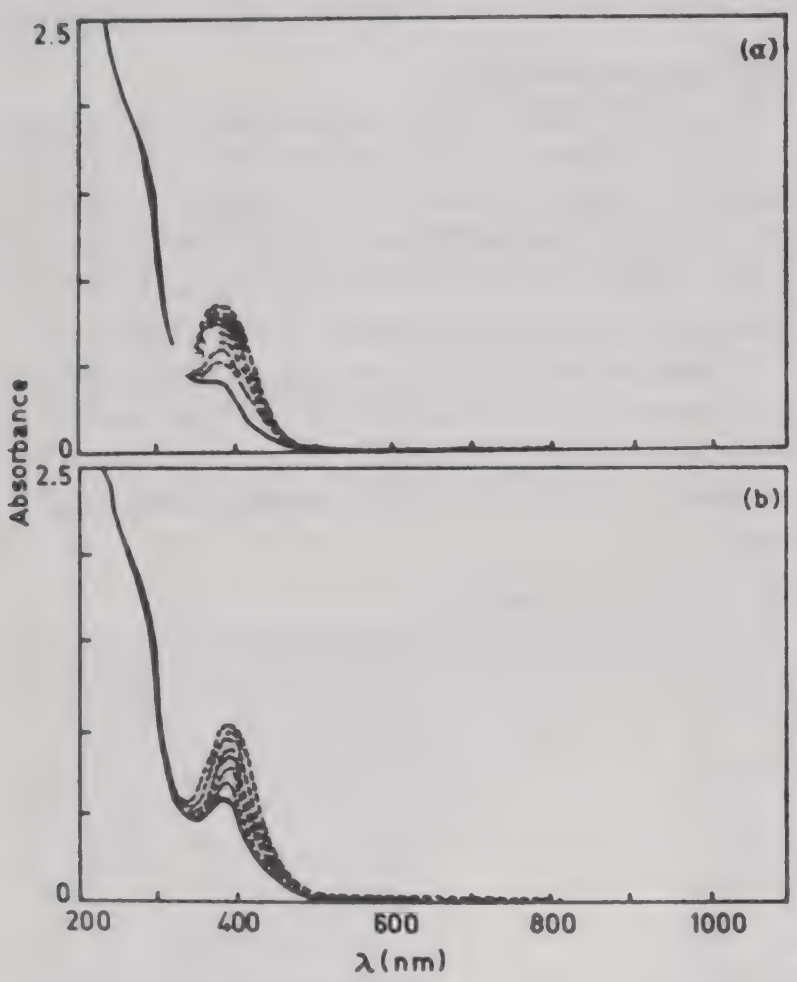

Fig. 1—(a) The UV-vis. absorption spectral change during carbonylation of [Ru(EDTA-H)(H_2O)] in water at *p*H = 5 (1×10^{-3} *M*) with time (——) soon after preparation (----) after 4 h; in 15 min intervals at 303°K and path length 1 = 1 cm.

Fig. 1—(b) The UV-vis. absorption spectral change during carbonylation of [Ru(PDTA-H)(H_2O)] in water at *p*H = 5(1×10^{-3} *M*) with time (——) soon after preparation, (----) after 4h; in 15 min intervals at 303°K and path length 1 = 1 cm.

The equilibrium constant K_{CO} was calculated by reported method[20].

Results and discussion

The UV-visible spectra recorded in doubly distilled water at *p*H 5 saturated with CO show an increase in absorbance at (λ_{max} = 390-386 nm) with time. Representative absorption spectra of [Ru(EDTA-H)(H_2O)] and [Ru(PDTA-H)(H_2O)] in aqueous solution saturated with CO are depicted in Fig. 1a and 1b, respectively. The maximum increase in absorbance was observed at 390 and 386 nm and assigned to MLCT M → CO band. The reversible binding of CO is confirmed by flushing nitrogen through the solution which displaces CO and the original spectrum of the complexes was obtained. This reflects on the low stability of Ru(III) carbonyl complexes over those of Ru(II) carbonyl species which are more stable because of greater softness and lower value of electronegativity of Ru(II) as compared to Ru(III).

Carbonylation of the complexes does not cause a reduction of Ru(III) to Ru(II). This was confirmed by the measurement of $E_{1/2}$ of Ru(III)/Ru(II) couple in D.C. and differential pulse polarograms of the solutions. Under N_2, the $E_{1/2}$ values lie at −0.18 volts (RuPDTA) and −0.15 volts (RuEDTA) while under CO the Ru(III)/Ru(II) couple shift towards more negative side and lie at −0.25 volts in RuPDTA and −0.20 volts in RuEDTA. This behaviour was also seen in CO binding to Ru(III) Schiff base complexes[21-23].

On dissolution of the complexes **1** and **2** in aqueous media Cl^- is immediately displaced by water to form aquo complex and later by displacement of H_2O by CO to form carbonyl complexes. The lability of chloro group is very important for catalysis of the complexes in carbonylation reaction[24].

The discrimination in binding of CO depends on the polarity of the solvents as well as the electron-donating substituent attached. A good σ donor increases[25] the electron density on ruthenium(III) and assists in the labilization of H_2O molecule in a nucleophilic displacement reaction.

From the data in Table 1 the equilibrium constant for carbonylation K_{CO} was comparatively more for [Ru(PDTA-H)(H_2O)] **2** compared to [Ru(EDTA-H)(H_2O)] **1**. It may be due to the inductive effect of the methyl group attached to ethylenediamine collar

in PDTA complex. The stability of carbonyl complexes with respect to the ligands (EDTA and PDTA) decreases in the order RuPDTA> RuEDTA. The same trend was also reported elsewhere[26]. The stability K_{CO} of the [Ru(EDTA-H)(CO)] complex at 25° agrees very well with that obtained indirectly[16] by kinetic method.

The thermodynamic parameters associated with reversible binding of CO to complexes **1** and **2** are given in Table 1. Since the overall reaction involves a displacement of H_2O molecule by CO the enthalpy should depend on the labilization of H_2O molecule in the complexes and depends[25] on the extent of σ donation and π-backbonding of the ligands present in the coordination sphere of the metal ion. The stability of the carbonyl complex of Ru(III)EDTA-H and Ru(III) PDTA-H complexes are about an order to magnitude lower than that of Ru(III) schiff base complexes[20-22]. The complexes exhibit discrimination towards CO binding as compared to oxygen[21,23]. The lower stability of Ru(III) carbonyls seems to be predominantly due to decrease in the $d\pi$-$p\pi$ back-bonding of CO in these complexes. From the thermodynamic data the enthalpy values which are a measure of metal ligand bond strength are more endothermic in [Ru(EDTA-H)(CO)] **3** as compared to [Ru(PDTA-H)(CO)] **4** complex which reflects on a weaker M-CO bond strength in **3** as compared to **4**. The entropy is more positive in **3** compared to **4** indicating a loss of vibrational and rotational degrees of freedom of CO on coordination to the metal ion.

References

1 Collman J P, Brauman J I, Iverson B L, Sessler J L, Morris R M & Gibson Q H, *J Am chem Soc*, 105 (1983) 3052.

2 Perutz M F, *Annu Rev Biochem*, 48 (1979) 327.

3 Perutz M F, *Proc R Soc London Ser B*, 208 (1980) 135.

4 Uemori Y & Kyuno E, *Inorg Chim Acta*, 165 (1989) 115.

5 Moffat K, Deatherage J F & Seybert D W, *Science* (Washington D C), 206 (1979) 1035.

6 Baldwin J, *J mol Biol*, 136 (1980) 103.

7 Collman J P, Brauman J I, Collins T J, Iverson B & Sessler J L, *J Am chem Soc*, 103 (1981) 2450.

8 Traylor T G, Koga N & Deardurff L A, *J Am chem Soc*, 107 (1985) 6504.

9 Suslick K S, Fox M M & Reinert T J, *J Am chem Soc*, 106 (1984) 4522.

10 Traylor T G, Koga N, Deardurff L A, Swepston P N & Ibers J A, *J Am chem Soc*, 106 (1984) 5139.

11 Kushkin N Yu, *Koord Khim*, 12 (1986) 147.

12 Bhattacharya A A, Nagel C C & Shore S G, *Organometallics*, 2 (1983) 1187.

13 Catlon R & Farthing R H, *Aust J Chem*, 24 (1971) 903.

14 Halpern J, James B R & Kemp A L W, *J Am chem Soc*, 88 (1966) 5142.

15 Yeh A & Taube H, *Inorg Chem*, 19 (1980) 3740.

16 Taqui Khan M M, Amjad Hussain, Moiz M A & Naik R N, *Polyhedron*, 8 (1989) 2199.

17 Taqui Khan M M, Bajaj H C, Shirin Z & Venkatasubramanian K, *Polyhed* (1991) in Press.

18 Taqui Khan M M, Venkatasubramanian K, Bajaj H C & Shirin Z, *Indian J Chem*, (In Press).

19 Taqui Khan M M, Hussain A, Ramachandraiah G & Moiz M A, *Inorg Chem*, 25 (1986) 3023.

20 Rose N J & Drago R S, *J Am chem Soc*, 81 (1959) 6138.

21 Taqui Khan M M, Khan N H, Kureshy R I & Boricha A B, *Inorg Chim Acta*, 174 (1990) 175.

22 Taqui Khan M M, Khan N H, Kureshy R I, Shaikh Z A & Boricha A B, *Inorg Chim Act*, 170 (1990) 213.

23 Taqui Khan M M, Kureshy R I & Khan N H, *Inorg Chim Acta*, 181 (1991) 119.

24 Taqui Khan M M, Halligudi S B, Shukla S & Sheikh Z A, *J mol Catal*, 57 (1990) 301.

25 Isied S S & Taube H, *Inorg Chem*, 15 (1976) 3070.

26 Taqui Khan M M, Moiz M A & Hussain A, *J coord Chem*, 23 (1991) 245.

Indian Journal of Chemistry
Vol. 31A, November 1992, pp. 886-888

Synthesis and characterization of chloro-, acetylacetonato-, and alkoxo-nonaisopropoxodizirconatoiron (III) derivatives

A Shah, A Singh* & R C Mehrotra†

Department of Chemistry, University of Rajasthan, Jaipur 302 004

Received 25 November 1991; revised and accepted 27 May 1992

Dizirconiumnonaisopropoxo derivatives of iron (III) of the types $FeCl_2\{Zr_2(OPr^i)_9\}$, $FeCl\{Zr_2(OPr^i)_9\}_2$, $FeX_2\{Zr_2(OPr^i)_9\}$ and $FeX\{Zr_2(OPr^i)_9\}_2$ (X = OMe, OPr^i, OBu^t, acac) have been synthesized and characterized on the basis of elemental analyses and spectral, magnetic and molecular weight measurements.

The use of (binary- and mixed-) metal alkoxides as molecular precursors for electronic and ceramic materials is an area of current interest and has recently been reviewed[1-4].

Although many examples of heterometal alkoxides[5,6] of iron (II & III) are known in the literature, very little is known about derivatives of the type $X_{3-n}Fe\{Zr_2(OPr^i)_9\}_n$ (where X = Cl, OMe, OPr^i, OBu^t, acac; $n = 1$ or 2). The derivatives of the type $Cl_{3-n}Fe\{Zr_2(OPr^i)_9\}_n$ are especially interesting because of their potential as precursors[6] for heteropolymetallic alkoxide compounds. The chelated metal alkoxide complexes possess the advantage of controlling the reactivity[7,8] to function as modifiers during the conversion of metal alkoxide derivatives to mixed-metal oxides via sol-gel process.

In this paper, we report the synthesis and characterization of novel heteroleptic nonaisopropoxodizirconatoiron (III) complexes.

Experimental

Anhydrous ferric chloride (Fluka) was purified by sublimation in a current of dry chlorine gas prior to use. Solvents in parentheses were dried over and distilled from Na/benzophenone (benzene), CaH_2 (isopropyl- and tertiary butyl alcohols), $Mg(OMe)_2$ (methyl alcohol) followed by azeotropic fractionation after adding 1-2 ml of an anhydrous appropriate azeotrope forming (C_6H_6 or Pr^iOH) solvent. Acetylacetone (BDH) was dried over anhydrous $MgSO_4$ filtered and fractionated over $Al(OPr^i)_3$.

All manipulations and reactions were carried out in oven dried (130-140°C) quick-fit glassware under strictly moisture-free atmosphere.

Infrared (4000-200 cm^{-1}) and reflectance spectra in nujol were recorded on a Perkin-Elmer 557 and Beckman DK-2 spectrophotometers respectively. Magnetic susceptibility measurements were carried out on a Bruker Magnetic Balance by the Gouy method using $Hg\{Co(SCN)_4\}$ as calibrant. The diamagnetic corrections (χ_{dia}) were calculated from Pascal's constants[9]. Molecular weights were determined ebullioscopically in benzene on a Gallenkamp apparatus.

Zirconium was estimated as ZrO_2 after precipitation as mandelate. Iron was estimated colorimetrically as ferric thiocyanate on a Bausch and Lomb spectronic 21 instrument. Alkoxy groups were estimated by dichromate oxidation method[10].

Preparation of heterobimetallic alkoxides of iron (III)

A number of interesting heterometal alkoxo complexes of iron (III) have been prepared by metathetical reactions involving iron (III) chloride or a nonaisopropoxodizirconatoiron (III) chloride and an appropriate alkoxo-, nonaisopropoxo-, dizirconato-, or acetylacetonato- ligand, as illustrated by the following typical examples:

(a) $FeCl_2\{Zr_2(OPr^i)_9\}$ (1)

To a benzene (~40 ml) suspension of anhydrous ferric chloride (0.86 g, 5.30 mmol) was added portion-wise solid potassium dizirconiumenneaisopropoxide** (3.99 g, 5.29 mmol) and the resulting mixture was stirred for 2 h, followed by refluxing for ~ 1 h. The precipitated potassium chloride (0.39 g, 5.30 mmol) was removed by filtration and an orange yellow solid product was isolated from the filtrate in quantitative yield by removing the volatiles under reduced pressure. The product **1** was volatilized unchanged in analysis at a bath in temperature of 205°C under reduced pressure (0.1 mm in ~ 50% yield.

†Present address: Vice-Chancellor, University of Allahabad, Allahabad 211 002

**Calculated on the basis of potassium metal used and isolated as solid by stripping off the volatiles under reduced pressure.

By carrying out the reaction of $FeCl_3$ and $K\{Zr_2(OPr^i)_9\}$, (1:2 molar ratio), a volatile product $FeCl\{Zr_2(OPr^i)_9\}_2$ (**2**) was isolated as a yellowish brown solid.

(b) $Fe(OMe)_2\{Zr_2(OPr^i)_9\}$

Potassium methoxide** (0.64 g, 9.13 mmol) was added portionwise to a benzene (~ 50 ml) solution of $FeCl_2\{Zr_2(OPr^i)_9\}$ (3.86 g, 4.58 mmol). The resulting mixture was stirred for 2 h at room temperature, followed by refluxing for ~ 2h. The yellowish brown solid product (**3**) was isolated in ~ 100% (2.97 g) yield by filtering off precipitated KCl (0.68 g, 9.17 mmol) and taking the benzene solution to dryness under reduced pressure. The product was further purified in ~ 70% yield by volatilization at a bath temperature of 180°C under reduced pressure (0.1 mm).

Adopting the above procedure by interacting appropriate reactants in required molar ratios, derivatives **4-10** were isolated quantitatively and volatilized (178 ± 12°C/0.1 mm) unchanged in high yields. The analytical data of all the complexes are presented in Table 1.

Table 1—Characterization data of heterobimetallic alkoxide derivatives of iron (III)

Compd	Colour Volatility (°C/mm)	Found (calcd), %		
		Fe	Zr	OR
1	Orange yellow 205/0.1	6.60 (6.54)	21.88 (21.68)	63.21 (63.28)
2	Yellowish brown 210/0.1	3.63 (3.67)	24.32 (24.00)	69.96 (69.98)
3	Yellowish brown 180/0.1	6.70 (6.71)	22.16 (21.98)	63.96 (73.18)
4	Brown 185/0.1	6.32 (6.29)	20.78 (20.54)	73.10 (73.18)
5	Dark brown 188/0.1	6.12 (6.09)	20.24 (19.91)	58.21 (58.06)
6	Reddish brown 190/0.1	5.72 (5.77)	19.11 (18.84)	54.82 (59.94)
7	Brown 162/0.1	3.63 (3.68)	24.32 (24.07)	70.26 (70.19)
8	Brown 165/0.1	3.60 (3.62)	23.88 (23.64)	72.76 (72.74)
9	Dark brown 165/0.1	3.54 (3.59)	23.48 (23.43)	68.36 (68.30)
10	Orange brown 188/0.1	3.52 (3.53)	23.46 (23.04)	67.14 (67.18)

Results and discussion

Anhydrous freshly sublimed ferric chloride undergoes metathesis with potassium nonaisopropoxodizirconate (1−) to give, sequentially, $FeCl_2\{Zr_2(OPr^i)_9\}$ (**1**) and then $FeCl\{Zr_2(OPr^i)_9\}_2$ (**2**) according to Eqs. 1 and 2.

$$FeCl_3 + K\{Zr_2(OPr^i)_9 \xrightarrow{\text{benzene}} \underset{(\mathbf{1})}{FeCl_2\{Zr_2(OPr^i)_9\}} + KCl\downarrow \quad \ldots(1)$$

$$\mathbf{1} + K\{Zr_2(OPr^i)_9\} \xrightarrow{\text{benzene}} \underset{(\mathbf{2})}{FeCl\{Zr_2(OPr^i)_9\}_2} + KCl\downarrow \quad \ldots(2)$$

Formation of **2** can also be effected conveniently in high yields by carrying out the reaction of $FeCl_3$ with two equivalents of $K\{Zr_2(OPr^i)_9\}$ in benzene.

$$FeCl_3 + 2K\{Zr_2(OPr^i)_9\} \xrightarrow{\text{benzene}} \mathbf{2} + 2HCl\downarrow \quad \ldots(3)$$

1 and **2** serve as precursors for a number of other interesting derivatives, e.g.,

$$\mathbf{1} + 2KX \rightarrow FeX_2\{Zr_2(OPr^i)_9\} + 2KCl\downarrow \quad \ldots(4)$$

3, X = OMe; **4**, X = OPr^i; **5**, X = OBu^t; **6**, X = acac

$$\mathbf{2} + KX \rightarrow FeX\{Zr_2(OPr^i)_9\}_2 + KCl\downarrow$$

7, X = OMe; **8**, X = OPr^i; **9**, X = OBu^t; **10**, X = acac

All these heterobimetal alkoxo complexes (Table 1) are coloured, volatile, hydrocarbon soluble, and highly moisture-sensitive solids. A noteworthy feature of these derivatives is the monomeric behaviour of the freshly prepared samples in boiling benzene. However, on being stored for 1-2 days, the samples show molecular complexity of generally two, except the derivatives **6** and **10** which remain monomeric.

The structurally relevant infrared bands for the new derivatives (**1**: 325, 370, 460, 495, 570, 610, 955, 1040, 1130, 1140; **2**: 360, 425, 445, 540, 1000, 1120, 1150; **3**: 435, 455, 555,830, 930, 1000, 1130, 1150; **4**: 465, 520, 570, 840, 1010, 1140, 1165; **6**: 410, 530, 1000, 1110, 1145, 1575; **7**: 475, 550, 1005, 1125, 1155; **8**: 445, 515, 565, 840, 945, 1010, 1130, 1160; **9**: 430, 500, 510, 1000, 1115, 1150 cm^{-1}) are assigned on the basis of published data on metal alkoxides[11] in the range 1160-1130 ν(alkoxy), 1030-930 ν(C−O) and 570-410 ν(M−O) cm^{-1}.

The bimetallic derivative **1** exhibits ν(Fe−Cl) bands at 370 and 325 cm^{-1}. The former band is close to ν(Fe−Cl) in $FeCl_3$-dioxane (380 cm^{-1}) (ref. 12) and $FeCl_3$ (4-cyanopyridine) (372 cm^{-1}) (ref. 13), for which trigonal bipyramidal geometry has been suggested and actually observed by

X-ray diffraction study respectively. The band at 325 cm^{-1} may be ascribed to ν(Fe−Cl) bridging. For the derivative **2**, the occurrence of only one band at 360 cm^{-1} assignable as ν(Fe−Cl) may be indicative of a five-, or six-coordinated geometry.

The diffuse reflectance spectral studies[14] of new heterobimetallic alkoxides of iron (III) (absorption maxima, cm^{-1}): **1**: 6565, 7505, 8520, 12780; **2**: 6570, 7500, 8520, 12790; **3**: 6500, 7505, 8525, 12730; **4**: 6665, 7590, 8600, 13470; **5**: 6480, 7460, 8540, 12725; **7**: 6380, 7690, 8815, 13335; **8**: 6740, 7690, 8820, 13340; **9**: 5150, 6310, 7370) as expected are not informative, although some indications about probable geometries may be obtained. Derivatives **1-5** and **7-2** showed absorptions in the range 5100-7600 cm^{-1} which can be assumed to be a mixture of the overtone of the C−H stretching and bending modes. The bands observed in the range 12000-13400 cm^{-1} could be due to the $^6A_1 \rightarrow {}^4T_1$, $^4T_2$ transitions in a distorted octahedral environment around the iron atom.

The room temperature magnetic moment values for the complexes (**6**) and (**10**) are in the range 5.70-5.90 B.M., indicating high spin nature[15] of the derivatives. However, the aged samples of **1-5** and **7-9** exhibit magnetic moments in the range of 4.20-4.95 B.M., which could be due to the weak intermolecular antiferromagnetic interactions[16], which are also reflected in the associated nature of the complexes, through bridging (chloro or alkoxo) groups in these complexes.

Acknowledgement

The partial financial support by the Department of Science and Technology, New Delhi, is greatly appreciated. One of us (A. Shah) is thankful to the CSIR, New Delhi for the award of a fellowship.

References

1 Mehrotra R C, *Mat Res Soc Symp Proc*, 121 (1988) 81; *J Non-cryst Solids*, 121 (1990) 1; *Chemtracts*, 2 (1990) 389.
2 Bradley D C, *Chem Rev*, 89 (1989) 317; *Phil Trans R Soc Lond*, A330 (1990) 167.
3 Livage J, Henry M & Sanchez C, *Prog Solid State Chem*, 18 (1988) 259.
4 Hubert-Pfalzgraf L G, *New J Chem*, 11 (1987) 663.
5 (a) Shah A, Singh A & Mehrotra R C. *Indian J Chem*, 26A (1987) 485:
(b) Shah A, Singh A & Mehrotra R C, *Inorg chim Acta*, 141 (1988) 289.
(c) Shah A, Singh A & Mehrotra R C, *Indian J chem*, 28A (1989) 392.
(d) Gupta R, Singh A & Mehrotra R C, *Indian J Chem*, 29A (1990) 596.
(e) Gupta R, Singh A & Mehrotra R C, *Indian J Chem*, 30A (1991) 592.
6 Dubey R K, Shah A, Singh A & Mehrotra R C, *Recl Trav chim Pays-Bas*, 107 (1988) 237.
7 Nass R & Schmidt H, *J Non-Cryst Solids*, 121 (1990) 329 and references therein.
8 Babonneau F, Coury L & Livage J, *J Non-Cryst Solids*, 121 (1990) 153.
9 Selwood P W, *Magnetochemistry* (Interscience, New York) 1956.
10 Bradley D C, Halim F M A & Wardlaw W, *J chem Soc*, (1950) 3450.
11 (a) Bradley D C, Mehrotra R C & Gaur D P, *Metal alkoxides* (Academic Press, New York) 1978;
(b) Barraclough C G, Bradley D C, Lewis J & Thomas I M, *J chem Soc* (1961) 2601;
(c) Rao C N R, *Chemical applications of infrared spectroscopy* (Academic Press, New York) 1963.
12 Fowles G W A, Rice D A & Walton R A, *J chem Soc* (*A*), (1978) 1842.
13 Maeda Y & Takashima Y, *Inorg nucl chem Lett*, 12 (1976) 313.
14 Lever A B P, *Inorganic electronic spectroscopy*, 2nd edn (Elsevier, Oxford), 1982.
15 (a) Figgis B N & Lewis J, *Progr inorg Chem*, 6 (1964) 37.
(b) Earnshaw A, *Introduction to magnetochemistry* (Academic Press, London) 1968.
16 Marray K S, *Coord chem Rev*, 12 (1974) 1.

Indian Journal of Chemistry
Vol. 31A, November 1992, pp. 889-891

Synthesis and characterization of homo and hetero trinuclear alkoxides

Gangadhar G Talele & Pabitra K Bhattacharya*
Department of Chemistry, Faculty of Science,
M S University of Baroda, Baroda 390 002

Received 7 October 1991; revised 30 April 1992;
accepted 9 July 1992

Trinuclear complexes of the type $[L'Cu(OR)_2.M(OR)_2CuL^2]$ $(ClO_4)_2$ where $L' = L^2 = 1$, 10-phenanthroline, 2, 2-bipyridyl and M = Cu(II) or Ni(II), $R = CH_3$, OPr^i have been prepared and characterised by elemental analyses, IR spectra and magnetic measurement studies.

The synthesis of homo and hetero trinuclear complexes of transition metal ions with various types of organic ligands have been reported[1-3]. Among the alkoxide bridged complexes are the trinuclear Cu(II) complexes with alkoxy bridges[4,5] and some homo and hetero termetallic isopropoxides of non-transition metal ions[6]. Hatfield *et al* have reported trinuclear Cu(II) complexes with terminal and bridging amino alcohols[7]. Binuclear complexes[8] of the type $[LCu(OR)_2CuL]ClO_4$ have been reported from our laboratory. In the present note we describe the synthesis of homo and hetero trinuclear complexes with di-methoxy or isopropoxy bridges of the type $[L\,Cu(OR)_2M(OR)_2CuL]ClO_4$, where M = Cu(II) or Ni(II).

Experimental

All the chemicals used were of AR grade. Methanol and isopropanol were dried by known methods[9]. Copper and nickel were determined by complexometric titrations after decomposition with acid[10]. Carbon, hydrogen and nitrogen were determined in the microanalytical laboratory of the department. Magnetic measurements in the solid state were carried out by the Guoy method at room temperature. IR spectra of the complexes were recorded in the region 4000-650 cm^{-1} in KBr phase on a Shimadzu IR 408 and the electronic spectra were recorded on a Shimadzu UV/Visible recording spectrophotometer (UV-240 graphicord) in the region 350-850 nm using barium sulphate as a reference material.

Preparation of complexes

$[LCu(ClO_4)_2]$

A solution of copper acetate (3.993 g, 0.02 mol) in methanol (100 ml) was thoroughly mixed with a solution of 1, 10-phen (3.964 g, 0.02 mol) or 2, 2′-dipy (3.1238 g, 0.02 mol) in methanol (~50 ml). To this solution, sodium perchlorate (5.616 g, 0.04 mol) dissolved in methanol (~80 ml) was added with stirring. The complex $[LCu(ClO_4)_2]$ precipitated out immediately in the form of blue crystals. The solid was filtered, washed with dry methanol and dried *in vacuo* at room temperature.

$[LCu(OR)_2LiClO_4]$

[Phen $Cu(ClO_4)_2$] (5.311 g, 0.012 mol) or [bipy $Cu(ClO_4)_2$] (5.023 g, 0.012 mol) was suspended in dry methanol or isopropanol (~80 ml). $LiOCH_3$ (0.9112 g, 0.024 mol) or $iOPr^i$ (1.5846 g, 0.024 mol) dissolved in dry methanol or isopropanol (~ 50 ml), was added and the mixture refluxed for 5 h. The resulting solution was cooled and the precipitate formed was filtered, washed with dry methanol and dried *in vacuo* at room temperature.

$[LCu(OR)_2M(OR)_2CuL]$ $(ClO_4)_2$

The trinuclear complexes were prepared by the following two methods:

(i) [Phen $Cu(ClO_4)_2$] (4.4265 g, 0.01 mol) or [bipy $Cu(ClO_4)_2$] (4.1865 g, 0.01 mol) was suspended in dry methanol or isopropanol (~100 ml) and to this was added $LiOCH_3$ (0.7594 g, 0.02 mol) or $LiOPr^i$ (1.3205 g, 0.02 mol) dissolved in ethanol (~50 ml) and refluxed for 5 h. After cooling, copper perchlorate (1.828 g, 0.005 mol) was added and the solution again refluxed for 5 h. The resulting product was cooled, filtered and washed with dry methanol and dried *in vacuo* at room temperature.

(ii) [$PhenCu(OCH_3)_2LiClO_4$] (4.122 g, 0.01 mol) or [$phenCu(OiPr)_2$ $LiClO_4$] (4.883 g, 0.01 mol) or [$dipyCu(OCH_3)_2LiClO_4$] (3.882 g, 0.01 mol) or [dipy $Cu(OiPr)_2LiClO_4$] (4.441 g, 0.01 mol) was suspended in dry methanol or isopropanol (~ 100 ml), respectively. To this was added copper perchlorate (1.852 g, 0.005 mol) or nickel perchlorate (1.8282 g, 0.005 mol) and the mixture refluxed for 5 h. The resulting product was filtered, washed with dry methanol and dried *in vacuo* at room temperature.

Results and discussion

When $CuL(ClO_4)_2$ is reacted with half equivalent of metal perchlorate in the presence of lithium alkoxide, a trinuclear complex is formed. The reactions can be represented as follows:

Table 1—Characterization data of the complexes

Sl. No.	Empirical formula	Analysis Found (Calc.), %				μ_{eff} (BM)	Visible spectral bands (nm)
		M	N	C	H		
1.	[phen.Cu$(OCH_3)_2$Cu$(OCH_3)_2$Cu.phen] $(ClO_4)_2$ $Cu_3C_{28}H_{28}N_4O_{12}Cl_2$	20.59 (21.81)	6.85 (6.40)	38.85 (38.41)	3.01 (3.23)	2.944	630
2.	[dipy.Cu$(OCH_3)_2$Cu$(OCH_3)_2$Cu.dipy] $(ClO_4)_2$ $Cu_3C_{24}H_{28}N_4O_{12}Cl_2$	23.62 (23.07)	7.28 (6.78)	35.30 (34.89)	3.12 (3.41)	2.548	585
3.	[phen.Cu$(Opr^i)_2$Cu$(Opr^i)_2$Cu.phen] $(ClO_4)_2$ $Cu_3C_{36}H_{44}N_4O_{12}Cl_2$	19.06 (19.32)	6.11 (5.68)	41.91 (43.83)	3.98 (4.49)	2.658	580
4.	[dipy.Cu$(Opr^i)_2$Cu$(Opr^i)_2$Cu.dipy] $(ClO_4)_2$ $Cu_3C_{32}H_{44}N_4O_{12}Cl_2$	19.78 (20.31)	6.73 (5.97)	39.52 (40.96)	4.35 (4.69)	2.902	575
5.	[phen.Cu$(OCH_3)_2$Ni$(OCH_3)_2$Cu.phen] $(ClO_4)_2$ $Cu_2NiC_{28}H_{28}N_4O_{12}Cl_2$	Cu = 14.21 (14.61) Ni = 6.45 (6.75)	6.64 (6.44)	38.04 (38.68)	3.03 (3.24)	2.78	625
6.	[dipy.Cu$(OCH_3)_2$Ni$(OCH_3)_2$Cu.dipy]$(ClO_4)_2$ $Cu_2NiC_{24}H_{28}N_4O_{12}Cl_2$	Cu = 14.95 (15.47) Ni = 6.82 (7.14)	6.46 (6.82)	34.87 (35.10)	3.11 (3.41)	2.88	590
7.	[phen.Cu$(Opr^i)_2$Ni$(OPr^i)_2$Cu.phen]$(ClO_4)_2$ $Cu_2NiC_{36}H_{44}N_4O_{12}Cl_2$	Cu = 12.35 (12.94) Ni = 5.96 (5.98)	6.05 (5.70)	43.80 (44.05)	4.04 (4.48)	3.74	620
8.	[dipy.Cu$(OPr^i)_2$Ni$(OPr^i)_2$Cu.dipy]$(ClO_4)_2$ $Cu_2NiC_{32}H_{44}N_4O_{12}Cl_2$	Cu = 13.10 (13.61) Ni = 6.02 (6.29)	5.59 (6.00)	40.53 (41.18)	4.35 (4.75)	3.20	590

$$2LCu(ClO_4)_2 + 4\ LiOR + M(ClO_4)_2 \rightarrow [LCu(OR)_2M(OR)_2CuL]\ (ClO_4)_2 + 4\ LiClO_4$$

$$LCu(ClO_4)_2 + 2\ LiOR \rightarrow [LCu(OR)_2LiClO_4] + LiClO_4$$

$$2[LCu(OR)_2Li]\ ClO_4 + M(ClO_4)_2 \rightarrow [LCu(OR)_2M(OR)_2CuL]\ (ClO_4)_2 + LiClO_4$$

(where R = CH_3, Pr^i; L = phen, bipy; and M = Cu(II), Ni(II)

The elemental analyses of the complexes correspond to the expected composition, but in some cases the values have been found to be unsatisfactory. Normally, in alkoxides, carbon hydrogen analysis is not possible because of their susceptibility to hydrolysis, leading to the formation of alcohol which evaporates.

However, Cu(II) alkoxides are less susceptible to hydrolysis and, hence, C, H and N values are within the expected range in most of the cases. The analytical data are presented in Table 1.

A general structure involving the coordination of two $(NN)M(OR)_2$ with the central metal ion through four alkoxy bridges can be assigned on the basis of the analytical data. This is further supported by the spectral characteristics of the complexes.

The IR spectra of these complexes exhibit the expected bands. The absorption frequencies for bridging ν(C−O+OR) have been observed at 1170-1120, 940-920 and 870-810 cm^{-1}, which correspond to the bridging ν(CO+OR) bands observed in the complexes of bimetallic alkoxides in which two metal atoms are linked through the oxygen of the alkoxy group[11].

The bands of dipyridyl and 1,10-phenanthroline in the complexes appear as two groups of doublets in the range 1590-1560 cm^{-1} and 1500-1430 cm^{-1}. The bands are shifted from the position of the free ligand bands and support coordination of the dipyridyl or 1, 10-phenanthroline.

A broad absorption band ~ 600 nm in the visible spectra of all the complexes corresponds to the three transitions $B_{2g} \leftarrow B_{1g}$, $A_{1g} \leftarrow B_{1g}$, $E_g \leftarrow B_{1g}$ as expected of square planar Cu(II) complexes. In case of hetero dinuclear complex with Ni(II) also, one band is observed in the region of study. The band due to the Ni(II) centre merges with the Cu(II) band. In case of trinuclear Cu(II) complexes, magnetic moments per copper atom are much less than one unpaired electron. This indicates that there is superexchange

between three Cu(II) centres, which are bridged through alkoxy oxygen. In case of methoxy bridged hetero trinuclear complexes, magnetic measurements correspond to two unpaired electrons showing that there is no superexchange between two Cu(II) centres and Ni(II) has a square planar structure. But in hetero-trinuclear complexes with an isopropoxy bridge, the magnetic moment corresponds to more than two unpaired electrons per molecule, showing some paramagnetism due to the Ni(II) centre. This indicates that there is distortion of square planar geometry around the Ni(II) in this complex.

Acknowledgement

We are thankful to the UGC, New Delhi, for the award of a teacher fellowship to one of us (GGT).

References

1 Gruber S J, Harris C M & Sinn E, *Inorg nucl chem Lett*, 3 (1967) 495; *J chem Phys*, 49 (1968) 2183.
2 Patel K V & Bhattacharya P K, *Polyhedron*, 5 (1986) 731.
3 Nishida Y, Keiji I, Hisashi O & Kida S, *Chem Lett*, (1989) 1251.
4 Masahiro M, Hisashi O & Kida S, *Bull chem Soc Japan*, 53 (1980) 2871; *Inorg chim Acta*, 42, (1980) 233.
5 Ferguson G, Langrio R C, Parker D & Mathes K, *J chem Soc Commun*, 22 (1985) 1605.
6 Agrawal M & Mehrotra R C, *Polyhedron*, 4 (1985) 845.
7 Mahone H & Hatfield W E, *Acta chem Scand Ser (A)*, 40 (1986) 41.
8 Talele G G & Bhattacharya P K, *Indian J Chem*, 28A (1989) 796.
9 Vogel A I, *A text book of practical organic chemistry*, 4th Edn (Longman, New York) 1986.
10 Vogel A I, *A text book of quantitative inorganic analysis*, (Longman, New York), 1961.
11 Mehrotra R C, Gaur D R & Bradley D C, *Metal alkoxides* (Academic Press, London) 1978.

Indian Journal of Chemistry
Vol. 31A, November 1992, pp. 892-895

Synthesis and characterization of some transition metal picrate complexes with isonicotinic acid hydrazide

Rakesh Bajaj & C L Jain
Department of Chemistry, M M H College, Ghaziabad

and

S K Gupta* & Krishan Lal
Materials Characterization Division,
National Physical Laboratory,
Dr K S Krishnan Marg, New Delhi 110 012
Received 19 December 1991; revised 18 March 1992;
accepted 11 June 1992

The mixed ligand complexes of Cr(III), Fe(II), Co(II), Ni(II), Cu(II) and Zn(II) picrates with isonicotinic acid hydrazide (INH) of the type $[M(pic)_n (INH) (MeOH)_n]$ (where n = 1, 2 or 3) have been prepared and characterized by elemental analysis, conductance, molecular weight, magnetic susceptibility, electronic, IR and EPR spectra. The investigations indicate that metal ions have octahedral structure but low symmetry distortion exists in some cases.

Isonicotinic acid hydrazide (INH) and its complexes are well known for their medicinal uses[1-3]. In this note, we report the synthesis of metal picrate complexes with INH and their characterization by atomic absorption spectroscopy, magnetic susceptibility, osmometry, electronic, IR and EPR data.

Experimental

The chemicals used were of Merck or BDH quality and solvents were purified and made anhydrous employing standard procedure.

Preparation of d-metal picrates

Silver picrate was first prepared by direct reaction of silver hydroxide with picric acid[4]. The picrates of transition metals [Cr(III), Fe(II), Co(II), Ni(II), Cu(II) and Zn(II)] were synthesized by double decomposition method. The aqueous solutions of metal chloride/iodide were reacted with silver picrate in molar ratio [3:1/2:1]. The products obtained were recrystallized from methanol. The molecular weight of each complex was determined by Osmometer method using benzil (diphenyl glyoxal) as reference, yield, 85 to 90%.

Preparation of mixed ligand complexes

A methanolic solution (2%) of isonicotinic acid hydrazide was refluxed on water bath for 1 h with the respective metal picrate in methanol (95%, 150ml) in 1:1 (metal-ligand) ratio. The complexes so obtained were washed with benzene and pet. ether and dried *in vacuo* over anhydrous calcium chloride, yield, 70-80%.

The purity of the complexes was checked by TLC. The elemental analysis was carried out by combustion method (Table 1). The metal analysis was carried out by Perkin Elmer atomic absorption spectrometer, 2380. The conductance was measured on Merk-V Mc-1 conductometer (M/s. Electronic Instruments Ltd., England) in DMF. The densities and molecular weights were determined using micropycnometer and vapour pressure osmometer. Magnetic measurements were carried out using Princeton magnetometer model 155. The IR spectra were recorded on Perkin-Elmer spectrophotometer in the 4000-200 cm^{-1} region. The electronic absorption spectra were recorded on Cary 14 spectrometer. The EPR spectra were recorded as powdered samples on X-band Varian make E-112 spectrometer with 100KHz magnetic field modulation using DPPH as a standard.

Results and discussion

The complexes studied are insoluble in nonpolar solvents but soluble in some polar solvents like pyridine, nitrobenzene and DMF. The molar conductance values (10^{-3} *M*) of the complexes suggest their non-electrolytic nature.

The corrected magnetic moments (Table 1) show that Ag(I) and Zn(II) complexes are diamagnetic. The magnetic moment values of Cr(III), Fe(II), Co(II) and Ni(II) complexes are near to the spin only values, which are indicative of the octahedral stereochemistry[5]. The small discrepancy may be due to the distortion existing around the metal ions as discussed later in EPR results. For Cu(II) complex, a magnetic moment of 1.90 B.M. is in good agreement for tetrahedrally distorted square planar stereochemistry[6,7].

In the electronic spectrum of Cr(III) complex, three bands at 17925, 23620 and 38425 cm^{-1}, are assigned to the charge transfer transitions $^4A_{2g}(F) \rightarrow {}^4T_{2g}(F)$, $^4T_{1g}(F)$ and $^4T_{1g}(P)$ respectively[8,9]. The values of 10Dq, LFSE, B_{35} and β_{35} have been found to lie in the range accepted for octahedral Cr(III) complexes[9]. In Fe(II) complex, one strong band observed at 10942 cm^{-1} ($\varepsilon_{max} = 3.3$) may be assigned

Table 1—Characterization data of mixed ligand complexes

Complex Colour	D.T.(°C)	λ_M Ohm^{-1} cm^2 mol^{-1}	Found (Calc.),%				μ_{eff} BM (300 K)
			C	H	N	M	
$[Cr(Pic)_3$ (INH) (MeOH)] Green	241	51.24	32.02 (33.13)	1.87 (1.88)	18.52 (18.55)	5.62 (5.74)	4.23
$[Fe(Pic)_2$ (INH) $(MeOH)_2]$ Black	228	28.26	31.61 (33.65)	2.48 (2.66)	17.81 (17.67)	7.81 (7.85)	3.76
$[Co(Pic)_2$ (INH) $(MeOH)_2]$ Dark yellow	242	46.12	32.98 (33.51)	2.62 (2.65)	17.42 (17.59)	8.41 (8.23)	4.82
$[Ni(Pic)_2$ (INH) $(MeOH)_2]$ Yellowish green	238	47.12	32.76 (33.52)	2.61 (2.65)	17.54 (17.60)	8.12 (8.20)	3.43
$[Cu(Pic)_2$ (INH) $(MeOH)_2]$ Green	239	30.02	33.42 (33.29)	2.57 (2.64)	17.52 (17.48)	8.94 (8.81)	1.90
$[Zn(Pic)_2$ (INH) $(MeOH)_2]$ Yellow	246	26.24	33.02 (33.21)	2.46 (2.63)	17.42 (17.43)	9.02 (9.05)	0.08
[Ag(Pic) (INH) $(MeOH)_2]$ Golden yellow	236	19.04	29.42 (30.87)	2.46 (2.57)	14.74 (14.76)	18.98 (18.97)	0.06

to the transition $^5T_{2g} \rightarrow {}^5E_g$ (D) (ref. 9,10). The electronic spectrum of Co(II) complex exhibits three bands at 9750, 19950 and 22725 cm^{-1} assigned to $^4T_{1g}$ $(F) \rightarrow {}^4T_{2g}$ (F), $^4A_{2g}$ (F), and $^4T_{1g}$ (P) transitions in octahedral geometry[10,11]. In Ni(II) complex bands at 9630, 17809 and 27400 cm^{-1} ($\varepsilon_{max} = 2.72$, 3.08 and 2.88) due to transitions $^3A_{2g}$ $(F) \rightarrow {}^3T_{2g}$ (F), $^3T_{1g}$ (F) and $^3T_{1g}$ (P) were observed[12]. The calculated values of ligand field parameters were found to be higher than the earlier reported values of octahedral Ni(II) complexes[13] which suggests the presence of distorted octahedral geometry around Ni(II). For Cu(II) complex, three bands observed at 15250, 17740 and 20240 cm^{-1} corresponding to the transitions $^2B_{1g}$ $\rightarrow {}^2A_{1g}$, ^2E_g, $^2B_{2g}$ suggest the tetragonally distorted square planar stereochemistry[14].

In the infrared spectrum of isonicotinic acid hydrazide, strong bands observed at 1670, 1550, 1340 and 1140 cm^{-1} have been assigned[15] to $\nu C=O$ (amide band I), $\nu C=N$ of imine - N (amide band II), $\nu C=C + \nu C=N + \nu CO + \nu CN$ (amide band III) and $\nu NCO + \nu CO$ (amide band IV) respectively. The shift of the amide band I to lower wavenumber by 25-35 cm^{-1} indicates that the bond between INH and the metal ion is through the oxygen of the carbonyl group. Amide band II also suffers a negative shift of 20-25 cm^{-1} due to the involvement of azomethine-N atom in coordination. The intense absorption bands at 1550 and 1515 cm^{-1} have been assigned to antisymmetric stretching vibrations of $\nu C=C + \nu C=N$ of pyridine ring and NO_2. Since there was no change in the position or intensity of these bands, these were not involved in bonding. The bands at 1190 and 1060 cm^{-1} have been assigned to $\delta(NH)$ and $\delta(NH_2)$ respectively. In the complexes, some new bands with medium to weak intensities at 3050-3150 cm^{-1} may be assigned due to νNH vibrations of the ligand. The broad bands at 3600-3300 cm^{-1} may be assigned to OH vibration of methanolic group of the complex. In the far IR spectra[14,15] $\nu(M-N)$ was observed as follows: $\nu Cr-N$, 470; $\nu Fe-N$, 472; $\nu Co-N$, 472; $\nu Ni-N$, 475; $\nu Cu-N$, 472; $\nu Zn-N$,474 and $\nu Ag-N$, 476 cm^{-1} and $\nu(M-O)$ as; $\nu Cr-O$, 325; $\nu Fe-O$, 390; $\nu Co-O$, 420; $\nu Ni-O$, 340; $\nu Cu-O$, 336; $\nu Zn-O$, 320 and $\nu Ag-O$, 390 cm^{-1}.

The EPR measurements of the complexes were undertaken in order to get information about different types of magnetic and non-magnetic interactions[17,18] (Fig. 1). In order to make a quantitative interpretation of the spectra, the computation of half width $(\Delta H_{\frac{1}{2}})_{cal}$ due to dipole-dipole interaction was done according to Vanvleck theory by using the relation[18,19] $(\Delta H_{\frac{1}{2}})_{cal} = 2.35\, g\beta\, [3/5\, S(S+1)\, \Sigma r_{jk}^{-6}]^{\frac{1}{2}}$ where S is the spin quantum number of the ion, r_{jk} is the distance between the ion j and k, g is the Lande splitting factor and β is the Bohr magneton. Since the X-ray data for these complexes are not available and we wish to

Table 2—Data of density, mean spin distance, EPR linewidth, *g*-values and computed dipolar width for complexes

Sample	Density gm/cm³	Mean spin distance Å	Experimental line width ΔH_{pp} Oersteds	g-values	Comparison with Van-vleck theory	
					$(\Delta H_{\frac{1}{2}})^{**}_{cal}$ Oersteds	$(\Delta H_{\frac{1}{2}})_{exp}$ Oersteds
$Cr(Pic)_3$ (INH) (MeOH)	2.5	8.4	400	$g_{av} = 2.0037$	109.0	346.4
$Fe(Pic)_2$ (INH) $(MeOH)_2$	3.4	7.0	Signal-I 80	gI = 2.0812	87.4	69.3
			Signal-II 120	gII = 4.4189	185.5	103.9
$Co(Pic)_2$ (INH) $(MeOH)_2$	2.2	8.1	42	$g_1 = 2.0685$	57.4	36.4
				$g_2 = 2.1240$		
				$g_3 = 2.3145$		
$Ni(Pic)_2$ (INH) $(MeOH)_2$	3.1	7.3	320	$g_1 = 2.0224$	147.2	277.1
				$g_2 = 2.3632$		
				$g_3 = 3.6450$		
$Cu(Pic)_2$ (INH) $(MeOH)_2$	2.4	7.9	45	$g_1 = 2.0546$	61.9	39.0
				$g_2 = 2.1118$		
				$g_3 = 2.3041$		

*ΔH_{pp} = denotes the full linewidth between maximum slope points
**$\Delta H_{\frac{1}{2}} = 3/2\ \Delta H_{pp}$ = half width between half power points

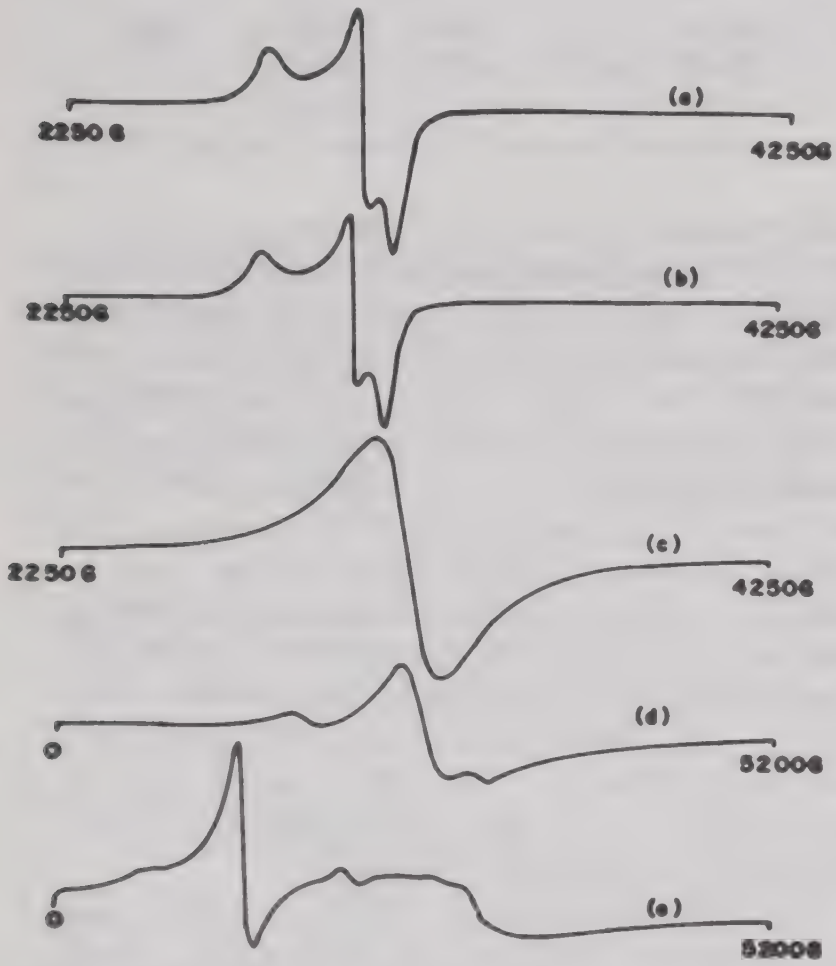

Fig. 1—EPR signals observed at liquid nitrogen temperature for (a), Cu(II); (b), Co(II); (c), Cr(III); (d), Ni(II) and (e), Fe(II) picrate-INH complexes

estimate only the relative contribution of dipolar interaction to line width, it was thought worthwhile to assume that all the complexes have a cubic structure, so that $r_{jk}^{-3} = N\rho/M$ where N is Avogadro number, ρ is density and M is the molecular weight of the complexes (Table 2). Due to large anisotropy in *g*-values, the spectra of Cu(II), Co(II) and Ni(II) complexes have been found to spread out in one of the arms and these spread out portions which gives information[20] about the *g*-values namely $g_1 < g_2 < g_3$ indicating that an unsymmetrical crystal field is acting on these ions. It seems that these ions are located in the site of nearly cubic symmetry but having orthorhombic distortion[20,21]. For Cr(III) complex[17,21,22], the single line peak is due to $M_s = \frac{1}{2} \leftrightarrow -\frac{1}{2}$ transition of octahedrally bound Cr(III). In the case of Fe(II) complex[23,24] an asymmetric and weak line at $g = 2.1$ is due to Fe(II) ion in a nearly cubic environment with a distribution of lower symmetry distortions whose average value is quite small while a strong peak at $g = 4.4$ is due to strong asymmetric potential. The experimental linewidths for Cu(II), Co(II) and Fe(II) complexes are smaller than those expected from dipolar coupling alone. This suggests the presence of exchange interaction in these complexes as evident from their Lrentzian EPR line shapes. However, in the case of Cr(III) and Ni(II) complexes, experimental widths were large although EPR signals were Lorentzian in shape. It appears that in the case of Cr(III), the $M_s = \frac{1}{2} \leftrightarrow -\frac{1}{2}$ transition has been broadened due to the contribution of $3/2 \leftrightarrow 1/2$ and $-1/2 \leftrightarrow -3/2$ transitions whereas the broad peak of Ni(II) complex may be because of the overlapping of two expected resonances (S = 1) due to weak cubic potential at the Ni(II) site[17,22,23].

References

1 Norman B W, *Martindale extra pharmacopoeia* (Pharmaceutical Society of Great Britain Press, London), 1975, p 1872.

2 *Chemeotherapy of tuberculosis*, edited by E Winder (Barry Butterworth, London) 1964, p 111.
3 Srivastava K N, Das S & Lal R A, *Indian J Chem*, 25A (1986) 85.
4 Nakagawa K, Amita K, Mizuno H, Inoue Y & Kakushi T, *Bull chem Soc Japan*, 60 (1987) 2037.
5 Mitchisen D A, *Britain Medical Bulletin*, 40 (1984) 184.
6 Dunn T M, *Modern coordination chemistry*, edited by J Lewis & R G Wilkins (Interscience Publishers Inc, New York) 1960, p 229.
7 Kato K, Jonassen H B & Fanning J C, *Chem Rev*, 64 (1964) 99.
8 Clark R J H & Williams C S, *Inorg Chem*, 4 (1965) 350.
9 A B P Leer, *Inorganic electronic spectroscopy* (Elsevier, NY) 1968, p 249.
10 Teotia M P, Rastogi D K & Malik W U, *J inorg nucl Chem*, 35 (1973) 3015.
11 Mathews R W & Walton R A, *Inorg Chem*, 10 (1971) 1433.
12 Campbell M J M, *Coord chem Rev*, 15 (1975) 279.
13 Chaurasia M R, *J inorg nucl Chem*, 37 (1975) 1547.
14 Ferguson J, *J chem Phys*, 35 (1961) 1612.
15 Nakamoto K, *Infra-red spectra of inorganic and coordination compounds* (Wiley-Interscience, New York) 1970.
16 Miyazawa T, Shimanouchi & Mizushima S I, *J chem Phys*, 29 (1958) 611.
17 Bowers K D & Owen J, *Rept Prog Phys*, 18 (1955) 304.
18 Misra B N & Gupta S K, *J Mag Resonance*, 12 (1973) 126.
19 Vanvleck J H, *Phys Rev*, 74 (1948) 1168.
20 Kneubuhl F K, *J chem Phys*, 33 (1960) 1074.
21 Ayscough P B, *Electron spin resonance in chemistry* (Methuen, London) 1967.
22 Bleaney B & Stevens K W H, *Rept Progr Phys*, 16 (1953) 118.
23 Walsh W M, Rupp L W & Wyluda B J, *Paramagnetic resonance: Proceedings of first international conference* vol 2, edited by W Low (Academic Press, NY) 1963, p 836.
24 Rai R, Gupta S K, Suri D K & Ali S Z, *Physica Status Solidi (b)*, 124 (1984) K167.

Indian Journal of Chemistry
Vol. 31A, November 1992, pp. 896-897

Tetraoxomolybdato and tetraoxotungstato complexes of iron(II) diimines

Vasanthi Lakshmanan, K S Nagaraja† & M R Udupa*
Department of Chemistry, Indian Institute of Technology, Madras 600 036

Received 22 July 1991; revised 23 January 1992; accepted 20 March 1992

The interaction of tetraoxomolybdate or tetraoxotungstate with iron(II) diimines gives compounds of the type ($LFeO_2MO_2$) (L = 2,2'-bipy, 1,10-phen; M = Mo or W). The magnetic studies suggest the presence of high spin iron(II) in the complexes. The IR spectral studies indicate the bonding of diimine to iron(II) and the bidentate nature of MO_4^{2-} group ligated to iron(II). Thermal decomposition behaviour of the complexes is reported. Iron(II) and molybdenum(VI) or tungsten(VI) are bridged by dioxo groups completing tetrahedral geometry.

Several iron-molybdenum-sulphur cluster complexes have been investigated[1,2] due to their relevance in nitrogenase. But the reports[3] on iron-molybdenum-oxygen complexes are sparse. In the present note, we describe the preparation and characterization of $[L_2FeO_2MO_2]$ L = 1,10-phenanthroline, (phen) or 2,2'-bipyridyl, (bipy); M = Mo or W.

Experimental

The chemicals employed were pure (laboratory grade).

Preparation of di-μ-oxo (1,10-phenanthroline) iron(II) dioxomolybdenum(VI), [*(phen)FeO₂MoO₂*] (**1**)

Aqueous solution of $FeSO_4.7H_2O$ (10 mmol, 30 cm^3) and 1,10-phenanthroline dihydrate (30 mmol, 30 cm^3) were mixed when a deep red solution of $[Fe(phen)_3]^{2+}$ was obtained. To this an aqueous solution of $Na_2MoO_4.2H_2O$ (10 mmol, 30 cm^3) was added and stirred. The *p*H of the solution was adjusted to 4.5 by the dropwise addition of 1*N* HCl when a pink coloured precipitate of the complex separated out. It was washed with water, methanol, acetone and dried; yield 65%.

[(phen)$FeWO_4$], (**2**), [(bipy)$FeMoO_4$] (**3**) and [(bipy)$FeWO_4$] (**4**) were obtained by following a similar procedure.

†Department of Chemistry, Loyola College (Autonomous), Madras 600 034

The elemental analyses were carried out by following the conventional procedures[4]. Tungsten was precipitated as barium tungstate and determined by gravimetric method. TG-DTA analyses were carried out on a recording Stanton Redcroft STA-780 thermal analyser. The samples were heated in a Pt crucible at a heating rate of 10°C min^{-1}. Magnetic susceptibility measurements were made at room temperature on a Gouy balance and the TIP and diamagnetic corrections were incorporated. Electronic, infrared and far infrared spectra were recorded on Perkin-Elmer, Cary-2300 and Perkin-Elmer 983 spectrophotometers respectively. The IR and far IR spectra were recorded in KBr and polyethene medium respectively

Results and discussion

The elemental analyses data (Table 1) are in agreement with the suggested compositions of the complexes. The complexes undergo thermal decomposition in air in a single step to give Fe_2O_3 and MoO_3. The X-ray diffraction pattern[5] of the residue exhibited lines due to Fe_2O_3 and MoO_3. The IR absorptions at 990, 870, 590 and 310 cm^{-1} (νMoO) and at 560, 470 and 330 cm^{-1} (νFeO) confirm[6] the proposed phase (Fe_2O_3 + MoO_3). The exothermic peaks in DTA curves at 370 and 400°C may be attributed to the oxidation of the organic ligand leading to the formation of metal oxides. The end products in the case of **3** and **4** are found to be a mixture of Fe_2O_3 and WO_3 as evidenced by X-ray diffraction pattern. The initial decomposition temperatures suggested that iron-tungsten complexes are more stable than iron-molybdenum complexes. The phen complexes decompose at higher temperatures than bipy complexes. This higher thermal stability may be due to an increased conjugation in phen as compared to that in bipy ligand.

The magnetic moment values, 4.8-5.0 B.M., correspond to the presence of four unpaired electrons in the complexes. Iron(II) in the high spin state has $d^6(t_{2g}^4\ e_g^2)$ configuration accounting for the four unpaired electrons. The observed electronic absorptions around 510 and 390 nm are assigned[7] to $d(Fe)\rightarrow\pi_1$ (bipy) and $d(Fe)\rightarrow\pi_2$(bipy) charge transfer transitions respectively. The intraligand $\pi_1\rightarrow\pi_2$ transition was observed[8] around 300 nm.

The IR spectral bands at 1575 and 1550 (bipy) and at 1630 and 1570 cm^{-1} (phen) are attributed to νCN and νCC. A positive shift (20-30 cm^{-1}) compared to free

Table 1—Analytical, magnetic, TG-DTA data of [$LFeMO_4$]

S.No.	Complex	Found (Calc.), %			$\mu_{eff.}$ (B.M.)	Temp. range (°C)	Wt loss (%) Calc. (Found)	Phases formed	DTA peak Temp (°C)
		N	Fe	Mo/W					
1.	[(phen) $FeMoO_4$]	7.0 (7.2)	14.0 (14.1)	23.9 (24.2)	4.81	260-420	39.8 (41.5)	Fe_2O_3 + MoO_3	340 400
2.	[(phen) $FeWO_4$]	5.9 (5.8)	11.5 (11.6)	37.1 (37.6)	4.89	265-500	33.4 (35.1)	Fe_2O_3 + WO_3	410 450
3.	[(bipy) $FeMoO_4$]	7.3 (7.5)	14.8 (15.0)	25.2 (25.8)	4.88	290-470	43.4 (41.2)	Fe_2O_3 + MoO_3	350 450
4.	[(bipy) $FeWO_4$]	6.3 (6.1)	12.1 (12.3)	39.7 (39.9)	4.91	300-500	35.6 (34.8)	Fe_2O_3 + WO_3	400 440

ligand positions indicates coordination through the diimine nitrogen atoms. Compounds **1** and **2** showed IR spectral absorptions at 900, 850 and 790 cm^{-1} due to ν(MoO) and complexes **3** and **4** exhibited three bands due to ν(WO) at 950, 900 and 880 cm^{-1}, thus indicating the bidentate mode[9,10] of MO_4 coordination. The splitting of the bands and the observation of higher frequency bands suggest that MO_4 behaves as a bidentate bridging ligand. The bands at 240 and 290 cm^{-1} are assigned[11] to ν(Fe-N). It is proposed that the diimines coordinate to iron(II) and (MO_4) functions as bidentate bridging ligand towards iron atom.

Acknowledgement

One of the authors (VL) thanks CSIR, New Delhi, for the grant of a Research Fellowship.

References

1 Coucouvanis D, *Acc Chem Res*, 14 (1981) 201.

2 Stiefel E I, *Proceedings of the fourth international conference on chemistry and uses of molybdenum*, edited by H F Barry & P C H Mitchell (Climax Molybdenum Corporation), 1982, 58.

3 Joshwa Anthony Raj D, Nagaraja K S & Udupa M R, *Transition Met Chem*, 11 (1986) 176.

4 Basset J, Demy R C, Jeffery G H & Mendham J, *Vogel's textbook of quantitative inorganic analysis* (ELBS, London), 1978.

5 *Inorganic index to powder diffraction file*, 9 - 209, 16 - 855, edited by L G Berry (JCPDS, Pennsylvania) 1971.

6 Nakamoto K, *Infrared spectra of inorganic and coordination compounds* (John Wiley, New York), 1977.

7 Krumholz P, Serra O A & De Paoli M A, *Inorg chim Acta*, 15 (1975) 25.

8 Bryant G M, Fergusson J E & Powell H K J, *Aust J Chem* 24 (1971) 257.

9 Wienstock N, Schulze H & Muller A, *J chem Phys*, 59 (1973) 5063.

10 Mitchell P C H & Parker D A, *J chem Soc Dalton Trans*, (1976) 1821.

11 Ferraro J R, Basile L J & Kovacic D L, *Inorg Chem*, 5 (1966) 391.

Indian Journal of Chemistry
Vol. 31A, November 1992, pp. 898-900

Acid hydrolysis of iminodiacetatotetraammine cobalt(III), $[Co(NH_3)_4idaH](ClO_4)_2$ complex

Chinmay Chatterjee* & Mary Stephen
Department of Chemistry, Indian Institute of Technology, Powai, Bombay 400 076

Received 3 December 1991; revised and accepted 4 May 1992

The acid catalysed dissociation of iminodiacetatotetraammine cobalt(III) complex has been studied in the $[HNO_3]$ range of 0.05-0.40 mol.dm^{-3} at I=0.50 mol. dm^{-3} ($NaNO_3$), in the temperature range 35-50°C. The reaction exhibits a solvent deuterium-isotope effect k_{D_2O}/k_{H_2O} = 2.32 at 40°C. The solvent deuterium isotope effect is consistent with a rapid pre-equilibrium protonation followed by rate determining ring opening, and excludes a mechanism involving concerted attack by $[H_3O]^+$. The magnitude of the solvent isotope effect, suggests an A-1 type reaction to give a five-coordinate intermediate.

The opening of chelate rings in cobalt(III) complexes in acidic solution is well documented. Detailed, kinetic studies have been reported for phosphato[1], oxalato[2], malonato[3] and carbonato[4] complexes. In contrast, very little kinetic and mechanistic information is available on the opening of aminopolycarboxylate and amino acid chelate rings in acidic media[5]. Rate studies involving potential tridentate aminopolycarboxylate ligand viz., iminodiacetic acid (ida), acting as a bidentate chelating agent in the metal complexes are rare[6] and thus warrant further investigation.

Experimental

cis-Diaquatetraammine cobalt(III) perchlorate and iminodiacetatotetraammine cobalt(III) perchlorate were prepared following the literature methods[6,7] and the purity of the complexes were ascertained by elemental and spectral analysis.

AR grade sodium nitrate and nitric acid were used to adjust the ionic strength and the acidity of the reaction medium, respectively.

Kinetic measurements

The aquation rates were monitoring spectrophotometrically using a Varian Superscan-3 UV-visible spectrophotometer. The course of acid catalysed aquation reactions were followed by measuring the decrease in absorbance at 503 nm where the molar extinction coefficients of the reactant and the product differ appreciably. From the spectral analysis the end product is identified as *cis*-$[Co(NH_3)_4(H_2O)_2]^{3+}$ ion, indicating the absence of any complication due to reverse anation reaction. Since the complex precipitates in perchlorate medium, the reactions were carried out in aqueous nitric acid.

The kinetics of acid catalysed aquation reaction in $[HNO_3]$ range 0.05-0.4 mol dm^{-3} at an ionic strength of 0.50 mol dm^{-3} adjusted with sodium nitrate was followed over a range of temperature 35-50°C. The rates were determined *in situ* following the method described in the literature[8]. The experimental conditions were so chosen that pseudo-first order rate law was applicable and the value of the observed first order rate constant, k_{obs}, were evaluated from the plots of $-\log(A_t - A_\infty)$ versus time (t) which were linear in every case.

Results and discussion

The observed pseudo-first order rate constants, k_{obs}, have been determined over a range of nitric acid concentrations, temperatures and ionic strengths. The variation of k_{obs} with acid concentration at different temperatures is illustrated in Fig. 1 and the results suggest the operation of two concurrent paths as shown in Eq. (1).

$$k_{obs} = k_1 + k_2[H^+] \quad \ldots . (1)$$

where k_1 is the first order rate constant for spontaneous aquation and k_2 is the second order rate constant describing acid catalysed pathway. The k_1 and k_2 values at different temperatures, as obtained from the intercepts and slopes of Fig. 1 are summarised in Table 1, along with the activation parameters, $\triangle H^{\neq}$ and $\triangle S^{\neq}$ values, corresponding to the acid catalysed path evaluated using the transition state equation.

Table 1—Rate and activation parameters for the acid catalysed aquation of $[Co(NH_3)_4idaH]^{2+}$
[complex] = 0.003 mol dm^{-3}

Temp (°C)	I(mol dm^{-3})	10^4k_1(s^{-1})	10^4k_2(mol^{-1} dm^{3}s^{-1})
35	0.5	0.40 ± 0.01	3.20 ± 0.05
35	1.0	0.40 ± 0.02	4.90 ± 0.16
40	0.5	0.70 ± 0.10	5.33 ± 0.30
45	0.5	1.05 ± 0.15	8.45 ± 0.25
50	0.5	1.50 ± 0.14	15.38 ± 0.40
$\triangle H^{\neq}$ (kJ mol^{-1})		82.1 ± 8.0	90.50 ± 8.20
$\triangle S^{\neq}$ JK^{-1} mol^{-1})		−65.9 ± 9.2	−20.30 ± 6.30

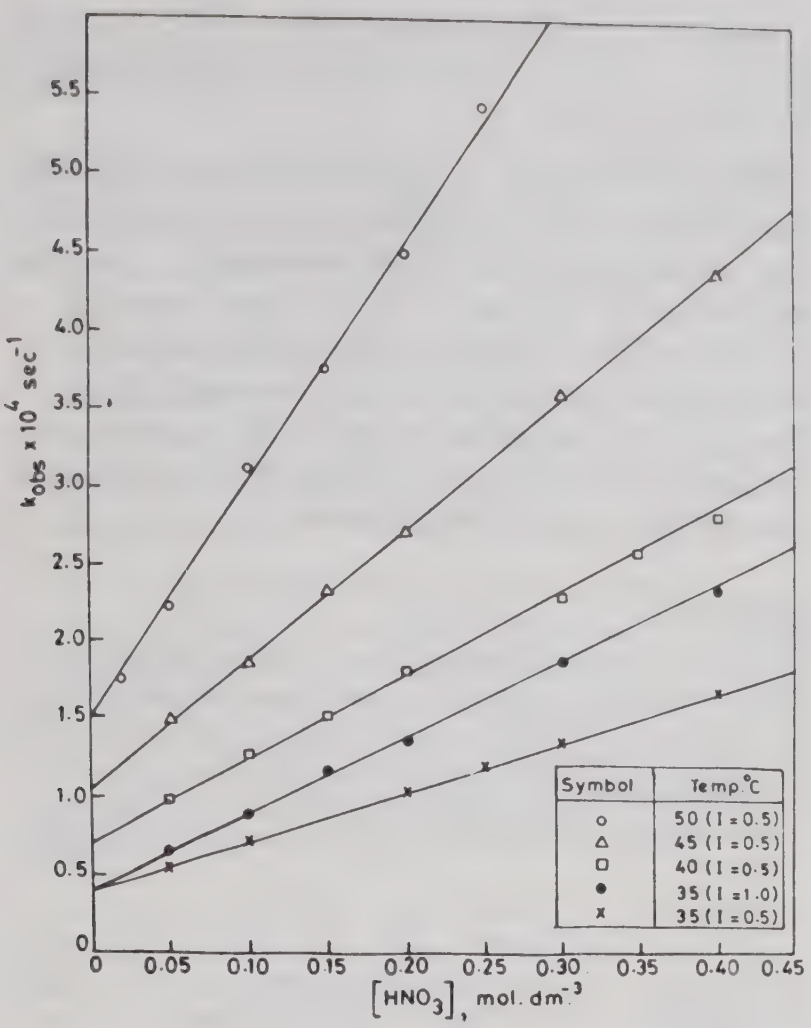

Fig.1—Effect of [acid] on k_{obs} at different temperatures and ionic strengths. ($[Co(NH_3)_4\ idaH]^{2+}$ = 0.003 mol dm^{-3})

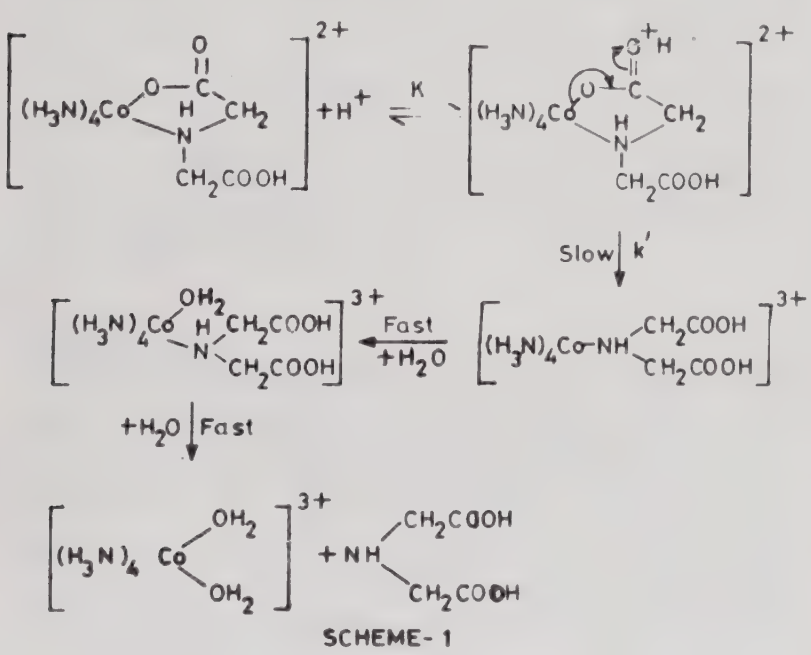

A sequence of changes consistent with the kinetic results for the acid catalysed process is depicted in Scheme 1.

According to Scheme 1, the catalytic rate constant k_2 is related to K and k' by the relation (2).

$$k_2 = k'K/(1 + K[H^+]) \quad \ldots . (2)$$

The absence of any deviation from linearity for the k_{obs} versus $[H^+]$ plot even at the highest [acid] used indicates that $K[H^+] << 1$ and hence Eq. (2) reduces to $k_2 = Kk'$. The comparison of the values of k_1 and k_2 indicates that the protonated species is much more labile than the unprotonated species. This can be rationalized by considering that acid catalysis involves protonation of the carboxylato chelate in a pre-equilibrium step. Strong bonding between oxygen atom of the ligand and H^+ in the protonated form of the complex leads to electron withdrawal from the Co—O bond, thereby facilitating its fission and providing a means for the facile entry of a water molecule from the solvation sheath to form the aqua iminodiacetic acid complex ion. Protonation of a carboxyl oxygen in octahedral cobalt(III) carboxylates has been reported by several workers[9].

The uncatalysed path can be visualised to be involving the attack of a solvent molecule in the rate-determining step. The mechanism of the acid catalysis depicted in Scheme 1 needs detailed discussion. Spectral data and product analysis indicate that acid catalysis involves opening of iminodiacetato ring. According to Scheme 1, ring opening probably involves protonation of the carboxyl oxygen in a rapid pre-equilibrium step followed by slow rate-determining opening of the chelate ring with Co—O bond cleavage. In the subsequent step Co—N bond cleavage becomes faster as the iminodiacetato ligand looses its chelate effect due to protonation of the carboxylate end. An alternative mechanism involving concerted attack by H^+ and H_2O can also be considered. However, it is possible to distinguish between these two mechanisms by using solvent deuterium isotope effects[10]. For the stepwise pre-equilibrium mechanism (Scheme 1), k_{D_2O}/k_{H_2O} should be greater than one since D_2O is less acidic than water, and hence the substrate will be able to compete with the solvent for deuterion in D_2O more effectively than for the proton in H_2O. However, for a rate determining proton transfer step k_{D_2O}/k_{H_2O} is expected to be less than one[5]. The solvent deuterium isotope effect was determined at 40°C [Table 2], giving k_{D_2O}/k_{H_2O} =

Table 2—Solvent deuterium isotope effect for $[Co(NH_3)_4\ idaH]^{2+}$ ion at 40°C and at I = 0.5 mol dm^{-3} ($NaNO_3$)

Medium HCl[a] (DCl[b]) (mol dm^{-3})	$10^4 k_{obs}$ (s^{-1})	$k_H(^{\prime}k_D) \times 10^4$ (mol^{-1} dm^3 s^{-1})
0.1	1.34(2.55)	
0.2	1.84(3.83)	4.48 ± 0.2 (10.42 ± 0.6)
0.3	2.30(4.65)	
0.4	2.68(5.75)	

a_{H_2O} solvent, b_{D_2O} solvent, k_H (k_D) = acid catalysed rate constant.

2.32, fully consistent with a rapid pre-equilibrium protonation. Mechanisms involving concerted attack by H^+ and H_2O are, therefore, excluded in this system.

The acid catalysed ring opening reaction could occur either by an A-1 or an A-2 type mechanism as shown below :

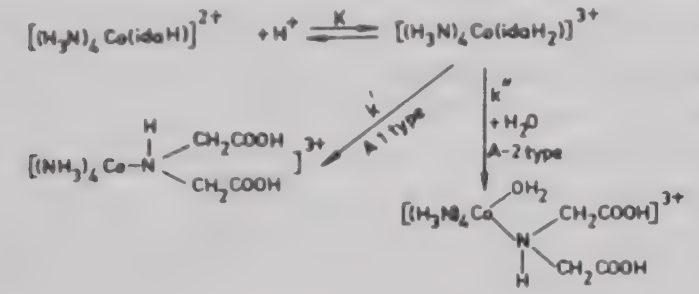

For an A-1 reaction the rate constant $k_2 = k'K$, while for the A-2 situation, $k_2 = k''K[H_2O]$. The A-1 mechanism would involve decomposition of the protonated species to give a five coordinate intermediate, while the A-2 mechanism would involve nucleophilic attack by water on the protonated species. The k_{D_2O}/k_{H_2O} ratio in the range (1.9-2.6) has been considered typical for A-1 type hydrolysis, and is much larger than the values of 1.3-1.4 which have been observed for A-2 reactions[10]. The present evidence ($k_{D_2O}/k_{H_2O} = 2.32$) thus favour an A-1 mechanism for the dissociation of the title complex.

The effect of ionic strength on the aquation rate has been studied at 35°C using sodium nitrate and nitric acid. The uncatalysed rate constant, k_1, remains unaffected by the variation in ionic strength as expected. The acid dependent rate constant, k_2, increases with an increase in ionic strength (Table 1). The equilibrium constant, K, generally increases with increase in ionic strength and hence the observed increase in k_2 can be attributed to the increase in K.

References

1 Lincoln S F & Stranks D R, *Aust J Chem*, 21 (1968) 57.
2 Roy J & Banerjea D, *J inorg nucl Chem*, 38 (1976) 1313.
3 Chatterjee C & Das S, *J coord Chem*, 15 (1986) 147.
4 Dasgupta T P & Harris G M, *J Am chem Soc*, 93 (1971) 91.
5 Hay R W & Basak A K, *Inorg chim Acta*, 69 (1983) 1.
6 Bhattacharya P & Banerjee P, *Bull chem Soc Japan*, 68 (1985) 3593.
7 Springborg J & Schaffer C E, *Inorg Synth*, 18 (1978) 83.
8 Chatterjee C & Phadke S V, *J chem Soc, Dalton*, (1987) 2095.
9 Vlcek A A, *Advances in the chemistry of coordination compounds* edited by S Krischner (Macmillan, New York) (1971) pp.590.
10 Hay R W & Jeragh B, *J chem Soc, Dalton*, (1979) 1343.

Indian Journal of Chemistry
Vol. 31A, November 1992, pp. 901-902

Cation exchange chromatographic separation of a number of metal ions in ammonium iodide media

Mohd Ibrahim Nasir* & Ashok Mahan
Department of Chemistry, University of Allahabad, Allahabad 211 002

Received 7 January 1992; revised 23 March 1992; accepted 8 June 1992

The cation exchange behaviour of 11 metal ions in NH_4I at various concentrations (0.096-2.08 *M*) has been studied with Dowex 50W-X4 resin (200-400 Mesh, NH_4^+-form). The distribution coefficients are determined by batch technique to evaluate the conditions for column chromatographic separation. A number of binary, ternary and quaternary separation of synthetic mixtures have been reported.

While anion exchange resin in iodide media provides a clear-cut separation of some elements[1,2], procedures based on the use of cation exchange resin have been found to be more convenient. Except the separation of cadmium from zinc reported by Kallmann *et al.*[3], no work has been published so far on the cation exchange in iodide media. The present note reports a systematic investigation of cation exchange behaviour of 11 metal ions in ammonium iodide media in eight different concentrations in the range 0.096-2.08 *M*.

Experimental

Stock solutions (0.05-0.10 *M*) of various metal ions were prepared as reported elsewhere[4]. The solutions were standardized by the complexometric methods[5,6]. An aqueous solution of ammonium iodide (4.0 *M*) (Sisco chem) was prepared and standardised for the iodide content. The cation exchange resin Dowex 50W-X4 (200-400 Mesh, H^+-form, Fluka AG) was pretreated and converted to NH_4^+ form, standardised and air-dried before use. The resin capacity and moisture content was determined by the usual methods and were 3.16 meq/g and 24% respectively.

The distribution coefficients (D) were determined by the batch equilibration technique as described elsewhere[4]. In achieving the various separations by column chromatography, the general procedure previously described[4] has been followed unless otherwise stated. In order to facilitate the flow of the eluting agents, the porcelain pieces were placed alongwith the resin bed. The resolution of the synthetic binary, ternary and quaternary mixtures are shown in Fig. 1. Both the ternary and quaternary mixtures were prepared in 0.096 *M* ammonium iodide solution,while the binary mixtures of Cd-Mg and Zn-Al were prepared in 0.32 *M* and 0.80 *M* ammonium iodide solution respectively. The metal ions eluted are shown in Fig. 1.

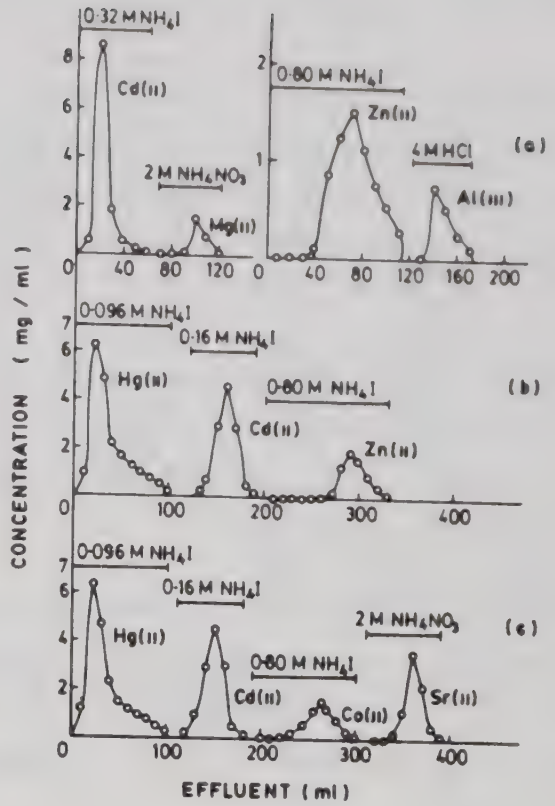

Fig. 1—Separation curves of binary, ternary and quaternary mixtures of metal ions on Dowex 50W-X4

Results and discussion

The affinity of a metal ion towards a cation exchange resin can be described by binding the metal ion in a complex. The sorption will be less, if the complex formed has a little positive, zero or a negative charge. The sorption of the cations investigated initially decreases as the iodide concentration increases, as shown in Table 1.

The Hg(II) and Cd(II) ions are weakly sorbed due to strong complex formation of negatively charged species mainly, MI_4^{2-} (refs 7-9). The moderate sorbed metal ions, Zn(II), Co(II), Ni(II), Mn(II) and Mg(II), have poor tendencies to form negatively charged species, and that too only at high concentrations of iodide[7,10]. The strongly sorbed cations, Al(III), Ca(II), Sr(II) and Th(IV) are retained by the resin due to their poor complexing nature and high positive charge. At higher concentrations of ammonium

Table 1—Distribution coefficients (D) and separation factors $\alpha(\alpha^{M}_{Hg})$ of metal ions in 0.096-2.08 *M* aqueous ammonium iodide on Dowex 50W-X4

Metal ion	Ammonium iodide concentration (*M*)									
	0.096		0.16		0.80		1.44		2,08	
	D	α	D	α	D	α	D	α	D	α
Mg(II)	150.79	23.50	128.12	22.00	13.58	3.60	7.23	3.10	4.87	3.00
Al(III)	1982.10	309.70	1628.96	280.60	40.02	10.80	13.15	5.70	6.61	4.10
Ca(II)	268.15	41.90	235.71	40.60	26.40	7.10	9.43	4.10	7.88	4.90
Mn(II)	172.90	27.10	148.21	25.50	17.54	4.70	7.55	3.20	7.33	4.60
Co(II)	60.80	9.50	53.12	9.20	16.32	4.40	11.23	4.80	5.12	3.20
Ni(II)	160.51	25.10	137.50	23.70	18.52	5.00	9.33	4.00	7.28	4.60
Zn(II)	72.22	1130	59.58	10.20	15.92	4.30	9.29	4.00	8.83	5.50
Sr(II)	T.S.	V.V.H.	T.S.	V.V.H.	562.52	152.00	402.27	174.90	336.68	213.00
Cd(II)	36.60	5.70	27.87	4.80	6.98	1.80	3.78	1.60	2.56	1.60
Hg(II)	6.40		5.80		3.70		2.30		1.58	
Th(IV)	1455.20	227.30	1201.23	207.10	50.51	13.60	25.00	10.80	23.68	14.90

T.S.: Shows almost total sorption.
V H.: Indicates very high α value.

Table 2—Expected metal ion complexes in ammonium iodide solution (0.096-2.08 *M*)

Metal ion	Complex formed	Complex nature	References
Hg(II)	HgI_4^{2-}	Very strong	8
Cd(II)	CdI_4^{2-}	Strong	
	CdI_3^-	less stable	8,9,12
	CdI_5^{3-}	less stable	13
Zn(II)	ZnI_4^{2-}	weak	1,3
Mn(II)	MnI_4^{2-}	unstable	10
	MI_6^{4-}	unstable	

All the metal ions investigated except Hg(II) form neutral complexes in the above iodide solution.

iodide solutions, these metal ions form a neutral species, and therefore, have not been taken by cation exchange resin[11]. The metal ions and their complexes formed with ammonium iodide are presented in Table 2. The ammonium iodide solution (0.096 *M*) was found most suitable for the chromatographic separation of Hg(II) and Cd(II) ions. This concentration was found to be appropriate since no precipitate of HgI_2 took place and also at this concentration, the separation factors ($\alpha = Di/Dj$, where i and j are two different metal ions) are the highest, as shown in Table 1. In addition, at such a low concentration, the iodide do not interfere in metal ions estimations. Moreover higher α values predict a more quantitative separation. The very high α values for Sr(II) which shows a lower trend at low concentrations of ammonium iodide solution are due to total sorption of Sr(II) by the resin as shown in Table 1. The separation of Zn from Ni in 0. 0 *M* NH_4I could not be achieved as both Zn and Ni pass together in the effluent of 0. 0 *M* ammonium iodide solution.

As ammonium is the secondary cation in the present case, it causes no difference at low salt concentrations. However, at higher concentrations, the association of the secondary cation with a resin invasion is strong. Such associated complexes are too large to enter the resin[14].

Acknowledgement

The authors are thankful to Prof W U Malik, Vice-Chancellor, University of Allahabad for providing the necessary facilities.

References

1 Kallmann S, Oberthin H & Liu R, *Analyt Chem*, 30 (1958) 1846.
2 Raptis S & Muller K, *Clin chim Acta*, 88 (1978) 393.
3 Kallmann S, Oberthin H & Liu R, *Analyt Chem*, 32 (1960) 58.
4 Nasir M I & Mahan A, *Indian J Chem*, 31A (1992) 285.
5 Flaschka H A, *EDTA titrations* (Pergamon, New York) 1964.
6 Vogel A I, *A text book of quantitative inorganic analysis* (ELBS, London) 1985.
7 Stokes R H, *Trans Faraday Soc*, 44 (1948) 137.
8 Marcus Y & Eliezer I, *J inorg nucl Chem*, 25 (1963) 867.
9 Nanjundiah C & Narayan R, *Trans SAEST*, 16 (1981) 233.
10 Misumi S & Aihara M, *Talanta*, 19 (1972) 549.
11 Siegel A, *Geochim Cosmochim Acta*, 30 (1966) 757.
12 Alberty R & King E, *J Am Chem Soc*, 73 (1951) 517.
13 Cyr H M, *Comprehensive inorganic chemistry*, edited by M C Sneed & R C Brasted (Van Nostrand, New York) 1955.
14 Qureshi M, Tandon S N & Varshney R G, *J Indian chem Soc*, LVIII (1981) 290.

ANNOUNCEMENTS

Nominations Invited for CSIR Young Scientist Awards: 1993

Nominations are invited by the Council of Scientific and Industrial Research (CSIR) for the 1993 CSIR Young Scientist Awards. The awards are to be given for research contributions made primarily in India during the past five years. The age of nominees should not be more than 35 years as on 26 September 1992. Regularly employed scientists working in CSIR system are eligible.

The awards, each of the value of Rs 10,000 are given annually in the following disciplines: (1) Biological Sciences, (2) Chemical Sciences, (3) Earth, Atmosphere, Ocean and Planetary Sciences, (4) Engineering Sciences, and (5) Physical Sciences (including instrumentation).

Nominations should be sent by December 1992 as per the prescribed proforma (20 copies) along with one set of reprints of research papers published during last 5-year period to the Head, Human Resource Development Group, Extramural Research Division, CSIR Complex, Pusa, New Delhi 110012. The proforma for nomination may be obtained from the above address.

Nominations Invited for Shanti Swarup Bhatnagar Prizes in Science and Technology : 1993

Nominations are invited by the Council of Scientific and Industrial Research (CSIR) for the Shanti Swarup Bhatnagar (SSB) Prizes in science, including engineering and technology for the year 1993. The SSB prizes are to be given for research contributions made primarily in India during the past five years. The age of the nominees for the 1993 SSB prizes should not be more than 45 years as on 31.12.1992.

The SSB prizes, each of the value of Rs 50,000 may be awarded for notable and outstanding research, applied or fundamental, in the following disciplines: (1) Biological Sciences, (2) Chemical Sciences, (3) Earth, Atmosphere, Ocean and Planetary Sciences, (4) Engineering Sciences, (5) Mathematical Sciences, (6) Medical Sciences, and (7) Physical Sciences.

Nominations should be sent as per the prescribed proforma (25 copies) along with one set of reprints of significant publications of last 5-year period by 1 February 1993 to the Head, Human Resource Development Group, Extramural Research Division, CSIR Complex, Pusa, New Delhi 110 012. The proforma for nomination may be obtained from the above address.

RECENT ADVANCES IN SPINNING TECHNOLOGIES

A.T.D.C. A. I. R. I. REGIONAL CENTRE

Special Issue of

Indian Journal of Fibre & Textile Research

The December 1992 issue of the *Indian Journal of Fibre & Textile Research* is being brought out as a special issue on ***"RECENT ADVANCES IN SPINNING TECHNOLOGIES"***.

Guest edited by Prof. K R Salhotra, the issue will contain the following invited papers:

- Influence of fibre properties in air-jet spinning — W Oxenham
- Influence of harvesting, ginning and mill cleaning systems on rotor-spinning performance — J B Price
- A new ring-and-traveller system as the key to more production from the ring spinning machine — H Stalder
- Factors effecting changes in the structure and properties of open-end rotor-spun yarns — C A Lawrence & E Finikopulos
- Future prospects of rotor spinning — J V Kasparek
- Present status of OE rotor spinning and the influence of some raw-material parameters on the yarn quality — Josef Ripka
- Recent developments in two-for-one (TFO) twisting and their relevance to Indian textile units — A K Agrawal, R G Patil, K A Patel & J M Grover
- Friction spinning — A critical review — N Balasubramanian
- Wrap spinning technology — A critical review of yarn properties — V Subramaniam & Peer Mohamed
- Response of polyester-viscose blends to air-jet spinning — R C D Kaushik, K R Salhotra & G K Tyagi
- An overview of spinning technologies: Possibilities, applications and limitations — K R Salhotra
- Production of international quality yarn — P Balasubramanian
- Influence of annealing on the properties of air-jet and ring yarns — A K Sengupta, R Chattopadhyay & D Daspal
- Spinning of synthetic fibres & blends on rotor-spinning machine — S M Ishtiaque

The contents of this special issue are bound to be of immense use to researchers, technologists, managers and industrialists and would serve as a valuable reference.

Price	**Rs 100.00**	**£18.00**	**$35.00**

Orders accompanied by Bank Drafts/Cheques drawn in favour of PUBLICATIONS & INFORMATION DIRECTORATE, NEW DELHI may be sent to the Sales & Distribution Officer, Publications & Information Directorate (CSIR), Dr. K.S. Krishnan Marg, New Delhi 110 012.

FREE GIFT WITH COMPLETE SET

GOLDEN OFFER

You can now book your copies of the attractive, lavishly illustrated popular science titles under CSIR GOLDEN JUBILEE SERIES in advance and also get a

FREE GIFT

Titles in print

BODY'S BATTLES

By **Bal Phondke**

Unfolds the story of the inner defence organisation of the body, the diversity and specificity of its armament and its round the clock vigil that meets every threat to it.

84 pages; Price: Rs.15 (Paperback), Rs. 18 (Hardcover)

MINING THE OCEAN

By **T K S Murthy**

Reveals, the timeless secrets of the seas and the secret bounty that they hold in reserve.

106 pages; Price: Rs. 12 (Paperback), Rs. 20 (Hardcover)

HIS MASTER'S SLAVE

By **Tapan Bhattacharya**

Tells the non-specialist the riveting story of the modern day genie of the bottle, the PC.

88 pages; Price: Rs. 10 (Paperback), Rs. 18 (Hardcover)

INSIDE STARS

By **Biman Basu**

Provides a privileged glimpse into star nurseries, tracking the luminescent trail to fiery senescence and death of stars to reveal the mysteries and marvels of cosmic drama.

90 pages; Price: Rs. 10 (Paperback), Rs. 18 (Hardcover)

PLASTIC FEAST

By **Subodh Jawadekar**

Celebrates the dawn of the plastics era and elaborates the myriad ways in which plastics touch our lives. A veritable feast of plastics, very palatable to the readers.

96 pages; Price: Rs. 12 (Paperback) Rs. 20 (Hardcover)

CERAMICS ARE FOREVER

By **B C Sharma**

Highlights the fascinating versatility of ceramics and provides an excellent close-up of the symbiotic relationship between man and materials.

84 pages; Price: Rs. 11 (Paperback), Rs. 20 (Hardcover)

ARTIFICIAL INTELLIGENCE

By K.D. Pavate

Unveils the many facts of Artificial Intelligence

98 pages; Price: Rs.13 (Paperback), Rs.21 (Hardcover)

Forthcoming Titles

HARDY COMPOSITES

MAN IN SPACE

MIND MASTER

You may place an order for all 10 titles by sending Rs.120.00 (for paperback) or Rs.200.00 (for Hardcover) including postage by Demand Draft/M.O. payable to "Publications and Information Directorate". The titles already published will be sent to you as soon as the payment is received and the forthcoming titles will be sent by post as soon as they are published, one every month. With every order you will receive a free gift.

For further information write to:
Sales and Distribution Officer
Publications and Information Directorate (CSIR)
Dr. K S Krishnan Marg, New Delhi 110 012

OUR AGENTS: – BANGALORE, Navakarnataka Publications Pvt. Ltd., Embassy Centre, 11, Crescent Road, Kumara Park East, Bangalore - 560 001; BHOPAL, Ajay Publishers & Distributors, 74, Motia Park, Behind Moti Masjid, Bhopal-460 001; BOMBAY, Strand Book Stall, Sir Ferozeshah Mehta Road, Fort, Bombay - 400 001, Universal Book Corporation, 546, Kalabadevi Road, Dhobi Talao, P.B. No.2540, Bombay - 400 00; CALCUTTA, Manisha Granthalaya (P) Ltd., 4/3 B, Bankim Chatterjee Street, Calcutta-700 073; MYSORE, People's Book House, J.M. Place Road, Mysore - 570 024; NEW DELHI, Sangam Book Depot, 4378/4B, Ansari Road, Darya Ganj, New Delhi - 110 002, UBS Publishers Distributors Ltd., 5, Ansari Road, Darya Ganj, New Delhi - 110 002; PATNA, Sunil News Agency, Yogiatoli, Patna - 860 001; PUNE, Satish Book Distributors, 27/B, Siddharth Chambers, Opp. Balwant Chowk, Budhwar Peth, Pune 411 002.

Printed & Published by Dr. G.P. Phondke, Director, Publications & Information Directorate (PID)
Dr. K.S. Krishnan Marg, New Delhi 110 012, at PID.

NEW!

NEW!

NEW!

AIR TIME

Catch the ***Action Spirit*** *for its*

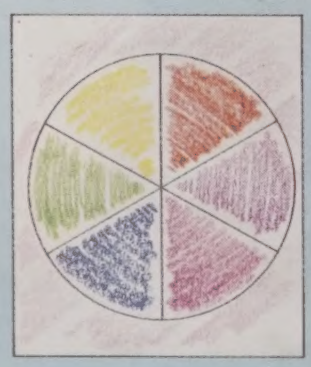

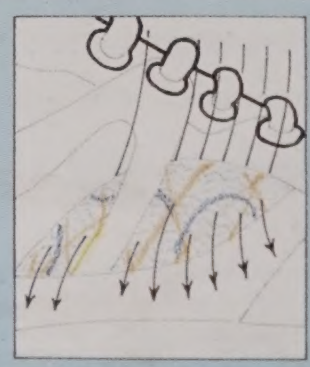

- QUALITY
- GENTLE GRIP
- MULTIPLE COLOURS
- DIFFERENT SIZES
- AIRY
- CUSHIONE INSOLE

action® SHOES

DL-18023/92
RN 7090/63